

# **Accelerating antimalarial drug discovery through repositioning**

**Holly Matthews**

School of Environment and Life Sciences  
College of Science and Technology  
University of Salford, Salford, UK

Submitted in Partial Fulfilment of the Requirements for the  
Degree of Doctor of Philosophy, April 2015

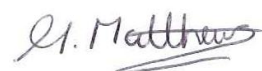
## DECLARATION

---

I certify that this thesis, which I submit to the University of Salford a partial fulfilment of the requirements for a Degree of Doctor of Philosophy, is a presentation of my own research work. Wherever contributions of others are involved, every effort is made to indicate this clearly with due reference to the literature and acknowledgement of collaborative research and discussions. The content of this thesis has not been submitted for a higher degree at this or any other university.

Part of the work presented in this thesis has been accepted for publication:

Matthews, H., Usman-Idris, M., Khan, F., Read, M. and Nirmalan, N. J. (2013) 'Drug repositioning as a route to anti-malarial drug discovery: preliminary investigation of the *in vitro* anti-malarial efficacy of emetine dihydrochloride hydrate'. *Malaria Journal*, 12, 359.



---

Holly Matthews

## CONTENTS

---

DECLARATION.....	ii
CONTENTS .....	ii
LIST OF FIGURES .....	ix
LIST OF TABLES .....	xii
ACKNOWLEDGEMENTS .....	xiv
ABBREVIATIONS .....	xv
ABSTRACT .....	xvi
CHAPTER 1.....	1
INTRODUCTION .....	1
1.1 Malaria: a historical perspective .....	1
1.2 Life Cycle.....	2
1.3 Disease symptoms.....	3
1.4 Discovery of the malaria parasite and its complex life cycle .....	3
1.5 History of malaria prevention and treatment.....	5
1.5.1 Mosquito Control .....	5
1.5.2 Quinine and its synthetic derivatives .....	6
1.5.3 The Malaria Eradication Programme .....	7
1.5.4 The impact of the antifolate drugs.....	10
1.5.5 The amino alcohols and artemisinins.....	11
1.6 Malaria today .....	13
1.6.1 The status of vaccine development .....	13
1.6.2 Current mosquito control measures .....	14
1.6.3 Current chemotherapy recommendations .....	15
1.7 Drug discovery.....	17
1.7.1 The golden era of drug discovery.....	18
1.7.2 Target-based drug discovery.....	19
1.7.2.1 Validated antimalarial drug targets .....	21
1.7.2.2 Problems with target-based drug discovery .....	22
1.7.3 Phenotypic drug screening.....	23
1.7.4 Drug repositioning.....	24
1.7.5 Phenotypic screening for malaria .....	26
1.7.6 Drug repositioning for malaria .....	27
1.8 Future directions .....	27
1.9 The objectives of the PhD .....	28

CHAPTER 2.....	29
GENERAL MATERIALS AND METHODS .....	29
2.1 <i>In vitro</i> culture of <i>Plasmodium falciparum</i> .....	29
2.1.1 Preparation of complete mediim .....	29
2.1.2 Washing Medium .....	29
2.1.3 Preparation of human blood for culture of <i>Plasmodium falciparum</i> .....	29
2.1.4. <i>In vitro</i> <i>Plasmodium falciparum</i> culture .....	30
2.1.5 Routine maintenance of a <i>Plasmodium falciparum</i> culture .....	30
2.1.6 Estimation of parasitaemia .....	30
2.1.7 Preservation in liquid nitrogen.....	31
2.1.8 Retrieval from liquid nitrogen .....	31
2.1.9 Sorbitol synchronisation.....	32
2.2 Drug susceptibility assays.....	32
2.2.1 Preparation of existing antimalarial primary stock solutions .....	32
2.2.2 SYBR Green microtitre plate assay for <i>Plasmodium falciparum</i> .....	32
2.2.3 SYBR Green flow cytometry method for <i>Plasmodium falciparum</i> .....	33
2.2.4 Calculation of IC <sub>50</sub> and IC <sub>90</sub> values .....	33
CHAPTER 3.....	34
OPTIMISATION OF FLUORESCENCE-BASED DRUG SUSCEPTIBILITY ASSAYS .....	34
3.1 INTRODUCTION .....	34
3.1.1The WHO microtest.....	34
3.1.2 Radioactive isotope incorporation .....	35
3.1.3 ELISA-based assays .....	36
3.1.4 SYBR Green-based microtitre plate assay .....	37
3.1.5 SYBR Green-based Flow cytometric method .....	38
3.2 METHODS .....	40
3.2.1 Optimisation of the SYBR Green Microtitre plate assay (SG-MicroPlate).....	40
3.2.2 Optimisation of the SYBR Green Flow Cytometry assay (SG-FCM) .....	40
3.2.3 Comparison of the Giemsa microscopic test, SG-MicroPlate and SG-FCM .....	40
3.2.4 Optimisation of 96 well plate culture of <i>P. falciparum</i> .....	41
3.2.5 Optimisation of a medium-throughput SG-MicroPlate assay .....	41
3.2.6 Time-course analysis of DHA treatment using SG-FCM .....	42
3.2.7 Stage-specific effects of DHA using SG-FCM .....	42
3.2.8 IC <sub>50</sub> determination of existing antimalarials against K1 parasites .....	43
3.3 RESULTS .....	44
3.3.1 Optimisation of the SG-MicroPlate assay for malaria .....	44

3.3.2 Optimisation of the SYBR Green Flow Cytometry assay (SG-FCM) .....	44
3.3.3 Comparison of the Giemsa microscopic test SG-MicroPlate and SG-FCM .....	46
3.3.4 Optimisation of medium-throughput SG-MicroPlate assay for malaria .....	47
3.3.5 SG-FCM for detailed <i>in vitro</i> investigations of parasite killing .....	48
3.3.5.1 Time-course analysis of DHA treatment .....	48
3.3.5.2 Stage-specific effects of DHA .....	51
3.3.5.3 Determination of baseline IC <sub>50</sub> values for existing antimalarials .....	51
3.4 DISCUSSION .....	53
3.4.1 Fluorescence-based drug susceptibility assays for malaria .....	53
3.4.2 Validation of SYBR Green staining procedures .....	53
3.4.3 SG-MicroPlate optimisation .....	54
3.4.4 SG-FCM for detailed <i>in vitro</i> investigations of parasite killing .....	56
3.4.5 Conclusion .....	57
CHAPTER 4.....	58
SCREENING FDA APPROVED DRUG LIBRARIES FOR ANTIMALARIAL ACTIVITY .....	58
4.1 INTRODUCTION .....	58
4.2 METHODS .....	64
4.2.1 Preliminary screening of the ENZO library for antimalarial activity.....	64
4.2.2 Preliminary screening of LOPAC compounds for antimalarial activity .....	64
4.2.3 MeSH annotation of hit compounds from LOPAC and ENZO libraries.....	65
4.2.4 Tanimoto similarity of MeSH compound with existing antimalarials .....	66
4.2.5 Secondary phase screening of selected ENZO compounds .....	66
4.2.6 Secondary phase screening of LOPAC compounds .....	66
4.2.7 Accurate IC <sub>50</sub> determination of selected compounds .....	67
4.3 RESULTS .....	67
4.3.1 Preliminary screening of the ENZO library for antimalarial activity.....	67
4.3.2 Preliminary screening of the LOPAC compounds for antimalarial activity .....	70
4.3.3 MeSH annotation of hit compounds from LOPAC and ENZO libraries.....	70
4.3.4 Tanimoto Similarity of selected MesH categories.....	71
4.3.5 Second-phase screening of selected compounds .....	73
4.3.6 IC <sub>50</sub> determination of selected compounds .....	75
4.4 DISCUSSION .....	77
4.4.1 Preliminary screening of the ENZO and LOPAC library for antimalarial activity .....	78
4.4.2 MeSH annotation of hit compounds .....	79
4.4.2.1 Anticancer compounds for malaria .....	79
4.4.2.2 Antipsychotics, immune suppressants and antibiotics for malaria .....	80

4.4.3 Tanimoto similarity of hit compounds .....	81
4.4.4 Secondary phase screening selected compounds.....	82
4.4.5 Accurate IC <sub>50</sub> determination of selected compounds .....	84
4.4.5.1 Antihistamines for malaria .....	84
4.4.5.2 Antiarrhythmic compounds for malaria.....	85
4.4.5.3 The anti-emetic, serotonin receptor antagonist for combination with emetine 86	
4.4.5.4 The anti-amoebic compound for malaria .....	86
4.4.6 Conclusion .....	87
CHAPTER 5.....	88
ANTIMALARIAL ACTIVITY OF EMETINE DIHYDROCHLORIDE HYDRATE .....	88
5.1 INTRODUCTION .....	88
5.2 METHODS .....	92
5.2.1 Determination of cephaeline IC <sub>50</sub> in <i>P. falciparum</i> strain K1 .....	92
5.2.2 Comparison of cephaeline and emetine cellular toxicity.....	92
5.2.3 Time-course analysis of emetine and dihydroartemisinin against K1 parasites.....	92
5.2.4 Stage-specificity of emetine .....	93
5.2.5 Determination of the killing profile for emetine against K1 parasites.....	93
5.2.6 Preliminary comparison of JC-1 and SYBR Green staining .....	94
5.2.7 JC-1 and SYBR Green following chloroquine treatment.....	95
5.2.8 Loss of mitochondrial membrane potential after atovaquone and emetine treatment .....	95
5.3 RESULTS .....	96
5.3.1 Comparison of cephaeline and emetine dose response .....	96
5.3.2 Comparison of cephaeline and emetine cellular toxicity.....	96
5.3.3 Time-course analysis of dihydroartemisinin and emetine dihydrochloride hydrate..	97
5.3.4 Stage-specific effects.....	99
5.3.5 Determination of the parasite killing profile for emetine against <i>P. falciparum</i> K1 .	100
5.3.6 Parallel staining with JC-1 and SYBR Green.....	104
5.3.7 JC-1 and SYBR Green following high-dose chloroquine treatment.....	105
5.3.8 The effect of emetine on mitochondrial membrane potential.....	106
5.4 DISCUSSION .....	106
5.4.1 Comparison between emetine and its natural derivative, cephaeline .....	107
5.4.2 Time-course analysis of emetine.....	108
5.4.3 Stage-specific effects and cytosytatic vs. cytotoxic activity of emetine .....	109
5.4.4 Detailed killing profile analysis of emetine against <i>P. falciparum</i> strain K1 .....	111
5.4.5 The effect of emetine on malaria parasite mitochondria .....	112

5.4.6 Conclusion .....	114
CHAPTER 6.....	116
DRUG INTERACTION ANALYSIS OF EMETINE DIHYDROCHLORIDE HYDRATE.....	116
6.1 INTRODUCTION .....	116
6. 2 METHODS .....	120
6.2.1 Fixed ratio drug interaction assay .....	120
6.2.2 Isobologram preparation and analysis for fixed ratio data.....	120
6.2.3 Application of the CalcuSyn assay to define antimalarial drug interactions.....	121
6.2.4 Validation of the CalcuSyn assay for malaria .....	122
6.2.4.1 Optimisation of drug dosing and treatment period.....	122
6.2.4.3 Recovery of parasites treated with the atovaquone-proguanil combination ...	124
6.2.5 CalcuSyn analysis of emetine with existing antimalarials .....	124
6.3 RESULTS.....	125
6.3.2 Fixed ratio combination of dihydroartemisinin and emetine .....	125
6.3.3 Analysis of the interaction between dihydroartemisinin and emetine using CalcuSyn .....	126
6.3.4 Validation of the CalcuSyn assay for malaria .....	128
6.3.4.1 Optimisation of drug dosing and treatment period.....	128
6.3.4.2 Non-constant ratio of combination of Atovaquone and Proguanil .....	133
6.3.4.3 Recovery of parasites treated with the atovaquone-proguanil combination ...	134
6.3.5 Combination of emetine and existing antimalarials using the CalcuSyn constant ratio method.....	135
6.4 DISCUSSION .....	139
6.4.1 Comparison of the fixed ratio and CalcuSyn methods for drug interaction analysis	139
6.4.2 Validation of the CalcuSyn method for malaria using the malarone combination...	142
6.4.3 CalcuSyn analysis of emetine with existing antimalarials .....	144
6.4.4 Conclusion and future directions .....	146
CHAPTER 7.....	148
GENERAL DISCUSSION .....	148
7.1 SYBR Green-based methods for antimalarial drug screening and development.....	148
7.1.1 SYBR Green-based methods for drug susceptibility.....	148
7.1.2 SYBR Green-based methods for drug interaction analysis.....	149
7.1.3 Conclusions and future directions for drug susceptibility assays .....	150
7. 2 Drug repositioning for malaria .....	152
7.2.1 Conclusions and future directions for antimalarial drug repositioning .....	153
7.3 Antimalarial activity of emetine dihydrochloride hydrate .....	153

7.3.1 Conclusions and future directions for the antimalarial development of emetine ...	155
APPENDIX .....	157
Appendix I: SYBR Green staining of <i>P. falciparum</i> for fluorescence confocal microscopy. ...	158
Appendix II: An example of Giemsa stained <i>P. falciparum</i> parasites (strain K1) following treatment with dihydroartemisinin (DHA).....	159
Appendix III: An example of the flow cytometer output obtained during the generation of dose response curves, for dihydroartemisinin against <i>P. falciparum</i> strain K1, using the SYBR Green-based Flow cytometer method .....	161
Appendix IV: Percentage inhibition table for each compound from the ENZO library against <i>P. falciparum</i> strain K1 at a concentration of 2.5 $\mu$ M .....	167
Appendix V: Tanimoto similary fingerprints for identified LOPAC and ENZO library hits with existing antimalarials.....	179
Appendix VI: Optimisation of the ondansetron dose response against <i>P. falciparum</i> , strain K1. ....	182
Appendix VII: Preliminary screen of cephaeline compared with emetine against strain K1, <i>P. falciparum</i> . ....	183
Appendix VIII Preliminary investigation of the comparison between the cellular toxicity of emetine and cephaeline against the HepG2 cell line.....	184
Appendix IX: Fluoresence microscopy of JC-1 stained malaria parasites. ....	186
Appendix X: Optimisation of the atovaquone proguanil combination against <i>P. falciparum</i> strain K1.....	187
Appendix XI: Recovery of <i>P. falciparum</i> strain K1 parasite after exposure to atovaquone or proguanil, either alone or at a non-constant ratio combination. ....	188
REFERENCES .....	194



## LIST OF FIGURES

---

Figure 1.1	<i>Plasmodium</i> life cycle
Figure 1.2	The global distribution of Malaria since pre-intervention (a) and current (2013) malaria distribution data (b)
Figure 1.3	Antimalarial drug timeline
Figure 1.4	Target-based and drug repositioning development timelines
Figure 3.1	The effect of parasite density dilution on fluorescence intensity of SYBR Green 1
Figures 3.2	Comparison of infected and uninfected blood samples using SG-FCM
Figure 3.3	Confocal microscopy of the malaria parasite
Figure 3.4	Dose response curves for dihydroartemisinin against the K1 strain
Figure 3.5	Comparison of parasite growth in a 96 well plate and 12.5 cm <sup>3</sup> flasks following exposure to a 3 point dose series of chloroquine and dihydroartemisinin
Figure 3.6	The effects of complete media on the SG-Microplate method
Figure 3.7	Short time-course analysis (48 h) for DHA treatment of K1 parasites
Figure 3.8	Extended time-course analysis of <i>Plasmodium falciparum</i> strain K1 exposure to DHA
Figure 3.9	The effects of dihydroartemisinin on schizont development
Figure 3.10	Dose response curves for dihydroartemisinin (a), chloroquine (b) atovaquone and proguanil
Figure 4.1	The structure of the 5 LOPAC compounds previously shown have antimalarial activity IC <sub>50</sub> <5 nM against <i>Plasmodium falciparum</i> strain 3D7
Figure 4.2	An exemplar panel of the ENZO library preliminary screen against <i>Plasmodium falciparum</i> , strain K1
Figure 4.3	SYBR Green-based Flow cytometric data for the treatment of <i>Plasmodium falciparum</i> (strain K1) malaria with dihydroartemisinin (DHA) and five LOPAC compounds
Figure 4.4	MeSH category distribution of the top 60 ENZO and LOPAC hits
Figure 4.5	An example of the structural clustering for the previously defined MeSH categories with a range of existing anti-malarials
Figure 4.6	Second-phase screen of selected ENZO library compounds
Figure 4.7	Second-phase screen of three selected LOPAC compounds
Figure 4.8	Accurate IC <sub>50</sub> determination of the four selected ENZO/LOPAC Library compounds
Figure 5.1	The structure of emetine dihydrochloride hydrate, cephaeline hydrochloride and dehydroemetine for comparison

Figure 5.2	Dose response of cephaeline against <i>Plasmodium falciparum</i> , strain K1
Figure 5.3	Dose response curves for emetine and cephaeline against HepG2 cells following 48 (a) and 120 (b) hours of exposure
Figure 5.4	Time-course analysis of dihydroartemisinin (DHA) in parallel with emetine (Eme) and the combination
Figure 5.5	<i>In vitro</i> stage progression of <i>Plasmodium falciparum</i> K1 parasites following exposure to dihydroartemisinin and emetine
Figure 5.6	Stage-specific cytostatic/cytocidal analysis of emetine
Figure 5.7	The recovery of parasite productive growth following emetine exposure, day 21 analysis
Figure 5.8	The recovery of parasite productive growth following emetine exposure, day 28 analysis
Figure 5.9	<i>Plasmodium falciparum</i> strain K1 viability time-course for treatment with emetine dihydrochloride hydrate after 21 and 28 days of recovery
Figure 5.10	Antimalarial killing profile data extracted from Sanz <i>et al.</i> (2012)
Figures 5.11	Flow cytometer analysis of JC-1 stained <i>Plasmodium falciparum</i>
Figure 5.12	The percentage of fluorescent events recorded for parallel JC-1 and SYBR green staining of <i>Plasmodium falciparum</i> using the BDFACsVerse flow cytometer
Figure 5.13	Parallel JC-1 and SYBR Green staining of <i>Plasmodium falciparum</i> following 7 hour exposure to a high dose series of chloroquine
Figure 5.14	Parallel JC-1 and SYBR Green staining of parasites exposed to IC <sub>50</sub> doses of atovaquone and emetine for 24 hours
Figure 6.1	The derivation of the Median-Effect Principle and its extensions to Multiple Drug Effect Equation
Figures 6.2	Fixed ratio dose response curves for the dihydroartemisin-emetine combination
Figure 6.3	Isobolograms showing the FIC <sub>50</sub> and FIC <sub>90</sub> interactions between dihydroartemisinin and emetine
Figure 6.4	Dose effect analysis of the dihydroartemisinin-emetine interaction, using the CalcuSyn software program
Figure 6.5	Basic graphical representation of the interaction between dihydroartemisinin and emetine
Figure 6.6	Atovaquone-proguanil combination against <i>Plasmodium falciparum</i> malaria, strain K1
Figure 6.7	Atovaquone-proguanil combination using a higher doses-series of atovaquone
Figure 6.8	The effect of drug addition method on combinatory outcome of the atovaquone-proguanil combination

- Figure 6.9      The effect of incubation time on combinatory outcome of the atovaquone-proguanil combination
- Figure 6.10     Dose response curves for atovaquone (ATQ), proguanil (PG) and the constant ratio combination of the two drugs
- Figure 6.11     CalcuSyn analysis of the atovaquone-proguanil combination
- Figure 6.12     The non-constant ratio combination of atovaquone and proguanil after 72 hours
- Figure 6.13     Constant ratio data for the atovaquone proguanil combination after 72 hours
- Figure 6.14     Constant ratio data for the atovaquone proguanil combination after 20 days
- Figure 6.15     The constant ratio combination of dihydroartemisin and emetine
- Figure 6.16     The constant ratio combination of chloroquine and emetine
- Figure 6.17     The constant ratio (1:46) combination of atovaquone and emetine

## LIST OF TABLES

---

Table 1.1	Artemisinin and non artemisinin containing drug combinations for malaria treatment.
Table 1.2	The existing and novel drug targets in <i>Plasmodium falciparum</i>
Table 3.1	A range of fluorescent dyes used to study malaria by flow cytometry
Table 3.2	Drug concentration ranges selected to obtain dose response curves for atovaquone, chloroquine, dihydroartemisinin and proguanil against <i>Plasmodium falciparum</i> strain K1
Table 3.3	<i>In vitro</i> IC <sub>50</sub> (nM) sensitivity of the K1 strain to dihydroartemisinin at 48 and 72 h
Table 3.4	Comparison of the IC <sub>50</sub> values determined in the current study for existing antimalarials with values reported elsewhere in the literature
Table 4.1	The 56 most potent compounds identified from the ENZO Library preliminary screen
Table 4.2	Preliminary IC <sub>50</sub> estimates based on the second phase SG-MicroPlate screen of 9 compound selected from the ENZO library
Table 5.1	A Summary of the <i>in vitro</i> anti-malarial efficacy and selectivity of emetine and its analogues
Table 5.2	Parameters for Lipinski's rule of 5 are shown for emetine, cephaeline and dehydroemetine
Table 5.3	Dilution procedure with fresh erythrocytes (varying haematocrits) at days 7, 14 and 20
Table 5.4	IC <sub>50</sub> values for the positive control, cisplatin, and the two test compounds emetine and cephaeline against the HepG2 cell line
Table 5.4	The Parasite Reduction Ratio (PRR), Parasite Clearance time (PCT) and Lag phase for the treatment of <i>Plasmodium falciparum</i> , strain K1 parasites with emetine dihydrochloride hydrate
Table 6.1	Various drug interaction models that have been developed and used since (1870)
Table 6.2	The first dose plate set up for analysis of the atovaquone (ATQ) Proguanil (PG) interaction using the constant ratio design for CalcuSyn
Table 6.3	The second dose plate set up for analysis of the atovaquone (ATQ) proguanil (PG) interaction using the constant ratio design for CalcuSyn
Table 6.4	Fourth dose plate set up for analysis of the atovaquone (ATQ) proguanil (PG) interaction using the constant ratio design for CalcuSyn
Table 6.5	Drug doses used for the existing and antimalarial combinations with emetine using the CalcuSyn analysis method
Table 6.6	The interaction between dihydroartemisinin and emetine against <i>Plasmodium falciparum</i> (strain K1) at 6 different fixed ratios

Table 6.7	Recommended symbols and descriptions for defining synergism or antagonism using the combination index method
Table 6.8	The combinatory index values (CI) for the ATQ + PG constant ratio combination (1:15987) at the ED <sub>50</sub> , ED <sub>75</sub> and ED <sub>90</sub> levels of inhibition
Table 6.9	The combinatory index values (CI) for the dihydroartemisin-emetine combination at a constant ratio of 1:10
Table 6.10	The dose effect parameters for the chloroquine-emetine combination
Table 6.11	The combinatory index (CI) values for the atovaquone emetine combination at the ED <sub>50</sub> , ED <sub>75</sub> and ED <sub>90</sub> levels of inhibition

## ACKNOWLEDGEMENTS

---

The work presented in this document would not have been possible without the help of a number of fantastic people. Firstly, I would like to express my special appreciation and thanks to my supervisor, Dr. Niroshini Nirmalan for the tremendous support, guidance and endless encouragement you have given me throughout the PhD. Your dedication to your work is truly an inspiration and the advice and lessons I have learnt from you will serve me well in my future endeavours. You have made my time at Salford incredibly enjoyable and I simply could not have wished for a better supervisor.

Next, I would like to thank our research collaborators Dr. Martin Read (University of Manchester) and Dr. Farid Khan (Protein Technologies Ltd.) for their helpful guidance and provision of the drug libraries, without which none of this work would have been possible. I would like to thank all other members of the malaria research group at the University of Salford. In particular, Maryam Idris-Usman for sharing my PhD experience with me and all of the masters and undergraduate students that I have had the pleasure of supervising. I would also like to express immeasurable gratitude to technical staff at Salford who were always more than willing to help with any lab related issues and have lent me various pieces of equipment over the years. Particularly, Jon Deakin for advice with CalcuSyn and Manisha Patel for help with the ‘temperamental’ Flow Cytometer. I must also thank my undergraduate supervisor, Professor Hilary Hurd (Keele University), who was the original inspiration for my pursuit of a career in malaria research.

I would especially like to thank my parents Jean and Darryl Matthews and my boyfriend, Stephen Colclough for their continuous encouragement during the last 3.5 years. Without their support, both emotional and financial, successful conclusion of the work would not have been possible. I would also like to mention Archie and Ted (the dogs) for being unmovable, faithful writing companions.

Finally, I would like to acknowledge the PhD Scholarship from the University of Salford, and numerous awards for national and international conference attendance from the Salford Postgraduate Research Fund. Through these opportunities I have attended various conferences which has encouraged my personal development as a scientific researcher.

## ABBREVIATIONS

---

ACT	Artemisinin combination therapy
ATQ	Atovaquone
CQ	Chloroquine
DHA	Dihydroartemisinin
FDA	Food and drug administration (USA)
EC <sub>50</sub>	half maximal effective concentration
ED <sub>50</sub>	half maximal effective dose
EMA	European Medicines Agency
Eme	Emetine dihydrochloride hydrate
GNF	Genomics institute of the Novartis research foundation
IC <sub>50</sub>	half maximal inhibitory concentration
PG	Proguanil
PRR	Parasite reduction ratio
PCT	Parasite clearance time
WHO	World health organisation
WRA	Walter Read Army Institute of Research

## ABSTRACT

---

Of the plethora of parasitic diseases that afflict mankind, malaria remains the most significant with 100-300 million cases reported annually and 600,000 fatalities. Treatment and control measures have been hampered by the emergence of drug resistance to most antimalarial therapies. Early signs of drug resistance to the current frontline option, the artemisinins, make it imperative that novel drug candidates are discovered. One possible short-term solution is drug repositioning, *via* screening existing FDA-approved (Food and Drug Administration agency) drug libraries for antimalarial activity. Towards this goal, two, fast, simple, and reliable *in vitro* SYBR Green-based drug susceptibility assays were optimised. The first, the SYBR Green microplate method offered a medium throughput option that was used to screen two FDA-approved libraries (Z score =  $0.68 \pm 0.06$ ), LOPAC and ENZO (~700 compounds). Approximately 60 hits, defined as > 50 % inhibition at 2.5  $\mu$ M, were identified by the preliminary screen. The SYBR Green flow cytometer method, capable of providing direct parasitaemia estimates and stage-specific information, was used for second-phase characterisation of the hits. From these, anti-amoebic compound emetine dihydrochloride hydrate was identified as a potent inhibitor of the multidrug resistant *Plasmodium falciparum*, strain K1, with an  $IC_{50}$  of 47 nM (95 % confidence interval 44.92-49.17). Further characterisation of the compound involved analysis of the parasite killing profile, to determine the parasite reduction ratio (PRR) and parasite clearance time (PCT) as well drug interaction analysis with existing antimalarials. Emetine was shown to have a similar killing profile to atovaquone inferring a similar mitochondrial mode of action, corroborated by fluorescence staining with the JC-1 mitochondrial probe. Taken together, emetine's pharmacokinetic matching and synergy with atovaquone provide an exciting drug combination for further investigation. The relatively high hit rate presented in the study, and *in vitro* workflow outlined for emetine, also showed drug repositioning to be a promising option for antimalarial drug discovery.



# CHAPTER 1

---

## INTRODUCTION

### *1.1 Malaria: a historical perspective*

Despite decades of effort to eradicate or at least control malaria, it remains one of the most widespread and devastating diseases to afflict mankind. Its history extends to antiquity (Balint, 2001; Cox, 2002; Krungkrai *et al.*, 2010). Indeed, it has been said our primate ancestors were recognisably malarious before they were recognisably human (Harrison, 1978). Earliest evidence of the disease comes from Chinese scripts dating back to 2700 BC. Other ancient references appear on Mesopotamia clay tablets (2000 BC) and Egyptian papyri (1570 BC) (Cox, 2010). Since then, the hallmark characteristics of malaria, namely: paroxysmal intermittent fevers, enlarged spleens and a tendency of epidemic occurrence, have been reported in every civilised society. Extending from the Hippocrates in ancient Greece (400 BC), to the Romans throughout their empire, and in the writings of Assyrian, Indian, Arabic, and European physicians (Carter and Mendis 2002; Cox, 2002). In addition to ancient symptomatic descriptions, recent empirical evidence has shown the existence of *Plasmodium falciparum* malaria in Egyptian mummies from the Fayum depression in 800 BC (Lalremruata *et al.*, 2013) and in amber preserved mosquitos (in the Dominican Republic) from the mid-Tertiary period 25-400 million years ago (Poinar, 2005). Extending through Darwinian descent, malaria has therefore had a huge impact on human exploration, colonisation and development of the world as we know it today (Harrison, 1978). Even referred to as the ‘scientific control of nature’, many historical figures including, Alexander the great, Emperor Titus Ceaser, Oliver Cromwell, Otto II and Pope Gregory V are thought to have succumbed to the disease (Carter and Mendis 2002, Harrison, 1978). More recently malaria, along with other diseases has had a huge impact on the world wars, where it is said that for every man lost in battle, another was lost to malaria. Commonly, the conditions of war encouraged the spread and resurgence of the disease (Cox, 2002; Harrison, 1978).

The name malaria originated from the association of the disease with marshy areas and the misguided belief that it was caused by miasmas, ‘bad air’ in Italian ‘Mal’aria’, rising from the swamps. Scientific understanding of malaria and its association with the mosquito vector did not begin until the end of the 19<sup>th</sup> century. The complex life cycle of the parasite involving an insect vector (females of *Anopheline* species) and an intermediate

vertebrate host, took almost 70 years to elucidate (Cox, 2010; Harrison, 1978). Four species of malaria infect man: *P. falciparum*, *P. vivax*, *P. malariae*, and *P. ovale* (Biamonte *et al.*, 2013; Greenwood *et al.*, 2008), the latter of which has now been divided into two sub-species *P. ovale curtisi* and *P. ovale wallikeri* (Sutherland *et al.*, 2010). More recently, it has been shown the *P. knowlesi*, which is known to cause malaria in long-tail macaques is also found consistently in man (Vythilingam *et al.*, 2008).

### 1.2 Life Cycle

Following the bite of an infected anopheline mosquito, sporozoites are inoculated into the subcutaneous tissue of the invertebrate host. This motile form rapidly migrates to the blood stream where it circulates (~30mins) until it reaches and invades the hepatocytes. Within the hepatocytes, pre-erythrocytic schizogony occurs whereby the parasites undergo asexual multiplication. Subsequently, 5-10 days after the initial infection thousands of merozoites are released into the blood circulation where they invade erythrocytes. In *P. vivax* and *P. ovale* infections, some sporozoites differentiate into hypnozoites and remain dormant in the hepatocyte cells for months until they are re-activated, causing a relapse of the malaria infection. Once inside the erythrocytes, the parasite undergoes a further amplification step where it transforms from a ring, to a trophozoite and finally, as a result of DNA replication and schizogony, a multinucleated schizont. Upon schizont rupture, commonly 8-32 merozoites are released from each red blood cell and are capable of invading yet more red blood cells (although odd numbers of daughter merozoites can also be produced). Repeated erythrocytic cycles, which occur every 48 hours in all human malaria species apart from *P. malariae* (72 hour cycle) and *P. knowlesi* (24 hour cycle), are responsible for the non-specific clinical symptoms of the disease (tertian and quartan fevers). A small percentage (~1%) of merozoites transform into gametocytes (sexual form) and await ingestion by a mosquito during a subsequent blood meal. The asymptomatic gametocytes can persist for weeks and are responsible for malaria transmission (Biamonte *et al.*, 2013; Delves *et al.*, 2012; Flannery *et al.*, 2013; Jensen and Mehlhorn, 2009; Rosenthal, 2008).

In the mosquito, the sexual phase of the parasite life cycle is initiated by the fertilization of the male and female gametes to create a zygote. This brief diploid stage allows sexual recombination, and is a key source of genetic variation (Gregson and Plowe, 2005). The zygote develops into a motile ookinete that migrates and through the gut wall and forms an oocyst. Further replication in the oocyst results in the release of thousands of sporozoites that migrate to the mosquito salivary gland. The mosquito stage is completed in

approximately 2 weeks (Delves *et al.*, 2012; Jensen and Mehlhorn, 2009; Rosenthal, 2008). The next blood meal along with the complimentary inoculation sporozites completes the parasite life cycle (Figure 1.1).

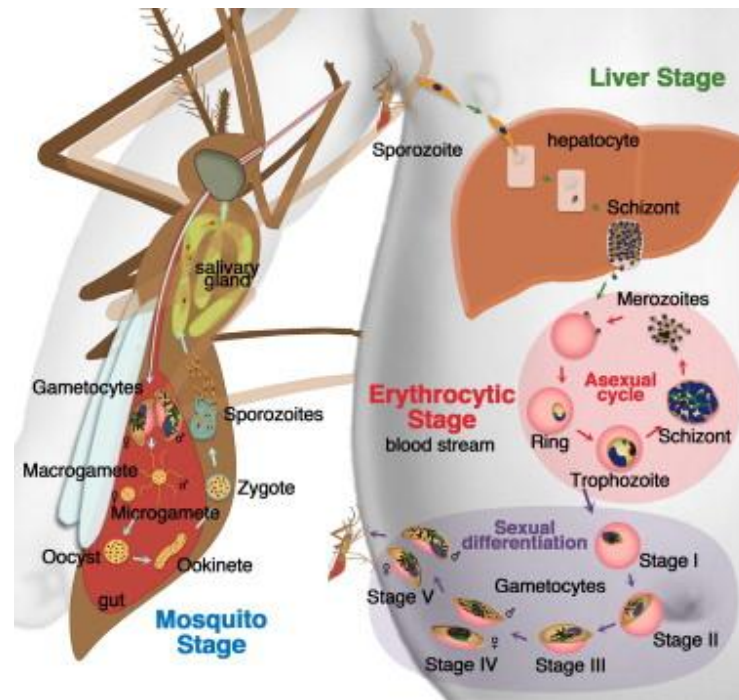


**Figure 1.1 *Plasmodium* life cycle** showing the parasite development at the Liver, Erythrocyte and mosquitoes stages. (Source: Biamonte *et al.*, 2013)

### 1.3 Disease symptoms

Of the four human malarias, *P. falciparum* is the most lethal and responsible for over 90% of malaria-related deaths (Hyde, 2007). This is the only species capable of causing severe disease, which is characterised by the parasites ability to sequester in various organs including the brain (Greenwood *et al.*, 2008). This occurs during an overwhelming erythrocytic stage infection and can lead to cerebral malaria (coma), vital organ dysfunction, acidosis, respiratory distress, and severe anemia. In children, hypoglycaemia, seizures and severe anemia are common manifestations (Krungskrai *et al.*, 2010).

### 1.4 Discovery of the malaria parasite and its complex life cycle

Although the outline of the life cycle can be regurgitated almost effortlessly by a modern malariologist, the extensive body of work defining the complex relationships between man, mosquito and parasite should not be overlooked. Indeed the discovery of the parasite and the mode of malaria transmission remain some of the most important and interesting findings in the history of parasitology (Cox, 2002). The story began in 1880 when French army surgeon, Charles Louis Alphonse Laveran identified and detailed a protozoan

parasite in the blood of a human malaria sufferer (Harrison, 1978). The initial unanimous resistance to the finding is not surprising considering that this was the first report of a parasite inhabiting a human erythrocyte. Furthermore, the ‘miasma theory’ that had reigned for almost 2500 years was not completely out of favour (Cox, 2010). It was only a recent idea, with the advent of the germ theory and the development of microbiology as a discipline by Louis Pasteur and Robert Koch in 1878-1879, that specific living micro-organisms could be causative agents of disease (Cox, 2010; Harrison, 1978). Investigations at the time were therefore intensified in the direction of finding the ‘bacteria’ responsible for malaria fever. Indeed, Edwin Klebs and Corrado Tommasi-Crudeli claimed as such, when they reported that a bacterium (*Bacillus malariae*), isolated from the Pontine marshland, was capable of causing febrile infections and enlarged spleens in rabbits (Cox, 2010; Smith and Sanford 1985). Undeterred, Laveran continued to ‘follow the pigment’ and described various stages of the erythrocytic cycle, documenting quinine induced parasite clearance and the association of corpuscle (schizont) rupture and fever. His eventual visualization of the exflagellation process became harder to ignore and in 1890 ‘Laveran’s germ’ was finally accepted by the majority of the community. He was later awarded the Nobel Prize for Medicine in 1907 (Harrison, 1978). Further definition of the erythrocytic stage cycle and species characteristics was catalysed by technical advances in staining procedures leading to the use of Giemsa staining (methylene blue eosin stain, Dimitri Leonidovitch Romanowsky 1891) and the development of the oil immersion microscope (Carl Zeiss 1882-4), (Cox, 2010).

Disease transmission, however, remained a mystery until Patrick Manson, after showing filarial worms were transmitted by mosquitos, suspected the same to be true for malaria. Postulated by the coincidently high prevalence of mosquitoes in the marshy associated with malaria, Manson recruited British army surgeon Ronald Ross to work on the project. Based in India, Ross’ initial observation of Laveran’s exflagellation proved only that the mosquito midgut environment did not kill the parasite as the same could be observed in infected blood on a microscope slide. However, on 20<sup>th</sup> August 1897 (mosquito day), Ross discovered an oocyst on the wall of the mosquito midgut, and in doing so provided the first empirical evidence that the parasite could undergo further development in the mosquito (Harrison, 1978). In the meantime Canadian William MacCullum, had described a sexual recombination event in a related avian parasite *Haemoproteus columbae*. He proposed that the formation of a vermicle (ookinete) through the fusing of two distinct

bodies, one flagellated and motile, the other sessile and egg-like was also likely to occur in malaria (Cox, 2010). Both Ross and Manson were more concerned with what happened post oocyst formation and expected to find, in the mosquito, a hardened free living form of the parasite ready to be discharged into the external environment (Harrison, 1978). Circumstance favoured Ross, and, forced to work on an avian (pigeon) model of malaria, in 1898 he discovered the presence malaria parasites (*Plasmodium relictum*) in the salivary gland of a culicine mosquito (Cox, 2010). He later showed that uninfected birds could be experimentally infected by malarious mosquitoes. Hot on his heels, the Italians, Giovanni Battista, Grassi, Amico Bignami and Giuseppe Bastianelli proved Ross' inclinations that the same cycle occurred in the human system and that mosquitos of the genus *Anopheles* were specifically responsible for human malaria transmission (Cox, 2002; Harrison, 1978). Fortunately, Ross' painstaking hard work and persistence did not go unnoticed and deservedly he claimed the Nobel Prize for the discovery of Malaria transmission in 1902 (Harrison, 1978). In fact, the life cycle of *Plasmodium* was incompletely understood for almost another 50 years, until Henry Shortt and Cyril Garnham (1947) showed that the 10 day lag phase following mosquito inoculation, was due to the hepatic stage prior to the erythrocytic cycle. Their collaboration with an American, Wojciech Krotoski, in 1982 solved the final conundrum, *P.vivax* was capable of producing dormant liver stages that could recrudesce several months or even years later (Cox, 2002; Cox, 2010; Harrison, 1978; Schlitzer, 2007).

### *1.5 History of malaria prevention and treatment*

#### *1.5.1 Mosquito Control*

In the early-mid 20th century efforts to control the disease were aimed at eliminating the *Anopheline* vector. Breeding sites situated close to residential areas were drained of swamplands and standing water sources. Puddles and pot holes were layered with oil to prevent egg laying and larval development. Overall, some improvements were made. A major breakthrough was the discovery of the insecticidal properties of dichlorodiphenyltrichloroethane (DDT) in 1939. The military were first to apply DDT for public health purposes in Southern Italy 1944, as opposed to its development as an agricultural pesticide. DDT then went on to play an important role during the latter years of the Second World War in preventing malaria (Sadasivaiah *et al.*, 2007).

### 1.5.2 Quinine and its synthetic derivatives

For many years quinine was the only chemotherapeutic agent available for directly targeting the malaria parasite during human infection. Quinine, the bark extract of the Peruvian *Cinchona* tree species, was first discovered in the 17<sup>th</sup> century by the Jesuit priests, who learned of its potential from indigenous practices. Word soon spread throughout Europe and other areas of the world regarding the medicinal properties of the ‘Jesuit bark’ for the treatment of agues. It wasn’t until 1820 that quinine was isolated from the bark along with other alkaloids such as quinidine, quinamine, cinchonine and cinchonidine. The quinine content of cinchona trees varied not only between species but also within the same plantation, leading to inconsistent reports of therapeutic efficacy. Numerous expeditions sought to obtain the seeds from the best plants to maximise yield. Charles ledger and his native servant Manuel Mamani discovered a species with particularly high quinine content (11-13%), *Cinchona ledgeriana*, and successfully exported seeds to Britain. For this betrayal and ultimately the loss of South America’s monopoly on quinine production Mamani was severely beaten and later died as a result of his injuries. The British, failing to realise the potential of this find, sold the seeds to the Dutch in 1865, leading to a Dutch monopoly (97%) on the production of quinine in the 1800s (Kitchen *et al.*, 2006).

The limited supply and resultant high cost of quinine during World War I prompted the search for cheaper, synthetic alternatives in the early 1900’s (Jensen and Mehlhorn, 2009). This led to the development of the quinoline classes: the 4-aminoquinolines the 8-aminoquinolines and the amino alcohols. Quinine itself was known to have toxic liabilities, such that sustained use could result in tinnitus, hypoglycaemia, abdominal pain, visual impairments, vertigo, hepatic injury, asthma, and psychosis (Achan *et al.*, 2011).

Investigations into tissue staining identified the first synthetic antimalarial, methylene blue (by Paul Ehrlich 1891). Further work led to the development of pamaquine (plasmochin 1926/27) and later primaquine, creating the 8-aminoquinoline class; of which, tefenoquine is a more recently identified member. However, toxicity associated with glucose 6-phosphate dehydrogenase deficiency, methaemoglobinaemia, and severe gastrointestinal disturbances precluded the use of the early derivatives (Peters, 1999). Renewed American interest in primaquine (during the Korean War), was a result of its particular effectiveness against liver-stage parasites and its potential to tackle relapsing *P. vivax* infections. In 1932

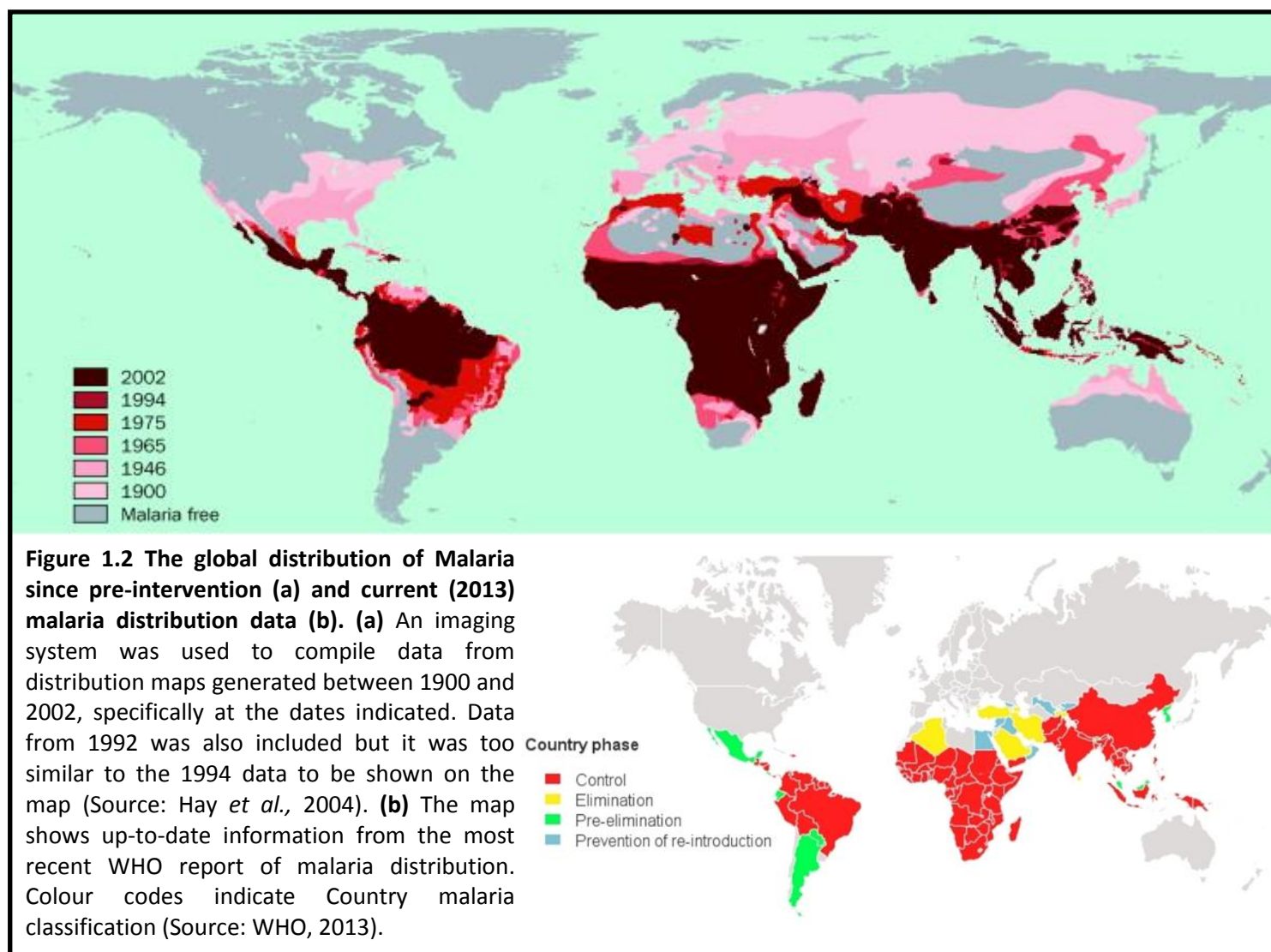
another dye, 9-amino acridine, atabrine, was also shown to be a potent antimalarial. Unfortunately, like methylene blue, atabrine discoloured skin and eyes and rumours that it caused impotence resulted in compliance issues (Kitchen *et al.*, 2006). The most significant breakthrough came when Andersag and co-workers modified atabrine by replacing its acridine ring with a quinoline ring creating the 4-aminoquinoline resochin (later to be renamed chloroquine) in 1934. However, concerns about its toxicity in humans meant that the drug didn't become available for malaria treatment until 1946 (Coatney, 1963; Krafts *et al.*, 2012; Schlitzer, 2007).

### *1.5.3 The Malaria Eradication Programme*

Due to its therapeutic success, both as a prophylactic and curative drug, chloroquine was soon included in the malaria eradication programme (1955) alongside DDT, to elicit a two-pronged attack against the parasite and mosquito (Dondorp *et al.*, 2010; Jensen and Mehlhorn, 2009). The unprecedented reduction in morbidity and mortality that ensued resulted in elimination of the disease from Europe in 1975, and its redefinition to tropical and subtropical regions (Figure 1.2). Unfortunately, the success of DDT and chloroquine was short-lived. The intensified efforts were not financially sustainable in underdeveloped countries. The disease remained, as it is today, inexorably linked to poverty and the prospect for eradication of African malaria was as unattainable as ever.

Environmental concerns arose about the use of DDT instigated by the publication of Rachel Carson's 'Silent Spring' in 1962, highlighting the harmful effects of bio-accumulation in both wildlife and human health. The use of DDT was further hampered by the onset of insecticide resistance. Consequently, although DDT was never banned, its usefulness was restricted. The situation was worsened by evidence of chloroquine resistance (Figure 1.3), initially at the Thailand-Cambodia border (1957), then independently in South America (1959) and finally in East Africa (1974) where it dispersed rapidly to the west of the continent. Duly, the eradication campaign was abandoned in 1972 (Greenwood *et al.*, 2008).

The next 50 years saw an incessant downfall of chloroquine, from the most widely used drug to the most ineffective (Dondorp *et al.*, 2010; Payne, 1987; Randrianarivelojosia *et al.*, 2009; Valecha *et al.*, 2009). This instigated investigations into the mechanism of action and causes of resistance to chloroquine.





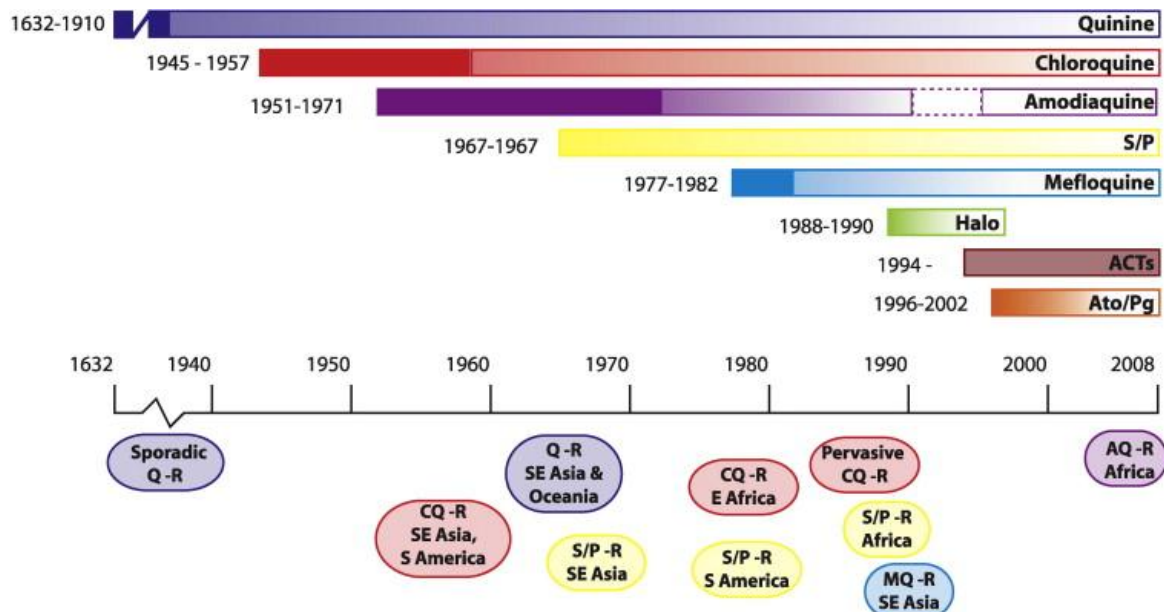


**Figure 1.3 Antimalarial drug timeline.** Numbers to the left of coloured bars indicate when the drug was first in use and the first sign of resistance appeared (also represented by the dark shaded regions of the bars). Coloured ovals dictate the geographical regions of resistance development. The dashed lined in the Amodiaquine bar indicates a break in it's used due to toxicity concerns. (Source: Eklund and Fiddock, 2008)

The drug was shown to kill the parasite indirectly by accumulating in the food vacuole, where it interfered with haeme sequestration. Haem is a toxic bi-product of haemoglobin digestion, a major source of amino acids for the parasites. It is usually detoxified *via* conversion, through bio-crystallization, to haemozoin (malaria pigment) (Djimde *et al.*, 2001; Hyde, 2007). In resistant *P. falciparum* parasites, alterations in a transporter protein, chloroquine resistance transporter (PfCRT), located on the membrane of the digestive vacuole ensures that the build-up of chloroquine within the vacuole is progressively diminished, together with the killing properties of the drug (Djimde *et al.*, 2001; Hyde, 2007). The resistance phenotype is attributable to multiple mutations on the *pfcr*t gene (encoding PfCRT) (White, 2004). A single mutation in the *pfcr*t gene, where threonine (T76) is substituted for lysine at position 76, has been shown to be responsible for resistance (Djimde *et al.*, 2001). The complexity of the trait arises from the finding that this mutation can only occur on the back of several other *pfcr*t mutations, which themselves do not cause resistance (Dondorp *et al.*, 2010; Plowe, 2009). Additional copy number polymorphisms in the *P. falciparum* multi-drug resistance gene, *pfmdr* 1, have also been associated with varying levels of chloroquine resistance. However, this also seems dependent on the presence of the *pfcr*t mutations (Djimde *et al.*, 2001).

The failure of DDT and chloroquine triggered a resurgence and fresh outbreaks of the disease. A period of despondency ensued, resulting in a unanimous acceptance that the

burden of malaria would remain indefinitely. Plans for eradication were abandoned and discussions turned to renewed efforts to treat and control the disease (Carter and Mendis, 2002).

#### *1.5.4 The impact of the antifolate drugs*

Fortunately, the rampant resurgence of the disease was stalled by the discovery of another class of antimalarial drugs, the antifolates. Originally developed for the treatment of tumours, the success of the antifolates meant that they were soon applied to other systems of rapidly dividing cells, such as bacteria and parasites. Proguanil was the first antifolate shown to be effective against *Plasmodium*, in 1945 during the Second World War (Nzila, 2006). Structurally similar to proguanil, pyrimethamine and cycloguanil were shown to target the dihydrofolate reductase (DHFR) enzyme in the folate pathway. This enzyme is present in both the parasite and the human host. Fortuitously, anti-DHFR drugs have a much higher affinity for the parasite enzyme than the human orthologue. The antifolate class was further expanded once it was discovered that sulfa drugs block *de novo* folate synthesis. The parasite can synthesise folate *de novo*, thus it transpired that sulfadugs were also effective at targeting the folate pathway in malaria (Nzila, 2006). Sulphonamide drugs and sulphones: namely, sulfadoxine, sulfalene, sulfone, and dapsone inhibit dihydropteroate synthetase (DHPS) activity in the folate pathway. Unique to the parasite, this enzyme is essential for biosynthesis of coenzymes in the folate metabolic pathway. Although proguanil and pyrimethamine have been used in monotherapy, the sulfadugs (apart from dapsone) had poor efficacy and unacceptable toxicity. Success came when the class I antifolates (DHPS inhibitors) and class II antifolates (DHFR inhibitors) were combined. Although not considered combination therapy, as both drugs act on the folate pathway, the combination was found to have synergistic activity and was more effective than either drug used alone (Gregson and Plowe, 2005). Together the class I and class II antifolates effectively block the folate pathway and the production of important reduced folate cofactors. The folate cofactors are essential for the synthesis and metabolism of certain amino acids, therefore, a consequence of antifolate treatment is the inhibition of DNA synthesis (Hyde, 2005; Hyde, 2007). During the erythrocytic cycle, the parasite undergoes a huge amplification step for which DNA synthesis is a pre-requisite. The parasite's high demand for nucleotides at this stage, and its preference for endogenous folate, make the folate pathway an excellent drug target and the basis for the success of the antifolates as antimalarials. The most extensively used combination is fansidar (SP), a

fixed-dose drug combination comprised of sulfadoxine and pyrimethamine approved by the FDA in 1983 (Gesase *et al.*, 2009; Kitchen, Vaughn and Skillman, 2006; Ridley, 2002). Fansidar was largely employed to target chloroquine-resistant parasite populations in the late 1980s and for some years it effectively replaced chloroquine as a first line treatment for *P. falciparum* malaria (Miller and Su, 2011). Unfortunately, resistance to fansidar, and consequently resistance to other antifolates ensued (Figure 1.3), and developed fairly rapidly in response to drug pressure (Koram *et al.*, 2005; Ratcliff *et al.*, 2007; White, 2004). Single mutations in either of the *dhps* and *dhfr* genes were enough to provide some degree of protection against the drug and led to localised reduction in drug susceptibility (Plowe, 2009). The current situation of widespread highly resistant parasite populations is a consequence of a stepwise acquisition of mutations, each bestowing a further reduction in susceptibility to the drug (Gregson and Plowe, 2005; White, 2004). Treatment failure is characterised by a double mutation on the *dhps* gene and a triple mutation on the *dhfr* gene. An additional fourth mutation has also emerged on the *dhfr* gene in Asia which denotes a high level of resistance to SP as well as the chlorproguanil-dapsone combination (Gesase *et al.*, 2009; Plowe, 2009). It is suspected that, although low level resistance can develop locally, high level resistance arose from only two ancestral origins; once in South America and once in South East Asia, the latter of which eventually disseminated to Africa (Figure 1.3). It is noteworthy that the pattern of sulfadoxine/ pyrimethamine resistance is akin to the spread of chloroquine resistance (Plowe, 2009).

#### 1.2.5 The amino alcohols and artemisinins

Malaria related impacts during the Vietnamese war (1954-1975) led to the intensification of efforts into antimalarial drug discovery by both the Americans and North Vietnamese (Milner and Su, 2001). The 15 year drug discovery programme (1963-1976), initiated at the Walter Reed Army Institute of Research (WRA), culminated in the discovery of two aryl amino alcohols, mefloquine and halofantrine, as novel antimalarials. The compounds were shown to be effective against chloroquine-resistant strains and were advanced quite rapidly for public use. Mefloquine and halofantrine were granted FDA approval by 1989 and 1992 respectively (Croft, 2007). Unfortunately, their lifetime was limited as resistance developed rapidly (Figure 1.3), particularly, when the drugs were used alone (Ridley, 2002). This was not entirely surprising considering their relatedness to the quinolines. Additional limitations associated with both mefloquine and halofantrine included

toleration issues, with increasing reports of neuropsychiatric disturbances and cardiotoxicity (Croft, 2007; Na-Bangchang and Karbwang, 2009; Ridley, 2002). The high cost of the compounds also prohibited their widespread use in sub-Saharan Africa (Ridley, 2002).

The North Vietnamese took a different direction and sought help from their wealthy Chinese neighbours, who set up an intensive top-secret project, Project 523. The aim of the project was to trawl ancient scriptures of traditional Chinese medicine with the hope of finding an efficacious herbal remedy for the disease. After testing more than 2000 plant compounds, *Artemisia annua* (qinghao) was found (Dondorp *et al.*, 2010; Miller and Su, 2011). Following improved extraction procedures and elucidation of its sesquiterpene lactone structure, more potent, water-soluble (artesunate and artelinate) and oil soluble (artemether and arteether) derivatives were synthesised (Meshnick *et al.*, 1996; Ridley, 2002). Widespread drug resistance to the existing antimalarials and the ensuing resurgence in malaria mortality led to the artemisinin derivatives being fast-tracked for medicinal use. Fortunately, the neurotoxicity problems seen in animal studies did not manifest clinically, and to this day the drugs remain safe, well tolerated, and highly effective in most areas of the world (Meshnick *et al.*, 1996; Rosenthal, 2008). Employed since the 1990s the artemisinins have saved countless lives and fought back in what was otherwise a losing battle (Figure 1.3). With no new alternatives available to replace the artemisinins, in the way SP replaced chloroquine, initial reports of early signs of artemisinin resistance appearing at the Thailand-Cambodia border set alarm bells ringing. There was once a perception that the artemisinins were less prone to resistance development due to their short-half life, rapid parasite clearance times and the resultant short selective window for resistance development. However, at this historical epicentre for the emergence of multidrug resistance, ideal conditions of uniquely high drug pressure, propagated by the use of sub-lethal doses, poor compliance with treatment regimes and low malaria transmission have allowed resistant populations of chloroquine (1957), sulfadoxine/pyrimethamine (1982) and more recently mefloquine (1990s) parasites to originate and establish (Alker *et al.*, 2007; Dondorp *et al.*, 2009; Krungkrai *et al.*, 2010; Plowe, 2008). After over 30 years of artemisinin monotherapy evidence of resistance came from slower parasite clearance, persistence for more than 7 days alongside adequate drug concentrations and re-emergence of parasites after 28 days of treatment (Krungkrai *et al.*, 2010; Noedl, 2008; WHO, 2010). A specific region of the kelch gene (K13) is now also

used as a genetic marker to identify artemisinin-resistant parasites (Tun *et al.*, 2015). The growing number of cases reported in the field was accompanied by the ability to generate resistance in laboratory strains *in vitro* (Krungskrai *et al.*, 2010). As a consequence, efforts to contain the spread of artemisinin resistance were intensified. Strategies involved the detection of all artemisinin resistant cases, the adoption artemisinin-based combination therapy regimes, the reduction of drug pressure in affected areas and the education of communities about the risk of using counterfeit drugs (Ioset and Kaur, 2009). Increased use of personal protective equipment (impregnated bednets) and mosquito control was also widely advocated (WHO, 2010). Since the early reports in 2005/2006, other, less severe cases (the proportion of patient's still parasitaemic on day 3 of treatment) at the Myanmar-Thailand, China–Myanmar borders and in one province of Vietnam have also been reported (Dondorp *et al.*, 2009; Ioset and Kaur, 2009). More worryingly however, a recent survey using the K13 marker has identified artemisinin resistant *P. falciparum* parasites in Myanmar, just 25 km from the Indian border (Tun *et al.*, 2015). Referred to as the gateway to the global spread of drug resistance, these recent reports at the Indian border provide further evidence that trajectory of artemisinin resistance is following that of the previous antimalarials. As the artemisinins are currently the main component of antimalarial treatment programmes throughout the world, prevention of the imminent spread of resistance to high transmission areas is, evidently, vital (Bhattarai *et al.*, 2007; Miller and Su, 2011; Obonyo and Juma, 2012; WHO, 2010).

### 1.6 Malaria today

The Malaria World report estimated that in 2012 there were 207 million cases (uncertainty range: 135–287 million) and 627,000 deaths (uncertainty range: 473,000–789,000). Most cases (80%) and deaths (90%) occurred in Africa and the tragedy is multiplied by the fact that a majority of these preventable deaths occur in children (77%) under the age of 5 (Wells, 2011; WHO, 2013). Areas that achieved eradication in the 1970s and 1980s maintain this status, but the disease persists in the poorest areas of the world that span the equator (See Figure 1.2 a and b) where the situation fluctuates between worse and better (Cox, 2002).

#### 1.6.1 The status of vaccine development

The tools that we have available today, chemotherapy and insecticides, are the same as those deployed over 60 years ago during the eradication era. Resistance to both is an

ongoing challenge (Na-Bangchang and Karbwang, 2009; White, 2004). Despite the fact that it has been over 40 years since sterile immunity was generated in humans, in response to A bite from infectious irradiated mosquitoes, there is still no effective vaccine available (Heppner, 2013). The manufacture and administration of an attenuated whole parasite vaccine has proved too challenging. Subunit vaccines have failed to achieve comparable efficacy. The most promising candidate to date is the pre-erythrocytic stage vaccine candidate RTS/S/AS01. This vaccine targets the sporozoite stage and is based on a region of the circumsporozoite protein, fused to the surface antigen of the hepatitis B virus and combined with a potent adjuvant. RTS/S/AS01 has now entered clinical trials with predicted licensure in 2015 (Guerin *et al.*, 2002, Seidlein and Bejon 2013). Despite reports of only 50% efficacy, the malaria community is hopeful that the candidate could help save countless lives. Other subunit vaccines target blood-stage merozoites, or gametocytes for transmission blocking purposes (Seidlein and Bejon 2013). Unfortunately there has been poor immunogenicity in the blood-stage candidates, possibly owing to the fact that the vaccine would have to induce a stronger immune reaction than the merozoite itself during a normal course of infection (Hill, 2011). The main disadvantage of the ‘altruistic’ transmission blocking vaccines are that prevention at the community level manifests in no immediate or direct benefit for the sufferer (Guerin *et al.*, 2002). It is unlikely that any candidate targeting a single antigen will provide complete protection, and a multistage, multicomponent vaccine would be the most feasible option for success (Guerin *et al.*, 2002; Heppner, 2013; Seidlein and Bejon 2013). The added complexity of such a candidate obviously poses more challenges and is unlikely to materialise in the near future (Hill, 2011).

### *1.6.2 Current mosquito control measures*

In terms of mosquito control, indoor residual spraying (IRS) remains an important component of control programmes. The most commonly used insecticide class for IRS is the pyrethroids. There are a few other options available, but they are more expensive. The use of insecticide treated bednets (ITN) and the more recently developed long-lasting insecticide treated bednets (LLITN), with a 3 year lifespan, have had a marked impact on malaria prevention in recent years. A combination of these vector control interventions is recommended. One problem is that all available mosquito nets are treated with pyrethroids. Unfortunately, there is already resistance to pyrethroids in the in the field, therefore, careful monitoring and insecticide rotation for IRS are imperative to curtail

widespread resistance development until other effective insecticide classes are developed (WHO, 2013).

### 1.6.3 Current chemotherapy recommendations

The history of malaria drug discovery has demonstrated that the parasite has been effortlessly capable of developing resistance against all purified single compound antimalarials used to date (Figure 1.3). For this reason, there has been a definitive abandonment of monotherapy. The idea is, that alongside the synergistic or additive activity conferred by a combination, there will be mutual protection against resistance bestowed to each of the partner drugs. The current recommendation by the World Health Organisation for uncomplicated malaria is artemisinin-based combination therapy (ACT) (Grandesso *et al.*, 2006; Valecha *et al.*, 2009). One such combination is lumefantrine-artemether (For other examples see Table 1.1). The combination has been shown to be synergistic (Schlitzer, 2007). Lumefantrine is a more recent member of the amino-alcohol class. It is structurally similar to halofantrine, less potent, but comparatively well tolerated due to the absence of cardiac side effects (Katrak *et al.*, 2009; Schlitzer, 2007). Other non-artemisinin-based combinations are also available (Table 1.1) and deployed regionally where necessary (Yeka *et al.*, 2005). For the treatment of severe malaria quinine or one of the artemisinin derivatives, artemether or artesunate, are recommended (WHO, 2013). For the high risk groups: namely, pregnant women and children < 5 yrs, intermittent preventive treatment (IPTp and IPTi for pregnancy and infants, respectively) with the sulfadoxine-pyremethamine (SP) combination is recommended. The treatment is given at the same time as the diphtheria-tetanus-pertussis vaccination. Surprisingly, SP remains effective as a prophylactic, despite a high level of resistance in the field (Craft, 2008). Seasonal malaria chemoprevention (SMC) with amodiaquine, plus SP is recommended for children aged 3-59 months (Andrews *et al.*, 2014; WHO, 2013). Amodiaquine is a 4-aminoquinoline that is closely related to chloroquine but it is effective against chloroquine resistant strains, apart from those that display very high levels of resistance. However, toxicity is a restrictive factor of the drug with reports of agranulocytosis, myelotoxicity, hepatotoxicity and immune toxicity. Its use is therefore reliant on whether the benefits outweigh the cost (Na-Bangchang and Karbwang, 2009; Obua *et al.*, 2006; Ridley, 2002). Malarone, the atovaquone-proguanil combination is primarily used as a prophylactic for travellers from developed countries, due to its high cost. This restriction on use is thought to be the reason for a lack of widespread resistance development to the combination.

Although atovaquone is distinct from the existing antimalarial classes, resistance can develop readily to the compound when used in monotherapy (Ridley, 2002). For *P. vivax* chloroquine is still effective in most areas (Andrews, 2014; WHO, 2013).

Artemisinin-based combinations	Safety	PK match	Evidence of field resistance
Artemether-lumefantrine	+/-	-	some/no
Artesunate + mefloquine	+	-	some/some
Artesunate + SP	+/-	-	some/yes
Artesunate + amodiaquine	+/-	-	some/yes
Artesunate + pyronaridine	+/-	-	some/no
Dihydroartemisinin + piperaquine	+/-	-	some/no
Artesunate + Chlorproguanil-dapsone	+/-	-	some/unknown/unknown
<b>Non-Artemisinin combinations</b>			
Sulfadoxine-Pyrimethamine (SP)	+/-	+/-	yes/yes
Chloroquine + SP	+/-	-	yes/yes
Amodiaquine + SP	+/-	-	yes/yes
Quinine + SP	+/-	-	some/yes
Mefloquine + SP	+/-	-	some/ yes
Quinine + tetracycline	-	+/+	some/no
Quinine + Clindamycin	+	+	some/no
Atovaquone-proguanil	+	+/-	some/some
Chlorproguanil-dapsone	-	++	unknown/unknown

**Table 1.1 Artemisinin and non-artemisinin containing drug combinations for malaria treatment.** Abbreviations are as follows -= poor, +/- unclear, += acceptable, ++= desirable. Drugs with – in the title are approved whilst drugs with + are not. Red text indicates self-determined assessment based on citations read. (After: Kremsner and Krishna, 2004; Na-Bangchang and Karbwang, 2009).

Antibiotics such as doxycycline and clindamycin (Table 1.1) have also been used in combination therapy in recent years (Andrews *et al.*, 2014). Antibiotic activity against the malaria parasite was initially unexpected due the specificity of antibiotics against prokaryotic structures. However, the eukaryotic malaria parasite possesses two organelles that have their own DNA and bacteria-like machinery; namely, the mitochondria and the apicoplast, on which the drugs are most likely to act. Most usually causing a delayed death phenotype, where antimalarial activity is not detected until the second erythrocytic cycle following drug exposure (Schlitzer, 2007). Although the use of antibiotics has increased the number of combinatory options and diversified the available chemotypes, most current treatments rely on either an artemisinin derivative or compounds related to existing, failing chemotherapies.

Furthermore, recent concerns about the pharmacokinetic mismatch of current combinations have been expressed, particularly for high transmission settings (Kremsner and Krishna, 2004; Nandakumar *et al.*, 2006; Ramharther *et al.*, 2003). Disagreements as to



whether the killing profile of each drug in the combination should be similar or dissimilar, in order to exert the greatest effect, have arisen. It was previously thought that fast-acting compounds should be combined with slow-acting compounds to limit the chances of recrudescence infections. However, while a fast-acting rapidly excreted compound, such as an artemisinin derivative, is protected by its partner drug, the longer plasma half-life partner is left exposed. Sub-lethal concentrations of the partner compound towards the end of the treatment regime may therefore increase the risk of selecting drug resistant mutants (Na-Bangchang and Karbwang, 2009; Dondorp *et al.*, 2010; Koram *et al.*, 2005; Walsh *et al.*, 2007).

While eradication should ultimately be a long term goal, the foreseeable future should focus on protecting existing treatments against impending failure (Greenwood *et al.*, 2008). The longevity of second-generation compounds is questionable, and a formidable concern, due to widespread resistance against the parent molecules (Na-Bangchang and Karbwang, 2009). The desperate need for novel antimalarial drug classes can therefore not be overemphasised. Unfortunately, antimalarial drug discovery has always been and remains, to this day, a challenging endeavour.

### *1.7 Drug discovery*

Active drug discovery in general is not much older than a century, and the history of antimalarial drug discovery cannot be detached from contextual developments of medicinal science. Traditionally, disease treatments relied on the serendipitous discovery of natural product remedies, such as digitalis (foxglove) for the treatment of congestive heart failure, ipecacuanha (cephaelis plant bark or root) for the treatment of dysentery, aspirin (willow tree bark) for the treatment of fever and quinine (cinchona bark) for the treatment of malaria (Ng, 2009). The earlier use of dried and ground preparations, was followed by the isolation and purification of active components during the early 19<sup>th</sup> century. Indeed, quinine was extracted in 1820. In an attempt to synthesise quinine in 1856, William Henry Perkin created 'mauve' the first synthetic textile dye. From then onwards synthetic dyes had a profound impact on drug discovery (Schlitzer, 2007). With the advent of the germ theory (1870) and numerous observations that fungal contamination had an antagonistic effect on bacteria, a haphazard observation that eventually led to the discovery of penicillin by Alexander Fleming (1928), there was already an idea that such interactions could be exploited pharmacologically (Rubin, 2007). A major breakthrough, coined as the beginning of a revolution in drug discovery, was when Paul Ehrlich (1890)

stained the malaria parasite with methylene blue. Inadvertently this demonstrated the selectivity of chemical dyes for biological tissues, prompting the development of the drug receptor concept. Thereafter, medicinal chemistry was born out of the realization of a connection between drug structure and biological activity (Drews *et al.*, 2000).

There was no greater impact on human health than antimicrobial therapy. History dictates that even penicillin was an indirect consequence of investigations into the antibacterial properties of synthetic dyes. Gerhard Domagk (1927) tested numerous dyes against a novel *in vivo* mouse model of *Streptococcus pyogenes* infection. Prontosil, a sulfonamide derivative (sulphonamide active component discovered as a dye in 1909) synthesised by Fritz Mietzsch and Josef Klarer, was shown to be the most efficacious (1935). Most importantly, Domagk had induced a change of opinion: that the administration of a substance systemically could cure a bacterial infection (Rubin, 2007). Interestingly, during its interval of popularity (1937) prontosil was also tested against *P. falciparum* with 100 % cure rates (Gregson and Plowe, 2005). At the time, the use of the sulfa drugs was limited by their ineffectiveness against tuberculosis and pneumonia and the potential for resistance development. It wasn't until the 1950/1960s that interest in the compounds was re-ignited for an antimalarial indication. The eventual systemic challenge of bacterial infections with purified penicillin (Chain and Florey, 1938) led to the phenomenal success of a broad spectrum, specific, potent antibiotic with low toxicity that is still in use today (Rubin, 2007).

#### 1.7.1 The golden era of drug discovery

Other breakthroughs followed, and the mid part of the 20<sup>th</sup> century (1928-1962) was considered the golden era of drug discovery. Medicinal chemistry advanced and treatments became available for numerous indications including, malaria, tuberculosis, hypotension, diabetes, psychosis, analgesia, and septicemia (Burger, 1983). The drug discovery pipeline involved *in vivo* animal models to demonstrate biological activity, followed by the purification and synthesis of compounds. Subsequent lead optimisation involved structural modifications to enhance efficacy through derivatization (Pina, *et al.*, 2010). For malaria, animal models consisted of *P. relictum* in canaries (1926-1935), later *P. gallinaceum* in either chicks, ducklings or turkeys (1935-1948) and finally the rodent *P. berghei* model, that was first isolated from the thicket rat (central Africa, 1948) and remains widely used today (Burger, 1983). Eventually, *in vitro* culture methods replaced the preliminary *in vivo* investigations. Trager and Jensen made this transition possible for malaria in 1976, by

successfully culturing *P. falciparum* parasites, isolated from *Aotus trivirgatus* monkey, in human blood (Trager and Jensen, 1976). Accompanied with the genomics revolution (1980's), these advances instigated a more rational design approach to drug discovery (Kotz, 2012). Optimism ensued from the idea that a greater understanding of disease aetiology, molecular biology and cellular processes would lead to the identification of essential defined targets, and in due course an influx of novel chemotherapies (Chatterjee and Yeung, 2012; Jana and Paliwal 2007; Wells, 2010). For malaria this prospect was promoted by the sequencing of the *P. falciparum* genome (Gardner *et al.*, 2002) and the discovery that 60 % of the parasite proteins have no orthologues in humans (Guiguemde *et al.*, 2012).

### 1.7.2 Target-based drug discovery

The framework for a target-based drug design strategy is to identify a metabolically essential target, most commonly from genomic analysis. Ideally, the target should be specific to the disease causing organism to help mitigate adverse effects (Chatterjee and Yeung, 2012). Once the target has been genetically validated, through knock-out studies, an *in vitro* chemical assay is developed to permit high-throughput screening (Chatterjee and Yeung, 2012; Frearson *et al.*, 2007). At this point either druggable small molecules, obeying the rule of 5, or smaller fragments that conform to the rule of 3 are screened against the target (Blaazer *et al.*, 2014). Subsequently, hit compounds undergo structural optimisation to enhance the potency, selectivity and pharmacokinetic properties (Gilbert, 2013). X ray crystallography and computational 3D modelling can also be used to inform structural alterations (Jana and Paliwal, 2007; Gilbert, 2013). Selectivity can be determined by subsequent screening of hit compounds against related human targets and in cellular assays. Toxicology and resistance potential is also evaluated (Gilbert, 2013; Chatterjee and Yeung, 2012). A novel target is not considered fully validated until a drug acting on that target is shown to be effective in the clinic (Gilbert, 2013; Wells, 2010). Since this approach has been adopted for malaria, numerous putative targets have emerged in the literature (See Table 1.2) (Fidock *et al.*, 2004; Jana and Paliwal, 2007). These include as the cysteine proteases, protein farnesyl transferases, dihydrofolate reductase and phospholipid biosynthesis, to name a few (Gelb, 2007; Fidock *et al.*, 2004; Nwaka *et al.*, 2004; Winstanley, 2000).

Target Location	Pathway/ mechanism	Target molecule	Examples of therapies	
			Existing therapies	New compounds
Cytosol	Folate Metabolism	Dihydrofolate reductase	Pyrimethamine, Proguanil	Chlorproguanil
		Dihydropteroate synthase	Sulfadoxine, dapsone	
	Pyrimidine metabolism	Thymidylate synthase		5-Fluoroorotate
	Purine metabolism	HGPRT		Immucillin-H
	Glycolysis	Lactate dehydrogenase		Gossypol derivatives
		Peptidedeformylase		Actinonin
	Protein Synthesis	Heat shock protein 90		Geldanamycin
	Glutathione metabolism	Glutathione reductase		Enzyme inhibitors
	Redox system	Thioredoxin reductase		5,8-Dihydrooxy-1,4-napthoquinone
		Gamma-GCS		Buthionine sulfoximine
	Signal transduction	Protein kinases		Oxindole derivatives
	Shikimate	EPSPS		Glyphosate
	CDK	Pfmrk		Oxindole derivatives, thiophene sulfonamide
	Unknown	Ca <sup>2+</sup> - ATPase	Artemisinins	
Parasite membrane	Phospholipid synthesis	Choline transporter		G25
	Membrane transport	Unique channels	Quinolines	Dinucleoside dimers
		Hexose transporter		Hexose derivatives
Food vacuole	Haem polymerization	Haemozoin	Chloroquine	New quinolines
	Haemoglobin hydrolysis	Plasmepsins		Protease inhibitors, pepstatin
		Falcipains		Protease inhibitors, leupeptin
	Free radical generation	Unknown	Artemisinin	New peroxides
Mitochondrion	Electron transport	Cytochrome c oxidoreductase	Atovaquone	
Apicoplast	Protein synthesis	Apicoplast ribosome	Tetracyclines, Clindamycin	
	DNA synthesis	DNA gyrase	Quinolines	
	Transcription	RNA polymerase	Rifampin	
	Type II fatty acid biosynthesis	FabH		Thiolactomycin
		FabI/PfENR		Triclosan
	Isoprenoid synthesis	DOXP reductoisomerase		Fosmidomycin
	Protein farnesylation	Farnesyl transferase		Peptidomimetics
Extracellular	Erythrocyte invasion	Subtilisin serine proteases		Protease inhibitors

**Table 1.2 The existing and novel drug targets in *Plasmodium falciparum*.** Abbreviations: EPSPS, 5-enolpyruvyl shikimate 3-phosphate synthase; CDK, Cyclin dependent protein kinases; DOXP, 1-deoxy-D-xylulose-5-phosphate; GSC, glutamylcysteine synthetase; HGRT, hypoxanthine-guanine-zanthine phosphoribosyltransferase; PfENR, *Plasmodium falciparum* enoyl-ACP reductase. (After: Fiddock, 2004; Jana and Paliwal, 2007; Rosenthal, 2003).

Unfortunately, the heralded breakthrough has been disappointing, as clinical validation of novel targets has proven more difficult than expected (Wells, 2010). Although potent hits are readily identified and can be genetically validated, translational problems often arise at the whole parasite or animal model level. Referred to as *in vitro/ in vivo* disconnect, this has been the fate of numerous compound series produced against prospective novel targets in recent years (Chatterjee and Yeung, 2012; Gilbert, 2013). Indeed, enzyme inhibition failed to correlate with whole-parasite activity for the targets: lactate dehydrogenase (LDH), thioredoxin reductase (TrxR) and the fatty acid biosynthesis enzyme (FabI), despite extensive lead optimisation. Eventually, LDH and TrxR were deemed not druggable and FabI was shown to be dispensable during the intraerythrocytic cycle (Guiguemde *et al.*, 2013). A number of reasons have been put forward for the issue, mostly concerned with the lack of cellular context by which the hit compounds are identified. This results in unpredictable problems with cellular penetration, compound efflux, sequestration in lipid compartments, non-specific binding, alterations in protonation state of the molecule (in the enzyme active site) or undesirable kinetic properties (Gilbert, 2013). Despite our understanding of parasite biology, target identification is constrained by our existing knowledge base. Hindsight has led to the realisation that the parasite commonly uses novel modes of metabolism, cell division and trafficking, signalling and communication pathways. This means that the biological spectrum affecting a particular target is often poorly understood (Reaume, 2011). This incomplete knowledge results in unexpected adverse events and the poor attrition rates most frequently achieved (Jana and Paliwal, 2007).

#### *1.7.2.1 Validated antimalarial drug targets*

Despite almost 30 years of target-based drug discovery, the antimalarial development pipeline has struggled to deviate from three validated targets. These targets are based on the action of pre-existing antimalarials that were not developed in accordance with the modern fully rational, target-based drug discovery framework (Na-Bangchang and Karbwang, 2009). They include (1) the haemozoin pathway (chloroquine) the folate pathway, (anti-folates Dihydrofolate reductase and dihydropteroate synthase inhibitors) and the cytochrome bcl complex of the mitochondria, reportedly the principle target of atovaquone (Chatterjee and Yeung, 2012; Gilbert, 2013). In all cases, the antimalarial activity of the drug was discovered prior the identification of the target and mode of action. Even the activity of antifolates, often considered an exemplar class of targeted

antimalarials, was recognised in the form of Prontosil long before their development specifically for the indication (Rubin, 2007).

Furthermore, the majority of new antimalarials undergoing clinical development are actually resurrected from previous discovery programs. The second or third generation compounds are re-designed to be less toxic and retain efficacy where resistance to parent compounds is established (Gelb, 2007). One prospective example is Isoquine, a second-generation aminoquinoline, that is active against chloroquine and amidoquinoline resistant parasite strains (Nwaka *et al.*, 2004). However, the limited pool of refined targets and the pre-existing resistance capabilities of the parasite calls into question the longevity of such second generation compounds (Canfield *et al.*, 1995; Wells, 2010).

#### *1.7.2.2 Problems with target-based drug discovery*

The reduction in output of novel first class medicines is not restricted to malaria, a decline has been seen across the disease spectrum (Ashburn and Thor, 2004; Boguski *et al.*, 2009; Reaume, 2011). Since the 1990's the capital spent on research and development has increased, while the number of chemical entities reaching regulatory approval has decreased (Boguski *et al.*, 2009; Fidock *et al.*, 2004). This has called into question over-reliance on the target-based strategy and genetic approach to drug discovery (Kotz, 2012). A recent review indicated that in total there are 1065 drugs targeting 324 targets, 266 of these are human targets and the remainder constitute those targeting pathogens (Gilbert, 2013). In reality, selective compounds are rare due to conserved homology (Chatterjee and Yeung, 2012).

Focus on the target-based strategy has not been the only issue for malaria drug discovery. A persistent problem is that, although the malaria drug market is one of the largest in the world, with half a billion people needing treatment per annum, the majority of patients that require treatment cannot afford to pay for it (Craft, 2008). Unsurprisingly, the discovery and development of a drug product with a negligible profit margin is an unattractive investment for pharmaceutical companies (Craft, 2008; Muthyala, 2011; Winstanley, 2000). The profit from prophylactic drugs for travellers from developed countries can in no way compensate for the capital needed for treatment of the underdeveloped world (Craft, 2008). Fortunately, in recent years this 'not-for-profit' area has been subsidised by the formation of non-profit public, private and philanthropic partnerships, such as the Medicine for Malaria venture (1999) and the Bill and Melinda Gates foundation,

substantially increasing efforts into malaria drug discovery (Fidock *et al.*, 2004). As a result, the involvement of academia in drug discovery has become increasingly important (Kotz, 2012; Oprea *et al.*, 2011).

Ultimately, these academic and industrial partnerships have been formed on the back of a unanimous realization that the number of programs focussing on novel antimalarials, and the predominantly target-based approach that was being adopted, will be insufficient to sustain the antimalarial drug pipeline (Gelb, 2007; Gilbert, 2013; Wells 2010). The considerably long development time of *de novo* drug discovery is further hampered by the high failure rate of candidates, with compounds at the lead optimisation stage having only a 7% chance of becoming a drug. Moreover, once in use, there is a possibility the novel drug may only have a short window of effectiveness, as demonstrated by the antifolates. Accompanied by inevitable spread of artemisinin resistance, these factors, predict an imminent, potentially catastrophic void in the malaria drug market. Thus making it imperative that faster development processes are sought and adopted (Craft, 2008; Gelb, 2007).

### 1.7.3 Phenotypic drug screening

Towards the above mentioned aim, the drug discovery industry has turned to more traditional approaches in order to surmount the innovation gap caused by the dependence on target-based approaches (Boguski *et al.*, 2009; Reaume, 2011). Historically, antimalarial drug discovery has benefited from phenotypic screening and the whole-organism based approach (Chatterjee and Yeung; 2012). This top-down development process involves testing against the whole parasite followed by compound purification according to potency. Drug targets and mechanisms of action are defined retrospectively (Gilbert, 2013). Regardless of the vast amount of information known about the *Plasmodium* life cycle, the most important and by far most efficacious antimalarial classes, the quinolines and the artemisinins, were discovered serendipitously from ancient herbal fever cures in this manner (Chatterjee and Yeung, 2012). Remarkably, the oldest antimalarial agent, quinine, remains effective despite nearly 400 years of use (Achan *et al.*, 2011). This is particularly striking when compared with the targeted anti-folate class of drugs that succeeded in retaining efficacy for relatively short 5 year period (Craft, 2008). While the action of the quinolines has since been elucidated, the target or most likely targets of the artemisinins, the most promising new class of antimalarials, are still in dispute. Indeed, evidence has been put forward implicating the involvement of

haemoglobin and haem (Klonis *et al.*, 2011; Zhang and Gerhard, 2009), free radicals generated by the reduction of the endoperoxide bridge (Meshnick, 2002), reactive oxygen species generated by the activation on the mitochondrial electron transport chain (Mercer *et al.*, 2011) and the involvement of the calcium pump PfATP6 (ortholog of endoplasmic reticulum pump SERCA) (Valderramos *et al.*, 2010). It appears that the complex nature of the parasite infection cannot be defeated by simple single-targeted compounds. The superiority of plant-based compounds is perhaps due to the complexity of their promiscuous binding and the benefits incurred by multiple off-target effects that are altogether lacking in their synthetically refined counterparts. Such issues of resistance development towards existing antimalarials has prompted the obligatory adoption of combination therapy for malaria in recent years. This, in turn has inadvertently doubled the quota for a continued supply of affordable new antimalarials (Craft, 2008). The modern perspective of phenotypic screening aims to address these issues by acknowledging the advances made in medicinal chemistry over the past century. Referred to as ‘drug repositioning’ or ‘repurposing’ (Figure 1.4), this novel strategy uses phenotypic screening to identify novel indications for existing or abandoned pharmacotherapies (Boguski *et al.*, 2009; Medina-Franco *et al.*, 2013).

#### 1.7.4 Drug repositioning

There have been numerous success stories of drug repositioning for other diseases. For instance, Sildenafil (Viagra) was originally developed to treat cardiovascular diseases but is now widely used for erectile dysfunction (Fink *et al.*, 2002). Thalidomide was formally developed to treat morning sickness but was withdrawn due to adverse severe birth defects in children. The drug was later found to be uniquely effective for the treatment of Erythema nodosum leprosum and has more recently been patented for the treatment of a type of cancer (multiple myeloma) (Walker *et al.*, 2007). Bupropion (Wellbutrin) and Duloxetine (Cymbalta) were both originally developed to treat depression but are now repurposed as a smoking cessation aid and for stress urinary incontinence respectively (Boguski *et al.*, 2009). Clearly such fortunate medical triumphs highlight an opportunity that should not be missed by the malaria community.



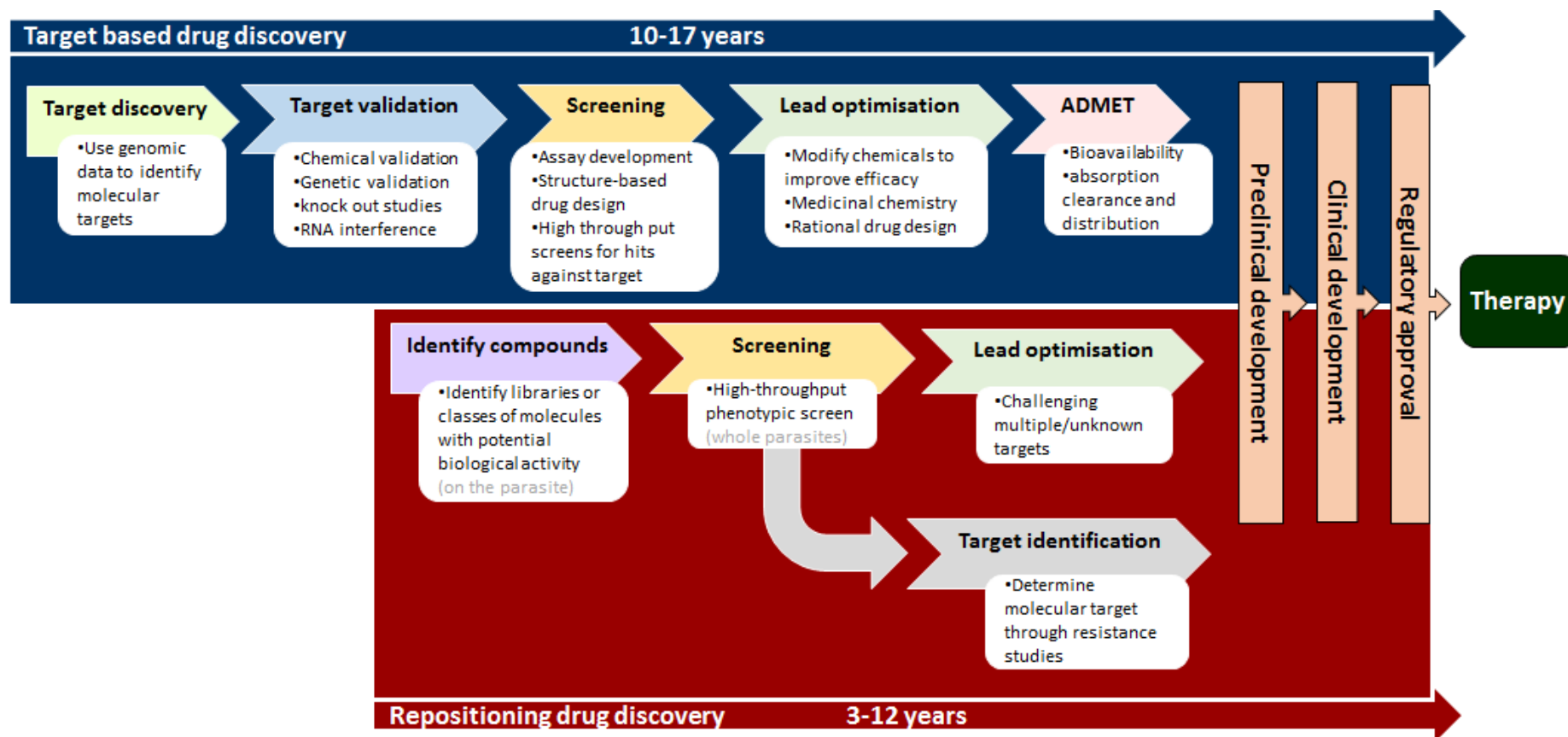


**Figure 1.4 Target-based and drug repositioning development timelines.** *De novo* drug discovery, which in the last 30 years has focussed on a target-based strategy, can take 10-17 years with only a < 10 % probability of success. The drug repositioning timeline is shorter (3-12). Frequently repositioned candidates have already been evaluated at several phases of the pipeline for their previous indication. ADMET, absorption, distribution, metabolism, excretion and toxicity information may already be available for the candidate and the drug may already be approved for human use by the EMEA or FDA. For parasitic disease when knowledge of the target is not essential, target identification can run in parallel to lead optimisation, clinical development and regulatory approval. (After: Ashburn and Thor, 2004; Frearson *et al.*, 2007 Wells, 2010)

In the last 5 years, the literature has been inundated with reports of drug repositioning for a range of different human and infectious diseases (Ekins *et al.*, 2011; Nzila, 2011; Oprea *et al.*, 2011). An approach that once relied only on serendipitous instances has been transformed into a more systematic method of drug discovery (Medina-Franco *et al.*, 2013). In effect, the strategy encompasses the benefits of the previous drug discovery methods; phenotypically, by using high throughput *in vitro* whole-cell screening and pharmacologically by exploiting diverse chemical libraries, the product of nearly 100 years of medicinal chemistry.

#### *1.7.5 Phenotypic screening for malaria*

Phenotypic screening for malaria has been made possible by recent developments of more high-throughput, whole-parasite screening techniques against the erythrocyte stages. These include the hypoxanthine incorporation assay, ELISA and SYBR Green-based methods. More recently high-throughput liver stage assays have also been developed (Derbyshire *et al.*, 2012). Demonstration of whole-cell activity means that the aforementioned issues often faced by targeted antimalarials, such as permeability and cellular efflux, have already been addressed. Selectivity and toxicity can be determined by screening against mammalian cell lines (Wells, 2011). One problem is that without prior knowledge about the target, structural alterations to improve compound activity are less informed (Gilbert, 2013). However, advances have been made in target identification using chemical proteomics, which could later be used to improve treatments by the creation of rationally designed second generation molecules (Gilbert, 2013; Kotz, 2012). Nevertheless, history has demonstrated that the most successful antimalarials are most likely to be those that display promiscuous binding and have multiple targets, which are much more difficult to elucidate and may have poor or narrow structural activity relationships (Chatterjee and Yeung, 2012; Melinda-Franco *et al.*, 2013). The over-emphasis on the importance of knowing the drug target prior to use has dominated opinion in the drug discovery arena in recent years. However, in practice this is not always possible. In many cases knowledge of the target is not always a requirement for regulatory approval (Kotz, 2010; Melinda-Franco *et al.*, 2013). For diseases like malaria, in particular, the need for the rapid deployment of an effective affordable antimalarial outweighs the idealism and benefits of knowing the target.

### 1.7.6 Drug repositioning for malaria

Drug repositioning has been made possible in recent years by the commercial and scholarly availability of chemically diverse compound repositories, produced by the pharmaceutical industry. The pharmacological advantages of screening such high quality libraries are that they permit quick access to innovative chemical entities that may act *via* novel and potentially, multiple targets in the malaria parasite. The value of identifying distinct, multiple-targeted antimalarials that would inherently help circumvent resistance is indisputable. Although devoid of target information, scaffolds of compounds that display varied degrees of activity can be used to inform structural optimisation and improve physiochemical properties. Early *in vitro* pharmacokinetic profiling and selection of compounds with favourable intrinsic properties will also enhance the chance of success (Chatterjee and Yeung, 2012). Generally, and of utmost importance for the discovery of antimalarial drugs, the pace of the drug repositioning development route is much more efficient (Figure 1.4), particularly if the selected compound libraries have already been approved by the Food and Drug Administration agency or the European Medicines Agency (Chatterjee and Yeung, 2012; Wells, 2010)

For diseases like malaria, where time and cost are significant factors, drug repositioning is an attractive, alternate approach to drug discovery (Figure 1.4). Not only will it offer an interim solution, while novel target-based drugs are developed, it may also help identify suitable candidates for combinatory regimes with existing antimalarials. Ultimately, this could help bridge the gap between the eventual failure of current antimalarials and future drug developments.

### 1.8 Future directions

The adoption of a balance between target-based drug discovery and drug repositioning will most likely be the best strategy (Gilbert, 2013). Existing target-based studies should be ongoing with the hope that the benefits of the last 30 years of scientific enquiry should materialise in the not too distant future. Novel drug repositioning approaches should simultaneously aim to identify drug targets, but such investigation should run in parallel and not prohibit development and regulatory approval of much needed drugs (Kotz, 2012).

Drug repositioning is often viewed as less scientific, when compared with the rational design target-based approach, due to its reliance on serendipity. However, the underlying hypothesis is that drugs are innately promiscuous, and access to unexplored chemical

space for a particular disease indication should permit the discovery of novel targets (Reaume, 2011). This is exemplified by a common finding that the moiety required for activity in the previous indication is often dispensable for the repositioned activity, seemingly the result of off-target effects (Gelb, 2007). Following this rationale, the hypothesis of the current study is that antimalarial hit compounds will be identified from a preliminary screening of two FDA approved drug libraries.

Subsequently, hit compounds should undergo more detailed characterisation in the academic setting so that early no-go and prioritization decisions can be made sooner (Chatterjee and Yeung, 2012). Indeed, for parasitic diseases, including malaria, preliminary screens of compound libraries, containing bioactive compounds with known safety profiles, have already begun (Baniecki, *et al.*, 2007; Chong *et al.*, 2006; Jones *et al.*, 2010; Lucumi *et al.*, 2010, Major and Smith, 2011). Despite the huge volume of hits identified, few have been taken beyond the hit identification stage, devaluing the approach as a fast-track strategy (Baniecki, *et al.*, 2007). The relatively refined compound screen (~700 compounds) proposed here will permit a self-contained workflow of hit identification, prioritization and characterisation. Finally, the study will serve to further validate drug repositioning as an effective paradigm for antimalarial drug discovery.

### *1.9 The objectives of the PhD*

1. To identify compounds that display potent *in vitro* antimalarial activity against the multidrug resistant *P. falciparum* K1 strain from medium-throughput phenotypic screens of two FDA approved drug libraries.
2. To further characterise the action of selected hit compounds by defining their IC<sub>50</sub> level of inhibition and killing profile.
3. Investigate the interaction of hit compounds with existing antimalarials, particularly artemisinin to determine suitability and potential for artemisinin-based combination therapy.

## CHAPTER 2

---

### GENERAL MATERIALS AND METHODS

#### *2.1 In vitro culture of Plasmodium falciparum*

All procedures were carried out in the pathogen laboratory (University of Salford) sterile hood (ESCO class II Biological safety cabinet), using aseptic techniques and pre-sterilised equipment. Virkon (Antec International, UK) was used to disinfect waste material before autoclaving and disposal. All routine culture methods are consistent with those employed by Read and Hyde (1993).

##### *2.1.1 Preparation of complete medium*

RPMI 1640 1x (+) L-Glutamine (+) 25 mM HEPES (4-(2-Hydroxyethyl)piperazine-1-ethanesulfonic acid) (Gibco, Life Technologies, UK) was used as the basis of the culture medium. Four additives; 2.5 g Albumin bovine serum fraction V (Sigma, UK), 2.5 ml 1 mg/ml hypoxanthine (Sigma, UK) in phosphate buffered saline (PBS) (Fisher Chemical, UK), 2.5 ml 40% glucose (Dextrose Anhydrous, Fisher Scientific, UK) in sterile water and 0.5 ml 50 mg/ml gentamycin (Sigma, UK) in PBS were transferred to a 50 ml falcon tube along with approximately 20 ml RPMI 1640 from a newly opened bottle. The contents of the falcon tube were allowed to dissolve and were subsequently passed through a 0.22 µm filter directly into the 500 ml bottle of RPMI 1640 medium using a 20 ml syringe. Following gentle mixing, the complete medium was stored at 2-8°C.

##### *2.1.2 Washing Medium*

A 500 ml bottle of pre-sterilised RPMI 1640 1x (+) L-Glutamine (+) 25mM Hepes (Gibco, Life Technologies, UK ) without additives was used as washing medium throughout the study and stored at 2-8°C for up to 2 weeks.

##### *2.1.3 Preparation of human blood for culture of Plasmodium falciparum*

To remove leukocytes, O+ whole blood (obtained from the human blood bank) was washed immediately before use. An equal volume of whole blood was added to two 50 ml falcon tubes and centrifuged for 5 mins and 3,400 rpm. Following centrifugation, blood plasma and the pale layer (the buffy coat-containing white blood cells) that forms on top of the red blood cells was removed. Blood was then re-suspended in an equal volume of washing medium and following centrifugation (as described previously) the supernatant,

along with the buffy coat, was discarded. The washing process was repeated 3x to ensure that all leukocytes were removed from the blood. For the latter of the three washes, complete medium not washing medium was used. Finally, full blood (100% haematocrit) was re-suspended in an equal volume of complete medium to give a final haematocrit of 50% and stored at 2-8°C until further use.

#### *2.1.4. In vitro Plasmodium falciparum culture*

To begin a new culture, 10 ml of complete medium and 0.5 ml of washed blood was added to a 50 ml culture flask and warmed to 37°C prior to the addition of the parasites. Approximately 0.5 ml of parasitised blood (retrieved from liquid nitrogen, refer to section 2.1.7) was then added to the warmed culture medium to give a final haematocrit of 5 %. Following inoculation, the parasite culture was gassed with a 5 % CO<sub>2</sub>, 5 % O<sub>2</sub> and 90 % N<sub>2</sub> gas mixture (BOC Limited, UK) and placed in the incubator (Leec culture safe touch 190 CO<sub>2</sub>, Leec Limited, Uk) at 37°C.

#### *2.1.5 Routine maintenance of a Plasmodium falciparum culture*

Parasites were routinely cultured at a final volume of either 10 ml or 30 ml in 25 cm<sup>3</sup> or 75 cm<sup>3</sup> flasks respectively. For experimental set up, smaller flasks (12.5 cm<sup>3</sup>) with a final culture volume of 5 ml were used. For each of the varying flasks volumes, the culture was maintained at approximately 5 % final haematocrit (for every 10 ml of complete medium 1 ml of 50 % haematocrit blood was added). The medium was changed at either 48 or 72 hour intervals. In brief, spent medium was removed and discarded without dislodging the parasitised blood layer that formed at the bottom of the flask. Subsequent to the estimation of parasitaemia (see section 2.1.6), the continuous culture was diluted to 0.5-1 % parasitaemia with washed blood (50 % haematocrit). New complete medium was added to give a final haematocrit of 5 %. Both washed blood and complete medium had been warmed prior to the dilution and re-suspension procedure. The culture was then gassed and placed in the incubator under conditions described previously.

#### *2.1.6 Estimation of parasitaemia*

One drop of concentrated parasitised blood (from the bottom of a culture flask) was transferred to the outer margin of a microscope slide. The blood was thinly smeared across the slide using a second slide and a single swift smooth action to obtain a monolayer of cells. The slide was then air dried at room temperature and fixed by rinsing in 100%

methanol. After an additional air drying step, the slide was immersed in Giemsa stain at room temperature for ~20 minutes. The Giemsa staining solution was prepared by diluting Gurr's Giemsa stain solution (BDH/VWR international limited, UK) 1:10 with Giemsa buffer. To prepare the buffer solution one tablet pH 6.4 (BDH laboratory supplies, England) was added to 1 litre of freshly distilled water. Following staining, the slides were rinsed with a gentle stream of tap water, dabbed dry and viewed under oil immersion (x 100) using a Leica DM 500 compound microscope. Parasitaemia was estimated by counting the total number of red blood cells per field of view (approx 100-200) and noting those containing parasites. Multiple infections were counted as one (as only one parasite is expected to reach full development). For each slide, at least 3 fields of view were counted from which the average percentage of infected cells was calculated.

#### *2.1.7 Preservation in liquid nitrogen*

A predominantly ring stage culture at approximately 15-20 % parasitaemia was selected for preservation in liquid nitrogen. In brief, the culture was centrifuged at 3,400 rpm for 5 min, the supernatant removed and the culture reconstituted to a 50 % haematocrit by adding an equal volume of warmed complete medium. Aliquots (0.5 ml) of the suspension were transferred into 2 ml cryotubes and 0.5 ml 20 % dimethyl sulfoxide (sterile filtered DMSO, Sigma, UK) in Ringer's solution (9 g NaCl, 0.42 g KCl and 0.25 g CaCl<sub>2</sub>/ Litre) was added. The tubes were immediately snap-frozen in liquid nitrogen for preservation and storage.

#### *2.1.8 Retrieval from liquid nitrogen*

Following an initial thawing period at 37°C the contents of the cryotube were transferred to a microcentrifuge tube and centrifuged at 14,000 rpm for ~1 min using the minispin (eppendorf, UK) centrifuge. Once the supernatant had been discarded the parasitised blood was gently re-suspended in 1 ml of 10% sorbitol (Fisher Scientific, UK) solution (in PBS) with continuous mixing. This was then centrifuged and the process repeated twice more with subsequent re-suspensions in 5 % sorbitol (in PBS) and finally, complete medium. Following the latter washing step in complete medium, the culture was re-suspended in complete medium and inoculated into a culture flask containing 0.5 ml of newly washed blood (50 % haematocrit) and 10 ml of complete medium (see 2.14).

### 2.1.9 Sorbitol synchronisation

During continuous culture *P. falciparum* parasites rapidly lose synchronisation. If synchronisation was required prior to experimental set-up, sorbitol synchronisation was used to obtain a predominantly ring stage parasite culture. Sorbitol (5 % w/v) was prepared in distilled water and filtered through a 0.22 µm filter. The sorbitol solution was then added directly to pelleted parasite culture (9 ml to 1 ml of culture pellet) and incubated for 5 mins at room temperature. Following this, the culture was centrifuged at 3,400 rpm for 5 mins and the supernatant was discarded. The parasite pellet was then subjected to three washing steps in complete medium, before re-suspension in complete medium at 50 % haematocrit. The synchronised parasite culture was used to set up a new culture as described previously (section 2.1.4).

## 2.2 Drug susceptibility assays

Initial optimisation experiments for SYBR Green-based assays are described in chapter 3. The final versions of the assays are described here.

### 2.2.1 Preparation of existing antimalarial primary stock solutions

The four selected existing antimalarials used in the current study were obtained from Sigma Aldrich, UK. Primary stock solutions were prepared in accordance with manufacturer instructions. In brief, atovaquone (MW = 366.84) was dissolved at 5 mg/ml (13.63 nM) in DMSO. For dihydroartemisinin (MW = 284.35) 1.4 mg of the powder stock was dissolved in 1 ml of DMSO to obtain a primary stock concentration of 5 mM. Proguanil was dissolved at 1 mg/ml in acetonitrile: water (60/40). All primary stock solutions were passed through a 0.22 µm porosity filter, aliquoted and stored at -20°C until further use. Chloroquine (MW = 515.86) was prepared freshly on the day of use. An initial stock solution was prepared at 5 mM (10.32 mg/ 4ml) and sterile filtered. For experimental set up, the primary stock solutions were further diluted with complete medium to give working solutions. Various amounts of the working solution were then transferred as required to achieve final test concentrations.

### 2.2.2 SYBR Green microtitre plate assay for *Plasmodium falciparum*

For the SG-MicroPlate assay a black bottom 96 well plate was used (Nunc, Denmark). Dependent upon the nature of the experiment treated infected blood, untreated infected blood (positive control) and uninfected blood (negative control) samples were suspended in complete medium, RPMI or PBS at a final volume of 100 µl and a haematocrit of either



5 or 10 %. One hundred microliters of SYBR Green 1 (nucleic acid gel stain 10,000 x, Sigma, UK) staining solution (5 x SG in wash medium or PBS) was added to each well. This gave a final well volume of 200  $\mu$ l and a SG concentration of 2.5 x. Final haematocrits were therefore also adjusted to 2.5 % and 5 % respectively. Following a 1 hour incubation period at room temperature, fluorescence intensity was measured from the top using a GENius plate reader (Tecan) set at 485 nm excitation and 535 nm emission wavelengths.

#### 2.2.3 SYBR Green flow cytometry method for *Plasmodium falciparum*

Following the drug treatment procedures, 50  $\mu$ l of 5 % haematocrit culture was transferred from the infected-blood control, the non-infected-blood control and each treatment flask, into separate eppendorf tubes (for plate experiments maintained at 2.5 % haematocrit the transfer volume was adjusted to 100  $\mu$ l). After a single washing step (in PBS, centrifugation: 90 seconds at 14, 0000 rpm) each pellet was re-suspended in 1 ml 5 x SYBR Green 1 solution (in PBS) and incubated in the dark for 20 minutes at room temperature. Subsequently, the samples were centrifuged for 90 seconds at 14,000 rpm, the supernatant was removed and discarded and samples were re-suspended in 250  $\mu$ l of 0.37 % formaldehyde solution in PBS (formaldehyde solution for molecular biology 36.5 %, Sigma, UK). After the addition of the fixative the samples were placed in the fridge at 4 °C for 10-15 minutes. Following fixation, the samples were washed 3 x in PBS and finally re-suspended in 1 ml of PBS. Fifty thousand events were recorded for each sample using the FITC channel of the BD FACsVerse flow cytometer system.

#### 2.2.4 Calculation of $IC_{50}$ and $IC_{90}$ values

For all dose response data sets, values were transferred from respective software programmes into Microsoft excel. The infected blood controls were set at 100% and percentage parasitaemia for drug treated samples was calculated relative to the infected control. For  $IC_{50}$  and  $IC_{90}$  calculations, data was further processed using Graphpad prism 5.0. Data was normalised so that the largest value in the data set corresponded to 100% and the smallest value corresponded 0%. Log-transformed drug concentrations were then plotted against the dose response and the  $IC_{50}$  and  $IC_{90}$  values were determined using nonlinear regression (Graphpad prism 5.0). The log(inhibitor) vs. Normalised response-Variable slope option was selected for  $IC_{50}$  calculation whilst the log(agonist) vs. Response-find ECanything with the F values set at 10 was used for the  $IC_{90}$  calculations.

## CHAPTER 3

---

### OPTIMISATION OF FLUORESCENCE-BASED DRUG SUSCEPTIBILITY ASSAYS

#### 3.1 INTRODUCTION

A pre-requisite for the screening of FDA-approved drug libraries containing hundreds of compounds, is the establishment and optimisation of medium-high throughput screening methods for the malaria parasite. Over the years, many drug screening assays have become available. Most focus on the erythrocyte stages of the parasite life cycle. These include; the WHO microtest, the radioisotopic test, enzyme-linked immunosorbent assays (ELISA) and more recently, the fluorometric assays that utilise DNA-binding fluorescent dyes (Basco, 2007; Co *et al.*, 2010). Details of each method will be discussed in the chronological order of discovery and suitability for use in the current study will be determined.

##### *3.1.1 The WHO microtest*

The traditional microscopy test, to determine the sensitivity of *Plasmodium falciparum* to antimalarial drugs, was first announced in 1978 (Rieckmann *et al.*, 1978). After further development by Wernsdorfer *et al.* (1980), the test gained support from the World Health Organisation (WHO). As a result, the WHO standard microtest kit was produced, and the procedure named accordingly (Payne and Wernsdorfer, 1989). The test uses microscopic evaluation to enumerate schizont maturation following growth in the presence of an antimalarial (Bacon *et al.*, 2007; Noedl, 2002). In brief, a Giemsa stained blood film is examined and 200 parasites are counted. Parasites with three or more nuclei are considered to have matured and are, therefore, not sensitive to the test drug. For drugs that affect nuclear division, such as pyrimethamine, three or more nuclei may develop even when the drug is effective. For this reason, the threshold is raised; schizonts with eight nuclei or more are considered mature. For adequate comparisons, the figure in the control sample must reach at least 10 % (WHO, 2001). The figures from the control and treated samples can then be used to determine the drug concentration that inhibits 50 % of parasite growth (IC<sub>50</sub>). This is a standard measurement used across disciplines to indicate the effectiveness of a particular compound. Still in use today, for both *in vivo* and *in vitro* experiments, the WHO microtest is a reliable, sensitive, and inexpensive epidemiological tool. It can, however, be subjective and is highly labour intensive (Bacon *et al.*, 2007; Noedl *et al.*, 2002; Rason *et al.*, 2008). Considering the large number of drugs to be tested, this method

would be too time-consuming. A more high-throughput method will therefore be necessary.

### 3.1.2 Radioactive isotope incorporation

The isotopic technique quantifies parasite uptake of various radioactive substrates as a measure of parasite growth (Smilkstein *et al.*, 2004). Commonly used substrates include (3H)-hypoxanthine (Desjardin *et al.*, 1979) and (3H)-ethanolamine (Elabbadi *et al.*, 1992). The former substrate is incorporated into nucleic acids whilst the latter is a precursor of phospholipids (Desjardin *et al.*, 1979; Elabbadi *et al.*, 1992). The principle behind the technique is that the parasite cannot produce these substrates itself and must, therefore, obtain them from its environment. A second condition is that the parasite must not be able to acquire a non-labelled form of the substrate from additional sources, such as the blood or medium. For this reason, the hypoxanthine method is slightly flawed as hypoxanthine is a common component of *P. falciparum* culture medium. This problem has been overcome by purine starvation prior to pulsing with the radioactive-label (Smilkstein *et al.*, 2004). The ethanolamine method, on the other hand, is devoid of this problem; the erythrocytes do not undergo phospholipid biosynthesis and the fatty acids and polar heads required are entirely absent from the growth medium (Elabbadi *et al.*, 1992). For both substrates, the multistep procedure involves an initial 24 hr incubation period in the presence of the test drug. After incubation, the samples are pulsed with the radioactive-label and returned to the incubator for an additional 24 h. At 48 h, the plates are removed from the incubator, freeze-thawed, and each sample is harvested onto fibre-glass paper. The paper is then dried and mixed with scintillation fluid. To determine IC<sub>50</sub> values, incorporation of the radioactive-label is measured by a liquid scintillation counter (Cerutti Junoir *et al.*, 1999; Noedl *et al.*, 2002; Rason *et al.*, 2008; Smilkstein *et al.*, 2004). The isotopic method is the most widely used technique for assessing *P. falciparum* drug sensitivity. Indeed, Bacon *et al.* (2007) refer to it as the ‘gold standard’. Like the WHO micro test, the isotopic method is extremely reliable. Its major shortfall is that it requires the handling of radioactive-isotopes. Not only are they expensive to buy, but, the equipment needed to process and dispose of them is also incredibly costly (Bacon *et al.*, 2007; Noedl *et al.*, 2002; Rason *et al.*, 2008; Smilkstein *et al.*, 2004). Although the isotopic technique is a more high-throughput method than the WHO microtest, it has a reduced sensitivity. To obtain adequate readings parasitaemia must reach 0.2-0.5%. This is a more serious problem for *in vivo* and *ex vivo* rather than *in vitro* culture systems, where starting parasitaemias can be

controlled (Noedl *et al.*, 2002). In view of the aforementioned problems, the handling of radioactive waste being the most limiting, the isotopic technique would not be suitable for use in our lab.

### 3.1.3 ELISA-based assays

The two enzyme-linked immunosorbent assays (ELISA) for malaria drug screening purposes were originally adapted from enzymatic assays (Co *et al.*, 2010). The more recent methods utilize two monoclonal antibodies against *P. falciparum*. The two most commonly used targets are histidine rich protein two (HRPII) and *P. falciparum* lactate dehydrogenase (pLDH) (Bacon *et al.*, 2007). As its name suggest HRPII is a histidine and alanine rich protein that is associated with parasite development (Noedl *et al.*, 2002). Localised to both the parasite, and the infected erythrocyte cytoplasm it is also found in pockets on the infected erythrocyte membrane and has been recovered from culture supernatants as a secreted water-soluble protein (Co *et al.*, 2010). The other target, pLDH, is an enzyme that catalyses the conversion of pyruvate to lactate, in the glycolytic pathway, and is essential for energy production and parasite growth. Conveniently, the parasite enzyme is distinct from the human form of LDH and can be used as indicator of parasite growth (Kaddouri *et al.*, 2006; Makler *et al.*, 1998; Co *et al.*, 2010).

The ELISA is now a widely used method for malaria drug susceptibility testing (Bacon *et al.*, 2007). The assay works by measuring changes in the levels of either target (pLDH or HRPII) as an indicator of parasite growth. Various groups have adapted different ELISA protocols using the different targets. For example, Druilhe *et al* (2001) developed the double enzyme-linked LDH immune-detection assay (DELI) using pLDH, Noedl *et al.* (2002) on the other hand developed the HRPII ELISA using HPRII. Although modifications have been made to improve assay performance for malaria drug screening purposes, all of the assays available follow the basic capture-ELISA procedure. Initially, the plates are coated with the primary antibody, specific for either HRPII or pLDH, and incubated overnight at 4°C. Following the incubation period, the plates are washed, leaving only the immobilised antibodies in the wells. Haemolysed infected blood can then be added to the pre-coated wells and incubated for 1hour at room temperature. This allows any antigen, for example HRPII, within the sample to bind to the antigen specific antibody. Subsequent to washing, the antibody-enzyme conjugate is added. Any unbound conjugate is then washed away and a colourless substrate is added to the wells. In the presence of the enzyme, which at this point is attached to the antibody-antigen-antibody sandwich, the

colourless substrate is converted into a coloured product. The absorbance can then either be read immediately, or at a later time point following the addition of a stop solution to prevent any further reactions. The intensity of this colour change, measured by a microtiter plate reader, corresponds to the level of parasite multiplication.

The ELISA-based methods offer high throughput, sensitive, non-subjective screening tests (Noedl *et al.*, 2002; Rason *et al.*, 2008). In addition, the more recently optimised DELI and HPRII methods have been shown to correlate well with the traditional, WHO microtest and radioactive-isotope, methods (Grimberg, 2011). However, the multistep procedure is time consuming, stage-specific and requires a minimum incubation time before detectable effects can be observed, while only providing indirect information about the response of the parasite to a test drug (Bacon *et al.*, 2007; Grimberg 2011; Noedl *et al.*, 2002). Furthermore, the commercial test kits available for both the pLDH and the HPRII ELISAs are expensive (Noedl *et al.*, 2005; Rason *et al.*, 2008). The individual assay components can be purchased separately for HPRII ELISA, but not for pLDH-based assays (Bacon *et al.*, 2007). The downfall is that the in-house procedure needs to be standardised which can be time-consuming and labour intensive (Noel *et al.*, 2005).

#### 3.1.4 SYBR Green-based microtitre plate assay

The use of SYBR Green in screening takes advantage of the fact that the parasite's host cells (human erythrocytes) are devoid of DNA. For this reason, the majority of fluorescence observed in a sample can be attributed to parasite DNA. SYBR Green is one of the most sensitive DNA stains available. It is a cyanine dye that binds to double stranded parasite DNA and once intercalated becomes highly fluorescent (Vossen *et al.*, 2010). For the purpose of drug screening, a lower fluorescence intensity reading, in comparison with the control sample, reflects a lower amount of DNA present, which in turn infers a decrease in parasite growth. The main advantages of the SYBR Green assay are that it is relatively simple, quick and inexpensive to perform (Rason *et al.*, 2008). Indeed, the one-step procedure involves the addition of dilute SYBR Green to the sample followed by a 1 hour incubation period in the dark at room temperature. The sample can then be read immediately (Smilkstein *et al.*, 2004). Apart from a fluorescent plate reader, no specialised equipment is required for the assay. In some studies the lysis of the erythrocytes prior to or during the staining procedure is included as an additional step to reduce background fluorescence (Johnson *et al.*, 2006; Moneriz *et al.*, 2009). One problem is that the SYBR Green dye can indiscriminately bind to non-parasite DNA as well as

parasite DNA. The presence of any remnant white blood cells in the sample may therefore interfere with the results, or cause a high background. The dye is also capable of binding to single stranded DNA and RNA but at a much lower affinity than double stranded DNA, again contributing to background interference (Smilkstein *et al.*, 2004). However, the results obtained by the relatively novel SG approach are comparable to those obtained *via* the more traditional methods (Rason *et al.*, 2008). Vossen *et al.* (2010) on the other hand suggests that for drug susceptibility assays a relatively high starting parasitaemia is required, indicating that the assay may be more suitable for *in vitro* culture systems, rather than as a field application, where such parameters can be controlled.

### 3.1.5 SYBR Green-based Flow cytometric method

Like the plate reader assays that use a fluorescent DNA stain, the flow cytometric method exploits the fact that circulating red blood cells predominantly lack DNA (Grimberg 2011). There are a multitude of fluorescent nucleic acid dyes available for use with a flow cytometer, each of which has varying specificities for DNA and/or RNA (Table 3.1) (Bianco, Battye and Brown, 1986; Hare and Bahler, 1986; Jackson *et al.*, 1977; Makler, Lee and Recktenwald, 1987; Shapiro and Mandy, 2007; Van Vianen *et al.*, 1993). In addition to the DNA stains, fluorescent antibodies against malaria blood cell surface antigens can be used to gain a clearer image of antigen expression during the parasite life course. Stains specific to human blood cells can also be employed to exclude unwanted cells from the analysis. This toolbox of dyes can be used individually or in conjunction with other dyes that have different wavelengths to gain more information about parasite response to drug exposure. Indeed, Malleret *et al.* (2011) used a tri-coloured method with which they were able to determine parasitaemia according to DNA content, using either Hoechst 33342 or SYBR Green as a DNA stain. In addition, they calculated the frequency of leukocytes, normocytes and reticulocytes by using an anti-CD45 antibody and dihydroethidium which stains both DNA and RNA (Malleret *et al.*, 2011). Others suggest that this exclusion process, adopted to avoid the confounding effects of reticulocytes and white blood cells, is not necessary, particularly when using an *in vitro* culture method. The RNA present in reticulocytes (1.5% of human blood) degrades within a few days of *in vitro* culture and any remnant white blood cells, left behind after the blood washing procedure can be easily identified on the flow cytometer output and thus eliminated due to the differential size of human DNA relative to the parasite genome (Grimberg, 2011).

Dye	Class	Specificity	Wavelength	Cell permeability
Hoechst 33258	Miscellaneous	DNA	ex345 em478	permeant
Hoechst 33342	Miscellaneous	DNA	ex355 em465	permeant
GFP		Varies	ex481 em507	permeant
SYTO-9	Cyanine stain	DNA/RNA	ex485/486 em598/501	permeant
SYBR Green	Miscellaneous	DNA	ex488 em522	impermeant
SYTO 16	Cyanine stain	DNA/RNA	ex488/494 em518/525	permeant
YOYO-1	Cyanine stain	Nucleic acids, high affinity for DNA	ex491 em509	impermeant
Acridine orange	Miscellaneous	DNA/RNA	ex503 em530	impermeant
SYTOX Green	Cyanine stain	Nucleic acids	ex504 em523	impermeant
Thiazole orange	Cyanine stain	Primarily RNA	ex509 em533	permeant
Ethidium bromide	Intercalating stain	Nucleic acids	ex510 em595	permeant
Propidium iodide	Intercalating stain	Nucleic acids	ex535 em617	impermeant
Hydroethidine	Intercalating stain	DNA (live parasites only)	ex365/535 em435/610	permeant
SYTO-61	Cyanine stain	Nucleic acids	ex628 em645	permeant

**Table 3.1** A range of fluorescent dyes used to study malaria by flow cytometry. (After Grimberg, 2011)

The fluorescence-based options are an attractive alternative to the more traditional methods used for drug susceptibility testing. They appear to be devoid of many of the tedious technical complications that plague the microscopic, isotopic and ELISA-based methods. The current study will aim to contribute to the growing body of evidence that the SYBR Green-based microtitre plate and flow cytometry methods are indeed reliable.

## 3.2 METHODS

### 3.2.1 Optimisation of the SYBR Green Microtitre plate assay (SG-MicroPlate)

An experiment was set up to determine the correlation between fluorescence intensity and parasite density. In brief, spent medium was removed from a continuous culture of *P. falciparum*, strain K1, and the parasitaemia was determined by blood smear. The parasitised blood (50 % haematocrit) was then diluted with RPMI to a range of starting haematocrits (2.5 %, 5 %, 10 %, and >10 %) before being transferred in duplicate (200 µl per well) to column 1 of a 96 well plate. A non-infected blood sample (5 % haematocrit) was also added to column 1, in duplicate, and served as a negative control. Two-fold serial dilutions were then performed using 100 µl of RPMI (columns 1-12) leaving a final volume of 100 µl per well. Additional controls included wells containing 100 µl of either wash medium or complete medium. The SG-MicroPlate staining procedure was carried out as described elsewhere (Chapter 2 section 2.2.2).

### 3.2.2 Optimisation of the SYBR Green Flow Cytometry assay (SG-FCM)

In order to establish whether the SG-FCM method described by Karl *et al.*, (2009) was reproducible, an unsynchronised parasite culture (~2 % parasitaemia) was stained in accordance with the methods described in chapter 2 (section 2.2.3). Comparisons were made, in parallel, between flow cytometric data and confocal microscopy of Giemsa stained blood smears, slides were stained with both Giemsa and SYBR Green and with SYBR Green only (See Appendix I for slide staining procedures).

### 3.2.3 Comparison of the Giemsa microscopic test, SG-MicroPlate and SG-FCM

The reliability of the SG-MicroPlate and SG-FCM methods were evaluated in comparison to the Giemsa microscopic test, by determining the 50 % inhibitory values of dihydroartemisinin against the K1 strain of *P. falciparum*. Synchronised ring stage cultures were diluted with fresh culture media to approximately 1 % parasitaemia (5 % hematocrit) and divided into 12.5 ml culture flasks (5 ml final culture volume). Doubling concentrations (1.25 nM, 2.5 nM, 5 nM, 10 nM, 20 nM and 40 nM) were added to the flasks in duplicate. A drug-negative control was included and the cultures were incubated at 37 °C. The first 7 of 14 flasks were exposed to the various DHA concentrations for 48 h whilst the replica flasks were exposed for a 72 hr time period. The two time points were selected to allow the analysis of the effects of DHA on parasite maturation and multiplication respectively. Subsequent to drug exposure, the three assays were completed



in parallel using the optimised staining procedures (Chapter sections 2.1.6, 2.2.2 and 2.2.3). In brief, 4 ml of spent, complete medium was removed and Giemsa blood smears were prepared for each sample. The haematocrit was then restored (to 5%) with 4 ml of warmed washing media. Triplicate samples were taken for SG-MicroPlate (100  $\mu$ l) and SG-FCM (50  $\mu$ l) analysis. Three experimental repeats were completed. The percentage fluorescence (SG-MicroPlate) or percentage parasitaemia (SG-FCM and Giemsa Microtest) comparative to the infected control samples were used to compile data, from the separate experiments. IC<sub>50</sub> values were determined using regression analysis (As described in Chapter 2 section 2.2.4) and compared *via* one-way ANOVA (Graphpad prism 5.0).

### 3.2.4 Optimisation of 96 well plate culture of *P. falciparum*

Strain K1 parasites were diluted to ~1% parasitaemia, treated with a series of chloroquine (200 nM, 250 nM, 300 nM) and dihydroartemisinin (2.5 nM, 5 nM and 10 nM) concentrations. Triplicate samples (200  $\mu$ l) were transferred to a 96 well plate at 2.5 % or 5 % haematocrit. Flask cultures were maintained at 5% haematocrit and grown in parallel. Following 48 h of incubation Giemsa stained blood smears were prepared for each sample (see Chapter 2, Methods 2.16 for details). For SG-MicroPlate analysis the previously optimised method was employed. In brief, 100  $\mu$ l of medium was removed from each well prior to the addition of the SG-staining solution to reduce background fluorescence. One hundred microliters of the parallel flask culture treatments were also transferred to the plate. The final volume of each well was therefore 100  $\mu$ l, before the addition of 100  $\mu$ l of SG (in RPMI 1640). (Note this means that the haematocrit from the flask cultures was diluted 1:1 in the plate from 5 % to 2.5 % haematocrit). The original 200  $\mu$ l final volume of the plate cultures was restored with the addition of SG staining solution, and thus the same haematocrit was maintained. Staining and analysis procedures were consistent with (Chapter 2, Methods 2.2.2).

### 3.2.5 Optimisation of a medium-throughput SG-MicroPlate assay

The following experiment was conducted in order to establish whether the previously optimised SG-MicroPlate protocol should be modified to include additional washings steps, following parasite growth in a 96 well plate format. A continuous culture of *P. falciparum* was diluted to ~ 3 % parasitaemia. Three conditions were set up, with both infected and non-infected blood, as follows: (1) 5 % haematocrit blood suspended in complete media and serially diluted with complete media (CM/CM P and CM/CM B for parasitised and uninfected blood respectively). Note: this was consistent with previous

experiments as there remains 100  $\mu$ l of complete media in each well prior to the addition of SG. (2) 5 % haematocrit blood suspended in complete media and serially diluted with RPMI (CM/RPMI P and CM/RPMI B). (3) Parasitised and uninfected blood washed in RPMI and re-suspended in RPMI at 5 % haematocrit before being serially diluted with RPMI (RPMI/RPMI P and RPMI/RPMI B). Initially, 200  $\mu$ l of each sample (in duplicate) was transferred to the first column of a black-bottom 96 well plate and serially diluted (1:1) with either complete media or RPMI as indicated above. One hundred microlitres of each mixture was discarded from the last well (leaving 100  $\mu$ l per well). The SG-MicroPlate method was employed (Chapter 2, section 2.2.2)

### *3.2.6 Time-course analysis of DHA treatment using SG-FCM*

In order to investigate the parasites response to DHA treatment in more detail and further validate the reliability of the SG-FCM, for stage-specific detection, a time-course analysis of DHA exposure during erythrocytic cycle progression of K1 parasites was completed, alongside Giemsa imaging. The experiments were initiated at the late ring/early trophozoite stage. The first study compared untreated control samples with DHA treatment, for a short time-course at regular intervals (4, 8, 24, 28, 32, 48 hours). The second study expanded the time-course to 24, 48 and 72 hour intervals. Parasites were treated with the previously determined IC<sub>50</sub> concentration of DHA and analysed at each time point using the SG-FCM method (Chapter 2, section 2.2.3).

### *3.2.7 Stage-specific effects of DHA using SG-FCM*

Following the validation the SG-FCM technique, this assay was used solely to determine whether stage specific effects of DHA could be analysed. During previous experiments drugs were added when parasites were predominately at the ring stage. This meant that at the 48 and 72 hour time points the parasites had entered a subsequent cycle and were analysed at the ring and trophozoite stage respectively. This routine effectively missed any effects on the schizont stage. As the cytometer is capable of discriminating between mononuclear (ring and trophozoite) and multinuclear (schizont) parasites, the aim of this experiment was to analyze the parasites at the schizont stage and establish whether DHA had an effect on schizont formation. To ensure parasites were treated with DHA for the duration of an erythrocyte cycle, a range of DHA concentrations (0.63 nM, 1.25 nM and 2.5 nM) were added, and analysed at schizont stage (45 hr incubation). Parasitaemia was estimated as described previously (Chapter 2, section 2.16).

3.2.8  $IC_{50}$  determination of existing antimalarials against K1 parasites

Following preliminary screens (data not shown), refined dose ranges were selected for atovaquone, chloroquine, dihydroartemisinin and proguanil to permit accurate  $IC_{50}$  calculation against the *P. falciparum* strain K1. The dose range selected for each antimalarial is shown in Table 3.2.

Atovaquone (nM)	Chloroquine (nM)	Dihydroartemisinin (nM)	Proguanil ( $\mu$ M)
0.64	100	1.25	3.77
1.28	150	2.5	7.54
2.56	200	5	15.08
5.11	250	10	30.15
10.22	300	20	60.31
20.45	350	40	120.61
40.89	----	----	241.22

**Table 3.2** Drug concentration ranges selected to obtain dose response curves for atovaquone, chloroquine, dihydroartemisinin and proguanil against *P. falciparum* strain K1.

Trophozoite stage parasites (0.5- 1%) were treated for 48 hours and parasitaemia was determined using the SG-FCM. Data were analysed in accordance with Chapter 2, sections 2.2.3 and 2.2.4.  $IC_{50}$  estimates were compared with those reported in the literature.

### 3.3 RESULTS

#### 3.3.1 Optimisation of the SG-MicroPlate assay for malaria

The fluorescence intensity of SYBR Green 1 nucleic acid dye was measured, for a range of parasite density dilutions, using the SG-MicroPlate assay. The results showed that as parasite density became more diluted, fluorescence intensity decreased. The results also indicated that complete medium, not washing medium or non-infected blood, had an inherently high level of fluorescence (Figure 3.1).

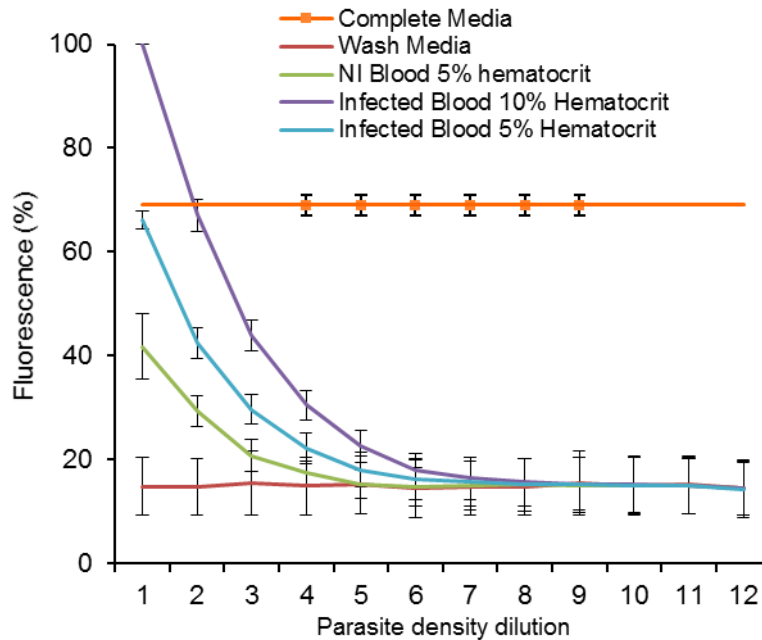
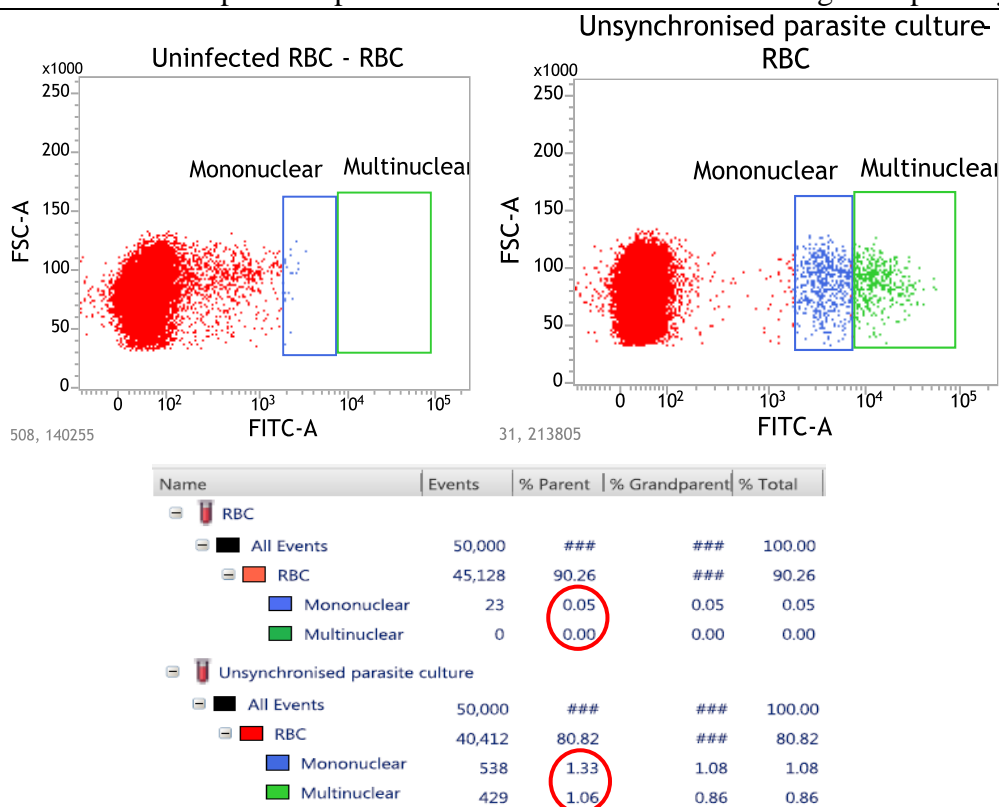


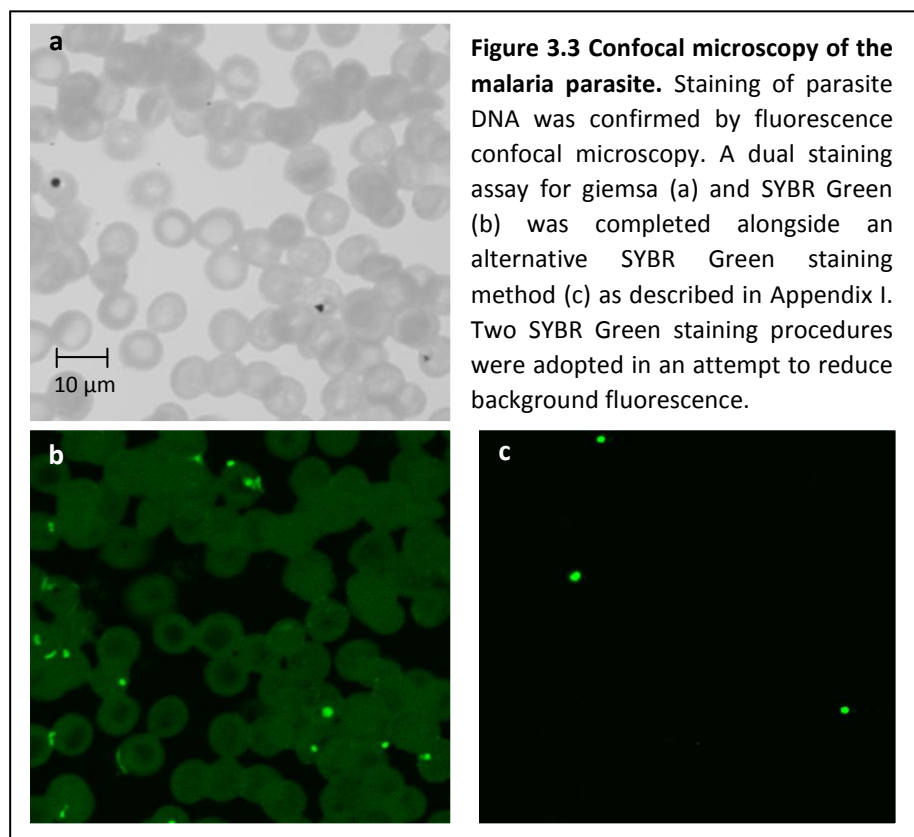
**Figure 3.1 the effect of parasite density dilution on fluorescence intensity of SYBR Green 1.** Parasitised blood (approx 3%) was diluted with RPMI (wash media) to either a 10 % or 5 % starting haematocrit. The infected samples were further (1:1) diluted 12 x alongside a non-infected blood control sample (5 % starting haematocrit) and subjected to the SG-MicroPlate assay. Complete media and RPMI served as controls. Error bars represent the standard error of two replica experiments

#### 3.3.2 Optimisation of the SYBR Green Flow Cytometry assay (SG-FCM)

A comparison of infected and non-infected blood samples showed that the SYBR Green 1-based flow cytometry assay can detect parasite DNA within the parasitised red blood cells (Figure 3.2). As demonstrated previously by Karl *et al.*, (2009), the unsynchronised culture presented two populations of varying fluorescence intensity on the cytometer output showing good labelling and differentiation of mononuclear and multinuclear parasites (Figure 3.2 b). The BDFACSverse software can be used to accurately determine parasitaemia by recording the percentage of infected cells relative to the total number of events recorded (red blood cells) (Figure 3.2 c).



**Figures 3.2 Comparison of infected and uninfected blood samples using SG-FCM.** Scatterplots based on forward scatter (FSC-A) and fluorescein isothiocyanate (FITC-A) (490/520) are examples of an uninfected blood sample (a) and an unsynchronised parasite culture (b). The gating strategy, adapted from Karl *et al.*, (2009), was employed to distinguish between mononuclear (rings and trophozoites) and multinuclear (schizonts) parasite stages. The % grandparent represents the % of mononuclear and multinuclear cells relative to the total number of events recorded. The % parent reflects the % of gated, uniform red blood cells displaying mononuclear and multinuclear fluorescence. The BD FACSVerse software program was used to determine the percentage of parasitised cells (c).



Fluorescence confocal microscopy images confirmed that SYBR Green 1 stained parasite DNA inside the erythrocytic cells (Figure 3.3). All samples were prepared from the same culture of *P. falciparum* strain K1 parasites. The dual giemsa and SYBR Green staining procedure (Appendix I a and b) permitted concurrent images (Figure 3.3 a and b) but showed a high level of background fluorescence and staining artefacts. The SYBR Green staining method (Appendix I c) used for Figure 3.3 c reduced background fluorescence and revealed parasitaemia estimates consistent with the giemsa staining (figure 3.3 a).

### 3.3.3 Comparison of the Giemsa microscopic test SG-MicroPlate and SG-FCM

SYBR Green flow cytometric (SG-FCM), micro titre plate (SG-MicroPlate) and traditional Giemsa microscopic (Giemsa) assays were compared by parallel analysis of the dihydroartemisinin dose-response for synchronised, ring stage, K1, *P. falciparum* cultures (Figure 3.4). IC<sub>50</sub> values for cultures sampled at 48 and 72 hr post drug exposure were determined (Table 3.3) and compared, using a one-way ANOVA (Graphpad prism). There were no significant differences between the three assays and although the IC<sub>50</sub> values appear to be consistently higher at 72 hours than at the 48 hour time point for all 3 assays (Figure 3.4), this difference was also shown not to be statistically significant. Exemplar Giemsa images and flow cytometer output can be found in Appendices II and III.

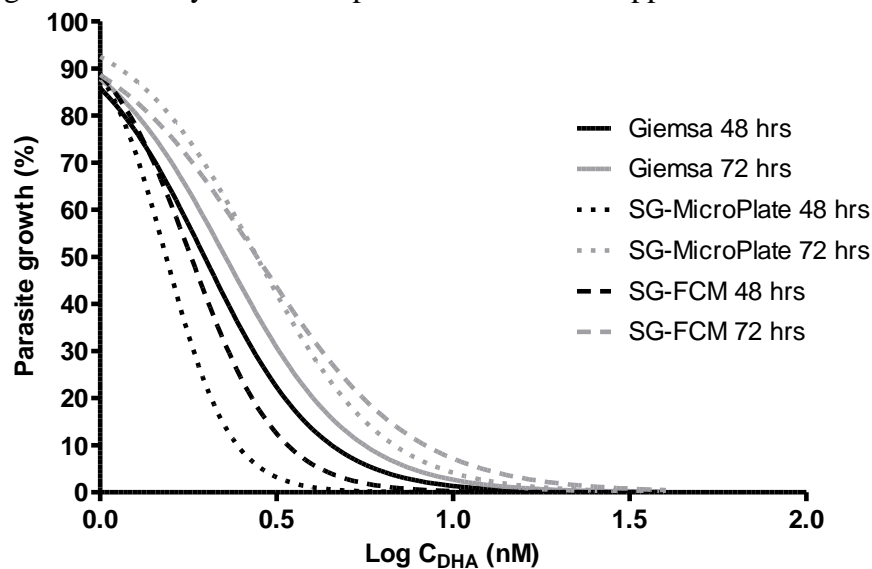


**Figure 3.4** Dose response curves for dihydroartemisinin against the K1 strain. A set of three parallel assays: namely, Giemsa microscopic test (Giemsa), SYBR Green microtitre plate assay (SG-MicroPlate) and the SYBR Green flow cytometer assay (SG-FCM). Data is from three independent cultures exposed to DHA for 48 or 72 h.

Time points	Giemsa IC <sub>50</sub> (nM)	SG-MicroPlate IC <sub>50</sub> (nM)	SG-FCM IC <sub>50</sub> (nM)
48 h	1.976 (1.60-2.45)	1.54 (1.12-2.11)	1.81 (1.30-2.53)
72 h	2.264 (1.85-2.78)	2.781 (2.26-3.42)	2.785 (1.87-4.14)

**Table 3.3** *In vitro* IC<sub>50</sub> (nM) sensitivity of the K1 strain to dihydroartemisinin at 48 and 72 h. Three assays were used to determine parasitaemia (i) Giemsa Microscopic test (ii) SYBR Green MicroPlate assay and (iii) the SYBR Green flow cytometer assay. Numbers in brackets are indicative of 95 % confidence intervals.

### 3.3.4 Optimisation of medium-throughput SG-MicroPlate assay for malaria

The Giemsa results of the initial comparison between plate growth and flask growth indicate that an equivalent growth rate can be achieved in a 96 well plate format, compared to the flask culture (Figure 3.5 a). A clear dose-response for chloroquine and dihydroartemisinin was also observed. These findings, however, are not mirrored in the SG-MicroPlate assay results that were completed in parallel (Figure 3.5 b). It appears that in the latter assay, only media composition and the amount of haematocrit have an effect on the absolute fluorescence reading obtained, and not parasite growth. The non-infected blood control also displayed a relatively high level of fluorescence.

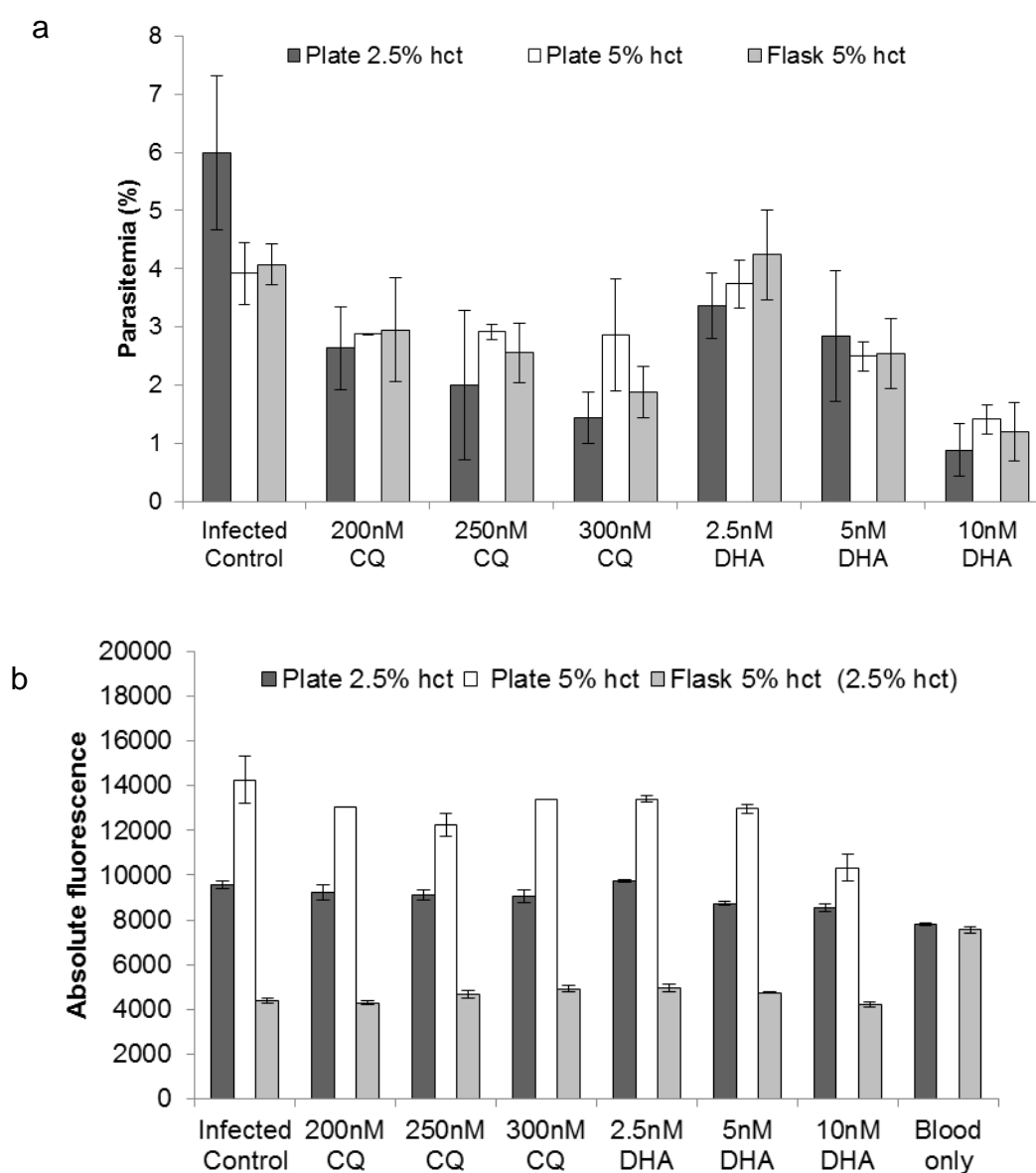


**Figure 3.5** Comparison of parasite growth in a 96 well plate and 12.5 cm<sup>3</sup> flasks following exposure to a 3 point dose series of chloroquine and dihydroartemisinin. Parasites were grown 96 well plate format at either 2.5 % or 5 % haematocrit or in a flask at 5% haematocrit. Viability was analysed using the Giemsa microscopic test (a) and the SG-MicroPlate method (b). For SG-MicroPlate analysis the flask culture was analysed at 2.5 % haematocrit (although grown at 5 %).

In order to overcome background fluorescence problems associated with the complete media, infected and non-infected blood was suspended and serially diluted in either complete media or RPMI (Figure 3.6). In the CM/CM conditions (suspended in complete media, diluted with complete media) there was a relatively high level of fluorescence irrespective of whether the blood was infected or non-infected. In the CM/RPMI condition (suspended in complete media, diluted with RPMI) a density dependent effect was observed. However, although the infected blood displayed higher fluorescence in this condition than the non-infected counterpart, a density-dependent effect was still apparent in the non-infected blood condition. In the RPMI/RPMI condition (suspended in RPMI, diluted with RPMI) the parasite density dilution effect observed in the infected blood was not seen in the non-infected blood.

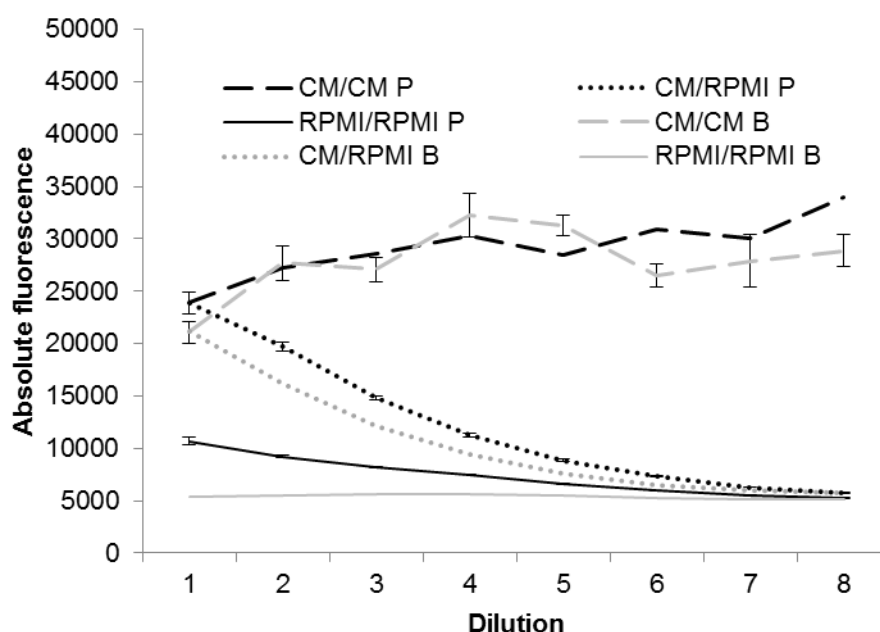
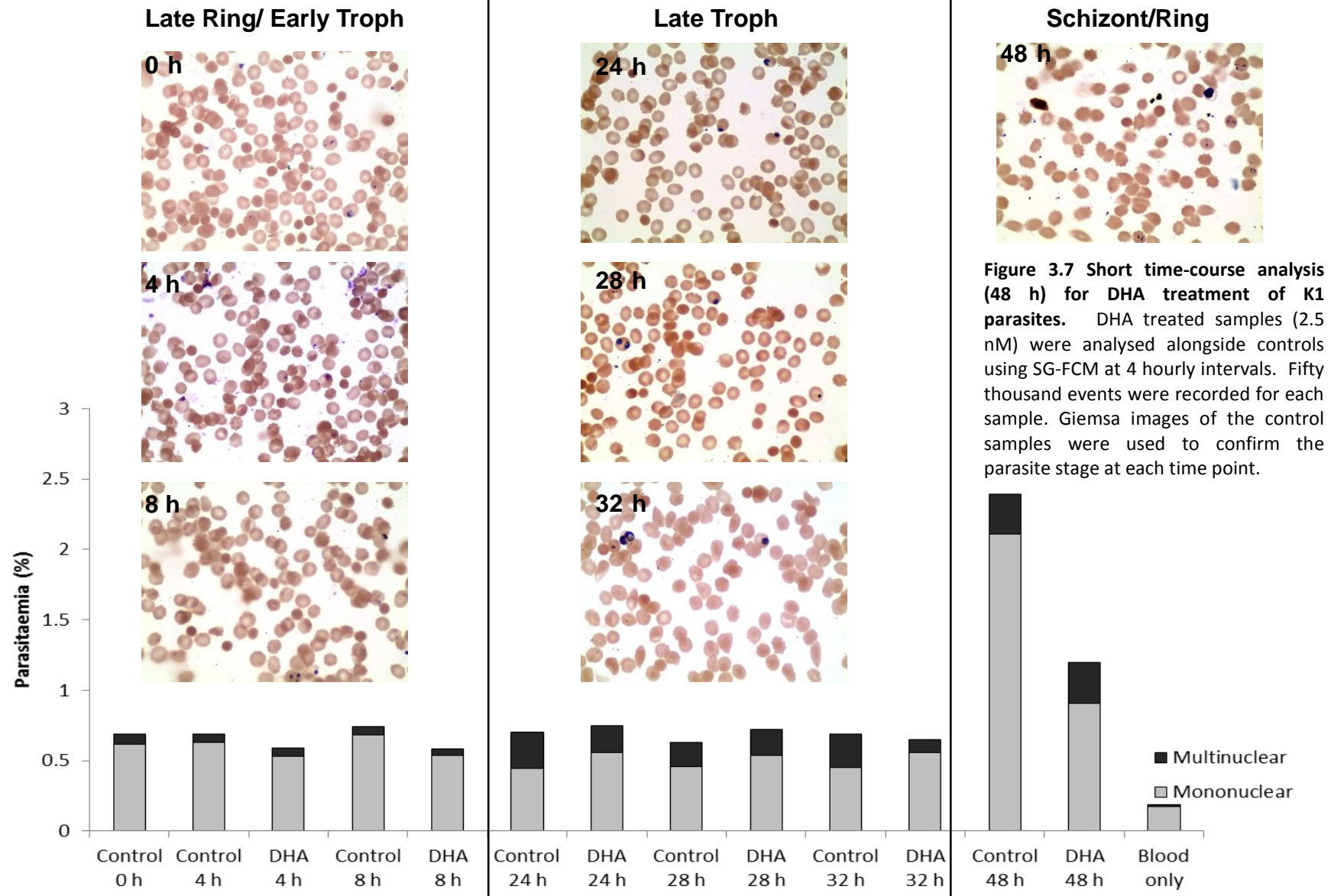


**Figure 3.6 The effects of complete media on the SG-Microplate method.** The serial dilution of infected blood (p), starting at 3 % parasitaemia, and uninfected blood (b) was analysed using the SYBR Green MicroPlate assay. Comparisons were made between blood suspended and diluted in either complete media /complete media (CM/CM), complete media/RPMI 1640 (CM/RPMI) or RPMI 1640/RPMI 1640 (RPMI/RPMI) respectively.

### 3.3.5 SG-FCM for detailed in vitro investigations of parasite killing

#### 3.3.5.1 Time-course analysis of DHA treatment





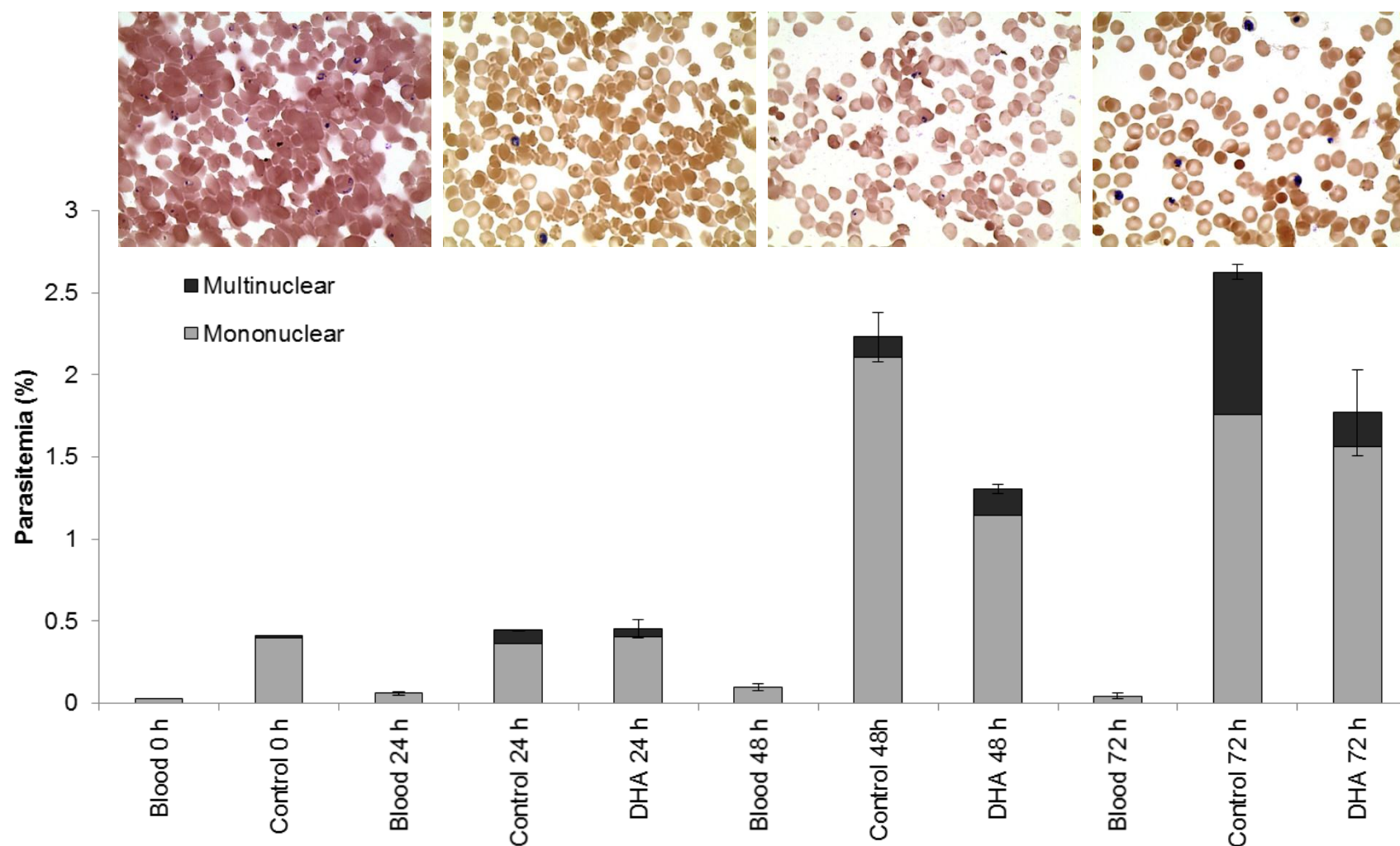


**Figure 3.8** Extended time-course analysis of *P. falciparum* strain K1 exposure to DHA. Control and DHA  $IC_{50}$  treated samples were analysed at 24h intervals for a 72 hour time-course. The percentage of mononuclear and multinuclear cells were recorded using SG-FCM. Error bars represent standard error of the mean (SEM) for duplicate samples. Giemsa imaging was used to confirm the parasite stage at each analysis point.

Time-course analysis data showed that drug induced alterations in parasitaemia could not be detected until parasites had entered a subsequent erythrocytic cycle (Figures 3.7 and 3.8). Indeed, no differences were detected during the short time-course until the schizont to ring transition was completed at 48 h (Figure 3.7). These findings were mirrored by the extended time-course at 48 h. Notably, there was a comparable rise in parasitaemia in both control and treated samples by the 72 hr time point while DHA-induced growth inhibition remained relatively constant (Figure 3.8). The results also appear to show a delay in parasite progression into multinuclear forms, particularly seen at the 32 hour reading (Figure 3.8).

### 3.3.5.2 Stage-specific effects of DHA

The SG-FCM assay was used to assess stage-specific effects of DHA and also effects on schizont development. The results show that the SG-FCM method has the potential to analyse stage specific effects during the course of drug treatment. The results also indicated that higher concentrations of dihydroartemisinin had a more pronounced effect on the disruption of schizont formation (Figure 3.9).

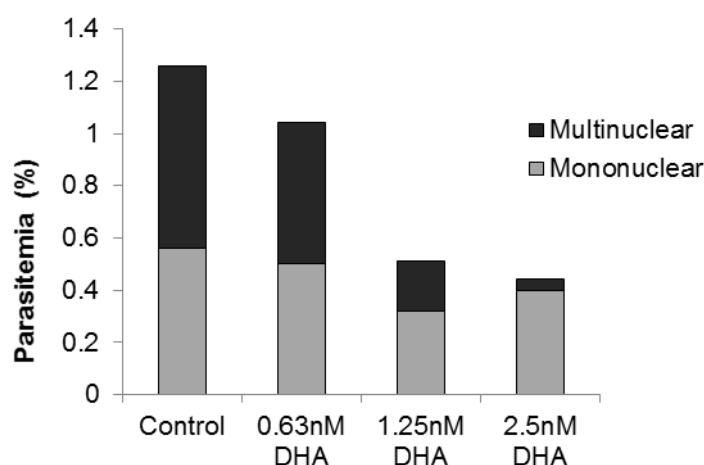
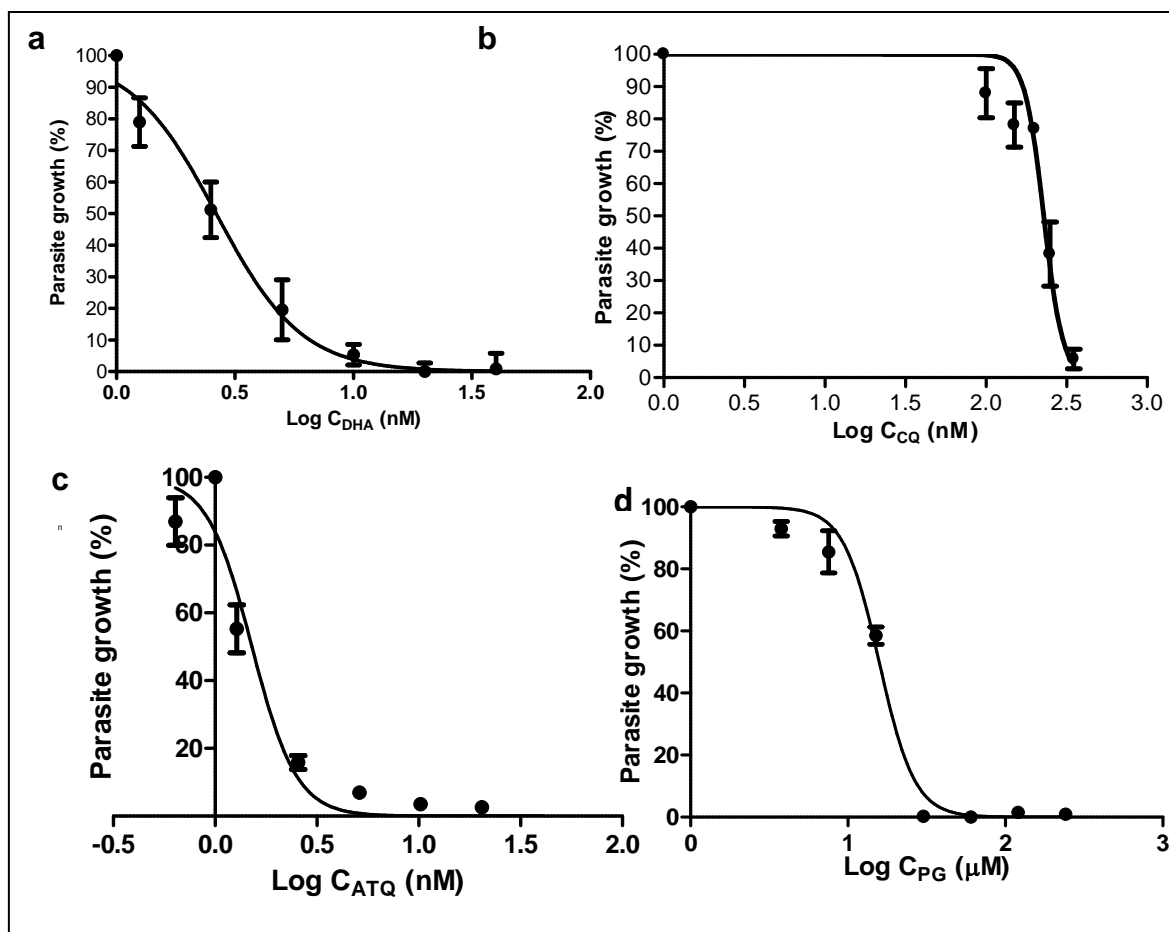


**Figure 3.9 The effects of dihydroartemisinin on schizont development.** A range of DHA concentrations were added at the schizont stage and the culture was incubated for 45 h under the conditions described previously. At the 45 hr time point the SYBR Green 1-based flow cytometer method was used to analyse the effects of DHA. Data are based on a single replica.

### 3.3.5.3 Determination of baseline $IC_{50}$ values for existing antimalarials

The dose-response curves generated (GraphPad Prism 5.0) using nonlinear regression analysis are shown in Figure 3.10. The  $IC_{50}$  values obtained for atovaquone, chloroquine, dihydroartemisinin and proguanil are displayed alongside those reported in the literature (Table 3.4). All values presented in the current study are within the range of those

determined elsewhere, although, they are consistently at the lower end of the scale (Table 3.4).



**Figures 3.10** Dose response curves for dihydroartemisinin (a), chloroquine (b) atovaquone and proguanil. Trophozoite stage parasites were treated for 48 hours with pre-selected dose ranges. The normalised dose response for each compound was plotted over log transformed drug concentrations.  $IC_{50}$  values were determined using nonlinear regression analysis (Graphpad prism 5.0). Error bars represent the standard error of the mean (SEM) for triplicate data.

Antimalarial	$IC_{50}$ against <i>P. falciparum</i> K1		Reference
	Current study	Literature reports	
Dihydroartemisinin	2.62 nM	$3.15 \pm 1$ $1.67 \pm 0.43$	Zongo <i>et al.</i> , 2011 Fivelman <i>et al.</i> , 2004
Chloroquine	228 nM	$255.86 \pm 65.58$ $266.58 \pm 15.06$	Vivas <i>et al.</i> , 2007 Fivelman <i>et al.</i> , 2007
Atovaquone	1.52 nM	$2.32 \pm 1.35$ $2.41 \pm 0.51$	Vivas <i>et al.</i> , 2007 Fivelman <i>et al.</i> , 2004
Proguanil	15.79 $\mu$ M	$34.27 \pm 2.894$	Fivelman <i>et al.</i> , 2004

**Table 3.4** Comparison of the  $IC_{50}$  values determined in the current study for existing antimalarials with values reported elsewhere in the literature.

### 3.4 DISCUSSION

#### *3.4.1 Fluorescence-based drug susceptibility assays for malaria*

The versatile fluorescent DNA stain-based technique is ideally suited for use in malaria studies (Grimberg, 2011). The FCM method tackles many of the aforementioned problems posed by pre-existing assays; it is objective, rapid, simple and labour-saving (Grimberg, 2011; Saito-Ito *et al.*, 2001). The procedure can be completed in a single step, this being the addition of the fluorescent dye. Washing and fixation are optional, dependent on the dye being used, and the operating procedures of the machine (Karl *et al.*, 2009; Malleret *et al.*, 2011; Grimberg, 2011). Despite numerous advantages, the use and popularity of the technique has been limited by the cost of the flow cytometry equipment, more so in the developing world, and by concerns about insufficient sensitivity. The latter, is possibly because the fluorescence intensity of some stains is not high enough to overcome auto-fluorescence, particularly in fixed samples (fixed red blood cells auto-fluoresce) (Saito-Ito *et al.*, 2001). For this reason, selection of a highly fluorescent dye, such as SYBR Green 1 is of paramount importance. Indeed, the robust data generated from both the SG-MicroPlate and SG-FCM assays performed here indicate that SYBR Green 1 is capable of overcoming background fluorescence, even in fixed samples. Two methods of staining and analysis with SYBR Green were optimised in the current study for different purposes. The SG-MicroPlate assay, for use as a medium-throughput preliminary screen, and the SG Flow cytometry-based method, for more accurate second-phase definition of selected hit compounds.

#### *3.4.2 Validation of SYBR Green staining procedures*

Initially optimisation of SG-based methods focussed on the validation of the staining procedures described by Karl *et al.* (2009). Parasitised blood was used to show that a density dilution effect could be detected using the SG-MicroPlate staining and analysis methods. Although the complete media displayed a high level of inherent fluorescence, the preliminary work indicated that the removal of 100  $\mu$ l of complete media, leaving 100  $\mu$ l per well (subsequently diluted 1:1 with the SG-staining solution), reduced background effects and permitted reproducible sensitivity. An unsynchronised culture was used to show that adoption of the SG-FCM method can provide accurate parasitaemia estimates and stage-specific information. Confocal microscopy was also used to visualize and confirm the staining of parasites within red blood cells. The second-phase of staining validation used the dihydroartemisinin dose response to compare the SG-based methods

with each other and with the traditional Giemsa microscopic test. Consistent with the finding presented here, Karl and colleagues (2009) showed that the SG-FCM method compared well with the 4 other *in vitro* assays; namely, the hypoxanthine incorporation assay, the pLDH ELISA, the SG-MicroPlate assay and the WHO microscopic test (Karl *et al.*, 2009). The particularly high concordance with microscopy, demonstrated here and in previous studies, is noteworthy as it is the only other method to count parasites directly (Bei *et al.*, 2010; Malleret *et al.*, 2011). Like the microtest, the FCM method is capable of resolving single, double or triple infections (Bei *et al.*, 2010). In fact some argue that it may even be more accurate, as early ring stage parasites can often be overlooked by microscopy (Saito-Ito *et al.*, 2001). In the current study, the compiled data for the Giemsa microscopic test shows minimal variation between experiments. However, the inherent subjectivity of the assay means that variation between different individuals and observer error for inexperienced users is likely. Such potential issues are absent from the more objective SG-based methods. Unlike the Giemsa microtest the FCM, however, is incapable of distinguishing between triple infections and early trophozoites (Bei *et al.*, 2011). Fortunately, for drug susceptibility screens, these factors are not problematic as the assay is mainly concerned with parasite multiplication or maturation via 48 hr or 72 hr assays respectively. Parasite multiplication is defined as the parasite's ability to grow and undergo nuclear division during schizont formation. Maturation, on the other hand corresponds to successful completion of the erythrocyte cycle in the presence of the test drug and also successful invasion of new red blood cells to begin the subsequent erythrocytic cycle (Grimberg, 2011). Overall, the dose response data and IC<sub>50</sub> values obtained for SG-based methods were in agreement with each other and with those obtained from the Giemsa microtest. There was a slight shift in the values obtained between the 48 and 72 hour time points but this was not shown to be statistically significant.

#### 3.4.3 SG-MicroPlate optimisation

Once the staining procedure had been validated, using flask cultures of *P. falciparum*, it was necessary to optimise growth and drug treatment in a 96 well plate format to achieve medium-throughput efficiency for the SG-MicroPlate assay. In order to overcome issues with poor parasite growth in the 96 well plates, gas exchange was improved through the use of gas permeable films and replacement of old gassing chambers. Different haematocrits were also selected to determine the optimal plate growth conditions. The Giemsa results indicated that parasite growth was sufficient at both the 5 % and 2.5 %

haematocrits and clear dose response to both antimalarials used in the study were observed. At the lower haematocrit, however, plate growth was either equal to or greater than flask growth at the standard 5 % haematocrit. Furthermore, there appeared to be no benefit bestowed by a 5 % haematocrit condition in the plate, even though the starting number of parasites would have been double. Taken together the results suggested that 2.5 % haematocrit may be optimal in the plate system. This is consistent with the literature, lower haematocrits are commonly used for plate growth experiments to permit a better surface area to blood volume ratio. This allows more efficient gas exchange and nutrient acquisition between parasites and the above culture media (Karl et al., 2009; Vossen et al., 2010). A further issue was that there was a discrepancy between SG-MicroPlate and Giemsa results as a comparable dose response pattern was not observed with the SG-MicroPlate readings. Despite previous in-house optimisation of the SYBR Green MicroPlate assay, other experiments have shown inconsistencies between the SG-MicroPlate and both the Giemsa and Flow cytometer assays (data not shown). The SG-Microplate data only showed absolute fluorescence differences between the variable haematocrits (Plate 2.5 % and Plate 5 %) and varying amounts of complete media (Plate 2.5 % and Flask 2.5 %). The earlier experimental method (Figure 3.1) that showed a parasite density dilution effect, represented by the CM/CM condition, also displayed a high level of background fluorescence for both infected and non-infected blood in the latter study, that overcome any SG staining that represented bound parasite DNA. One possibility was that the albumin from bovine serum (Sigma) used in the latter experiments contributed to higher background fluorescence than the AlbuMAX (lipid rich albumin from bovine serum, Gibco) used in the initial optimisation work. The trend observed in the CM/RPMI condition most likely represented a serial dilution of complete media with RPMI. However, the clear difference in the level of absolute fluorescence between the infected and non-infected blood indicated notable detection of parasite DNA. The RPMI/RPMI condition showed that when all of the complete media had been removed, the dilution of non-infected blood had no effect on fluorescence intensity. Therefore, the modest density dilution effect observed in infected blood series (RPMI/RMPI P) accurately represented parasite DNA. It was also possible that in the original SG-MicroPlate protocol the DNA from dead or dying parasites, outside the erythrocytes, may be recorded as live. Washing would also help reduce this confounding factor, improving the accuracy of the SG-MicroPlate assay and concordance with Giemsa staining and SG-FCM. Taken together, the data highlighted the importance of the inclusion of washing

steps in the SG-MicroPlate protocol in order to achieve true parasite density readings. Indeed, variable volumes of complete media could drastically alter the results this is particularly important for growth inhibition studies where parasitaemia may be low.

#### 3.4.4 SG-FCM for detailed *in vitro* investigations of parasite killing

Unlike any other currently available objective method, the unique advantage of the SG-FCM technique is that it offers the opportunity to gain more information about intra-erythrocytic parasite growth and development and to accurately monitor stage-specific effects in response to drug treatment (Izumiya *et al.*, 2009; Grimberg, 2011.) Indeed, the corroboration of the SG-FCM data and Giemsa images during time-course analyses provided further confirmation that the method can be used to accurately monitor mononuclear and multinuclear parasite transitions. The results of the current time-course and stage-specific investigations were in agreement, showing delayed progression to schizont formation under DHA drug pressure. The stage-specific data clearly demonstrated that this disruption in schizont formation is dose dependent. This is in line with previous findings that suggest artemisinins arrest parasite development at the ring stage (Klonis *et al.*, 2011). However, although differences in stage-specific detection can be reported here, stage-specific inhibition cannot be inferred, as the drug was present throughout the erythrocytic cycle and transition through parasite stages. To obtain true stage specific-data using the SG-FCM method any future work should direct drug exposure against a single parasite stage. This could be achieved by altering the treatment regime to a short 6 hr window of drug exposure, followed by washing, removal of the drug and subsequent re-incubation to permit completion of the 48 hr erythrocytic cycle. Wein *et al* (2010) suggest that a 72 hour treatment period is needed to obtain reliable data using the SG-based methods. Conversely, the data from both the time-course analysis and IC<sub>50</sub> determination of four existing antimalarials: namely, atovaquone, dihydroartemisin, chloroquine and proguanil, suggests that so long as the 48 hr treatment period spans the transition into the subsequent erythrocytic cycle, accurate drug inhibition and IC<sub>50</sub> data can be generated. Data presented here, irrespective of whether parasites were grown under flask or plate conditions (all analysed using SG-FCM) shows that 48 hr exposure initiated at trophozoite stage yields the expected dose response for the four existing antimalarials selected. The IC<sub>50</sub> values obtained were all within the range of the values reported elsewhere in the literature. The advantages of this treatment protocol are that it allows all stages of the parasite to be exposed to the drug, permits entry into a subsequent erythrocytic cycle and



ensures that early ring stages are not overlooked as all parasites should have entered the trophozoite stage at the time of the analysis. The data presented, therefore, indicates that parasite maturation rather than treatment period is important for analyzing the efficacy of antimalarials with different modes of action. Indeed focusing on multiplication only may overlook drugs with novel modes of action, for example targeting other organelles such as those involved in invasion. It is evident that a number of findings presented here highlight the importance of timing in the basic drug susceptibility assays. Firstly, the comparison study of the Giemsa microscopic test, the SG-MicroPlate and the SG-FCM assays revealed a slight shift in  $IC_{50}$  values between the 48 h and 72 h time points. Secondly, during the extended time-course analysis there was an increase in parasitaemia from the 48 hr to the 72 h reading. This suggests that some parasites may have become unsynchronized and had not entered the subsequent erythrocytic cycle at 48 hours, but had successfully invaded new erythrocytes by the 72 h time point. Thirdly, without alterations in the treatment and analysis protocol, the dose-dependent effects of DHA on schizont formation would have been missed.

#### *3.4.5 Conclusion*

In conclusion the above findings indicate that various factors such as: the parasite stage at which the drug is added, the drug treatment period, and the stage at which samples are taken for analysis could all affect the results and the detail of the information obtained from individual experiments. Evidently, consistency should be maintained between replicate experiments and the above mentioned variables considered when comparisons are drawn across different studies. The results of the current study empirically confirm that the SG-based methods are not only reliable but also offer fast, simple, quantitative, parasite detection devoid of human error and bias. Additionally, the more accurate SG-FCM option also offers the opportunity to obtain stage-specific information. The low cost of the reagent and the availability of the both the fluorescent plate reader and flow cytometer made the technique ideal for use in our laboratory. The proposed workflow was, therefore, to adopt both SG-based methods. The modified SG-MicroPlate assay would be employed, in accordance with the improved protocol to overcome Albumin-related fluorescence, for the preliminary screening of FDA approved compound repositories. The SG-FCM would be used, subsequently, for more detailed second-phase characterisation of antimalarial hits.

## CHAPTER 4

---

### SCREENING FDA APPROVED DRUG LIBRARIES FOR ANTIMALARIAL ACTIVITY

#### 4.1 INTRODUCTION

Since the late 2000's, the prospect of drug repositioning for malaria has received increasing attention (Guiguemde *et al.*, 2012). One of the earlier studies by Weisman *et al.* (2006), served as proof-of-concept that novel chemical scaffolds, capable of inhibiting the malaria parasite, could be identified from existing compound libraries. Using the YOYO-1 microplate method, the whole-parasite study screened 2,160 compounds and uncovered 36 novel inhibitors of *P. falciparum* (strains 3D7 and W2). Of these, 19 were approved therapeutics. The antimalarial hit list was further refined based on the drug delivery route and the closeness of the effective dose (EC<sub>50</sub>) against *P. falciparum*, to the current safe therapeutic window in humans. From these, 5 compounds: namely, propafenone, thioridazine, chlorprothixene, perhexiline and azlocillin were proposed as feasible candidates for further development (Weisman *et al.*, 2006).

Concurrently, another group, Chong *et al.* (2006) screened the Johns Hopkins Clinical Compound Library using the (<sup>3</sup>H)-hypoxanthine<sup>1,2</sup> incorporation assay. They selected 1,937 FDA approved drugs plus 750 approved for use outside America or undergoing Phase 2 clinical trials. Of these, 189 compounds displayed >50% inhibition at a concentration of 10 µM against *P. falciparum* strains 3D7, Dd2 or ItG. Further refinement came from the elimination of compounds that were cytotoxic drugs, topical therapies, known antimalarials and compounds previously shown to have antimalarial activity (Chong *et al.*, 2006). From the most potent of remaining compounds that offered potential starting points for lead optimisation, the group deemed the anti-histamine astemizole, as the most promising candidate. This compound is structurally related to the 4-aminoquinolines and likely to act *via* the inhibition of heme crystallization, therefore, not representing a completely novel antimalarial class (Chong *et al.* 2006; Lotharius *et al.*, 2014). However, the effectiveness of the compound against drug resistant strains *in vitro*, and against 2 mouse models in the 4-d suppression test *in vivo* raised optimism. Unfortunately, side effects were a concern as the compound had been withdrawn from its previous use due to adverse cardiovascular side effects linked specifically to QTc prolongation. The group emphasised that the drug was widely used before its withdrawal, which was largely due to the availability of safer alternatives. They also supposed that its

use for malaria would be relatively acute and intermittent when compared with the continuous everyday use as an anti-histamine (Chong *et al.*, 2006). A recent article by Lotharius *et al.*, (2014) suggests that the compound is no longer under consideration for repositioning in malaria, while reporting data regarding its cardiotoxicity and withdrawal from use in 1999. In fact, the discovery of its antimalarial properties was not until 2006 (Chong *et al.*, 2006) and the relevant safety data for doses applicable to malaria have not yet been published. Furthermore, recent studies have reported submicromolar potency ( $<10\text{ }\mu\text{M}$ ) of the compound against *P. berghei* liver stages (Derbyshire *et al.*, 2012) and the effectiveness of a chloroquine-astemizole hybrid molecule against CQ resistant strains both *in vitro* and *in vivo* (Musonda *et al.*, 2009), indicating that the molecule is not yet completely out of favour.

A larger screen, by Baniecki and colleagues (2007), investigated 79,000 small molecules for antimalarial activity using the fluorescent dye 4',6-diamidino-2-phenylindole (DAPI) plate reader method as a reporter of parasite growth. They identified 181 hits, defined as inhibiting 90 % of parasite growth, against either single or multiple parasite strains (Dd2, HB3 and 3D7) at a concentration of  $6\text{ }\mu\text{M}$  (Baniecki *et al.*, 2007).

The Lucumi group (2010) reported a high-throughput screening initiative on three compound libraries, namely the Library of Pharmaceutically Active Compounds (LOPAC), the library from the National Institute of Neurological Disorders and Stroke (NINDS) and the Library of uncharacterised compounds (Chembridge). A 384-well luciferase screen on 12,320 compounds, at  $5.5\text{ }\mu\text{M}$  concentrations, yielded a total of 163 compounds exhibiting a reduction in parasitaemia  $\geq 85\%$  in the drug sensitive 3D7 strain of *P. falciparum*. Through structural clustering, the group was able to identify 12 novel scaffolds. A 1,4-naphthoquinone moiety, similar to atovaquone, was deemed the most interesting chemotype because of its novel mechanism. They also propose the histamine antagonist, zolotadine, as an attractive lead (Lucumi *et al.*, 2010).

The success of these initial screens prompted a wide-scale drug discovery initiative involving three academic and corporate institutions: namely, The St Jude's children research hospital (Guiguemde *et al.*, 2010) GlaxoSmithKline (Gamo *et al.*, 2010) and Novartis (Plouffe *et al.*, 2008).

The St Jude Children's Hospital screened a total of 309,474 compounds against the *P. falciparum* strain 3D7 at fixed drug dose of  $7\text{ }\mu\text{M}$ , using various fluorescent-based DNA

stains to evaluate parasite growth (namely, YOYO-1, SYBR Green 1 and DAPI). This gave 1,300 hits with >80 % activity. The hit compounds were subjected to dose-response screens against multi-drug resistant strains, as well as counter screening against mammalian cell lines HepG2 and BJ, to determine toxicity. Cut offs were set at < 2 $\mu$ M effective dose (EC<sub>50</sub>) (against 3D7 or K1) and a  $\geq$  10 fold increase was considered a safe therapeutic window against the mammalian cell lines. A structurally diverse set of compounds was selected from the hits for further interrogation. Of the 172 validated hits, 58 displayed similar potencies ( $\leq$  3-fold shift in EC<sub>50</sub>) when analysed with a panel of seven *P. falciparum* strains with different chemo sensitivities. Reverse chemical genetic profiling showed that 80 % represented novel modes of action with regard to three well characterised antimalarial targets: Pyrimidine biosynthesis (specifically inhibition of the *P. falciparum* dihydroorotate dehydrogenase enzyme, PfDHOD), inhibition haem detoxification, which is usually converted to inert crystallised haemozoin by the parasite, using the *in vitro* haemozoin formation assay, and haemoglobin degradation through the analysis of *P. falciparum* falcipain-2 (PfFP-2) inhibition, an enzyme which is reported to have a critical role (Guiguemde *et al.*, 2010; Guiguemde *et al.*, 2012).

Gamo and colleagues (2010) at GSK screened a chemical library, the Tres Cantos Animalarial Compound Set (TCAMs) of nearly 2,000,000 compounds against *P. falciparum* strains 3D7 and Dd2. They identified 13,533 and 8,000 compounds capable of inhibiting parasite growth by 80 % and 50 % at 2  $\mu$ M, in the susceptible and multi-drug resistant strains respectively. Out of the verified hits only 15 % were considered cytotoxic by 50 % inhibition of the HepG2 cell line at 10  $\mu$ M. Encouragingly, the majority of the compounds are new to the malaria research community (82 %) and the data has been released into the public domain to promote further investigation and lead compound identification (Gamo *et al.*, 2010; Guiguemde *et al.*, 2012).

Novartis have been involved in various screening and lead optimisation programmes with numerous academic collaborators. One of their initial large scale screens identified ~6,000 possible drug discovery leads from a collection of 1.7 million compounds in the Genomics Institute of the Novartis Research Foundation (GNF) chemical library. The library was reported to have drug-like characteristics and high conformity to Lipinski's rule of 5. SYBR Green 1 staining was used to define hit compounds that displayed 50 % inhibition at a concentration of < 1.25  $\mu$ M against *P. falciparum* strain 3D7. Plouffe *et al.*, (2008) then employed *in silico* activity profiling to reveal potential mechanism of action of hit

compounds by adopting a guilt-by-association approach. Information was gathered from previous evaluations of the compounds across 131 cellular enzymatic assays. This helped inform cross-reactivity/toxicity information and the prediction of pathways and targets. Pooling of data, and discovering patterns amongst immense biological data sets, may be an effective tool in modern drug discovery. The expanded chemical space occupied by the 6,000 novel inhibitors offered the opportunity to discover a new-generation of antimalarials (Plouffe *et al.*, 2008). Since the initial investigations, various compound series have undergone lead optimisation, namely: the Benzamides (Wu *et al.*, 2009), 1H-imidazol-2-yl-pyrimidine-4,6-diamines (Deng *et al.*, 2010) and the Imidazolopiperzines (Wu *et al.*, 2011). The latter of which, in the form of the optimised derivative GNF 156, has recently completed phase 1 clinical trials (Guiguemde *et al.*, 2012).

One of the most successful reports to date of repositioning efforts for malaria came from a Novartis screen of 12,000 natural product compounds. These included pure, natural products and synthetic compounds with natural product features. The preliminary screen yielded 275 hits active at submicromolar concentrations. Of these, 17 were taken forward, based on the criteria that they were active against multiple drug resistant strains and were not cytotoxic (> 50% inhibition at 10  $\mu$ M in cell lines of neural, renal hepatic, and monocytic origin). Based on its desirable pharmacokinetic and physical properties, a synthetic compound related to the spiroazepineindole class surfaced as a promising candidate for lead optimisation. Synthesis and evaluation of 200 compound derivatives led to the selection of the optimised spiroindolone (spirotetrahydro beta-carboline) compound NITD609, that was shown to have an  $IC_{50}$  ~1nM against *P. falciparum* (Rottmann *et al.*, 2010; Yeung *et al.*, 2010). Most importantly, compound NITD609 (renamed KAE609) was shown to act *via* a new mechanism of action based on the inhibition of *Pf*ATP4 (Rottmann *et al.*, 2010; White *et al.*, 2014). KAE609 has now completed phase 1 and phase 2 clinical trials with a positive outcome (Guiguemde *et al.*, 2012; White *et al.*, 2014).

Although the successful outcome of the larger screening initiatives has resulted in two compounds entering clinical trials within 5 years post discovery (Guiguemde *et al.*, 2012), it is likely that more potentially medically valuable hits are awaiting lead optimisation. Indeed, it has been reported that since 2006 approximately six million compounds have been phenotypically screened in this manner (Spangenberg *et al.*, 2013), providing more hits (~ 20,000) than can reasonably be investigated (Meister *et al.*, 2011). For this reason a

revolutionary approach to drug discovery has made early screening data available in the public domain to encourage industrial and academic collaborations, and the development of a faster more efficient drug discovery paradigm (Burrows *et al.*, 2012; Spangenberg *et al.*, 2013).

In order to harness the usefulness of the screening information and overcome the practicalities of obtaining physical compound samples Medicines for Malaria Venture (MMV- not for profit public and private partnership) has refined the list of 19,876 compounds from the initial St Judes, Novartis, and GSK screens, to a set of just 400 compounds, now referred to as “The Malaria Box”. (Burrows *et al.*, 2012; Spangenberg *et al.*, 2013). The first filtering step was to include only commercially available compounds which reduced the collection from 20,000 to 5,000. The remaining compounds were thought to be good representatives of the chemical space occupied by the whole set. Next, they were subdivided into those that obey Lipinski’s rule of 5 and those that did not: namely: drug-like and probe-like groups respectively. Structural clustering was then used for each group so that representatives of each cluster were included in the final compound set. The aim was to maximise diversity while maintaining some cluster pairs that varied in antimalarial potency in order to help inform structure-activity investigations (Spangenberg *et al.*, 2013). The Malaria Box is now freely available, upon request, for a more rigorous definition and characterisation of antimalarial efficacy and activity against other diseases, on the condition that any data obtained is released into the public domain (Biamonte *et al.*, 2013; Burrows *et al.*, 2012).

Despite expectation for the Malaria Box to provide chemotherapies suitable for malaria eradication, and the collection is in no doubt an invaluable tool for malaria drug discovery, it is only a small fraction of the armamentarium of compounds available in a multitude of untested drug libraries that should not be overlooked. Indeed, the key to a “miracle cure” may even be embedded within those compounds that have been filtered out of contention. Accordingly, the objectives of the current study were to complete a preliminary single-dose phenotypic screen on the Screen-Well™ FDA approved drug library from ENZO, which to our knowledge has not yet been evaluated for antimalarial activity. The set of 640 chemically and pharmacologically diverse compounds, boast a rich source of bioactivities and the highest degree of drug-likeness available. The preliminary screen against the multi-drug resistant strain K1 had a rigorously low cut off point of 2.5  $\mu\text{M}$ , less than half of most previous reports, in an attempt to retain a refined, reliably potent short list. An

additional aim was to selectively corroborate some of the data published by the Lucumi group (2010) by completing secondary phase screening on the most potent antimalarial candidates identified (against 3D7) from the Library of pharmaceutically active compounds (LOPAC). Against a backdrop of emerging artemisinin resistance and a fast-depleting armamentarium of affordable antimalarial therapeutic options, it is critical that candidates from such preliminary screening initiatives are further investigated objectively and systematically to evaluate their therapeutic potential. Further characterisation of leads, to identify stand-alone antimalarial options and potential synergistic candidates for combination therapy with artemisinins or other existing antimalarials, is of utmost importance.

## 4.2 METHODS

### 4.2.1 Preliminary screening of the ENZO library for antimalarial activity

The ENZO library, which contains 640 chemically and pharmacologically diverse compounds, was kindly donated by Dr. Farid Khan (Protein technologies Ltd, Manchester Science Park, UK). The compounds were stored at -20 °C in a 96 well plate format, at a stock concentration of 400 µM (in DMSO). A relatively rigorous preliminary screen concentration of 2.5 µM was selected for all compounds. This meant that 1.25 µl of each compound (in DMSO) was transferred directly into 200 µl of parasite culture, ensuring that DMSO concentrations did not exceed 0.625 %. Each treatment was set up in duplicate and controls consisted of non-treated, parasitised blood, dihydroartemisinin treated samples (2.5 µM), and DMSO only treated cultures at 0.625 %. Plate cultures were initiated at 2.5 % haematocrit containing 0.5 - 1 % trophozoite stage parasites and incubated for 48 hours at 37 °C under a 5 % CO<sub>2</sub> 5 % O<sub>2</sub> and 90 % N<sub>2</sub> gas mixture as described previously. Following the treatment period 100 µl of PBS was added to each well (300µl final well volume), samples were mixed thoroughly and centrifuged at 1000 rpm for 3 minutes. A 200 µl aliquot of the supernatant was then removed from each well using a multichannel pipette to ensure that the parasitised blood was not dislodged from the bottom of the plate. The washing procedure was subsequently completed twice more with 200 µl PBS. Once the final washing step had been completed, and 200 µl of the supernatant discarded, the SG-MicroPlate staining and analysis procedure was performed as described elsewhere (section 2.2.2). A non-infected blood control sample (2.5 % haematocrit) was also included and background fluorescence was deducted from parasitised blood samples accordingly.

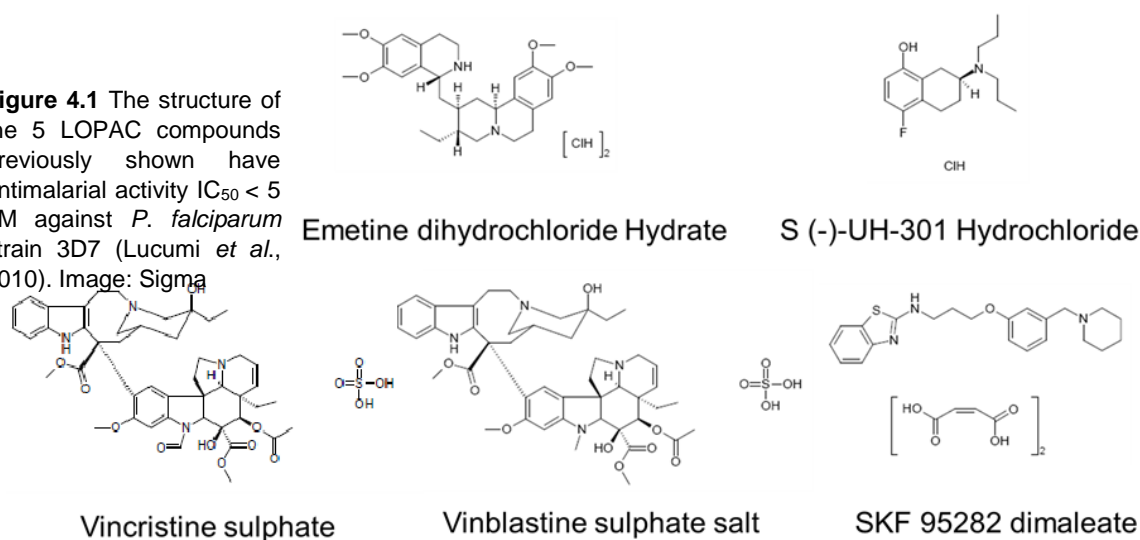
### 4.2.2 Preliminary screening of LOPAC compounds for antimalarial activity

Five compounds, previously reported by Lucumi *et al.* (2010) to be potent against *Plasmodium falciparum* strain 3D7 ( $IC_{50} \leq 5$  nM), were taken forward for preliminary screening against the multidrug resistant K1 strain. The compounds: Emetine dihydrochloride hydrate, SKF 95282 dimaleate, S (-)-UH-301 hydrochloride, Vinblastine and Vincristine (Figure 4.1), were selected from the Library of pharmaceutically active compounds (LOPAC). The LOPAC libraries were stored at -20 °C in a 96 well plate format at a concentration of 1 mM. Working stocks were prepared by diluting 1:10 with DMSO, and test concentrations prepared by further dilution with RPMI 1640. Parasites were treated with the respective  $IC_{50}$  of each compound (Lucumi *et al.*, 2010) and 10x the



$IC_{50}$  to account for the resistance phenotype of the K1 strain (5 ml flask format as described previously). In addition to corroborating the previous work published by the Lucumi and co-workers (2010) by analysing the potency of the selected compounds against K1, the LOPAC compounds were administered in combination with dihydroartemisinin (DHA). For the preliminary combination assays LOPAC compounds at  $IC_{50}$  were used with dihydroartemisinin 0.63 nM or 1.25 nM. The LOPAC 10 x  $IC_{50}$  treatments were co-administered with 0.63 nM dihydroartemisinin only, to enable the combinatory effects to be monitored. Infected blood and non-infected blood served as positive and negative controls respectively. Treated and control flasks were incubated under conditions described previously for 48 hours and analysed using SG-FCM. (Chapter 2, section 2.2.3).

**Figure 4.1** The structure of the 5 LOPAC compounds previously shown have antimalarial activity  $IC_{50} < 5$  nM against *P. falciparum* strain 3D7 (Lucumi *et al.*, 2010). Image: Sigma



#### 4.2.3 MeSH annotation of hit compounds from LOPAC and ENZO libraries

All compounds selected for the preliminary screen of the LOPAC library (n=5) against the multi-drug resistant K1 strain and the most potent 55/640 compounds from the ENZO library were searched using the NCIB PubChem database and their respective medical subject heading (MeSH) annotations were retrieved. This system was used as it is a reliable source and provides a controlled set of vocabularies to categorise compounds according to their known bioactivities and mechanism of action classifications (Plouffe *et al.*, 2008). The frequency distribution of the top 60 compounds within the identified MeSH categories was then plotted to establish whether novel classes of antimalarial inhibitors could be identified.

#### 4.2.4 Tanimoto similarity of MeSH compound with existing antimalarials

Once annotated and grouped according to their previously defined mechanism of action, each MeSH category was subjected to structural clustering analysis using the 2D Tanimoto index (PubChem), to determine whether the novel scaffolds were structurally distinct from existing antimalarials. Compounds were compared within each MeSH category and with a range of existing antimalarials including artemisinin, fansidar (pyremethamine and sulfadoxine), halofrantine, atovaquone, proguanil, five representatives of the quinolines: namely, chloroquine, mefloquine, amodaquine, primaquine and quinine, and two antibiotics previously used to treat malaria, clindamycin and doxycycline.

#### 4.2.5 Secondary phase screening of selected ENZO compounds

Second-phase screening of ENZO compounds involved the generation of a preliminary dose response curve and IC<sub>50</sub> determination using the SG-MicroPlate method. The dose range for each compound was based on the level of inhibition achieved during the preliminary screen at 2.5  $\mu$ M. For compounds displaying >80 % inhibition, 2.5  $\mu$ M was selected as the highest dose in the treatment series. For compounds with a lower level of inhibition between 60-80 % or < 60 % the highest dose was adjusted to 5  $\mu$ M and 10  $\mu$ M respectively. Two-fold serial dilutions were used to achieve a 6 or 7 point dose range. A total of 10 ENZO compounds were screened in this manner including the existing antimalarial atovaquone, which served as a positive control. A comparable level of DMSO was also serially diluted to ensure that the solvent was not responsible for any inhibitory effects observed. Duplicate treatments were set up for each compound, in complete media, at twice the final dose required (100  $\mu$ l/well) and subsequently diluted 1:1 with parasitised culture (1 % trophozoite, 5% haematocrit). Following 48 h of incubation under the conditions described previously, samples were analysed using the SG-MicroPlate method (Chapter 2 section 2.2.2).

#### 4.2.6 Secondary phase screening of LOPAC compounds

Out of the 5 compounds from the selected LOPAC library, three were taken forward for second-phase screening and preliminary IC<sub>50</sub> determination. These were, emetine dihydrochloride hydrate, SKF 95282 dimaleate, and S (-)-UH-301 hydrochloride. Based on the previously determined IC<sub>50</sub> values for the 3D7 strain (Lucumi *et al.*, 2010) and the relatively low level of inhibition observed against the multi-drug resistant strain K1, wide dose ranges were selected for each drug. For emetine, SKF and SUH 1 nM-100 nM, 1 nM-

200 nM and 10 nM-1000 nM concentration ranges, with up to 5 dose points, were selected respectively. Stock and working concentrations were prepared as detailed above. Treatments were set up in a 5 ml flask format and incubated for 48 hours under conditions described previously (Chapter 2). As there were only 3 compounds for the analysis the more accurate SG-FCM method was used to determine parasite growth following drug exposure (Chapter 2, Methods 2.2.3).

#### *4.2.7 Accurate IC<sub>50</sub> determination of selected compounds*

The most potent compounds from the second-phase screens of the ENZO and LOPAC libraries were taken forward for accurate IC<sub>50</sub> determination. Three compounds from the ENZO library were selected for further interrogation: namely, clemastine (histamine 1 receptor antagonist) propafenone (anti-arrhythmic) and one of the serotonin receptor antagonists (ondansetron). From the LOPAC library, SKF and SUH displayed a relatively huge shift in IC<sub>50</sub> values against the K1 strain compared to their previously reported potency against 3D7. For this reason, only Emetine dihydrochloride hydrate was considered for further investigation. Dose ranges were selected in line with the previous effective window identified in the second phase screens. For two of the ENZO compounds, propafenone and clemastine, the dose range selected was 0.04-2.5 µM. Ondansetron failed to show a dose response in the first three replicas of the experiment, therefore, the concentration range was gradually shifted until a clear dose response was apparent and an accurate IC<sub>50</sub> calculation could be achieved. For emetine the dose response selected was 10-100 nM. All treatments were initiated at trophozoite stage with a starting parasitaemia 0.5-1 % and a 2.5 % (plate) or 5 % (flask) haematocrit. Treatments were set up in triplicate and incubated for 48 hours under conditions described previously. Parasite growth was analysed using the more accurate SG-FCM method and the IC<sub>50</sub> was calculated using GraphPad Prism 5.0 (as described in Chapter 2, Section 2.2.4).

### 4.3 RESULTS

#### *4.3.1 Preliminary screening of the ENZO library for antimalarial activity*

The preliminary screen of the ENZO library revealed a 9.5 % hit rate (compounds that showed  $\geq 50$  % inhibition after 48 h treatment at 2.5 µM). Although the positive and negative controls were effective (Figure 4.2) and achieved a Z score of 0.68 ( $\pm 0.06$ ), additional validation of the assay came from known antimalarials within the initially blinded hit list (Table 4.1). For additional data refer to Appendix IV.

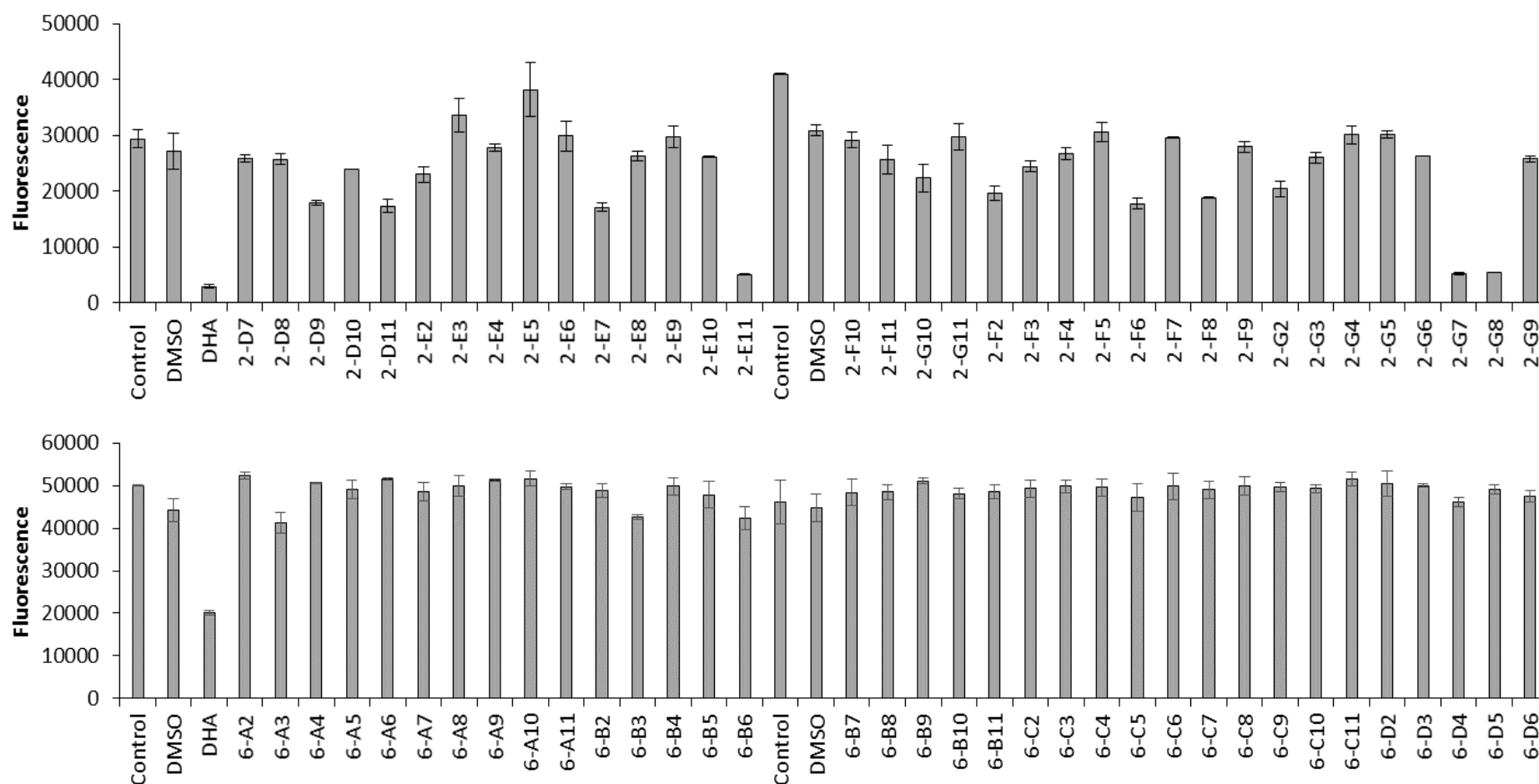


**Figure 4.2** An exemplar panel of the ENZO library preliminary screen against *Plasmodium falciparum*, strain K1. The complete collection of 640 compounds was screened at a rigorous concentration of 2.5 $\mu$ M. The treatment period was initiated when parasites entered at trophozoite stage and lasted for 48 hours. Untreated, DMSO-only and dihydroartemisinin treated samples (2.5  $\mu$ M) served as negative and positive controls, respectively. Background fluorescence from non-infected blood samples was deducted accordingly. The screening capacity was 70 test compounds per experiment. Additional controls were included in the centre as well as at the periphery of the plate to ensure that edge-effects were not a confounding factor. The SYBR Green MicroPlate assay was used to analyse growth in test samples relative to controls.

Name	% inhibition <i>P. falciparum</i> strain K1	Mechanism of action Medical subject heading (MeSH)
Artesunate	98.72	Antimalarial
Cyclosporin A	93.96	Immunosuppressant
Quinine·HCl·2H <sub>2</sub> O	91.54	Antimalarial
Propafenone	91.18	Anti-arrhythmic
Aclarubicin	87.69	Antiancer
Ivermectin	86.48	Antiparasitic (worms)
Clemastine	85.53	A histamine H1 antagonist
Mitoxantrone	85.14	Anti-cancer
Atovaquone	85.13	Antimalarial
Puromycin	84.56	Antibiotic
Sertaconazole	84.51	Antibiotic/ Antifungal
Plicamycin	83.88	Antineoplastic antibiotic
Doxorubicin·HCl	83.83	Anticancer/Anthracycline antibiotic
Chloroquine	82.99	Antimalarial
Artemisinin	81.32	Antimalarial
Vorinostat	80.04	Anticancer
Daunorubicin	80.03	Anticancer
Quinacrine	79.10	Antimalarial
Bortezomib	73.46	Anticancer
Fluoxetine	72.65	Selective serotonin inhibitor
Bromocriptine mesylate	68.98	Dopamine D2 agonist
Mitomycin C	68.87	Anticancer
Nisoxetine·HCl	67.59	Selective noradrenalin uptake inhibitor
Bopindolol	67.46	Beta blocker
Rifampicin	66.79	Antibiotic
Loperamide·HCl	64.73	Antidiarrheal
Niguldipine	63.92	Calcium channel blocker
Trifluoperidol	63.74	Antipsychotic
Idarubicin	62.53	Anticancer
Nicardipine·HCl	62.35	Calcium channel blocker
Telmisartan	61.39	Angiotensin receptor blocker
Fluspirilene	61.20	Antipsychotic
Ergotamine	60.52	A vasoconstrictor- migraine treatment
Maprotiline·HCl	60.27	Antidepressant
10-Hydroxycamptothecin	60.11	Anticancer
Ondansetron	59.93	Serotonin type 3 receptor antagonist
Dihydroergocristine	59.74	Vasodilator, Ergot alkaloid
Tiotropium Bromide	59.14	Anticholinergic bronchodilator for COPD
Trimethoprim	58.72	Antibiotic
Pimozide	58.71	Antipsychotic
Cilostamide	56.95	Phosphodiesterase PDE3 inhibitor
Ketanserin	56.12	Selective serotonin receptor antagonist
Rapamycin	55.84	Immunosuppressant
Spironolactone	55.45	Competitive antagonist of aldosterone receptor
Haloperidol	54.89	Antipsychotic
Amiodarone·HCl	54.78	Antiarrhythmic
Irsogladine	54.70	Mucosal protective drug (Treat peptic ulcer)
Mesoridazine besylate	54.67	Antipsychotic
Mycophenolic Acid	54.49	Immunosuppressant
Etazolate	54.45	Phosphodiesterase inhibitor
Pronethalol·HCl	54.07	non selective beta blocker
Dibenzepine	53.21	antidepressant
Thioridazine	53.16	antipsychotic
Sulfadiazine	52.16	antiparasitic (Toxoplasmosis)
Valaciclovir	51.59	antiviral
Terfenadine	51.27	H1 receptor antagonist

**Table 4.1 The 56 most potent compounds identified from the ENZO Library preliminary screen.** Tabular data shows the % inhibition for the ENZO library compounds against *P. falciparum* strain K1 at a concentration of 2.5  $\mu$ M. MeSH annotation of the compounds is also presented. The list includes 6 existing antimalarials.

#### 4.3.2 Preliminary screening of the LOPAC compounds for antimalarial activity

Five compounds from the LOPAC library, shown to display the most potent antimalarial activity by Lucumi *et al.* (2010) against *P. falciparum* strain 3D7, were screened in the current study for activity against the K1 strain. The data presented here infers all 5 compounds were less potent towards multiple-drug resistant strain (Figure 4.3).

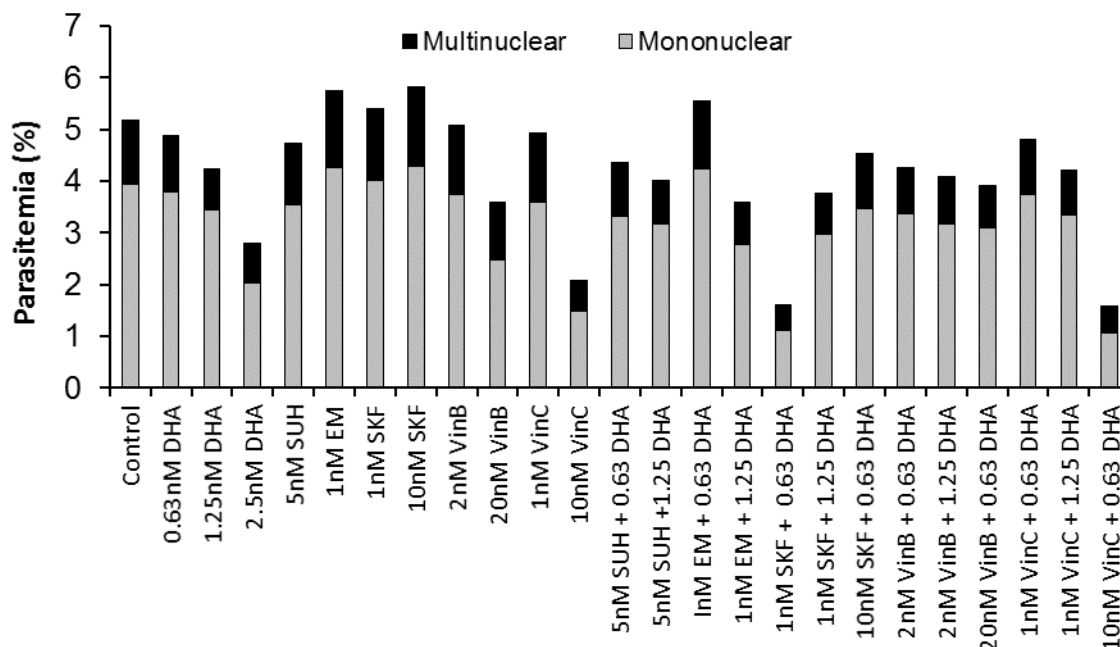
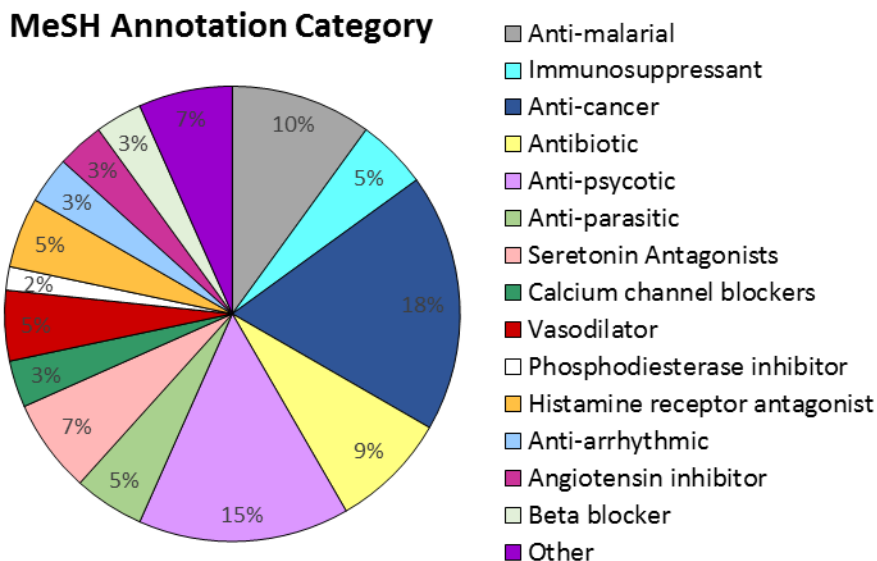


**Figure 4.3 SYBR Green-based Flow cytometric data for the treatment of *P. falciparum* malaria (strain K1) with dihydroartemisinin (DHA) and five LOPAC compounds.** The LOPAC compounds Emetine dihydrochloride hydrate (EM), SKF 95282 dimaleate (SKF), S (-)-UH-301 hydrochloride (SUH), Vinblastine (VinB) and Vincristine (Vinc) were either added alone or in combination with DHA for a 48hr treatment period. Parasitised blood and parasites treated with a range of DHA concentrations served as controls. Non-infected blood was also included and background fluorescence was deducted from all samples accordingly. Parasitaemia was determined using SYBR Green based flow cytometry and 50, 000 events were recorded for each sample.

Even at 10 x the  $IC_{50}$  values of the 3D7 strain, 50% growth inhibition was only achieved with one LOPAC compound, vincristine. The preliminary combination data between dihydroartemisinin and the LOPAC compounds: emetine dihydrochloride hydrate, SKF 95282 dimaleate, S (-)-UH-301 hydrochloride, vinblastine and vincristine showed that the combination had a slightly more potent effect on growth inhibition than when either drug of a pair is used alone, at some but not all of the doses analyzed. In particular the 1 nM SKF + 1.25 nM DHA combination shows a considerable reduction (Figure 4.3).

#### 4.3.3 MeSH annotation of hit compounds from LOPAC and ENZO libraries

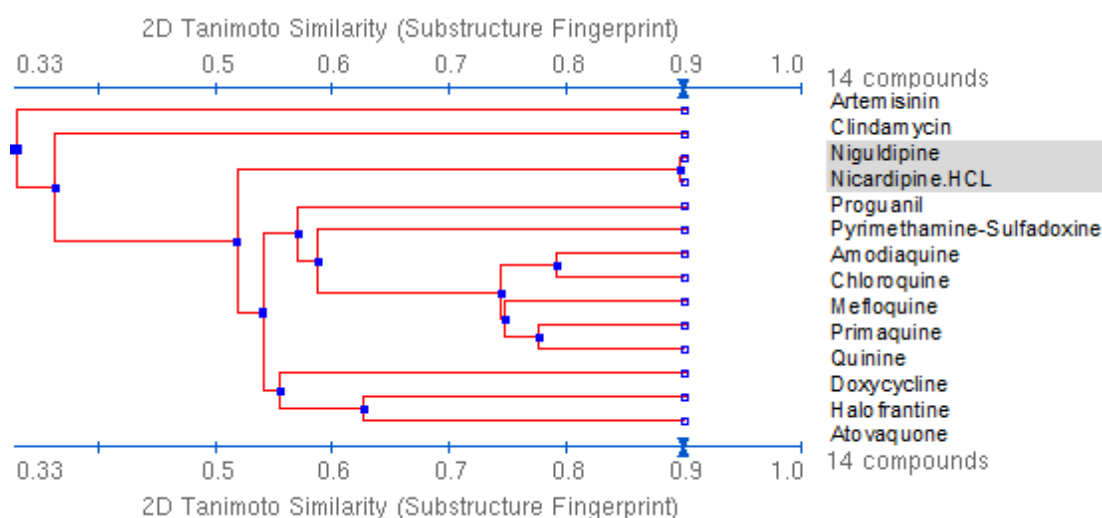
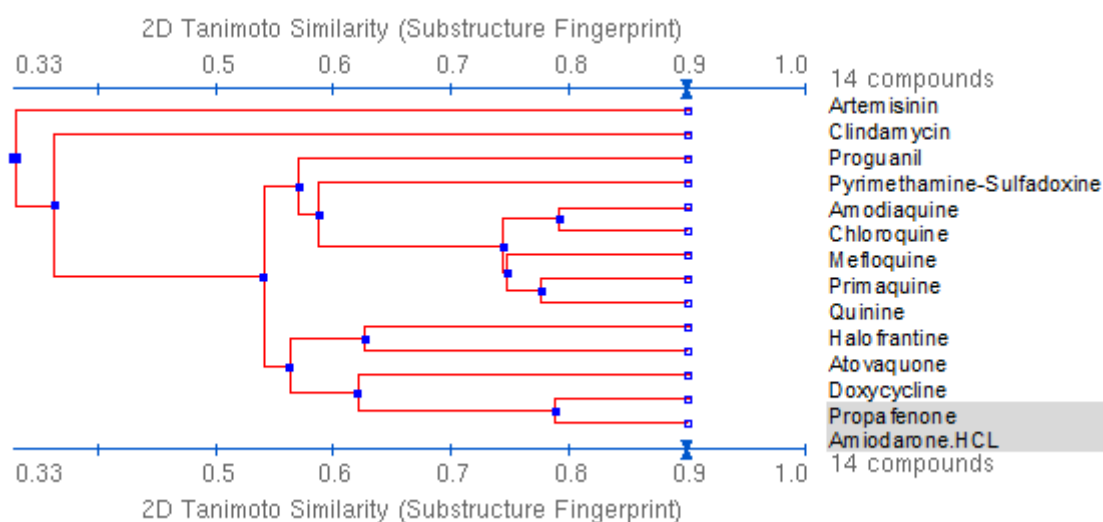
MeSH annotation of hit compounds revealed that they fell into 15 distinct mechanisms of action classifications. Some of the most common, apart from the existing antimalarials, were the anti-cancer and antipsychotic compounds (Figure 4.4).



**Figure 4.4 MeSH category distribution of the top 60 ENZO and LOPAC hits.** The 60 most potent compounds from the ENZO (55 compounds) and LOPAC (selected 5) library preliminary screens were grouped according to their previously defined mechanism of action classifications, as determined by Medical subject heading annotation (MeSH PubChem) to identify common classes with antimalarial activity.

#### 4.3.4 Tanimoto Similarity of selected MesH categories

Tanimoto similarity of the most desirable novel classes revealed that they were structurally distinct from a range of existing antimalarial classes. Compounds with an index of  $> 0.85$  were considered to have the same mechanism of action (Plouffe *et al.*, 2008). The quinolines formed a distinct cluster displaying at least 0.65 similarity to each other and served to validate the similarity method employed (Figure 4.5). Some of the novel classes also presented a high level of similarity to each other. Indeed, the calcium channel blockers displayed a similarity score of 0.896, whereas their highest similarity, when compared with existing antimalarials, was 0.517 and 0.515 for mefloquine and doxycycline, respectively (Figure 4.5 a). The anti-rhythmic compounds were only 0.787 similar to each other, whilst their highest similarity to an existing antimalarial was 0.62 with doxycycline (Figure 4.5 b). The highest similarity score for the serotonin and histamine receptor antagonists to the selected existing antimalarials was with halofantrine (0.636 and 0.706 respectively). The anti-parasitic category contained compounds that have different modes of action against different parasites. These compounds, therefore, also had varied degrees association to each other and the existing antimalarials (See Appendix V).

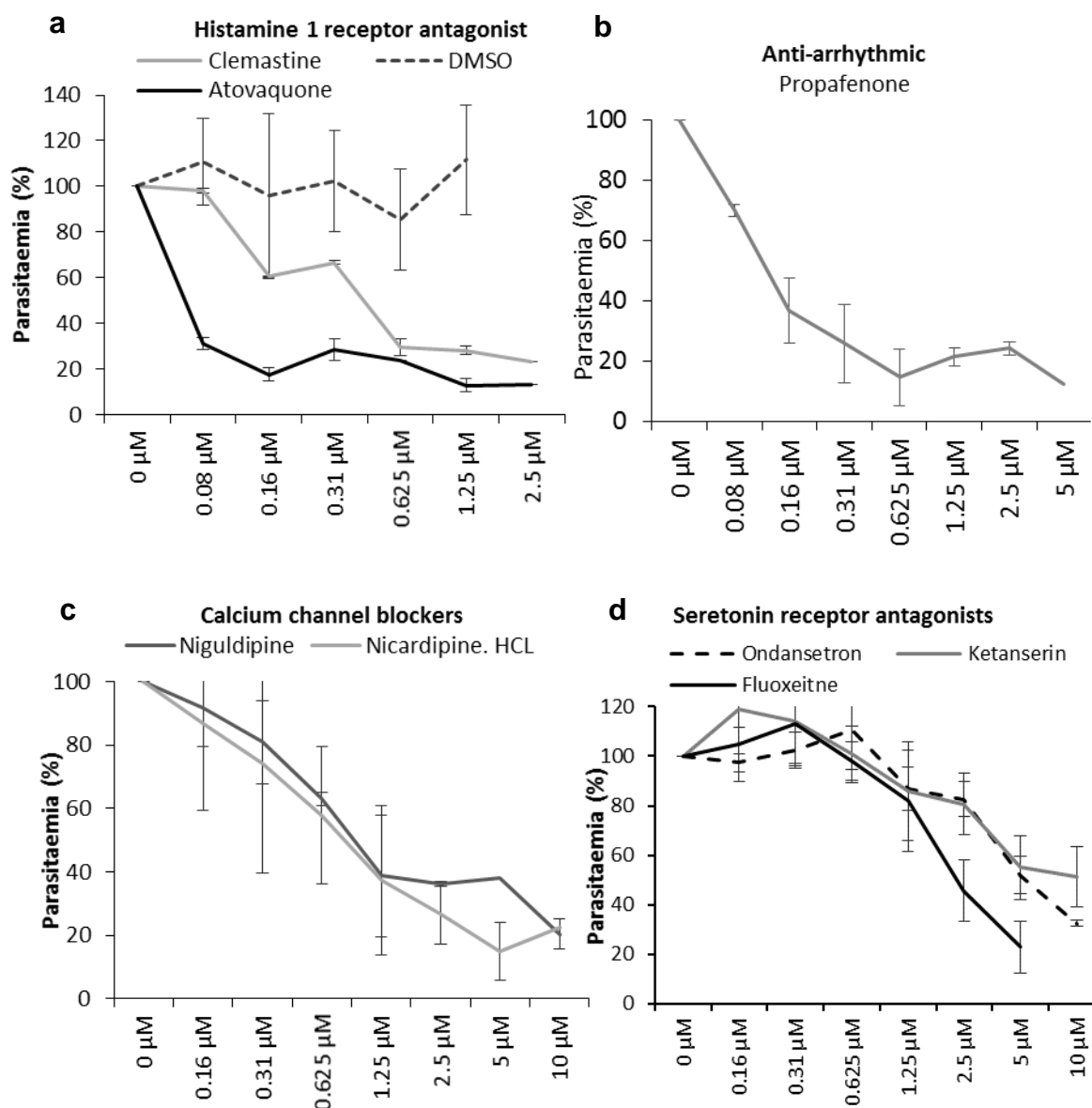
**a. Calcium channel blockers****b. Anti-arrhythmic**

**Figure 4.5** An example of the structural clustering for the previously defined MeSH categories with a range of existing anti-malarials. Namely, the calcium channel blockers and the anti-arrhythmic compounds. PubChem substructure fingerprint using the 2D Tanimoto similarity coefficient was employed to determine the similarity of the potentially novel anti-malarial classes with existing anti-malarials. In accordance with Gamo *et al.* (2010) compounds with a similarity index of  $\geq 0.85$  were considered to share a mode of action.



## 4.3.5 Second-phase screening of selected compounds

The second-phase screen of the ENZO library indicated that compounds, propafenone and clemastine were the most potent with  $IC_{50}$ 's of 0.12-0.16  $\mu$ M and 0.4-0.5  $\mu$ M respectively (Figure 4.6 a and b). For the remaining 7 compounds the  $IC_{50}$  estimates were 0.8-10  $\mu$ M (Figure 4.6 c-f and Table 4.2)



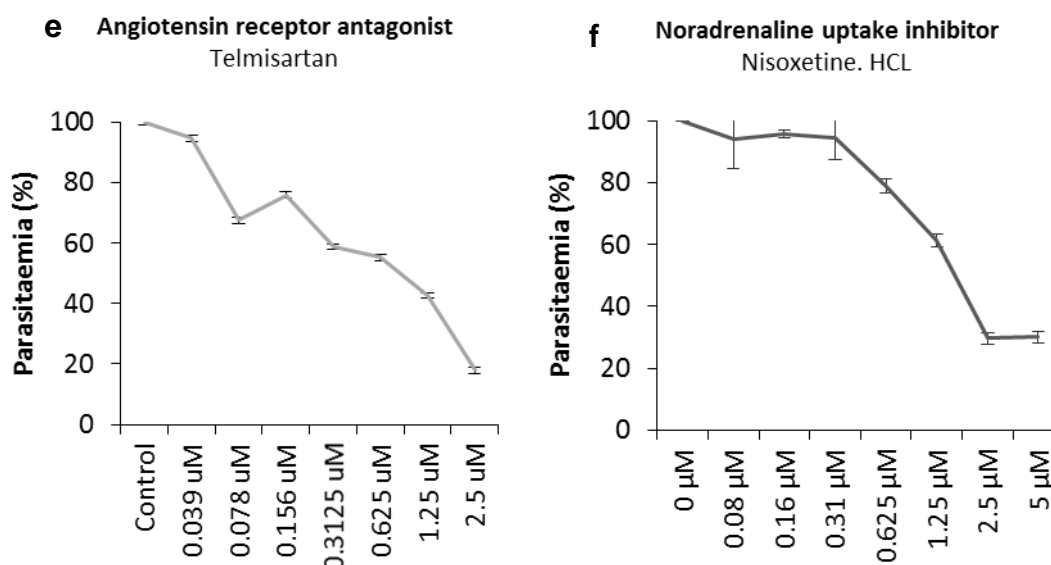
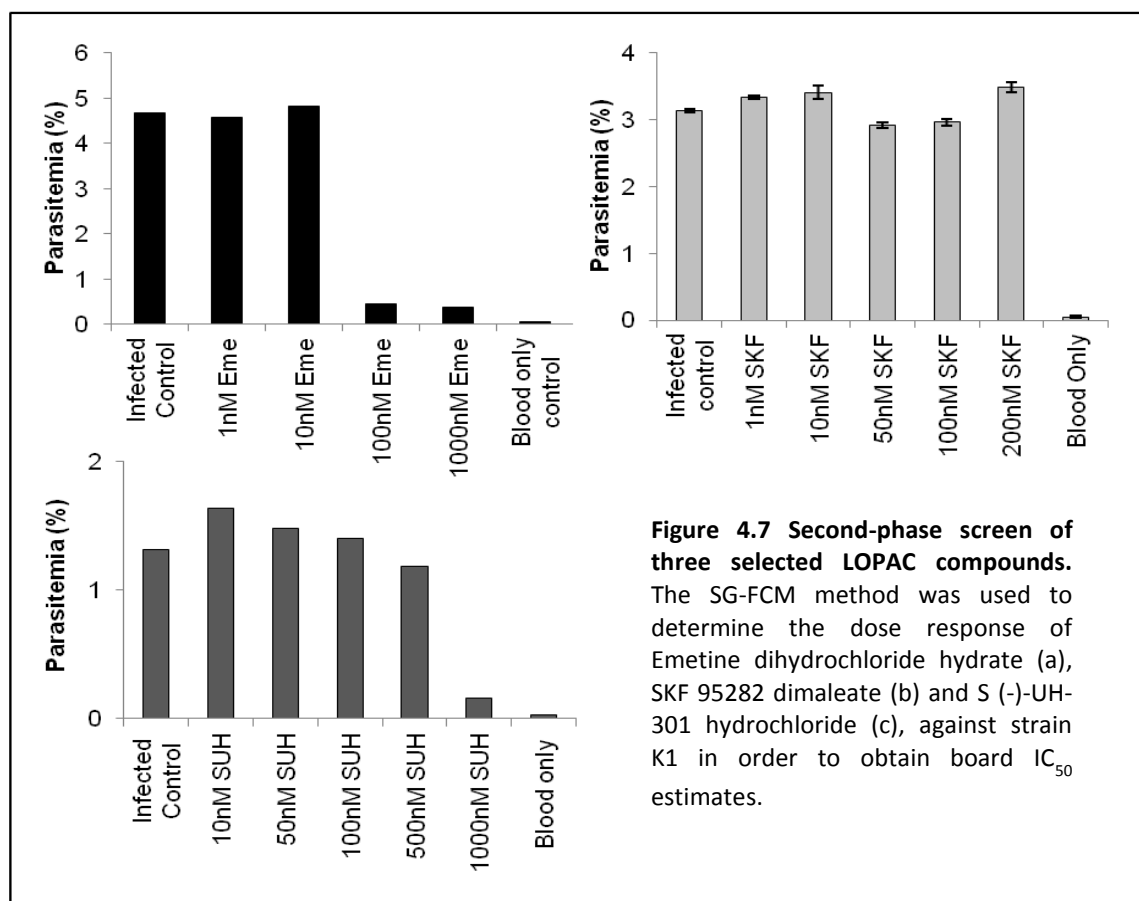


**Figure 4.6 Second-phase screen of selected ENZO library compounds.** Dose response curves were generated using the SG-MicroPlate method. The dose-range for each class was selected based on the potency of the preliminary screen. Classes analysed included anti-histamine receptor antagonist (this Figure also included the un-treated and the DMSO-only controls (a), anti-arrhythmic compound (b), calcium channel blocker (c), serotonin receptor antagonists (d), noradrenaline uptake inhibitor (e) and an angiotensin receptor antagonist (f).

Compound Name	Class	Preliminary IC <sub>50</sub> (μM)
Atovaquone	Antimalarial (positive control)	< 0.08
DMSO	N/A (Negative control)	No inhibition
Clemastine	H1 receptor antagonist	0.4-0.5
Propafenone	Anti-arrhythmic	0.12-0.16
Niguldipine	Calcium channel blocker	0.9-1.1
Nicardipine. HCL	Calcium channel blocker	0.8 -1
Fluoxetine	Serotonin receptor antagonist	2-2.5
Ondansetron	Serotonin receptor antagonist	5-7.5
Ketanserin	Serotonin receptor antagonist	> 10
Nisoxetine. HCL	Noradrenaline uptake inhibitor	1.5-2
Telmisartan	Angiotensin receptor blocker	0.9-1.1

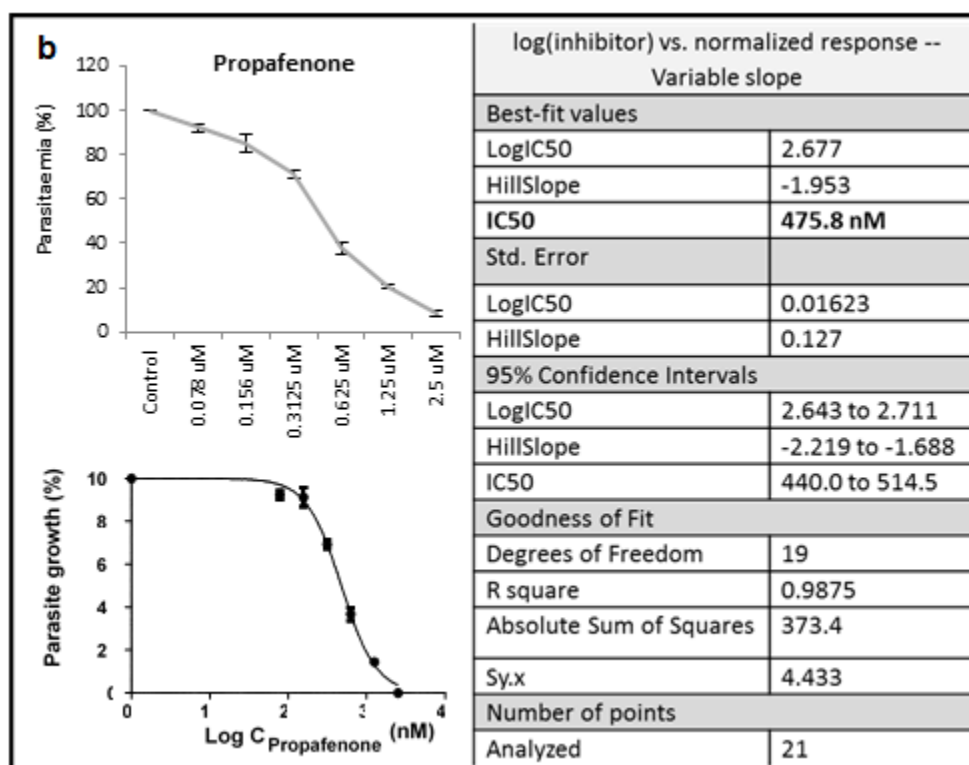
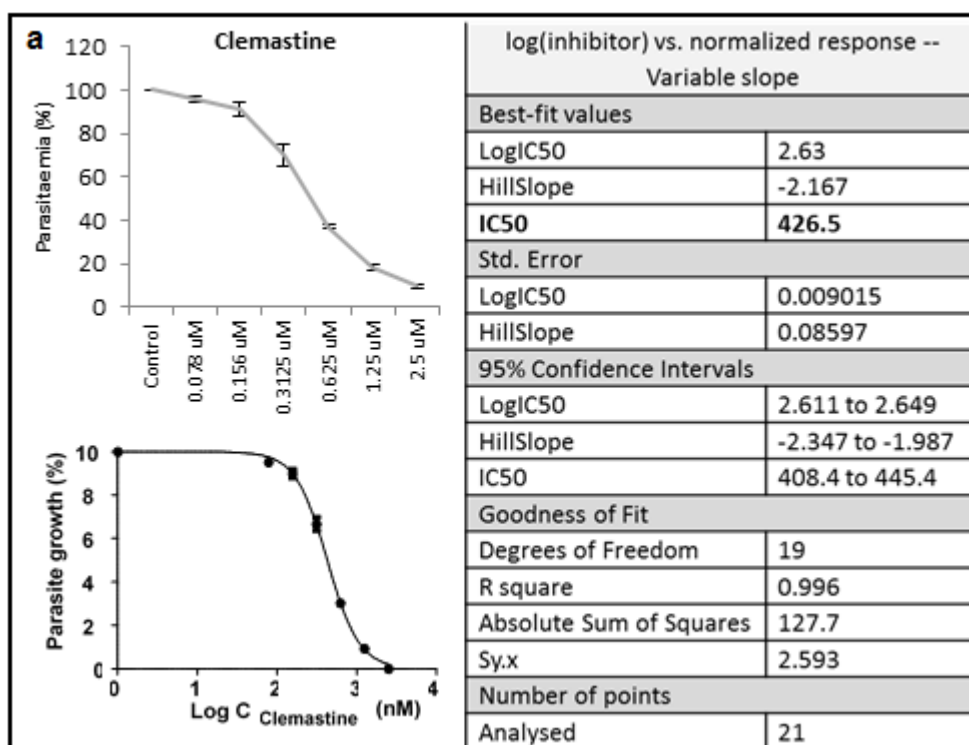
**Table 4.2** Preliminary IC<sub>50</sub> estimates based on the second phase SG-MicroPlate screen of 9 compounds selected from the ENZO library.

The second-phase screen of the LOPAC compounds emetine dihydrochloride hydrate (Figure 4.7 a), SKF 95282 dimaleate (Figure 4.7 b), S (-)-UH-301 hydrochloride (Figure 4.7 c), using the more accurate SYBR Green-FCM method, showed that 50% growth inhibition could be achieved at ~ 50 nM, >200 nM and ~750 nM respectively.



#### 4.3.6 $IC_{50}$ determination of selected compounds

The results showed that, out of the ENZO and LOPAC compounds, emetine was by far the most potent ( $IC_{50} = 47$  nM (Figure 4.8 d)). The two ENZO compounds clemastine and propafenone, selected for further study based their potency, were shown to have  $IC_{50}$ s just below 500 nM (Figure 4.8 a and b respectively). Ondansetron, selected for its anti-emetic potential, was shown to be a very mild inhibitor of the *Plasmodium falciparum* K1 strain ( $IC_{50} \sim 39$   $\mu$ M (Figure 4.8 c)).



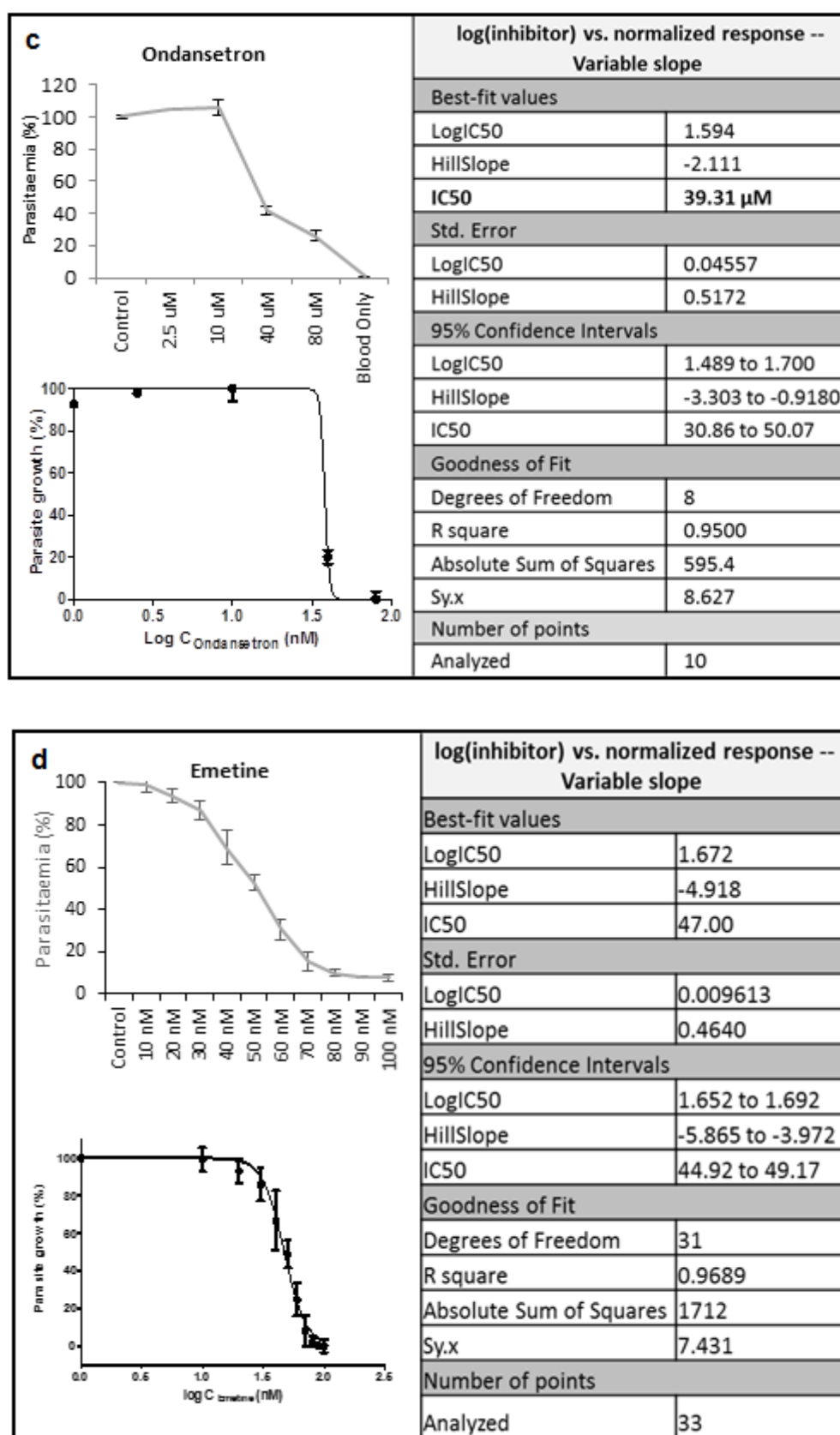


**Figure 4.8 Accurate IC<sub>50</sub> determination of the four selected ENZO/LOPAC Library compounds.** These included the ENZO Histamine receptor 1 antagonist clemastine (a), anti-arrythmic propafenone (b), serotonin receptor antagonist ondansetron (c), and the LOPAC compound emetine dihydrochloride hydrate (d) against *P.falciparum* K1 using the SYBR Green flow cytometer method. The compiled figures show the standard dose response curve, and the GraphPad Prism 5.0 output for normalised data against log transformed drug concentrations (Sy.x indicates the standard deviation of residuals).

#### 4.4 DISCUSSION

##### *4.4.1 Preliminary screening of the ENZO and LOPAC library for antimalarial activity*

The phenotypic screen of the ENZO library presented a relatively high hit rate (9.5%), compared with previous screens, possibly, owing to the bioactive nature and drugability of the small compound library (Weisman *et al.*, 2006). A hit was defined as a compound inhibiting >50 % growth at a single dose point of 2.5  $\mu$ M. These criteria are consistent with other single-dose screens (Plouffe *et al.*, 2008; Lotharius *et al.*, 2014). Some previous studies only included compounds presenting > 80 % inhibition, however, the single dose adopted in these studies was usually 3 or 4 fold higher than the concentration presented here (Gamo *et al.*, 2010; Guiguemde *et al.*, 2010; Lucumi *et al.*, 2010; Weisman *et al.*, 2006). Although there was some toxicity incurred by the solvent concentration (0.625% DMSO), the data was adjusted accordingly so that only inhibition above that of the DMSO control was considered. Some false-negative were identified by the screen (Appendix IV). For example, doxycycline is a known antimalarial inhibitor that did not appear in the hit list. The most likely reason for this is that assay time course selected for fast acting compounds. Antibiotics like doxycycline are known to induce a delayed death phenotype that would have been missed by the 48 SYBR Green screening assay. It is also unlikely that compounds were capable of promoting (in some cases more than double) parasite growth compared to the untreated controls (Appendix IV). Thus the extreme values of negative inhibition maybe due to interference from coloured compounds with an inherent fluorescence. However, the blind screening procedure employed the re-identification of known antimalarials in the hit list and a good Z score ( $0.68 \pm 0.06$ ) served to validate the hits obtained.

The results of the preliminary LOPAC screen indicated that there may be some resistance towards the 5 selected compounds in the multidrug resistant K1 strain when compared with the 3D7 data (Lucumi *et al.*, 2010). Nevertheless, Emetine dihydrochloride hydrate, SKF 95282 dimaleate, S (-)-UH-301, vinblastine and vincristine showed additional suppression, at some but not all of the doses tested, when they were co-administered with dihydroartemisinin. Possibly, indicating that they may be useful in artemisinin-based combination therapy.

#### 4.4.2 MeSH annotation of hit compounds

The 15 MeSH categories identified as displaying antimalarial activity are in agreement with other reports, providing further validation for the data obtained. Indeed, antibiotic, anticancer, antipsychotic and immune-suppressant compounds have commonly been identified in numerous high-throughput phenotypic screens against cyclic blood stages of the disease (Gamo *et al.*, 2010; Lotharius *et al.*, 2014; Plouffe *et al.*, 2008; Weisman *et al.*, 2006). This data should be viewed with caution as it must be pointed out that the MeSH distribution of hits, may actually represent the MeSH distribution of the whole library. However, it is noteworthy that the most potent compounds from the LOPAC library selected for further investigation were easily placed into MeSH categories outlined for the ENZO library. Further validating the categories as potentially novel antimalarial leads.

##### 4.4.2.1 Anticancer compounds for malaria

The anticancer compounds were most commonly identified within the hit list (18% of hits). There has been recent interest in repositioning anticancer therapies for malaria treatment. Indeed, inhibitors of the novel malaria drug target farnesyltransferase were originally developed for cancer treatment. The rationale for the exploitation of such cross discipline drug-targets highlights that the toxicity of any drug developed for cancer therapies will have been studied at considerably higher doses (Nzila *et al.*, 2010). Nzila *et al.*, 2010 quotes Paracelsus' law '*Sola dosis facit venenum* (only dose makes the poison)' suggesting that all drugs are poisons it is only the dose that dictates the severity. Interestingly, two out of the 5 compounds investigated from the LOPAC library were previously used as anticancer therapies (Lucumi *et al.*, 2010). Vinblastine and vincristine are chemical analogues originally isolated from the Madagascar periwinkle (*Catharanthus roseus*). Vinblastine is used for the treatment of Hodgkin's disease and advanced breast and testicular cancer whilst vincristine is used for leukemia and other types of lymphoma treatment (Oksman-Caldentey and Inze, 2004). Both vinblastine and vincristine act by inhibiting microtubule formation, and have been suggested to target nuclear division in the malaria parasite. Additional target could include other cellular processes dependent on microtubule function such as merozoite formation and erythrocyte invasion by daughter merozoites (Usanga *et al.*, 1986; Chakrabarti *et al.*, 2013). Despite the relatively toxic nature of anti-cancer compounds, only vincristine appears to be potent against the K1 strain. In order to reposition these compounds for malaria, doses that do not cause toxicity would have to be analysed for activity against malaria before vincristine could progress as

a viable candidate. Notably, vinblastine the least toxic of the two was shown to be less effective against K1. Indicating that general toxicity rather than parasite specificity may be the reason for the potency observed. The high (83 %) similarity between mammalian and parasite tubulin (Chakrabarti *et al.*, 2013) also infers that the general toxicity of such a target may be difficult to overcome.

Drug candidates for widespread malaria treatment need to be well tolerated and safe for use in children. The repositioning of anticancer therapies for malaria is therefore hampered by persistent underlying concerns about toxicity, strong side effects and resulting compliance issues (Lotharius *et al.*, 2014). The huge effort expended in developing a drug that could potentially have such problems is not feasible, particularly when other avenues for exploration have been presented. For this reason, despite the high prevalence of activity, anticancer compounds from the ENZO or LOPAC libraries were not considered further in the current study.

#### 4.4.2.2 Antipsychotics, immune suppressants and antibiotics for malaria

Out of next most prevalent categories namely: the antipsychotics (15%), the immune suppressants (5%) and the antibiotics (9%) the former was not taken forward due concerns about adverse effects. The latter two classes have already been widely reported in the literature for consideration and use in repositioning therapy for malaria respectively. Immunosuppressant compounds such as Cyclosporin A and rapamycin in particular have been studied extensively for their antimalarial potential (Bell *et al.*, 1994; Bobbala *et al.*, 2008). Unfortunately, their immunosuppressive properties are suggested to prevent repositioning of these compounds for malaria (Lotharius *et al.*, 2014). Numerous antibiotics such as the tetracyclines and clindamycin, a lincosamide antibiotic, have been used in combination therapy for malaria (Andrews *et al.*, 2014), however, there are growing concerns that further exploitation of this important class of compounds will only accelerate the dwindling efficacy for its primary antimicrobial indication.

Of the remaining categories the interesting groups that offered potentially novel antimalarial scaffolds were analysed for tanimoto similarity with existing antimalarials and other group members. The three remaining LOPAC compounds: Emetine, SKF and SUH aligned well with the selected categories: namely, antiamoebic (antiparasitic), histamine receptor antagonist and serotonin receptor antagonist respectively and were therefore included for structural similarity analysis.



#### 4.4.3 Tanimoto similarity of hit compounds

Various studies have employed similarity indexes to determine whether the chemical space occupied by novel antimalarial scaffold overlaps with the existing pharmacotherapies for malaria. In addition, structural similarity between novel chemical scaffolds can help inform lead optimisation of candidates. Compounds with differential potencies within the same cluster can be used to identify, and potentially modify, the structural components responsible for both off-target and on-target effects (Guiguemde *et al.*, 2010 Plouffe *et al.*, 2008).

In the current study the Tanimoto similarity index was used, firstly, to compare each MeSH category with a range of existing antimalarials, and secondly, to analyse the similarity of the compounds grouped within the same MeSH category. Compounds that were singly responsible for the identification of a particular MeSH category were grouped into 'other' and analysed for their similarity with known antimalarials only. Encouragingly, none of the novel scaffolds displayed a high degree of similarity with existing antimalarials (defined as  $> 0.85$  (Guiguemde *et al.*, 2010 Plouffe *et al.*, 2008)). Although data was further validated through the distinct cluster formed by the quinoline antimalarials their relative similarity coefficients were not particularly high. This is somewhat expected as structural alterations have been made to reduce the non-target effects of quinine, the parent compound, to make the synthetic derivatives such as chloroquine and mefloquine more tolerable.

Overall, the similarity clustering between compounds within each MeSH category was not that informative, possibly due to the diversity of the library and the particularly small compound set analysed ( $n \sim 55$ ). The only MeSH category to report a high level of similarity between the compounds was the calcium channel blockers, nifedipine and nifedipine HCL (0.896). The similarity of the other compound clusters was clearly affected by the specificity of the MeSH category. For example, the serotonin and histamine receptor antagonist classifications contained different families of antagonist that target different receptor types ( $H_1$  and  $H_2$  or  $5-HT_1$ ,  $5-HT_2$  and  $5-HT_3$  respectively). It is therefore perhaps not unexpected that compounds in these broad spectrum categories did not present a high degree of similarity to each other. Furthermore, although structure is related to activity, the reverse is not always so easily applicable. Indeed compounds that have the same function (activity) may bind to and inhibit different targets within a pathway for which the appropriate structure may be completely different (Plouffe *et al.*, 2008).

Indeed the angiotensin inhibitor telmisartan and spironolactone are known to act on the same pathway but are dissimilar in structure. Whereas, the high similarity of the calcium channel blockers would predict that they act on the same target.

In order to further refine the hit list for second-phase validation through dose response analysis, the most potent ENZO compounds from each category (propafenone, clemastine and telmisartan) were taken forward. Along with the three remaining LOPAC compounds that showed potential as ACT candidates. For the calcium channel blockers both compounds (nicardipine. HCL and nifedipine) were considered due to their high degree of structural similarity and the possibility of identifying structural activity relations. Although the preliminary screen indicated only a slight variation in potency, second-phase analysis may reveal a more profound difference. For the serotonin receptor scaffold, all compounds (fluoxetine, ondansetron and ketanserin) were taken forward for further validation. This cluster not only represented a relatively large proportion of hits (7%), but members of the class have previously been proposed as novel antimalarial candidates (Gamo *et al.*, 2010). The dissimilarity between the compounds and the lack of a huge variation in potency precluded the selection of fewer representatives (56-73% inhibition). From the 'other' category the most potent compound a noradrenaline uptake inhibitor, nioxetine. HCL, was also considered.

Once hit compounds have been validated, a more informative structural similarity analysis of the whole library would permit comparisons between active and inactive compounds. One foreseeable problem is that the relatively small library boasts a high level of diversity which may ultimately limit cluster size. However, the growing amount available data in the public domain, on preliminary screens, could be used for a larger scale *in silico* analysis of compounds designated to promising MeSH categories (Guiguemde *et al.*, 2012; Spangenberg *et al.*, 2013). This would not only to increase cluster size, but also help build structural activity relations and instruct structural lead optimisation.

#### 4.4.4 Secondary phase screening selected compounds

The second phase-screen of the ENZO library was in agreement with the preliminary screen. All of the selected compounds were validated as malarial inhibitors. The most potent compounds were the anti-histamine receptor antagonist, clemastine, and the anti-arrhythmic compound propafenone, both with estimated  $IC_{50}$ 's between 0.12-0.5 $\mu$ M (Table 4.2). This is consistent with the literature, as compounds from these classes have

previously been identified as submicromolar inhibitors of malaria (Chong *et al.*, 2006; Derbyshire *et al.*, 2012; Plouffe *et al.*, 2008; Weisman *et al.*, 2006). For the other categories: namely, angiotensin receptor antagonist, calcium channel blockers, noradrenaline uptake inhibitors and serotonin receptor antagonist the IC<sub>50</sub> estimates were between 1-10  $\mu$ M (Table 4.2). In addition to the erythrocytic stage antimalarial activity presented here, Derbyshire and colleagues have shown that telmisartan is also inhibitive to liver stage parasites (Derbyshire *et al.*, 2012). Unfortunately, the calcium channel blockers failed to show a distinct variation in potency hence would not be suitable for SAR investigations. The serotonin receptor antagonist, despite being the one of the most common classes, (although structurally diverse) were the least potent compounds in the second-phase screen. While these candidates are not ideal in their current formulations, they should be considered as novel antimalarial scaffolds for lead optimisation. To fit the criteria of an antimalarial candidate, compounds should display potent antimalarial activity, be effective against drug resistant strains, free of significant side effects and have good pharmacokinetic properties (Rottmann *et al.*, 2010). Indeed, these candidate are known to be bioactive, have been screened against a multidrug resistant strain and fall within the criteria outlined by MMV that suggest and IC<sub>50</sub> of  $< 1 \mu$ M as a good starting point for lead optimisation (Lotharius *et al.*, 2014).

The wider dose range selected for the second-phase screen of the 3 selected LOPAC compounds permitted a clearer estimation of the IC<sub>50</sub> against the multiple drug resistant strain K1. Despite the finding that the IC<sub>50</sub> fell within the  $< 1 \mu$ M range, two of the compounds the histamine receptor antagonist SKF 95282 dimaleate, and the serotonin receptor antagonist S (-)-UH-301 hydrochloride displayed a large shift when compared with the IC<sub>50</sub> obtained for 3D7 strain. Although multiple replicas were completed for SKF 95282 dimaleate no growth inhibition was observed at 200 nM, 200 x the previous reported IC<sub>50</sub> value (1 nM) for 3D7 (Lucumi *et al.*, 2010). For S (-)-UH-301 hydrochloride Lucumi *et al.*, (2010) reported an IC<sub>50</sub> value of 5 nM against 3D7, here we show that this level of inhibition is only achieved at a concentration of  $\sim 750$  nM against K1 (150 x). Although Lucumi *et al.* (2010) used luciferase-based assay and the current study adopted SYBR green-based flow cytometry, the IC<sub>50</sub> values determined for existing antimalarials were comparable between the two studies. Furthermore, as little as a 10 fold increase in IC<sub>50</sub> value is often reported as clinically significant resistance (Gelb, 2007). Thus the 200 x and 150 x shift significantly limits these compounds for further

antimalarial development. The most potent of the LOPAC compounds was Emetine dihydrochloride hydrate. Despite also showing an increase in the  $IC_{50}$ , the potency against a multidrug resistant strain was well within guidelines of a good antimalarial candidate and even conformed to the more stringent  $EC_{50} < 100$  nM potency cut-off outlined by Biamonte *et al.* (2013).

It was not within the remit of this study to investigate every hit obtained. Therefore based on potency, three compounds from the ENZO and LOPAC libraries were taken forward for the next phase of interrogation (accurate  $IC_{50}$  determination using the SG-FCM method). These included clemastine propafenone and emetine dihydrochloride hydrate. One compound from the serotonin class (ondansetron) was also progressed, not because of its potency against the malaria parasite, but for a secondary function as potential anti-emetic for combination with emetine. As its name suggested emetine induces strong emetic effects which would evidently cause serious compliance issues if it was deployed for the treatment of malaria. Combination with an anti-emetic may help nullify the adverse effects while bestowing the additional benefits of a combinatory regime, such drug synergy and a prolongation of resistance development.

#### 4.4.5 Accurate $IC_{50}$ determination of selected compounds

The  $IC_{50}$  obtained for 3 out of the 4 selected compounds was within the expected range, as predicted by the second-phase screens. Representatives of two classes of ENZO compounds, the anti-histamines and the anti-arryhtmics, have previously been reported to inhibit *P.falciparum*. The data presented here therefore further confirms their utility as antimalarial candidates. Clemastine and propafenone achieved an  $IC_{50}$  of 427 nM and 475 nM respectively, therefore further lead optimisation will be required. As Guiguemde *et al.*, (2010) emphasised, it is not claimed that hit compounds identified from such phenotypic screens are clinical candidates in their current formulation but they are reasonable starting points.

##### 4.4.5.1 Antihistamines for malaria

With regard to the histamine receptor antagonists, astemizole, was previously identified as the most promising candidate from a screen of 2,687 compounds against the erythrocyte stage parasite (Chong *et al.*, 2006). Since then there has been other studies reporting its potential as a hybrid with chloroquine against chloroquine-resistant strains (Musonda *et al.*, 2009) and its effectiveness against liver stage parasites (Derbyhire *et al.*, 2012). As of yet there is no empirical evidence indicating that astemizole or its derivatives have entered

clinical trials. Evidently the slow progress for this compound, compared with both the spiroindolone and Imidazolopiperazines derivatives that have advance quite rapidly (Guiguemde *et al.*, 2010; Guiguemde *et al.*, 2012), has been hampered by underlying cardiotoxicity issues (Lotharius *et al.*, 2014). This is not to say that work is not ongoing. More recently Roman and colleagues have managed to achieve 200 fold selectivity towards the parasite over hamster cells with benzimidazole analogues, structural derivatives of astemizole (Roman, Crandall and Szarek, 2013).

The antihistamine clemastine, shown here to be effective against blood stage malaria, has also been shown to be potent against liver stages parasites (Derbyshire *et al.* 2012). Unlike astemizole, this compound is still available over the counter. Interestingly, astemizole is considered to act via a similar mechanism to the quinolines, therefore not representing a novel antimalarial chemotype (Plouffe *et al.*, 2008; Lotharius *et al.*, 2014), however, the highest similarity reported against the quinoline derivatives, for clemastine was 0.495 with Amodiaquine. Indicating that some antihistamines may offer a novel mode of action. Finding a safe compound with potent effects against both the blood and liver stages would be ideal and is suggested to be a necessity if eradication goals are to be achieved (Derbyshire, Mota and Clardy, 2011). Indeed, the liver stage is a bottle neck in the parasite life cycle and until recently identification of compounds active against this stage was impeded by the lack of a high throughput screen. Out of the existing antimalarials, only primaquine and atovaquone are effective against the liver stage (Derbyshire *et al.*, 20012). Hence the unique opportunity of a safe novel drug scaffold that can potentially elicit a two pronged attack is a valuable asset.

#### 4.4.5.2 Antiarrhythmic compounds for malaria

Anti-arrhythmic compounds, including propafenone have been reported elsewhere to be active against blood-stage parasites (Plouffe *et al.*, 2008; Lowes *et al.*, 2011; Weisman *et al.*, 2006). This activity was also shown at relevant doses to the therapeutic window of its prior indication (Weisman *et al.*, 2006). Again cardiotoxicity was a concern, however, lead optimisation efforts have begun to create derivatives that address its cardiac ion channel and pharmacokinetic liabilities (Lowes *et al.*, 2011). Further work has focused on improvements in the bioavailability, toxicology and pharmacokinetics of the anti-arrhythmic compounds (Lowes *et al.*, 2012). Interestingly, propafenone has also been shown to be more potent in the drug resistant strain, K1 when compared with the susceptible strain, 3D7 (Lowes *et al.*, 2011).

#### 4.4.5.3 *The anti-emetic, serotonin receptor antagonist for combination with emetine*

The third ENZO compound, the serotonin receptor antagonist ondansetron, on the other hand presented considerably lower activity than inferred by both the preliminary and secondary screens. A new powder stock was purchased for this compound and dissolved in water (as indicated by sigma) as opposed to the previous suspension of the ENZO library in DMSO. This suggest that either the initial screens were inaccurate or there was a dissolvability problem with the newly purchased stock. This kind of discrepancy is not uncommon among phenotypic screens that often report a re-confirmation rate of only 75-80 % when a new stock is purchased (Guiguemde *et al.*, 2010; Plouffe *et al.*, 2008). Multiple dose response attempts were made (Appendix VI) but an IC<sub>50</sub> level of inhibition was not achieved until the dose range was significantly increased. Due to a lack of activity and the obvious detriment to the chances of a safe therapeutic window ondansetron may not be suitable for combination with emetine. Unless further work can validate the potency observed in the preliminary screens.

#### 4.4.5.4 *The anti-amoebic compound for malaria*

The high activity of the LOPAC compound Emetine dihydrochloride hydrate (IC<sub>50</sub> = 47 nM) was also re-confirmed. Although the compound has been identified repeatedly as a potent antimalarial in numerous high through-put screens, it has been largely overlooked as a potential candidate due to fears of toxicity. Emetine, originally derived from the root of *Carapichea ipecacuanha* (Ipecac), was previously used as a potent intestinal and tissue amoebicide. Adverse effects of the treatment included nausea and vomiting (emesis-hence its name). In fact, the drug was often exploited medicinally to induce vomiting. However after the 1980's its use was abandoned due to serious cardiotoxic complications, seen in a small proportion of patients (high cumulative doses), and availability of a safer alternative metronidazole. Initial toxicity issues are in fact a common affliction amongst novel classes of compounds identified as antimalarial inhibitors. The majority of libraries screened contain compounds for which the primary indication was a human disease and are therefore inherently active against human targets. Derivatization to reduced cardiotoxic effects of anti-histamine and anti-arrhythmic compounds has led to safer alternatives. With emetine as a potent starting point it may be possible to also use derivatization to overcome such issues. Furthermore the value of Emetine, a natural product compound used

previously for the treatment of a parasitic infection, with potentially multiple targets that could circumvent resistance should not be discounted.

#### 4.4.6 Conclusion

Given that 90 % of drug candidates fail during development (Ashburn and Thor, 2004), and the fact that there are no novel antimalarials in the foreseeable pipeline, drug-repositioning offers a much needed interim solution. The data presented here clearly supports the strategy as a viable option for antimalarial drug discovery. From a screen of < 700 hundred compounds we have identified at least 3 potent antimalarial candidates. In addition to that, other novel scaffolds have been shown to have antimalarial activity at < 1  $\mu$ M (MMV guidelines, Lotharius *et al.*, 2014). To make drug repositioning a valuable tool it is important that these hits are characterised on a more systematic basis with equal velocity and enthusiasm. Else, initial screening efforts that promise to help speed up drug development and rapidly progress candidates to the front line will be futile (Baniecki, *et al.*, 2007). The high activity of emetine against a multidrug resistant strain, K1, justifies its selection for further interrogation. Unlike the anti-histamine and anti-arrhythmic compounds its antimalarial potential has been commonly overlooked. In order to progress emetine as a viable antimalarial candidate intensive *in vitro* investigations to elucidate the killing profile, stage specificity and its suitability for combination with existing antimalarials will be employed. Once optimised the outlined workflow for emetine could be applied to other candidates. The more intensive *in vitro* investigations afforded by the focus of academic study rather than large scale industrial development should permit better *in vitro* to *in vivo* translation of hits.

Undoubtedly, the current voids in the malaria drug market highlight the fact that mankind could be faced with a potentially horrific, uncontrollable, resurgence of the disease if drug production does not meet the on-going demand. Therefore to make drug repositioning a viable short term option for anti-malarial drug discovery, hit compounds, like emetine, should be quickly advanced to second-phase screening programs. Where more detailed interrogation of the compound can be completed. The importance of effective interaction studies cannot be overemphasised as combination therapy is the future for malaria treatment. Without rapid progress of candidate antimalarials, the benefits of a fast-track drug discovery program will undoubtedly be lost.

## CHAPTER 5

---

### ANTIMALARIAL ACTIVITY OF EMETINE DIHYDROCHLORIDE HYDRATE

#### 5.1 INTRODUCTION

For almost 50 years, emetine was used as a standard, affordable treatment for amoebiasis and amoebic dysentery, caused by the protozoan parasite *Entamoeba histolytica* (Akinboye and Bakare, 2011). The natural plant-derived product was also given ‘over the counter’ in the form of Syrup of ipecac to induce vomiting in cases of poison (Akinboye *et al.*, 2012). Unfortunately the curtailment of its medicinal use, due to adverse cardiotoxic effects and the availability of a safer anti-amoebic drug (metronidazole), has precluded interest in the compound for antimalarial repositioning, despite being identified as a recurring hit in recent high throughput screens (Andrews *et al.*, 2014; Lucumi *et al.*, 2010; Plouffe *et al.*, 2008). However, its bioactive potential for other parasitic diseases has been considered. As early as 1966 the value of emetine as and antischistosomal compounds was realised when schistosomal haematuria’s disappeared in patients treated for amoebic dysentery (Dempsey and Salem, 1966). More recently emetine has been identified as a potent trypanocidal compound against both *Trypanosoma cruzi*, complete inhibition at  $< 5 \mu\text{g/ml}$  (Cavin *et al.*, 1987) and *T. brucei* with  $\text{IC}_{50} < 1 \mu\text{M}$  (Mackey *et al.*, 2006) or  $< 10 \mu\text{M}$  (Merschjohann *et al.*, 2000), the causative agents of Chagas disease and Sleeping Sickness respectively. *In vitro* activity against *Leishmania donovani* at  $0.03 \mu\text{g/ml}$  (Muhammed *et al.*, 2003) and *Toxocara canis* at  $109 \mu\text{mol/L}$  (Satou *et al.*, 2002) has also been demonstrated. However in most cases, the limited margin of safety against human cell lines was a cause for concern (Mackey *et al.*, 2006; Merschjohann *et al.*, 2000; Rosenkranz and Wink, 2008; Satou *et al.*, 2002). The reasons for perusing the compound for malaria repositioning are two-fold; firstly, the potential for a favourable dose-related toxicity profile against the malaria parasite and secondly the existence of a safer derivative. Most of the toxicity studies for emetine were carried out in the 1960’s, therefore, revisiting this area with post genomic technologies may offer new insight.

A review of existing literature suggests that the side effects of emetine are dose dependent (Akinboye and Bakare, 2011). One of the more recent studies showed that *in vitro* sensitivity of various amoebiasis strains ranged from  $25\text{--}35 \mu\text{M}$  (Bansal *et al.*, 2004), which is 700-fold higher than the antimalarial potency presented here against K1, 35,000-fold higher than  $\text{IC}_{50}$  for 3D7 (Lucumi *et al.*, 2010), and 1750-fold higher than the  $\text{IC}_{50}$  for



W2 (Genomics Institute of the Novartis Research Foundation database). This *in vitro* data has beneficial implications for its margin of safety as an antimalarial and indicates that the dose-dependent toxicity profile should be re-evaluated at a 'malaria appropriate' dose range. The majority of *in vivo* data and information about drug plasma concentrations is also dated. However, Asano *et al.*, (2001) recently provided some information about the pharmacokinetic and pharmacodynamic properties of the compound in humans. Healthy male volunteers were given 5, 10, 15, 20, 25 or 30 ml of a solution containing 0.503 mg/ml of emetine. This equates to a single dose of 2.5, 5, 7.5, 10, 12.5 and 15 mg respectively. Authors reported that between 10-84% of the initial oral preparation of emetine was found in vomit. If we consider that the highest dose would induce the most vomiting then it can be assumed that potentially only 16 % of the solution was absorbed equating to a total dose 2.4 mg (16 % of 15 mg). From this, a concentration of 6.2 ng/ml was measured in human plasma after 12 hours. Our *in vitro* investigations suggest that the IC<sub>50</sub> for emetine against the multi drug resistant strain K1 is 50 nM which is equivalent to 27.7 ng/ml (4.5 x more than 6.2 ng/ml). Notably, the 1 nM 3D7 efficacy reported by Lucumi *et al.* (2010) would equate to 0.55 ng/ml (which is 11.3 x less than 6.2 ng/ml). Asano *et al* (2001) showed that, once vomiting is corrected for, there was a linear relationship between the emetine dose ingested and the concentration in the blood plasma. Therefore in order to achieve a plasma concentration equating to IC<sub>50</sub>, the emetine dose given should be 10.8 mgs (4.5 x 2.4). This dose is well within the previously recommended dose for amoebiasis treatment of up to 60 mg per day for 6 days followed by 3 further treatments after day 9 (Ganguli, 2002). Obviously the aim is to achieve 100 % parasite killing, but up to 5 x this dose is achievable within the window of safety and our work showed that just 2 x the IC<sub>50</sub> dose was capable of inducing 90% inhibition (Figure 4.8). Due to the sporadic nature of the previously reported cardiotoxic events, mostly related to cumulative dosing after day 6, it is plausible that such issues could be avoided during malaria treatment, particularly if a shorter treatment periods were adopted. In the study by Asano *et al.* (2001) emetine was undetectable in blood plasma after 168 hour but persisted in the urine for up to 12 weeks. This is consistent with previous reports of detection in urine after 60 days and agrees with evidence that the compound accumulates in the liver and other organs. Indeed accumulation in organs is most likely responsible for cardiotoxic issues. What is more, such persistence could mean that parasites will be exposed to sub-optimal concentrations, encouraging the likelihood of resistance development. Conversely, the issue may be

advantageous for treatment of *P. vivax* infections if the hepatic concentrations could be exploited attack the dormant liver stages of this species.

Fortunately, prior to the introduction of metranidazole for amebiasis treatment, efforts were made to develop a safer alternative to the parent compound emetine. A synthetic modification of the drug (2, 3-dehydroemetine (DHE, Roche)) was shown to retain its amoebicidal properties while producing fewer side effects (Figure 5.1 Table 5.2). Other advantages were that it had a shorter period of bioactivity and was excreted more rapidly from most body organs including the heart. The oral resonate, although incompletely absorbed and thus requiring higher concentrations of the compound, was shown to be more tolerable and in fact more effective than the injection (Dempsey and Salem, 1966). Furthermore daily doses of up to 90 mg per day (intramuscular) have been recommended for the safer alternative (Nozaki and Bhattacharya, 2014), inferring that lethal *Plasmodium falciparum* doses could be achieved providing that DHE has comparable antimalarial activity to emetine. In practical terms, gastric irritation due to emetine could be further minimised by the adoption on novel drug formulation methods. Various coating options could be employed to ensure slow or pH-dependent release of the compound. For cerebral malaria intramuscular injection could also be an option when in-hospital patient monitoring is routine. Future biotechnological advances could also provide the option of nano delivery systems for emetine, to avoid the troublesome emesis and cardiotoxic side-effects (Allen and Cullis, 2004).

In vitro Data			
	Pf potency	Pf in vitro IC <sub>50</sub>	Selectivity Index
Emetine di-hydrochloride	High	K1: 26 ng/ml, 3D7: 0.55 ng/ml, D6: 72 ng/mL, W2:78 ng/mL	D6: 6, W2: 5
Klugine	High	D6: 37.7 ng/mL, W2:46.3 ng/mL	D6:>265, W2:>217
Cephaeline	High	K1: 3.8 ng/ml, 2807:27 ng/mL, INDO:11 ng/mL, D6: 38 ng/mL, W2: 27.7 ng/mL	D6: 132, W2: 193
Isoemetine	Inactive		NT
Isocephaeline	Low	D6: 186 ng/mL, W2: 290 ng/mL	D5:>54, W2:>35
7'-O-dethylisocephaeline	V. low	D6: 1500 ng/mL, W2: 3067 ng/mL	D6:>7, W2L>3
Psychotrine	Low	2807: 140 ng/mL, INDO: 390 ng/mL	
Tubulosine	High	K1: 20 ng/mL, 2807: 6 ng/mL, INDO: 11 ng/ml	W2: 0.9
Chloroquine	High	2807: 20ng/mL, INDO: 80 ng/mL, D6: 18ng/mL, W2: 176ng/mL	D6:>556, W2: >56
Artemisinin	High	D6: 14.3ng/mL, W2: 8.5ng/mL	D6:>699, W2: >1176

**Table 5.1 A Summary of the *in vitro* anti-malarial efficacy and selectivity of emetine and its analogues.** (NT: not tested, NC: Not cytotoxic at max dose 10 µg/mL, SI: Selectivity Index IC<sub>50</sub> VERO/IC<sub>50</sub> Pf. Data collated from Matthews *et al.*, 2013, Lucumi *et al.* 2010, Freidrich *et al.*, 2007, Wright *et al.*, 1991, Sauvin *et al.*, 1992, Muhammad *et al.*, 2003, Akinboya and Bakare 2011)

The synthetic derivative dehydroemetine is stated is commercially unavailable as production has been discontinued. The complex re-synthesis of the compound is not within the remit of the current study and therefore its antimalarial potency has not been evaluated. However, the existence such a derivative demonstrates that emetine is amenable to useful

chemical modification with the potential to deselect for toxicity. Furthermore, studies on closely related naturally occurring, structurally similar analogues of emetine support the hypothesis that minor structural differences in the molecule result in significant differences in pharmacology, toxicology and selectivity. For this reason the closely related natural analogue, cephaeline (Figure 5.1 table 5.2) will be compared it's for potency and toxicity against the malaria parasite and a mammalian cell line respectively.

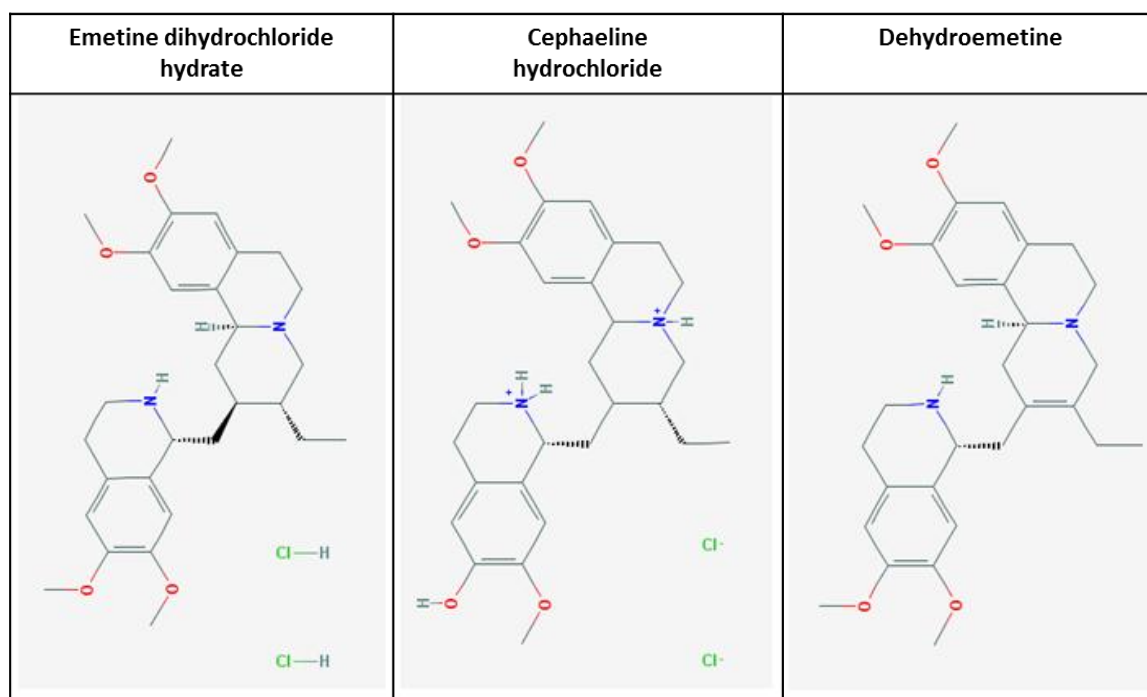


**Figure 5.1** The structure of emetine dihydrochloride hydrate, cephaeline hydrochloride and dehydroemetine for comparison (Source: PubChem).

Lipinski's rule of 5	Emetine		Cephaeline		Dehydroemetine
≤ 5 hydrogen bond donors	3*	1	3*	2	1
≤ 10 hydrogen bond acceptors	7	6	6	6	6
Molecular weight < 500	553.6 g/mol	480.6 g/mol	539.5 g/mol	466.6 g/mol	478.6 g/mol
LogP < 5	---	4.7	---	4.4	3.7

**Table 5.2** Parameters for lipinski's rule of 5 are shown for emetine, cephaeline and dehydroemetine. Violations of lipinski's rules are indicated in red. \*Compounds used in the current study emetine dihydrochloride hydrate and cephaeline hydrochloride (Source: PubChem).

The potential of emetine derivatives to provide a novel antimalarial class and the wealth of pre-existing information about structural activity relations justifies a more detailed interrogation of the compound as an antimalarial candidate. Towards this aim, the killing profile of emetine will be defined against the multidrug resistant *Plasmodium falciparum* parasites strain K1. Knowing a compounds killing profile should not only help inform decisions about appropriate pharmacokinetically-matched combinatory options but also

provide better *in vitro* to *in vivo* translation. Indeed, the recent upsurge of antimalarial hit compounds in the literature and the availability of better *in vitro* assays has meant that acquiring accurate *in vitro* pharmacokinetic data is imperative to prioritise candidates for *in vivo* evaluation.

## 5.2 METHODS

### 5.2.1 Determination of cephaeline $IC_{50}$ in *P.falciparum* strain K1

The ipecac alkaloid cephaeline hydrochloride (Sigma, UK) was analysed for antimalarial activity against the K1 strain. Following an initial preliminary screen (Appendix VII) an 8 point two-fold dose series from 0.78-100 nM was set up. Treatment conditions and  $IC_{50}$  determination were consistent with those described previously (Chapter 2). The emetine dose-response was completed in parallel to permit direct comparisons between the two compounds. Tanimoto similarity was also determined for the two analogues as detailed in (Chapter 4).

### 5.2.2 Comparison of cephaeline and emetine cellular toxicity

HepG2 cells were maintained in RPMI 1640 media containing 2mM l-glutamine, HEPES and substituted with 1 % non-essential amino acids, 10 % fetal calf serum (FCS) and 1 % Pen/strep. Incubations were at 37 °C under 5 %  $CO_2$ . Confluent cells were counted and seeded at 4000 cells/well and 2000 cells/well for 48 and 120 hour exposures, respectively. The drugs were added 24 hours after seeding to permit cell adherence prior to drug exposure. An initial experiment opted for a wide dose-range (25  $\mu$ M-3 nM) so that the inhibitory concentrations were not overlooked (Appendix VIII). A 25  $\mu$ M-0.39  $\mu$ M two-fold dose series of cisplatin (Sigma-Aldrich) was included on each plate as a positive control. Once the appropriate dose-range for cephaeline and emetine had been determined (200 nM-3.125 nM 2-fold dose series) the experiment was repeated to obtain accurate  $IC_{50}$  values.

### 5.2.3 Time-course analysis of emetine and dihydroartemisinin against K1 parasites

In order to gain further insight into the mode of action of emetine an *in vitro* time-course assay was completed. Parasites were treated with either  $IC_{50}$  DHA,  $IC_{50}$  emetine, or a combination of both compounds ( $IC_{50}$  DHA +  $IC_{50}$  Eme). Untreated controls were also analysed in parallel to the drug treatments. Duplicate treatments were initiated at late trophozoite stage and analysed for growth at 24, 48 and 72 hour time points using SG-FCM (Chapter 2 section 2.2.3). Parasite progression through the erythrocyte cycle stages

was also monitored due to the capability of the method to differentiate between mononuclear and multinuclear parasite forms. The proportion of multinuclear cells (schizonts) was then displayed as a percentage of the total number of parasitised cells recorded for each treatment at each time point. Giemsa staining was used for parasite stage confirmation.

#### 5.2.4 Stage-specificity of emetine

Parallel cultures previously synchronised at either ring or trophozoite stage were diluted to ~1 % parasitaemia. The culture was subdivided into control, or emetine treatments of  $IC_{50}$  (55 nM) and 10 x  $IC_{50}$  (550 nM) concentrations (2.5 % haematocrit) and incubated in accordance with standard conditions. Following a 6 hour treatment period 2 ml was removed from each condition, washed 3 x in complete media to remove the drug and re-suspended in an equal volume of complete media to restore the haematocrit to 2.5 %. Two hundred microliters of each condition, including the samples washed at 6 hours and the remaining samples that had not been washed and thus remained exposed to the drug, were then transferred to a 96 well plate. For each condition there were at least 4 replicates. The plate was placed in the humidifying chamber, gassed and incubated for 48 hours. Following the incubation period triplicate samples for each condition were analysed using the SG-FCM method as described previously.

#### 5.2.5 Determination of the killing profile for emetine against *K1* parasites

A more in depth method to determine the emetine killing profile against *P. falciparum* was employed. All procedures were consistent with those described by Sanz *et al.*, 2012. In brief, drug treatment was initiated at 10 x the  $IC_{50}$  (550 nM emetine) against an initial inoculum of  $10^6$  ring stage parasites/ml at 0.5 % parasitaemia 2 % haematocrit. The flask culture was incubated for 5 days (120 h). At 24 hours intervals the drug treatment was replenished to maintain a constant drug pressure and parasite recovery was analysed by limiting serial dilution. At each time point (0, 24, 48, 72, 96, and 120) an aliquot corresponding to  $10^5$  parasites was removed (1 ml) washed 3 x in complete media to remove the drug (centrifuged at 3000 rpm), and re-suspended in an equal volume to restore the original haematocrit. A 96 well plate was prepared from rows 2-12 by adding 100  $\mu$ l of 2 % haematocrit blood in complete media. To row 1 of the plate 150  $\mu$ l of the washed aliquot was added in quadruplicate. A 1:3 limiting serial dilution was performed by transferring 50  $\mu$ l of the parasitised culture in row 1 to row 2 (containing 100  $\mu$ l freshly prepared erythrocytes) mixing and again transferring 50  $\mu$ l to the adjacent well (row 3).

All wells were serially diluted in this manner. Half (50 µl) of each well was then discarded. Double the volume required was used for the serial dilution to ensure that evaporation and drying of a small volume in the flat bottom 96 well plate, whilst preparing the dilution, did not confound the results. Each well then received an additional 100µl of complete media so that the final volume was 150 µl and the haematocrit was reduced to 0.667% per well. The plate was placed in a humidifying chamber, gassed and incubated for 28 days under conditions described previously. During the course of the experiment each container was gassed every 3-4 days. Spent media was removed on days 7, 14 and 20 and replaced with fresh media and blood (see Table 5.3).

Day	Volume removed	Volume added	Haematocrit (fresh blood)	Final haematocrit per well
7	100 µl	150 µl	0.667 %	200 µl at 1 %
14	150 µl	150 µl	0.667 %	200 µl at 1.5 %
20	100 µl	200 µl	1.5 %	300 µl at 2%*

**Table 5.3** Dilution procedure with fresh erythrocytes (varying haematocrits) at days 7, 14 and 20. \*half removed (150 µl) and transferred to a second plate for day 21 analysis.

On day 21 and 28 triplicate samples were analysed for growth using the SG-FCM method. Parasitaemia plots for each well were used to determine which dilution was the last to render growth following exposure to emetine for the aforementioned treatment periods (0, 24, 48, 72, 96, and 120 h). The number of viable parasite was then back-calculated using the formula  $X^{n-1}$  (where X is the dilution factor and n is the number of wells able to render growth). Log transformed values ( $\text{Log}(X^{n-1}) + 1$ ) were plotted for the time-course. Two key mode of action parameters: namely the parasite reduction ratio (PRR) and parasite clearance time (PCT) were then calculated from the graph.

#### 5.2.6 Preliminary comparison of JC-1 and SYBR Green staining

Used also as a read out for parasite survival, the JC-1 assay was completed in parallel with the SYBR Green flow cytometer method to permit direct comparison. Briefly, a continuous culture of *Plasmodium falciparum* was diluted to ~1 % parasitaemia and split into two cultures flasks. The first flask served as an untreated control whilst the second flask was exposed to IC<sub>50</sub> DHA (2.5 nM). Following a 48 hr incubation period 50 µl of the respective control and treated culture flasks were transferred to eppendorf tubes. An additional 50 µl was taken from the untreated control sample and treated with 0.5 µl Carbonylcyamide m- chlorophenylhydrazine (CCCP -positive control and inducer of loss

of mitochondrial membrane potential) and incubated for 5 min in a humidifying chamber at 37 °C and 5 % CO<sub>2</sub>. Following a single washing step with PBS JC-1 (Molecular probes, Invitrogen, USA) was added to each tube to a final concentration of 6 µM (1.5 µl of stock solution into 50 µl parasite suspension). The samples were then incubated for 30 mins in a humidifying chamber at 37 °C and 5 % CO<sub>2</sub>. Parallel samples (Control, CCCP treated, and DHA treated) were also taken for SYBR Green staining (Chapter 2 section 2.4). Following staining samples were washed 3 x with PBS and analysed using flow cytometry (BD FACsVerse flow cytometer). The FITC and PI channels were used for JC-1 Green and JC-1 Red staining respectively. Red staining was also confirmed by fluorescence microscopy (Nikon Eclipse TE2000-S) see Appendix IX.

#### *5.2.7 JC-1 and SYBR Green following chloroquine treatment*

In order to establish whether loss of mitochondrial membrane potential could be detected prior to any evidence of parasite death (as determined by SYBR Green staining) a short treatment time-course was set up. Trophozoite stage parasites (2 % parasitaemia) were treated with a 0.3 µM, 3 µM and 30 µM chloroquine dose range for 7 hours. These parameters were consistent with those reported by Ch'ng *et al.* (2010) previously shown to induced loss of loss of mitochondrial membrane potential. Duplicate samples were set up for each treatment including untreated controls. The JC-1 and SYBR Green staining procedures were consistent with the methods described above (Section 5.2.5). CCCP exposure of additional untreated control samples also served the positive control.

#### *5.2.8 Loss of mitochondrial membrane potential after atovaquone and emetine treatment*

The experiment was initiated at ring stage with 2 % parasitaemia and 2.5% haematocrit. Parasites were treated for 24 or 72 hours with pre-determined IC<sub>50</sub> doses of atovaquone (0.8 ng/ml or 2.3 nM) and emetine (50 nM). Loss of mitochondrial membrane potential was determined by JC-1 staining (Section 5.2.5) concurrently with parasitaemia estimates using SG-FCM (Chaper 2 Section 2.2.3). Prior to staining parasite were exposed to CCCP treatment (positive control) for 5 minutes as described previously (Section 5.2.5)

### 5.3 RESULTS

#### 5.3.1 Comparison of cephaeline and emetine dose response

Despite displaying a tanimoto similarity score of 0.943 with emetine, cephaeline was shown to be 6 x more potent against the drug resistant strain with an  $IC_{50}$  of 8 nM compared with 47 nM previously reported for emetine (Figure 5.2).

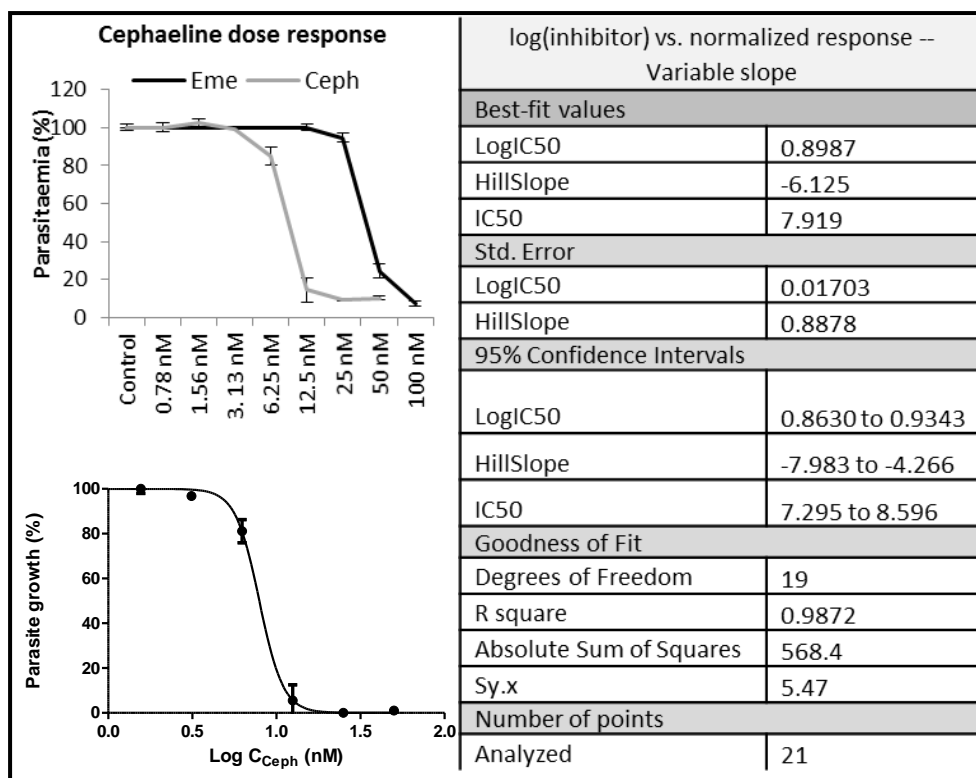


**Figure 5.2 Dose response of cephaeline against *P.falciparum*, strain K1.** The compiled image shows the parallel comparison of cephaeline and emetine dose response curves (a). Cephaeline dose response for log transformed drug concentrations (b). Nonlinear regression analysis output for accurate  $IC_{50}$  determination of cephaeline (c) using GraphPad Prism 5.0 (Sy.x indicates the standard deviation of residuals).

#### 5.3.2 Comparison of cephaeline and emetine cellular toxicity

The HepG2 cell line was used to evaluate the cellular toxicity of cephaeline and emetine. At both the 48 and 72 hour time points, there was a shift in the dose-response curves between two compounds (Figure 5.3).  $IC_{50}$  determination confirmed that the human cell line was more sensitive to cephaeline exposure when compared with emetine. The  $IC_{50}$  values obtained for the positive control, Cisplatin, were in line with estimates reported elsewhere (McAlpine *et al.*, 2014) and served to validate the data (Table 5.4).



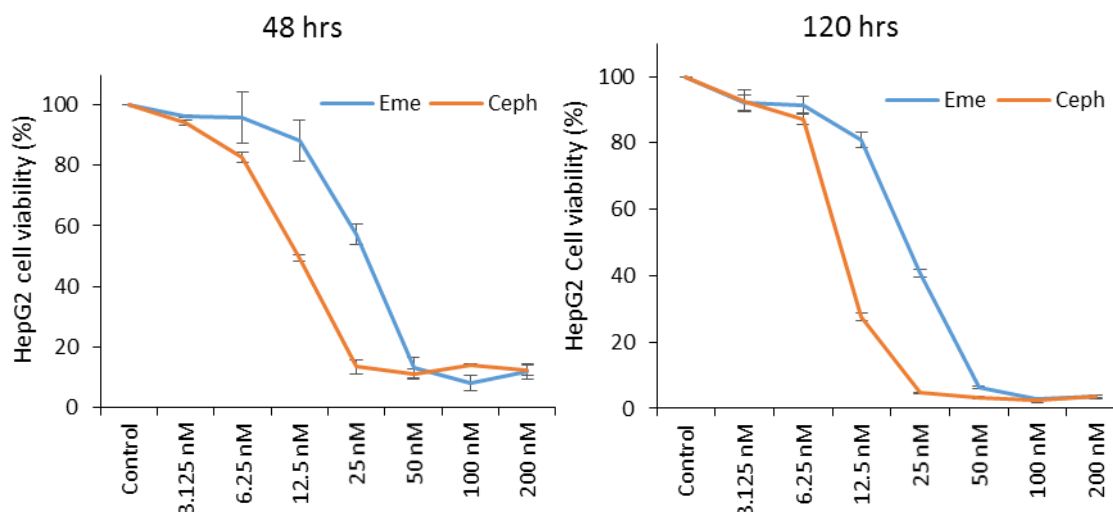


**Figure 5.3** Dose response curves for emetine and cephaeline against HepG2 cells following 48 (a) and 120 (b) hours of exposure. Cell viability was determined using the standard MTT assay. Error bars represent triplicate data.

	HepG2 IC <sub>50</sub>		
	Cisplatin + control (μM)	Emetine (nM)	Cephaeline (nM)
<b>48 h</b>	5.1 ± 1.37	25.2 ± 2.42	10.8 ± 0.64
<b>120 h</b>	3.6 ± 0.33	20.6 ± 1.32	9.7 ± 0.41

**Table 5.4** IC<sub>50</sub> values for the positive control, cisplatin, and the two test compounds emetine and cephaeline against the HepG2 cell line. Both the 48 and 120 hour time points were evaluated. IC<sub>50</sub> values were determined using nonlinear regression (GraphPad Prism 5.0) Averages are based on triplicate data. Standard error values for each estimate are also shown.

### 5.3.3 Time-course analysis of dihydroartemisinin and emetine dihydrochloride hydrate

The results of the time-course indicate that like dihydroartemisinin the effects of emetine only become apparent once a subsequent erythrocytic cycle has been entered. These effects were further pronounced upon successive cycle progression. However, apart from variations in potency, DHA and Eme showed no difference in the time of drug action (Figure 5.4).

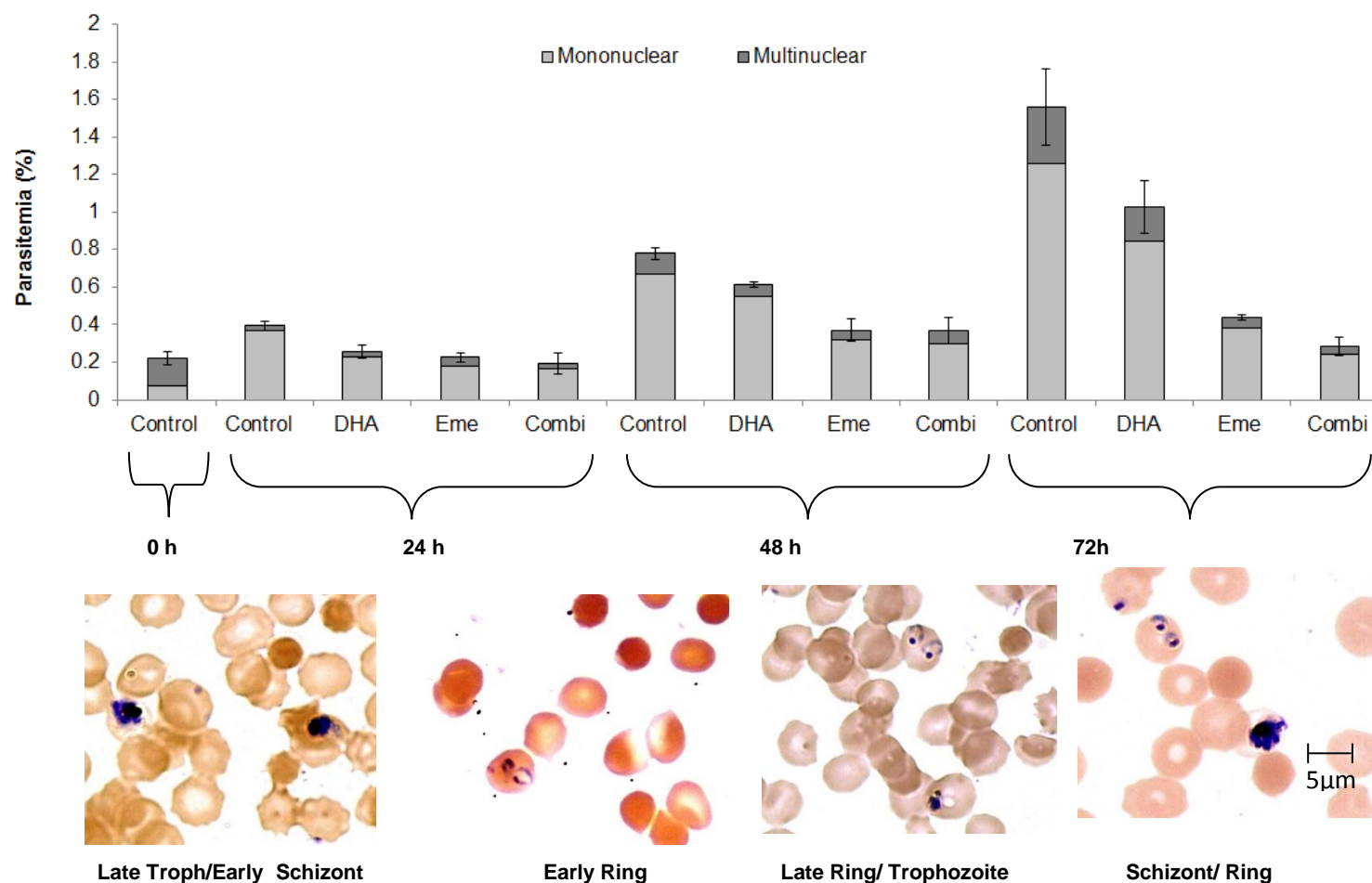


**Figure 5.4 Time-course analysis of dihydroartemisinin (DHA) in parallel with emetine (Eme) and the combination.** The respective  $IC_{50}$  doses of DHA, Eme and the combination ( $IC_{50} + IC_{50}$ ) were added at late trophozoite/schizont stage and analysed at 24 hour intervals during a 72 hour time-course. Drug susceptibility was analysed using the robust SYBR Green flow cytometer method to permit differentiation between mononuclear and multinuclear parasite stages. Giemsa staining of control samples was also used for confirmation of parasite progression through erythrocytic cycle.

Further investigation into stage-specific analysis (mononuclear vs multinuclear) revealed interesting variations in parasite progression patterns during the course of drug treatment. For dihydroartemisinin-treated samples, progress into the multinucleated schizont form imitated that of the untreated control samples. Emetine-treated samples, on the other hand showed a reversed pattern, representing a delay in parasite development. This data was corroborated by the fact that the combined effect of the drugs appeared to display a true amalgamation of the two (Figure 5.5).

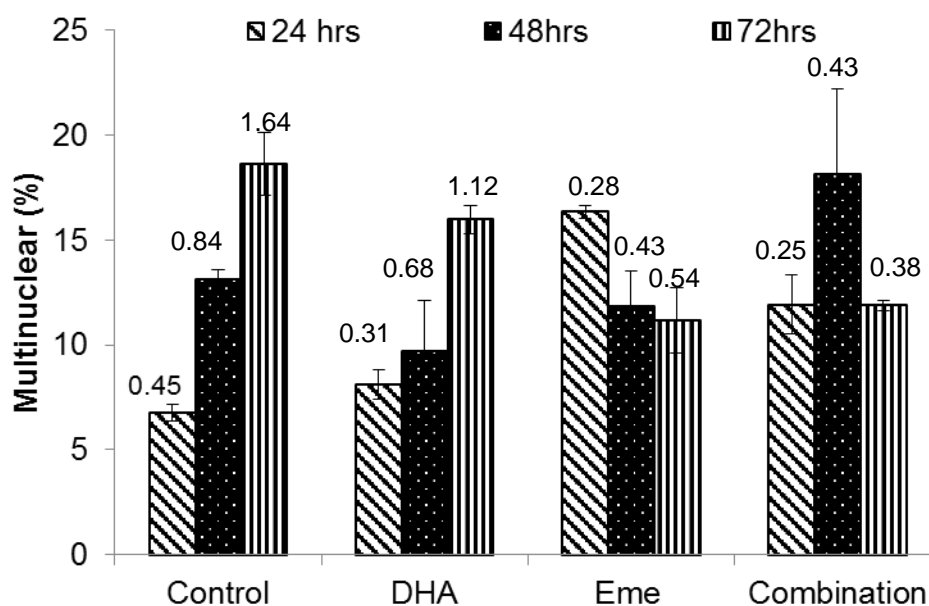


**Figure 5.5** *In vitro* stage progression of *P. falciparum* K1 parasites following exposure to dihydroartemisinin and emetine Trophozoite stage parasites were treated with IC<sub>50</sub> DHA (2.5 nM) and IC<sub>50</sub> emetine (50 nM) either alone or in combination for a 24, 48 and 72 hour time-course. The percentage of multinuclear cells (schizont) as a proportion of the total parasitaemia was recorded for each condition at each time point. The total parasitaemia is indicated by the numbers above bars.

#### 5.3.4 Stage-specific effects

Stage-specific effects show that treatment directed specifically against ring or trophozoites stage parasites for only a 6 hour period is capable of significantly reducing growth relative to controls by about ~ 20% in both cases (Figure 5.6).

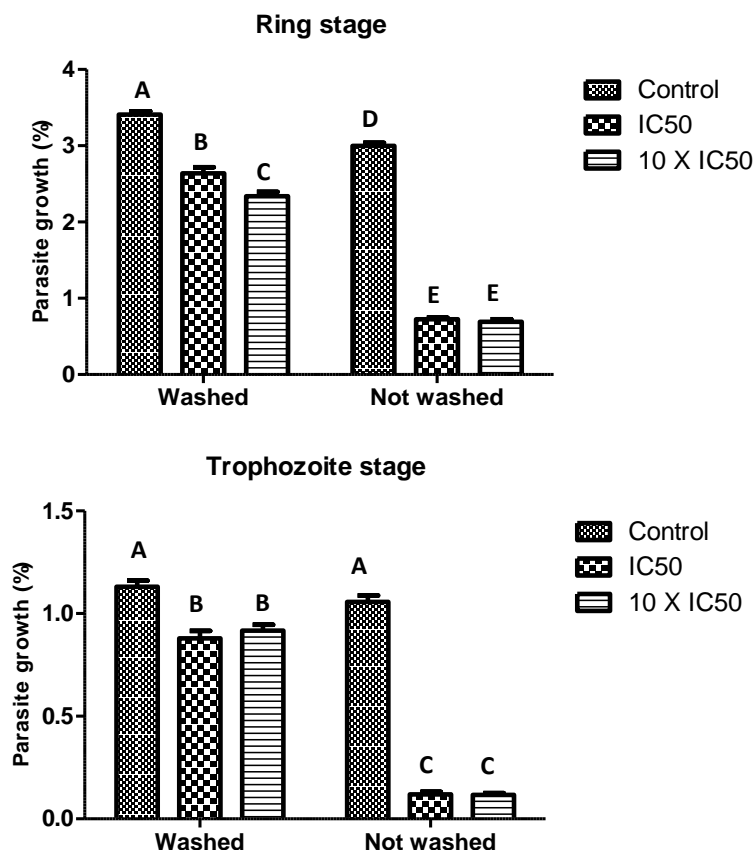


**Figure 5.6 Stage-specific cytostatic/ cytocidal analysis of emetine.** Ring (a) and trophozoite (b) stage parasite were treated for 6 hours before washing and removal of the drug and a further incubation of 42 hours. A parallel 48 hour exposure to emetine was also set up. Different letters indicate data that is significantly different as determined by one-way ANOVA (GraphPad Prism 5.0)

### 5.3.5 Determination of the parasite killing profile for emetine against *P. falciparum* K1

SG-FCM was used to analyse productive re-growth upon removal of the drug after 20 and 28 days of recovery. The data showed that the most diluted well able to render growth was dependent on the initial drug treatment period (Figures 5.7 and 5.8) Triplicate data was generally consistent between samples. Discrepancies only appeared where it was evident that the last viable parasite had been transferred to the subsequent dilution, in some cases leaving no evidence of growth in the previous dilution. Parasitaemia estimates from each replica were displayed separately. This was to prevent data based on averages confounding the definition of parasite growth at each dilution in a presence or absence manner. Both the 21 day (Figure 5.7) and 28 day (Figure 5.8) data indicated that emetine induced a lag phase in parasite killing of approximately 48 hours (Figure 5.9). Parasites were not able to withstand emetine exposure for 96 and 120 hours periods (Figure 5.9). The direct measure of parasite killing rate, the parasite reduction ratio (PRR) was determined by a decrease in parasite killing during 48 hours of the maximal killing phase, and the parasite clearance

time (PCT), the time needed to clear 99.9% of the parasite population, are shown in Table 5.5. When compared with a panel of existing antimalarials, the killing profile of emetine is most consistent with that of atovaquone.

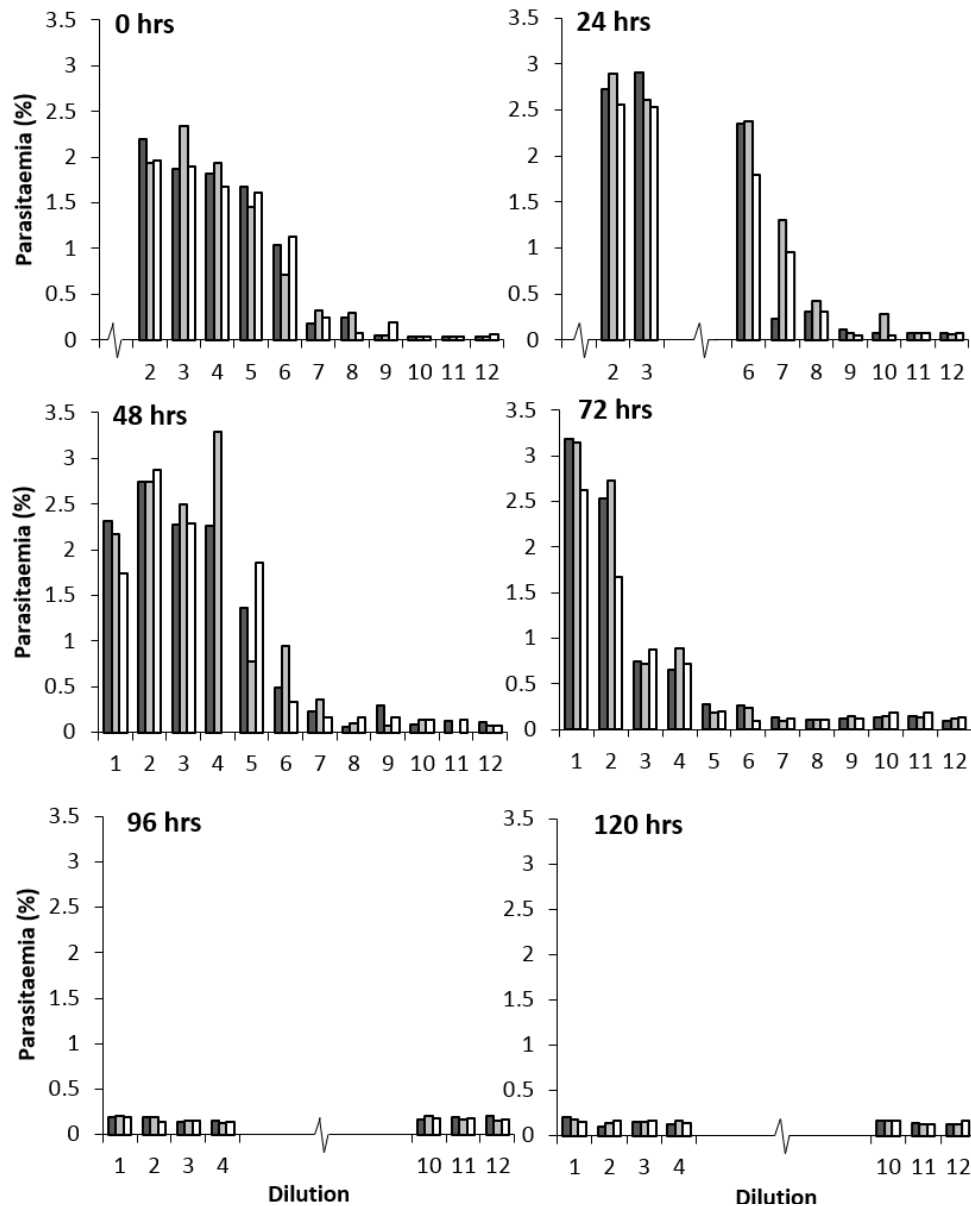


**Figure 5.7 The recovery of parasite productive growth following emetine exposure, day 21 analysis.** SYBR Green Flow cytometry was used to determine parasite regrowth on day 21. Parasites were subjected to the limiting serial dilution (aliquots corresponding to  $10^5$  parasites) following emetine exposure for either 0, 24, 48, 72, 96 and 120 hours treatment periods. Triplicate data points are shown separately to permit accurate determination of parasite growth at each dilution in a presence or absence manner. Axis breaks are present where data was not collected due to the consistency of the surrounding readings.

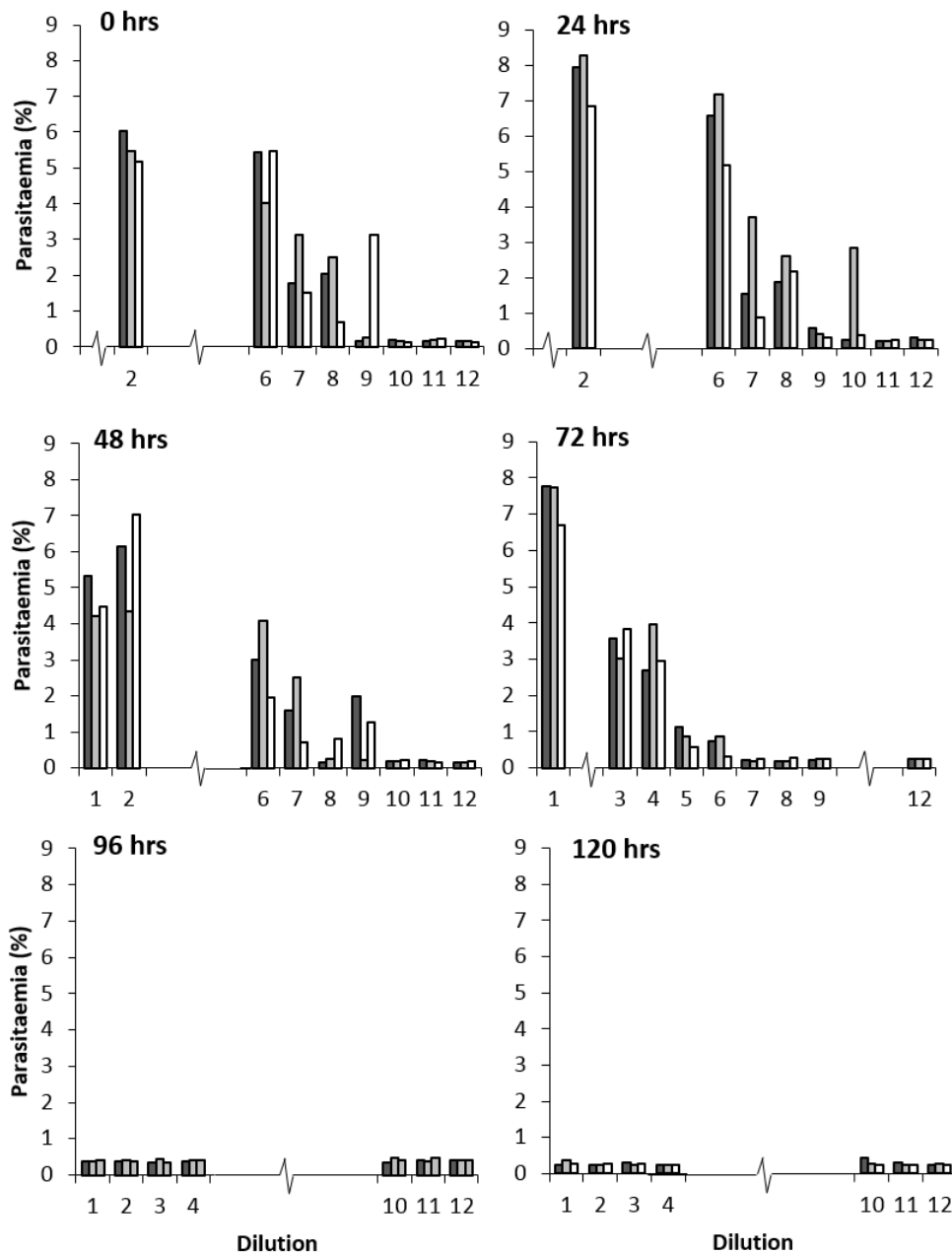


**Figure 5.8 The recovery of parasite productive growth following emetine exposure, day 28 analysis.** Day 28 data provides confirmation of parasite regrowth at day 21. Following treatment with emetine for either 0, 24, 48, 72, 96 and 120 hours an aliquot of  $10^5$  parasites was washed 3 x to remove the drug and subjected to limiting serial dilution. Parasitaemia was determined after a 28 day recovery period using SYBR Green Flow cytometry. The raw data was used to determine the last dilution at each time point able to render growth. Axis breaks are indicative of absent data points.

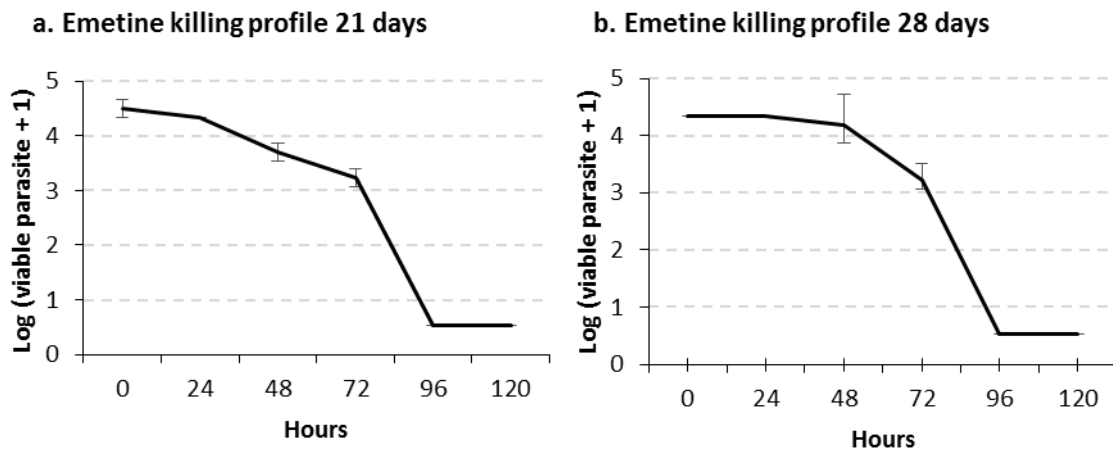
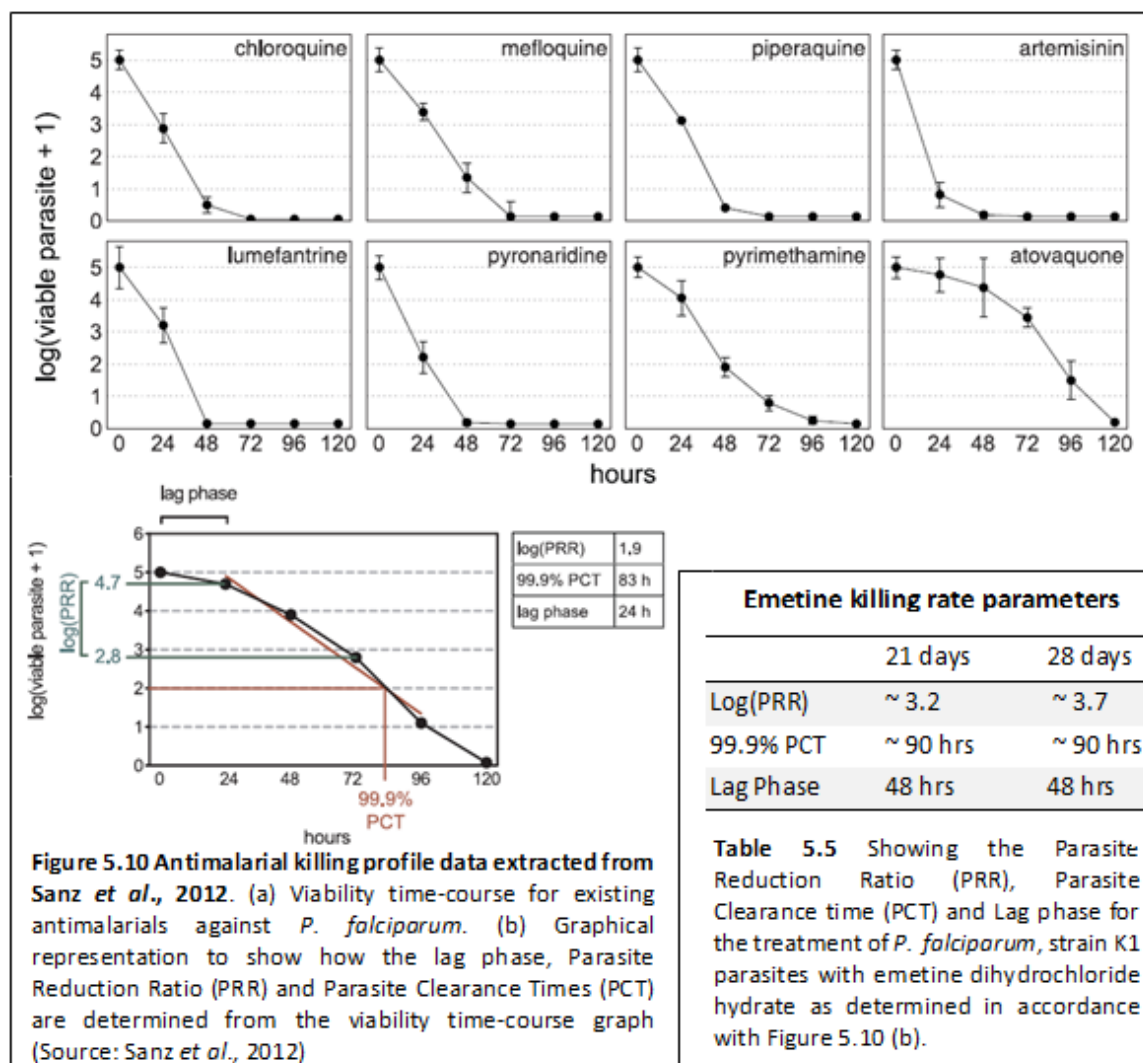
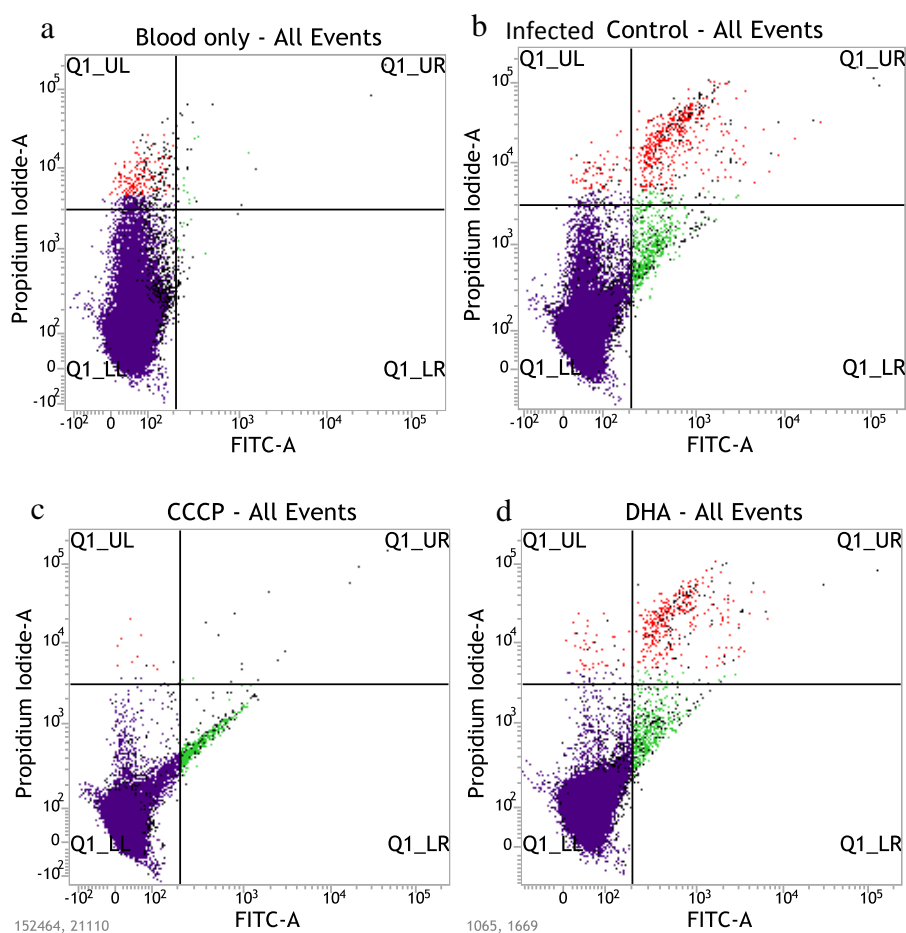


Figure 5.9 *Plasmodium falciparum* strain K1 viability time-course for treatment with emetine dihydrochloride hydrate after 21 days and 28 day of recovery. Error bars represent triplicate data and the experiment was repeated twice. The Y axis shows (log viable parasite +1) to allow representation of logarithms when number of viable parasites is equal to zero.



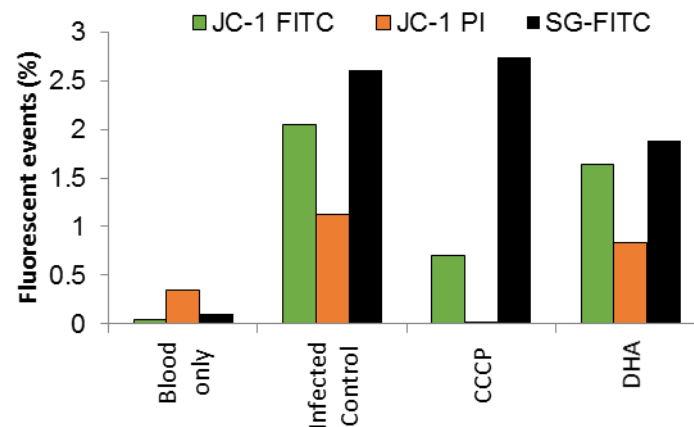
### 5.3.6 Parallel staining with JC-1 and SYBR Green

Figure 5.11 shows the gating procedure used, for JC-1 stained malaria parasites on the BDFACsVerse flow cytometer system, to obtain the percentage data shown Figure 5.12. The results indicated that the percentage of fluorescent events was comparable between the SYBR Green and JC-1 controls and DHA treated samples. In the CCCP treated sample, however, staining with SG and JC-1 was not consistent (Figure 5.12). The results showed that CCCP was effective in inducing loss of mitochondrial membrane potential in the malaria parasite, as shown by the reduction in JC-1 red fluorescence staining, while SYBR Green stained DNA remained intact (Figure 5.12). The lack of staining in the CCCP treated sample is also visible in fluorescence images taken in parallel (Appendix IX). The results showed some level of background fluorescence in the uninfected blood sample, particularly with the red analysis channel (Figure 5.11). Both JC-1 and SG staining appeared reduced in the DHA sample, after 48 hours of treatment, when compared with the untreated control (Figure 5.12).



**Figures 5.11 Flow cytometer analysis of JC-1 stained *P. falciparum*.** Dot plots of FITC against Propidium Iodide are shown for JC-1 stained blood only (a) infected control (b) CCCP treated (c) and DHA (d) samples. Colours indicate the gating procedure used to obtain statistical data.





**Figure 5.12** The percentage of fluorescent events recorded for parallel JC-1 and SYBR green staining of *P. falciparum* using the BDFACsVerse flow cytometer. Parasites were exposed to dihydroartemisinin (DHA) or CCCP (positive inducer of loss of mitochondrial membrane potential). Blood only and infected blood served as controls. JC-1 staining was determined using the FITC (JC-1 green) and Propidium Iodide (JC-1 red) channels. The gating procedure is shown in figure 5.11. SYBR Green staining was performed in parallel to confirm percentage parasitaemia. Fifty-thousand events were recorded for each condition in both assays.

### 5.3.7 JC-1 and SYBR Green following high-dose chloroquine treatment

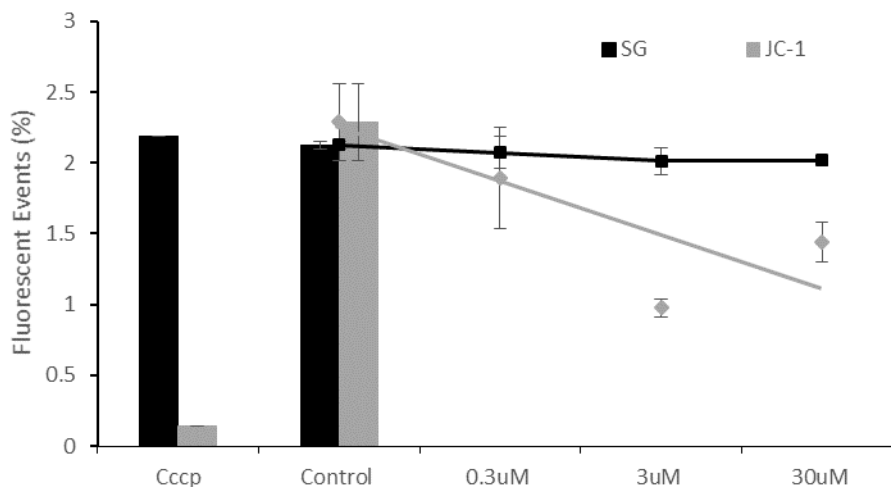


**Figure 5.13** Parallel JC-1 and SYBR Green staining of *P. falciparum* following 7 hour exposure to a high dose series of chloroquine. Strain K1 parasites were treated with high doses of chloroquine in an attempt to replicate finding of the Ch'ng *et al* (2010) and induce loss of mitochondrial membrane potential (reduction in JC-1 staining) during a short < 8 hour treatment period. The number of fluorescent events recorded for red and green JC-1 staining was pooled and compared with overall parasitaemia as determined by SYBR Green flow cytometry.

The results showed that loss of mitochondrial membrane potential can be induced by high concentrations of chloroquine (Figures 5.13). The positive control (CCCP treatment) was effective in the current experiment and background staining in the uninfected blood sample did not interfere with the results. While JC-1 staining was reduced, SYBR Green staining remained constant throughout the treatment series (Figure 5.13).

### 5.3.8 The effect of emetine on mitochondrial membrane potential

The results of the JC-1 assay showed that after 24 hours of incubation, emetine is capable of inducing loss of mitochondrial membrane potential in *P. falciparum* K1 parasite strain at a physiologically relevant IC<sub>50</sub> dose. What is more, the extent of mitochondrial depolarization was similar to that of atovaquone, a drug known to act via the mitochondria. Both drugs failed to induce mitochondrial depolarization at a level comparable to the positive control, CCCP. The SG-FCM data showed that parasitaemia remained consistent between the control, CCCP and atovaquone samples. However, the emetine treatment showed a 15-30 % reduction in parasitaemia (Figure 5.14 a). The 72 hour data provided confirmation that following parasite death the JC-1 assay can be used as a readout for parasite survival by staining the remaining live parasites. The decrease in red/green ratio was less marked in the ATQ and Eme treatments at this time point (Figure 5.14 b).

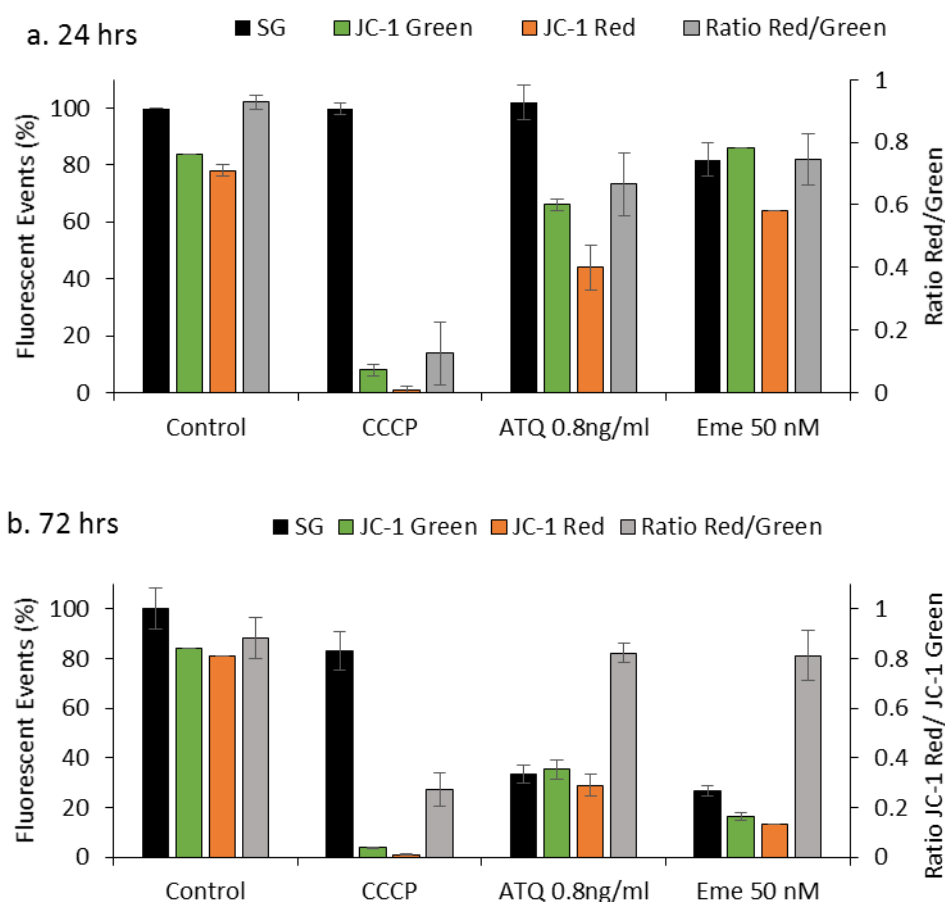


**Figure 5.14 Parallel JC-1 and SYBR Green staining of parasites exposed to IC<sub>50</sub> doses of atovaquone and emetine for 24 hours.** Drug treatment as initiated at ring stage and analysed at 24 (a) and 72 (b) hour time points for mitochondrial depolarization using the JC-1 assay. SG-FCM was completed to determine parasitaemia. CCCP treatment and untreated samples served as positive and negative controls, respectively. CCCP treatment was initiated immediately before staining for 5 minutes. As an indicator of loss of mitochondrial membrane potential the ratio of JC-1 Red/ JC-1 Green fluorescence was determined and plotted on a secondary axis. Error bars represent duplicate data.

## 5.4 DISCUSSION

### 5.4.1 Comparison between emetine and its natural derivative, cephaeline

The data showed that despite a tanimoto similarity score of 0.94, the slight structural difference between cephaeline and emetine resulted in a 6-fold shift in potency against the malarial parasite. Indeed cephaeline has been shown elsewhere to have potent activity against *P. falciparum* strains W2 and D6 (Muhammad *et al.*, 2003). The increase in potency presented here was, however, accompanied by a 2-fold increase in toxicity against the mammalian cell line HepG2, indicating that the structural difference between the two compounds does not favour the antimalarial development of cephaeline. This is in contrast to the finding of Muhammad *et al.* (2003) who showed that against *Leishmania donavani*, cephaeline is equally potent and 12 x less toxic against VERO cells when compared with emetine. Although, the study did show cephaeline to be toxic against four different human cancer cell lines (Muhammed *et al.*, 2003). Due to the recent interest in emetine for the treatment of other parasitic diseases, particularly the trypanosome infections, more *in vitro* toxicity information about emetine in human cell lines has become available. While IC<sub>50</sub> values for bloodstream forms of *Trypanosoma brucei* (39-40 nM) were comparable to animalarial potency, there was a 24-fold increase in the IC<sub>50</sub> (900-970 nM) against the human promyelocytic leukemia cell line, HL60 (Meschjohann, 2000; Rosenkranz and Wink, 2008). The Novartis-GNF screen, from which compounds were selected for the malaria box, determined IC<sub>50</sub> values for emetine, against *P. falciparum* 3D7 (drug susceptible) and W2 (chloroquine, quinine, pyrimethamine, cycloguanil, and sulfadoxine-resistant) strains as well as Huh7 (human hepatocellular carcinoma cell line), as 10 nM, 20 nM and 116 nM respectively. Taken together, the parasite potency and cytotoxicity data presented elsewhere provides a slightly better safety margin than would be predicted by our current study. In accordance with the data presented here, however, Akinboye *et al.* (2012) reported IC<sub>50</sub> values for emetine of 24-33 nM against the prostate cancer cell lines PC3 and LNCaP, but showed that they were able to reduce cytotoxicity through derivatisation of the N-2 position of the compound. In order to increase the therapeutic index of emetine for anticancer therapy the group created pH dependent prodrugs by modifying the N-2 position with thiourea, urea, sulfonamide, dithiocarbamate, carbamate and amide analogs. The derivatives were shown to less cytotoxic *in vitro* (0.079-10  $\mu$ M IC<sub>50</sub>). Further *in vivo* investigation of two of the analogs revealed no side effects in mice administered with 100 mg/kg for 5 days, while the comparable dose of emetine killed the

mice within 48 hours (Akinboye *et al.*, 2012.). However the N-2 position along with N-5 and C-9 have been reported as important functional moieties for biological activity (Akinboye and Bakare, 2011). Whether this is also the case for antimalarial activity is yet to be determined. This data along with the existence of the less toxic derivative, dehydroemetine, infers that small structural changes can alter on-target and off-target effects of this class of compounds. For this reason, emetine is a good starting point for a novel class of antimalarials. Further work, therefore, focused on the characterisation of emetine's antimalarial killing profile.

#### 5.4.2 Time-course analysis of emetine

The necessity of combination therapy for malaria treatment and the need for appropriate pharmacokinetic matching of compounds has emphasised the importance of defining a compound's killing profile. As artemisinins are known to be a fast acting antimalarials (Krishna *et al.*, 2004; Sanz *et al.*, 2012) the killing profile of emetine was compared with that of dihydroartemisinin during a 72 hour time-course. Both drugs were shown to induce a slight reduction in parasitaemia after 24 hours and the effect became more pronounced as the time-course progressed. On closer inspection of parasite stages, it can be noted that the drug induced reductions in parasitaemia were detected once the parasites had entered a subsequent erythrocytic cycle. The increase in parasitaemia between the 24 and 48 hour time points is possibly reflective of parasites during the schizont to ring transition at 24 hours becoming fully established and therefore detectable by SG-FCM at 48 hours. The result presented here would indicate that emetine is as equally fast acting as dihydroartemisinin, whether this is an artefact of the SG-FCM assay or true reflection on mode of drug action is questionable. Indeed, Wein and colleagues (2010) suggest that a 72 hour treatment period is required to achieve accurate results with the SYBR Green-based methods (Wein *et al.*, 2010). The issue is that arrested or dying parasites may be recorded as live due to the residual intact DNA inside the red blood cells. However, it is not only the selected drug susceptibility read-out that can be deceptive, but also drug mode of action. The phenomenon known as the post antibiotic affect (as it most commonly in response to antibiotic treatment) occurs when organisms are considered alive even though they are condemned/committed to death (Renneberg and Walber 1989; Zhanel *et al.*, 1991). In some cases, even after a short drug exposure period, drug effects are not observed until a second or third round of replication (Pasini *et al.*, 2013). The reverse can also be true, cytostatic organisms can appear dead but are dormant and can in fact resume productive

growth once the drug has been removed (Gorka *et al.*, 2013; Sanz *et al.*, 2012). Although there may be a limit to length of drug exposure when the commitment to death is irreversible. In contrast to Wein *et al.* (2010) we have shown elsewhere (Chapter 3) that standard IC<sub>50</sub> values can be achieved after 48 hour drug exposure providing, SG-FCM analysis is completed after the parasite entered into a subsequent erythrocyte cycle. Indeed, accurate results have been obtained when experiments were initiated at trophozoite stage and analysed 48 hours later, when the parasites were at trophozoite stage in the subsequent erythrocytic cycle. Rather than multiplication, viability is determined by maturation and the ability to continue development by successfully invading new red blood cells. Discrepancies in 48 hour data occur when samples are analysed during schizont to ring transition as shown here between the 24 and 48 hour readings. The time-course data presented here provides confirmation of this method, as the dose of DHA used in the current study achieved ~ 25 % inhibition at both the 48 and 72 analysis points. The lack of a comparable increase in parasitaemia for the emetine treated parasites at 72 hours resulting in different levels of inhibition at the 48 and 72 hour readings (~50% and ~70% respectively) could indicate a different mode of action to DHA, where parasite are delayed or arrested in their development cycle. Indeed, delayed parasite progression in emetine-treated samples, compared with the dihydroartemisinin treatment, was confirmed by further stage-specific interrogation (% multinuclear parasites). Parasites treated with the combination, on the other hand, appeared to display interference between the two compounds, ultimately leading to further reduction in parasitaemia. It must be noted that the combination dose used for each drug was equal to that of the drug alone, so reduced growth, following exposure to a drug combination that is not antagonistic, should be expected. This preliminary indication of different modes of antimalarial activity justifies a potential role for the drug in artemisinin combination therapy. However, the time-course data cannot dictate whether the delayed parasite progression induced by emetine is cytostatic or cytotoxic as a subsequent recovery period in the absence of drug exposure was not analysed. Stage-specificity can also not be determined as the drug was present throughout all stages of the life cycle.

#### 5.4.3 Stage-specific effects and cytostatic vs. cytotoxic activity of emetine

The subsequent experiment aimed to address issues in determining stage specificity and cytostatic vs, cytotoxic activity. This was achieved by treating either ring or trophozoite stage parasites for 6 hours followed by washing and growth in absence of the drug for 48

hours. A parallel continuous 48 hour exposure was also set up for comparison. Consistent with the method outlined by Gorka *et al.* (2013) the data would suggest that emetine was cytocidal to approximately 20% of parasites after just 6 hours of exposure while the greater inhibition at 48 hours could be confounded by the cytostatic activity of the compound. Differences were not huge between  $IC_{50}$  and  $10 \times IC_{50}$  doses and the drug appeared similarly effective against both ring and trophozoite stage parasites. The inference that emetine is potentially a fast acting compound whose target is present in multiple parasite stages is consistent with Wong *et al.*, 2014 who established the cryo-EM secondary structure for emetine bound to the Pf80s ribosomal complex, verifying the target binding site and mechanism of action of emetine against *P. falciparum*. Given the numerous actions of emetine reported in the literature, including but not limited to antiviral and anticancer properties (Akinboye and Bakare, 2011) it is possible that the cytosolic ribosome is not the only target of drug in the malaria parasite. Indeed, protein translation, one of the key targets of emetine in other organisms occurs in two other centres in the malaria parasite: namely, the mitochondria and the apicoplast (Wong *et al.*, 2014). Wong *et al.* (2014) suggest that emetine has a similar binding site to the antibiotic pactamycin. In the eukaryotic malaria parasite other antibiotics are known to target two prokaryotic structures, the apicoplast and the mitochondria (Schlitzer, 2007). It is therefore possible that emetine may also have an effect on protein translation in these organelles. In fact, drugs known to target the apicoplast have displayed a delayed death effect similar that of the post-antibiotic effect described above (Fiddock, 2008; *et al.*, Kremsner and Krishna, 2004). This would also imply a cytocidal rather than cytostatic mode of action after 6 hours treatment with the compound. Others suggest that emetine specifically targets eukaryotic protein synthesis and is not classified as an antibiotic (Mackey *et al.*, 2006). Grollman on the other hand showed that emetine acts in a similar manner to glutarimide antibiotics and is capable of interfering with ribosomal protein synthesis in mammalian, yeasts and plant cells. The resemblance further extended to the finding that extracts of *E.coli* resisted protein synthesis inhibition to both ipecac alkaloids and glutarimide antibiotics (Grollman, 1966). However protein synthesis has been shown to be a common target in protozoans including *Entamoeba histolytica*. Therefore, whether the emetine has single or multiple targets, of prokaryotic or eukaryotic origin, and the effects that these may have on the malaria parasite killing profile remains to be disputed. Contradictory to the suggestions of Gorka and colleagues (2013), it cannot be assumed that parasites would recover from a cytostatic period, of unknown duration, and achieve parasitaemia equating to

that of the untreated controls within the 48 hour time-course. The lower parasitaemia in 6 hour treated samples could reflect parasites that have become dormant, possibly even continued with cycle progression but at a slower rate than the unaffected counterparts. These parasites may not have entered a subsequent erythrocytic cycle at the time of analysis but may be viable and thus capable of doing so in the near future. A longer recovery period, in the absence of drug exposure, would therefore be necessary to accurately define the action of a compound as cytocidal. The required duration of the assay will depend on drug mode of action and rate of kill. Indeed even one of the fastest antimalarials, DHA has been known to induce a dormancy response lasting up to 20 days (Sanz *et al.*, 2012). For this reason, a more intensive investigation, lasting up to 28 days, was set up to determine emetine's speed-of-kill against *P. falciparum* strain K1.

#### 5.4.4 Detailed killing profile analysis of emetine against *P. falciparum* strain K1

Although the data revealed that emetine has a relatively slow killing profile, which is arguably less desirable due to the potential for resistance development if parasites are exposed to sub-optimal concentrations, it was within the remit of the existing antimalarials. In fact its speed of kill was pharmacokinetically similar to the actions of atovaquone. Like atovaquone, emetine was also shown to have a 48 hour lag phase. The parasite reduction ratio and parasite clearance times were also similar for the two compounds ranging from 2.9-3.7 and 90-93 hours respectively. Sanz *et al.* (2012) showed that when  $IC_{50}$  or in some cases  $3 \times IC_{50}$  doses were used for slow, medium and fast acting compounds the of killing rate of the compound was compensated by growth in the treated culture. Thus in agreement with their finding the current study adopted  $10 \times$  the  $IC_{50}$  of emetine to achieve the maximal killing rate. The advantages of the killing profile assay described by Sanz *et al.* (2012), and replicated here, are that it accurately measures parasite viability over time in response to drug treatment. The extended recovery period of up to 28 days means that the assay avoids erroneous interpretations of the dormancy response or post-antibiotic effect that often arises when metabolism, the accumulation of specific molecules or, as described above, DNA content are used as surrogates for parasite viability during or immediately after drug treatment. Indeed, drug treatment commonly induces an uncoupling of such parameters. Due to evidence of a good correlation between *in vitro* and *in vivo* PRR, the assay also permits some predictions about the *in vivo* situation. The *in vitro* PRR, a direct measure of parasite viability tends to be higher than the *in vivo* estimate that measures clearance of the parasite by the organism and is thus affected by a multitude

of pharmacokinetic and pharmacodynamic factors. Furthermore, as the lag phase is not affected by drug concentration and the killing rate and clearance times are not related to drug potency. The method also provides some information about the intrinsic mode of action of a compound. Sanz *et al.*, 2012 showed that compounds with similar rates of kill have similar modes of action. Indeed, two artemisinin derivatives, artesunate and artemether and two compounds known to impair mitochondrial function GW648495X and GW844520X, displayed similar reduction ratios and clearance times to artemisinin and atovaquone respectively. It is therefore possible that emetine has a similar mode of action to atovaquone. Atovaquone is known to act *via* the bc1 complex of parasite mitochondria through electron transport inhibition, ultimately impairing pyrimidine biosynthesis (Sanz *et al.*, 2012). Destabilization of the bc1 complex causes proton leakage and leads to mitochondrial depolarization (Srivastava and Vaidya, 1999). As an inhibitor of RNA/DNA and protein synthesis, the bacteria-like translation machinery of the mitochondria may therefore be another target of emetine. In cancer cells Boon-Unge *et al.* (2007) showed that emetine regulates alternative splicing in the *Bcl-x* gene, shown to be dependent on protein phosphatase 1, resulting in alterations in pro-apoptotic (Bcl-xS) and anti-apoptotic (Bcl-xL) ratio promoting apoptosis (Boon-Unge *et al.*, 2007). The drug has also been linked to the induction of mitochondrial-dependent apoptosis in *T. brucei*. Rosenkranz and Wink, 2008 also showed that loss of mitochondrial membrane potential was accompanied with other programmed cell death phenotypes such as DNA fragmentation (Rosenkranz and Wink, 2008).

#### 5.4.5 The effect of emetine on malaria parasite mitochondria

A study investigating mitochondrial depolarization in response to atovaquone treatment showed that parasites were able to withstand mitochondrial membrane disruption for up to 48 hours before the commitment to death was irreversible (Painter *et al.*, 2010). This is consistent with the 48 hour lag phase of atovaquone determined by the Sanz group (Sanz *et al.*, 2012). As emetine treatment also presented a similar lag phase to atovaquone, it is unlikely that the previous experiment of 6 hours of emetine exposure was due to cytotoxic effects of the drug. Painter and colleagues (2010) suggested that apoptosis did not ensue after mitochondrial disruption due to differences between metazoan and protozoan apoptosis pathways. In the protozoan parasite however, Ali and colleagues (2010) showed that induction of loss of mitochondrial membrane potential is accompanied with other markers of apoptosis such as caspase activity, although an apoptosis pathway independent



of the mitochondria may also exist (Ali *et al.*, 2010; Matthews *et al.*, 2012). It is possible that in some cases, rather than being a direct target of the mitochondria, loss of mitochondrial potential occurs as an indirect effect of parasite death, particularly when high, physiologically irrelevant doses are used. Indeed, a number of compounds have been reported to affect mitochondrial physiology at high concentrations (Srivastava and Vaidya, 1999). In order to analyse whether a drug is acting *via* the mitochondria, the time-course and dose will be important.

Mitochondrial depolarization can be determined by the JC-1 assay. Recently the assay has also been used as a readout for parasite viability (Pasini *et al.*, 2013). In this case JC-1 fluorescence is an indicator of the intact mitochondria of live parasites. The preliminary data presented here shows a comparable decrease in JC-1 and SYBR green staining following a 48 hour treatment period with DHA compared with non-treated controls. The results also confirmed that 5 minutes of treatment with CCCP (positive inducer-known to effect protein synthesis in the mitochondria) is capable of inducing loss of mitochondrial membrane potential in *Plasmodium falciparum* parasites without effecting DNA. This is consistent with the chronology of apoptosis where loss of mitochondrial membrane potential is an early early-onset feature of programmed cell death and DNA degradation is the end point (Ch'ng *et al.*, 2010). The comparability between SG and JC-1 staining served to validate the assay and the staining procedure adopted in the current study. In order to determine whether the assay can be used to help decipher antimalarial mode of action, loss of mitochondrial membrane potential was induced in a dose-dependent manner after 7 hours of incubation with chloroquine. These parameters were consistent with the Ch'ng group (2010) who induced loss of mitochondrial membrane potential within 6 hours, using higher concentrations of chloroquine. During the short time-course of chloroquine exposure presented here the reduction in JC-1 staining was not accompanied by a decrease in SYBR Green. This provides proof-of-concept that parasites can display physiological changes like loss of mitochondrial membrane potential in response to drug treatment prior to death as determined by DNA content. These high concentrations are confounded by toxicity issues and are therefore unlikely to reflect the true mode of drug action (Srivastava and Vaidya, 1999).

Therefore, in the subsequent investigations, physiologically relevant concentrations of emetine were used to establish whether the drug has an effect on parasite mitochondria. Ring stage parasite were treated with the IC<sub>50</sub> dose of the drug for 24 hours. Atovaquone, a

drug known to act *via* the mitochondria, with which emetine shares a similar killing profile was included in the assay at its respective IC<sub>50</sub>. A 24 hour time point was selected as atovaquone has been shown to be capable of mitochondrial disruption for up to 48 hours before parasite death ensues. SG-FCM staining was used in parallel to ensure that any effects observed were not due to reductions in parasitaemia. The results showed that after 24 hours, a reduction in JC-1 staining and a shift from red to green fluorescence (as determined by the red/green ratio) was observed at a similar magnitude for both ATQ and Eme. Staining in untreated control samples however was consistent between the SG and JC-1 assays. The positive control CCCP showed a more pronounced reduction in JC-1 staining and a greater shift from red to green fluorescence than either of the drug treated samples. As parasites were only subjected to a 5 minute treatment period with CCCP, a shorter time-course for treatment with the test compounds may permit more informative data. Indeed, Srivastava and Vaidya (1999) analysed mitochondrial membrane disruption in response to atovaquone and other existing antimalarials by staining parasite with the DiOC6(3) (3,3'-Dihexyloxacarbocyanine Iodide) probe for 20 minutes followed by a drug treatment period of 20 minutes before analysis (Srivastava and Vaidya, 1999). Although the JC-1 ratio was consistent between the atovaquone and emetine samples, some reduction in parasitaemia as indicated by SG, was observed in the emetine treated sample, potentially inferring that in addition to effects on the mitochondria emetine may also be operating *via* other targets in the parasite. The 72 hour data confirmed parasite death in response to drug treatment. The comparability between SG and JC-1 staining inferred that the 72 hour analysis was indicative of the remaining live parasites. The reduction in red/green ratio was also much less pronounced at this time point, indicating that parasites affected by ATQ and Eme treatment had already died. The data therefore further validates the JC-1 assay as a read-out for parasite viability, providing an appropriate time-course is adopted.

#### 5.4.6 Conclusion

Taken together the current data suggest that emetine has a similar killing profile to the existing antimalarial atovaquone. Primary data presented here infers that like atovaquone, emetine may target the mitochondria in the malaria parasite. However given the bioactive nature of the compound it is likely that other targets, in addition to the 80s cytosolic ribosome, exist. The detailed *in vitro* analysis of emetine provides a good background for defining appropriate treatment regimes for *in vivo* analysis of the drug. In the *in vivo*

situation it is important to maintain the inhibitory concentration for longer than the parasite is able to stay alive (Painter *et al.*, 2010). As an ameobicide, emetine was given for 6 days with further treatments after day 9. The data presented here confirms that 99.9% of malaria parasites are killed after 90 hours of treatment with the drug which has beneficial implications for the safety profile of emetine. Reducing the number of doses may help avoid cardiotoxic issues due to high cumulative concentrations of the compound. Derivatisation and novel drug delivery system may also lead to safer alternatives. Details about the pharmacokinetic profile presented here can also be used to inform decisions about appropriate combinatory options for the drug, with the aim to further reducing drug doses. The wealth of existing information on emetine and its analogues and the potential for investigations into structural activity relationships suggest that this molecule, discovered through repositioning, is uniquely placed to be advanced through rational drug design with the aim of delivering an affordable, effective and safe natural product drug class for malaria.

## CHAPTER 6

---

### DRUG INTERACTION ANALYSIS OF EMETINE DIHYDROCHLORIDE HYDRATE

#### 6.1 INTRODUCTION

The high priority for effective combinatorial regimes means that the analysis of drug interactions has become an important part of the antimalarial drug development pipeline (Bell, 2005). There is a limited number of chemotherapies available and novel candidates are usually combined with existing treatments (Bhattacharya *et al.*, 2009; Kremsner and Krishna, 2004; Sahu *et al.*, 2014). This is because the development of two novel compounds is doubly challenging and the benefits of the recent high-throughput phenotypic screens are yet to be realised. The current combination therapies recommended and available for malaria treatment are discussed elsewhere, along with their pharmacokinetic and resistance profiles (Chapter 1). Indeed, the ideal partner drugs for malaria treatment should have matching pharmacokinetics, synergise against drug resistant strains, be free of significant side effects, be relatively inexpensive and have no other antimicrobial activity (Canfield *et al.*, 1995; Kremsner and Krishna, 2004). In order to predict whether a particular combination will be efficacious, detailed interaction studies should be conducted. The values of combination therapy; namely, (1) better therapeutic efficacy, (2) the potential to impede or delay the onset of resistance, (3) dose reduction whilst maintaining potency and avoiding adverse effects, and (4) the potential for selective synergism or toxic antagonism, were realised much sooner for disease like cancer, AIDS and tuberculosis (Chou, 2010; Fivelman *et al.*, 2004; Kremsner and Krishna, 2004). Thus, it follows that the numerous methods to analyse drug interactions have evolved and been evaluated over the last century (Harasym *et al.*, 2010) (Table 6.1). However, the complexity of the task has meant that interpretations of the data has been varied resulting in confusion and conflict (Chou, 2006). The the issue predominantly lies with determining and defining synergy (Bell, 2005; Chou, 2006). Indeed, synergy can occur as a result of the drugs interacting physically or most often as a consequence of each drug interacting at the molecular level with (same or different) components of the target (Bell, 2005; Zimmermann *et al.*, 2007). Furthermore, a mutual event such as synergism has to be disassociated from one-sided events, where one of the drugs has no effect when used alone, such as enhancement, potentiation and augmentation (Chou, 2010). It is therefore too simplistic to suggest a synergistic outcome is when the combination of drugs A and B is greater than either drug alone ( $A+B > A$  or  $A+B > B$ ). For example,

if drug A and B each inhibit 60 % the combination cannot inhibit 120 % (Chou, 2006).

Drug interaction evaluation models	Date
Isobologram	1870
Loewe additivity	1926
Bliss independence response surface approach	1939
Fractional product method of Webb	1963
Multivariate linear logistic model	1970
Approach of Gessner	1974
Method of Valeriote and Lin	1975
Method of Drewinko <i>et al.</i>	1976
Interaction index calculation of Berenbaum	1977
Method of Steel and Peckman	1979
Median-effect method of Chou and Talalay	1984
Method of Berenbaum	1985
Method of Greco and Lawrence	1988
Method of Pritchard and Shipman	1990
Bivariate spline fitting (Sühnel)	1990
Models of Greco <i>et al.</i>	1990
Models of Weinstein <i>et al.</i>	1990

**Table 6.1** Various drug interaction models that have been developed and used since (1870)  
(After: Harasym *et al.*, 2010)

In attempting to identify the desirable occurrence of synergy, experimenters have realised that the definition of additivity is most important. Synergism and antagonism are referred to as a more than expected or less than expected additive effect, respectively (CalcuSyn manual, Biosoft). The majority of interaction methods are therefore based on two definitions of additivity Bliss independence and Loewe additivity (Feng *et al.*, 2009; Yeh *et al.*, 2009). Bliss independence (fractional product method) assumes that each drug acts independently. Therefore the issue of both drugs inhibiting 60% is resolved by the definition that additivity =  $1 - [(1-A)(1-B)]$  in this case  $1 - [(1-0.6)(1-0.6)] = 0.84$  so to be additive A + B would be expected to achieve 84% inhibition and deviation above or below this would be considered as synergistic or antagonistic respectively. Loewe additivity on the other hand dictates that a drug cannot interact with itself. Therefore if in fact A and B were the same drug the interaction can only be additive so 0.5 A and 0.5 B should be expected to achieve the same effect as drug 1 A or 1 B. Drug combinations are therefore additive if inhibition is constant along a line of equal effective dose. Hence the approach uses a line of constant inhibition (isobole) to define additivity. Deviations above the line (convex) are antagonistic and deviations below the line (concave) synergistic (Yeh *et al.*, 2009; Zimmermann *et al.*, 2007). After nearly 100 years of use the isobologram method remains one of the most trusted and widely accepted methods for determining synergy (Bell, 2005). Most commonly the malaria community have adopted either the checkerboard or fixed ratio methods to obtain data for isobologram preparation (Abiodun *et al.*, 2013, Bhattacharya *et al.*, 2009; Fivelman *et al.*, 2004; Fugi *et al.*, 2010; Gupta *et*

*al.*, 2002; Sahu *et al.*, 2014). The two methods employ different treatment regimes to characterise the drug interactions. In the checkerboard method the concentration of drug 'A' remains constant while the concentration of drug 'B' is varied and *vice versa*. While the fixed ratio method, originally developed to test drug interactions against bacteria, involves the serial dilution of both drugs at a range of fixed ratios (Fidock *et al.*, 2004). In addition to the isobologram, the sum of the fractional inhibitory concentration ( $\Sigma$ FIC) is calculated and the numerical output used to categorise the nature of the interaction at a particular level of inhibition ( $IC_{50}$ ,  $IC_{90}$ ). A value  $<1$  is synergism, equal to 1 is additivity,  $>1$  is antagonism). However the lack of standardised methods between different research groups, in particular the  $\Sigma$ FIC cut-offs for classifying an interaction as synergistic, additive or antagonist has meant that inconsistent inferences have appeared throughout the literature (Canfield *et al.*, 1995; Fivelman *et al.*, 2004; Gorka *et al.*, 2013; Mariga *et al.*, 2005). This is not unique to malaria drug interactivity studies and has in fact plagued the field of combinatory drug analysis over many decades. The lack of consensus, prompted efforts by Chou and Talalay to attempt resolution of the problem. Initially Chou aimed to define additivity in accordance with the theories outlined above and emphasised that equations can only be used to define additivity (Chou, 2010). Chou also argues that synergy is a physiochemical rather than statistical issue. Instead, Chou employed the physiochemical principle of the mass-action law and the mathematical principle of induction and deduction to create the median effect equations (Figure 6.1) (also referred to as the general theory of dose-effect analysis). Remarkably, the general theory of dose and effect has been proven to be a unified theory of four existing physiochemical equations namely; Henderson-Hasselbalch (pH ionization), Hill (higher order ligand binding saturation), Michaelis-Menten (enzyme kinetics), and Scatchard (receptor binding). After 35 years of research, the complex algorithms of median effect analysis were incorporated into a series of software programmes (CalcuSyn, CompuSyn), to permit the automated analysis, now widely employed in biomedical science (Chou, 2010; Feng *et al.*, 2009; Harasym *et al.*, 2010), even for other parasitological diseases (Corral *et al.*, 2014; Keiser *et al.*, 2011; Keiser *et al.*, 2012; Hu *et al.*, 2010). The advantages of the programmes are that they are capable of performing multiple-drug dose-effect calculations using the median effect method based on both the inputted data and values predicted by the mathematical models. Unlike the other methods, the entire shape of the growth inhibition curve is taken into account and the effects of the drug combination are quantified to see if they have greater effects together than expected from a simple summation of their individual effects

(Chou, 2010). Read-outs for this method are similar to that of the fixed ratio method and include the combination index, the isobologram plot and the dose reduction index, the equations for which are derived from the median effect equation (Figur 6.1). Although cut-off criteria for the combination index are comparable to those used for the  $\Sigma$ FIC calculation, the different degrees of synergism, additivity and antagonism are clearly defined providing a more stringent and accurate categorisation of the interaction (CalcuSyn manual 1996-2006). Applying an automated, non-subjective method to malaria drug interaction studies would help standardise interaction classifications and permit more reliable comparisons between research groups.

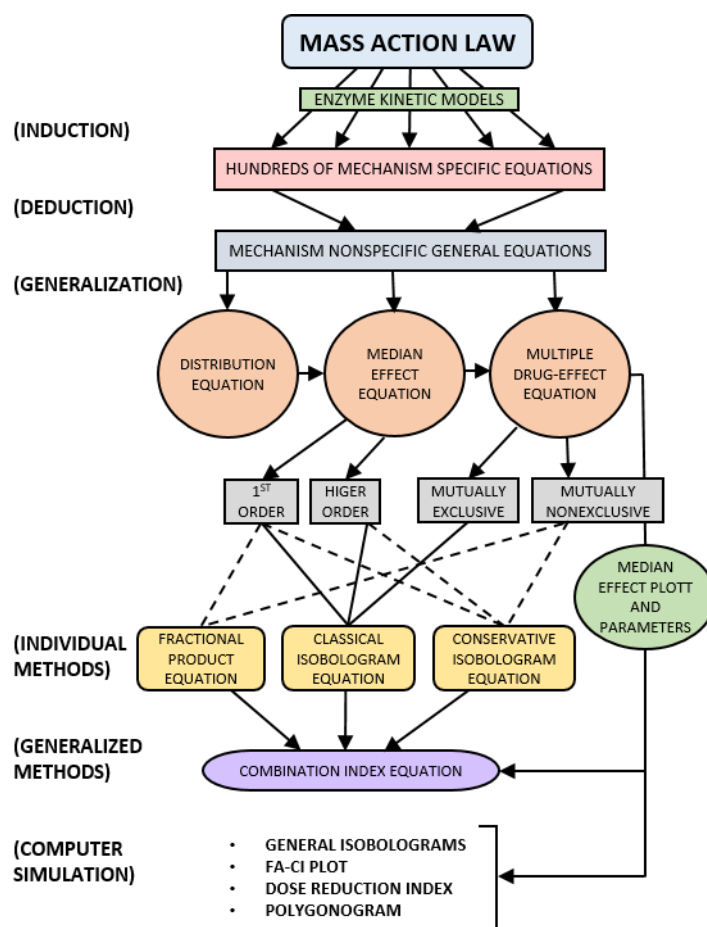


**Figure 6.1** The derivation of the Median-Effect Principle and its extensions to Multiple Drug Effect Equation (After: Chou, 2006)

In order to triage the potent antimalarial candidate emetine dihydrochloride hydrate, the nature of its interaction with the existing antimalarials chloroquine, dihydroartemisinin and atovaquone will be determined. Initially, the study will aim to validate the CalcuSyn method for malaria. This will be achieved by comparison with one of the existing methods, previously adopted by the malaria community, to analyse the interaction between emetine and dihydroartemisinin. For this, the fixed ratio method was nominated due to the following

advantages: it is not affected by the day to day variations of predetermined  $IC_{50}$  values, fewer calculation steps are required,  $IC_{50}$  calculations and regression curve fits are more accurate due to the generation of dose-response curves for each ratio calculated on the basis of 100-0 % parasite inhibition (Fivelman *et al.*, 2004). The combination will then be repeated using the CalcuSyn method so that comparisons can be drawn. Secondly, atovaquone-proguanil combination, known to be synergistic against malaria and commonly used in the field, will be evaluated using CalcuSyn to establish whether the expected classification will be assigned.

## 6. 2 METHODS

### 6.2.1 Fixed ratio drug interaction assay

To investigate whether the combined effects of emetine hydrochloride hydrate were synergistic, additive or antagonistic, an interaction assay previously described by Bhattacharya *et al.*, (2009) was employed. Dihydroartemisinin and emetine dihydrochloride hydrate were combined in four fixed ratios 4:1, 3:2, 2:3 and 1:4. In addition, each drug was administered alone for direct comparison with the combinations, hereafter referred to as the 5:0 and 0:5 ratios. Approximately eight-fold  $IC_{50}$  values were used as 100% ( $8 \times IC_{50}$  DHA = 20 nM and  $8 \times IC_{50}$  Eme = 400 nM). Thus for the first dilution the combinations were as follows for DHA (nM) : Eme (nM) 20:0, 16:80, 12:160, 8:240, 4:320 and 0:400 respectively. For each dilution thereafter drug concentrations were serially diluted two-fold. The  $IC_{50}$  for each compound (at the 5:0 and 0:5 ratios) therefore lay within the fourth dilution. Once drug stocks had been prepared in RPMI 1640, trophozoite stage parasites were diluted to ~ 0.5 % parasitaemia and transferred into individual 5 ml treatment and control flasks at 5 % haematocrit. Parasites were then treated with the various drug combinations, gassed (as described previously) and incubated for 48 hours at 37 °C. Duplicate preparations were set up for each ratio at each dilution. Following treatment, samples were analysed using SG-FCM. Giemsa staining of thin blood smears was also employed to permit parasite stage confirmation.

### 6.2.2 Isobologram preparation and analysis for fixed ratio data

Drug interaction studies for emetine dihydrochloride hydrate and dihydroartemisinin were performed using a modification of the fixed ratios method, employing 4 fixed ratios of 4:1, 3:2, 2:3 and 1:4.  $IC_{50}$  values were determined for each compound at each ratio as described



above and used to calculate fractional inhibitory concentration for each ratio using the equation below. Drug interactions were analysed both at IC<sub>50</sub> and IC<sub>90</sub> values.

$$\text{FIC} = \frac{\text{Fraction of drug concentration require to produce IC}_{50} \text{ when used in combination}}{\text{Fraction of drug concentration require to produce IC}_{50} \text{ when used alone}}$$

The FIC values for dihydroartemisinin at each ratio were then plotted against those calculated for emetine to obtain the isobologram trends. To investigate the interaction between dihydroartemisinin and emetine at each ratio the calculated FIC values for each compound were then added together to obtain the sum of the fractional inhibitory concentration ( $\Sigma\text{FIC}$ ) as per equation below.

$$\text{SumFIC } (\Sigma\text{FIC}) = \frac{\text{IC}_{50} \text{ of A in mixture}}{\text{IC}_{50} \text{ of A alone}} + \frac{\text{IC}_{50} \text{ of B in mixture}}{\text{IC}_{50} \text{ of B alone}}$$

Criteria consistent with Bhattacharya *et al.* (2009) were used to determine whether the effects of the combination were synergistic, additive or antagonistic. In brief, when the sum FIC calculations  $\Sigma\text{FIC} < 1$  synergism,  $\Sigma\text{FIC} \geq 1$  and  $< 2$  additive, interaction,  $\Sigma\text{FIC} \geq 2$  and  $< 4$  slight antagonism,  $\Sigma\text{FIC} \geq 4$  marked antagonism.

### 6.2.3 Application of the CalcuSyn assay to define antimalarial drug interactions

The CalcuSyn software program was developed to quantitatively assess drug interactions (Chou, 2010). The method, commonly used in cancer research, requires a different treatment regime than those described previously for the checkerboard and fixed ratio assays. In the current study, CalcuSyn was used to provide a different perspective on the interaction between dihydroartemisinin and emetine dihydrochloride hydrate. A constant drug ratio design was set up for the analysis. In brief, the IC<sub>50</sub> concentration for each drug was taken as a starting point. Below the IC<sub>50</sub> three 1:1 dilutions and above the IC<sub>50</sub> three doubling concentrations were selected to provide a sufficient dose range for each drug. For dihydroartemisinin, the doses ranged from 6.3 nM to 40 nM. For emetine the doses ranged from 63 nM to 400 nM. Co-administration of the compounds occurred at each level, for example the IC<sub>50</sub> of dihydroartemisinin was combined with the IC<sub>50</sub> of emetine and 2 x IC<sub>50</sub> DHA was combined with 2 x IC<sub>50</sub> Eme and so forth. Parasites were treated at trophozoite stage and incubated for 48 hours in a 96 well plate format. SYBR Green flow cytometry was used to determine drug susceptibility. Triplicate data was converted to an average percentage and analysed for the median effect using CalcuSyn software (Biosoft).

### 6.2.4 Validation of the CalcuSyn assay for malaria

#### 6.2.4.1 Optimisation of drug dosing and treatment period

In order to validate the CalcuSyn method as a useful tool for analysing drug interactions against the malaria parasite, the known synergistic drug combination, Atovaquone and proguanil (Malarone), was used. The initial experiment adopted the treatment regime outlined above and the doses selected were based on the respective  $IC_{50}$  values obtained previously for atovaquone and proguanil (Chapter 3). Refer to Table 6.2 for the individual dosage and plate set up. Triplicate samples were analysed by SG-FCM after 48 hours, the quadruplicate samples were used for Giemsa staining.

	1	2	3	4	5	6	7	8	9	10	11	12
<b>A</b>	Control				Control				Control			
<b>B</b>	ATQ 0.0875 ng/ml				0.0875 ng/ml + 0.575 ug/ml				PG 0.575 ug/ml			
<b>C</b>	ATQ 0.175 ng/ml				0.175 ng/ml + 1.15 ug/ml				PG 1.15 ug/ml			
<b>D</b>	ATQ 0.35 ng/ml				0.35 ng/ml + 2.3 ug/ml				PG 2.3 ug/ml			
<b>E</b>	ATQ 0.7 ng/ml				0.7 ng/ml + 4.6 ug/ml				PG 4.6 ug/ml			
<b>F</b>	ATQ 1.4 ng/ml				1.4 ng/ml + 9.2 ug/ml				PG 9.2 ug/ml			
<b>G</b>	ATQ 2.8 ng/ml				2.8 ng/ml + 18.4 ug/ml				PG 18.4 ug/ml			
<b>H</b>	ATQ 5.6 ng/ml				5.6 ng/ml + 36.8 ug/ml				PG 36.8 ug/ml			

**Table 6.2** The first dose plate set up for analysis of the atovaquone (ATQ) Proguanil (PG) interaction using the constant ratio design for CalcuSyn.

Due to the lack of a synergistic interaction predicted by the initial data numerous optimisation steps were trialled: firstly, the activity of the drug stocks was checked (Appendix X) and the experiment was repeated with an increased atovaquone dose series to account for a slight shift in the  $IC_{50}$  (Table 6.3). Samples were analysed for parasite growth as described above for the ATQ-PG first experiment.

	1	2	3	4	5	6	7	8	9	10	11	12
<b>A</b>	Control				Control				Control			
<b>B</b>	ATQ 0.175 ng/ml				0.175 ng/ml + 0.575 ug/ml				PG 0.575 ug/ml			
<b>C</b>	ATQ 0.35 ng/ml				0.35 ng/ml + 1.15 ug/ml				PG 1.15 ug/ml			
<b>D</b>	ATQ 0.7 ng/ml				0.7 ng/ml + 2.3 ug/ml				PG 2.3 ug/ml			
<b>E</b>	ATQ 1.4 ng/ml				1.4 ng/ml + 4.6 ug/ml				PG 4.6 ug/ml			
<b>F</b>	ATQ 2.8 ng/ml				2.8 ng/ml + 9.2 ug/ml				PG 9.2 ug/ml			
<b>G</b>	ATQ 5.6 ng/ml				5.6 ng/ml + 18.4 ug/ml				PG 18.4 ug/ml			
<b>H</b>	ATQ 11.2 ng/ml				11.2 ng/ml + 36.8 ug/ml				PG 36.8 ug/ml			

**Table 6.3** The second dose plate set up for analysis of the atovaquone (ATQ) proguanil (PG) interaction using the constant ratio design for CalcuSyn. The ATQ doses were shifted while the PG concentrations remained consistent with the previous experiment.

The second experiment was also unsuccessful in demonstrating synergy. A third experiment was designed to analyse the effect of treatment duration and the potential for

an order effect. The experiment was simplified by selecting only three dose points (low, mid and high) for each compound: namely 0.8, 1.6 and 3.2 ng/ml for atovaquone and 2.4, 4.6 and 9.2 µg/ml for proguanil. Parallel treatments were set up for two conditions ‘together’ or ‘separate’. In the ‘together’ condition compounds were added to the plate prior to the addition of the parasitised culture. In the ‘separate’ condition the parasitised culture was added to the plate followed by the addition of each compound separately. Additional alterations to the previous treatment regime was that the experiment was initiated against ring stage parasites not trophozoite and incubated for 72 not 48 hours. In the fourth experiment the atovaquone dose was reduced, the drugs were administered ‘together’ and treatment period employed in the previous experiment (initiated at ring stage and analysed 72 hours later) was maintained (Table 6.4).

	1	2	3	4	5	6	7	8	9	10	11	12
<b>A</b>	Control				Control				Acetonitrile:water			
<b>B</b>	ATQ 0.0975 ng/ml				0.0975 ng/ml + 0.575 µg/ml				PG 0.575 µg/ml			
<b>C</b>	ATQ 0.195 ng/ml				0.195 ng/ml + 1.15 µg/ml				PG 1.15 µg/ml			
<b>D</b>	ATQ 0.39 ng/ml				0.39 ng/ml + 2.3 µg/ml				PG 2.3 µg/ml			
<b>E</b>	ATQ 0.78 ng/ml				0.78 ng/ml + 4.6 µg/ml				PG 4.6 µg/ml			
<b>F</b>	ATQ 1.56 ng/ml				1.56 ng/ml + 9.2 µg/ml				PG 9.2 µg/ml			
<b>G</b>	ATQ 3.12 ng/ml				3.12 ng/ml + 18.4 µg/ml				PG 18.4 µg/ml			
<b>H</b>	ATQ 6.24 ng/ml				6.24 ng/ml + 36.8 µg/ml				PG 36.8 µg/ml			

**Table 6.4** Fourth dose plate set up for analysis of the atovaquone (ATQ) proguanil (PG) interaction using the constant ratio design for CalcuSyn. The ATQ doses were reduced but the PG concentrations consistent with the previous experiments.

#### 6.2.4.2 Non-constant ratio design

In order to determine whether the atovaquone-proguanil combination represents true antagonism at the ED<sub>75</sub> and ED<sub>95</sub> levels of inhibition, or whether there was a problem with the reliability of the read out method employed, a non-constant ratio design was set up. In brief, three dose points were selected for each compound that were previously shown to equate to IC<sub>25</sub> IC<sub>50</sub> and IC<sub>75</sub> levels of inhibition for a 72 hour treatment period (0.05, 0.2 and 0.8 ng/ml for atovaquone and 2.4, 4.6 and 9.2 µg/ml for proguanil). Each of the three doses of atovaquone was combined with each of the three doses of proguanil. Each dose was also administered singly as a control. Untreated and acetonitrile controls were also included in the experiment. All treatments were set up in triplicate. The plate was incubated under conditions described previously and analysed at 72 hours using the SG-FCM method. Data was plotted to allow visualisation of the absence or presence of a dose response for one drug when combined with a constant dose of the second compound.

#### 6.2.4.3 Recovery of parasites treated with the atovaquone-proguanil combination

As an extension to the non-constant ratio design experiment, following the 72 hour treatment period, the drug was removed and a limiting serial dilution was performed for each sample (in triplicate). In brief, 50 µl samples of each treatment were transferred to microcentrifuge tubes and washed 3x in 1 ml of complete media. The pellet was re-suspended in 100 µl of complete media so that the haematocrit was adjusted from 2.5 % to 1.25 %. Four 96 well plates were prepared by adding 200 µl of 1.25 % haematocrit to each well. Seven 10-fold limiting serial dilutions were performed by adding 20 µl of each sample to row A, mixing thoroughly and transferring 20 µl to row B and so forth until row H where the excess 20 µl was discarded. On day seven, 100 µl of spent media was removed from each well and replaced with fresh media and blood at 1 % haematocrit. Adjusting the final haematocrit to 1.75 %. The plates were and incubated for a further 10 days and analysed for growth using the SYBR Green procedures described elsewhere.

#### 6.2.5 CalcuSyn analysis of emetine with existing antimalarials

Following validation of the CalcuSyn method using the atovaquone-proguanil combination, the interaction between emetine and dihydroartemisinin was re-analysed using the optimised treatment regime. Subsequently the combinations between chloroquine and emetine, and atovaquone and emetine were also analysed using CalcuSyn. The doses used for each compound were based on previously determined IC<sub>50</sub> values and are shown in the Table 6.5.

Dose Level	Dose nM			
	Dihydroartemisinin	Chloroquine	Atovaquone	Emetine
A	0	0	0	0
B	0.625	28.75	0.136	6.25
C	1.25	57.5	0.272	12.5
D	2.5	115	0.544	25
E	5	230	1.088	50
F	10	460	2.175	100
G	20	920	4.35	200
H	40	1840	8.7	400
Ratio				
AM: Eme	1:10	4.6:1	1:46	---

**Table 6.5** Drug doses used for the existing and antimalarial combinations with emetine using the CalcuSyn analysis method. The ratio of the drug doses is also shown for Antimalarial (AM) to Emetine dihydrochloride hydrate (Eme) combinations.

## 6.3 RESULTS

## 6.3.2 Fixed ratio combination of dihydroartemisinin and emetine

The fixed ratio interaction assay was employed to decipher whether the combination between dihydroartemisinin and emetine was synergistic, additive or antagonistic. The dose response curves of each ratio are displayed in Figure 6.2. Dihydroartemisinin (a) and emetine (b) dominant combinations were plotted separately. The emetine dominant combinations, at the 1:4 ratio in particular, reduced parasite growth compared to the drug alone counterparts. Growth inhibition for the other drug ratios showed similar trend to that of the DHA-only or Eme-only dose response curves. Although the 4:1 drug ratio reduced growth less than the other combinations none of the fixed ratio treatments showed marked reductions in growth inhibition. This is consistent with the findings of the fractional inhibitory concentration analyses. In accordance with the criteria presented by Bhattacharya *et al.*, (2009) the sum 50% and 90% fractional inhibitory concentration ( $\sum\text{FIC}_{50, 90}$ ) data suggested that the combination between dihydroartemisinin and emetine is predominantly additive (indifferent). SumFIC values ranged from 0.9-1.4 at the 4 ratios tested (Table 6.6). A synergistic interaction was detected only at the  $\text{FIC}_{90}$  3:2 ratio and no antagonistic interactions were recorded for the combination using the  $\sum\text{FIC}_{50, 90}$  values as the determinant. Analysis of the isobologram plots, however, revealed a relatively prominent convex curve for the  $\text{FIC}_{50}$  level on inhibition indicative of antagonism (Figure 6.3 a). The  $\text{FIC}_{90}$  plot is consistent with the  $\sum\text{FIC}_{90}$  data also showing an additive interaction between dihydroartemisinin and emetine (Figure 6.3 b).

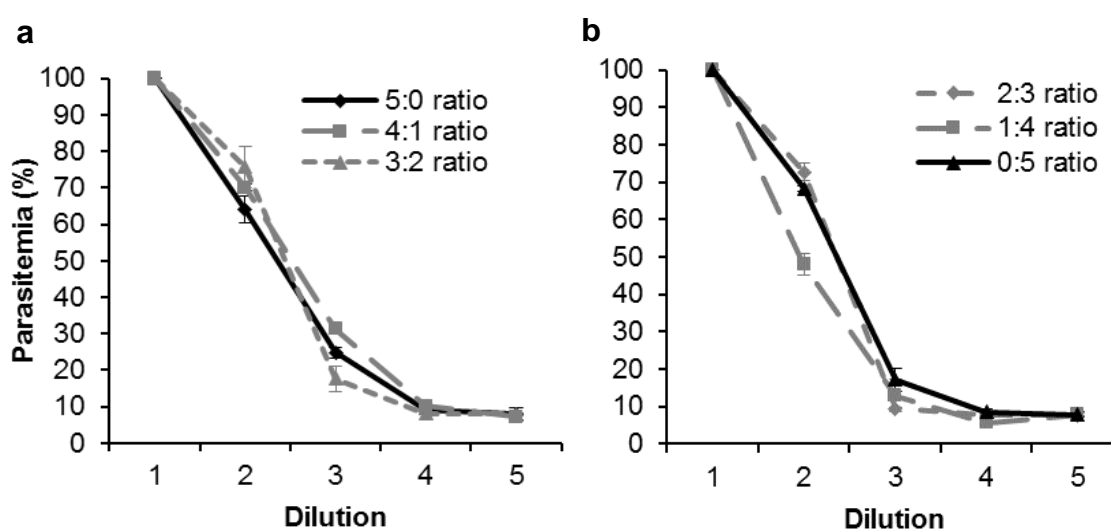


**Figure 6.2** Fixed ratio dose response curves for the dihydroartemisinin-emetine combination. Dihydroartemisinin dominant 5: 0, 4: 1 and 3: 2 (a) and emetine dominant 2:3, 1:4 and 0:5 (b) combinations are displayed separately. Error bars represent data completed in duplicate.

Ratio	CompA (DHA) FIC <sub>50</sub>	CompA (DHA) FIC <sub>90</sub>	CompB (Eme) FIC <sub>50</sub>	CompB (Eme) FIC <sub>90</sub>	$\Sigma$ FIC <sub>50</sub> s, interaction	$\Sigma$ FIC <sub>90</sub> s, interaction
5:0	1	1	0	0	n/a	n/a
4:1	0.914829	0.97142	0.412807	0.482675	1.327636, ADD	1.454094, ADD
3:2	0.638616	0.464741	0.837115	0.422492	1.475731, ADD	0.887233, SYN
2:3	0.421106	0.310655	1.059061	0.71155	1.480167, ADD	1.022206, ADD
1:4	0.238412	0.212022	1.167547	1.064742	1.405959, ADD	1.276764, ADD
5:0	0	0	1	1	n/a	n/a

**Table 6.6** The interaction between dihydroartemisinin and emetine against *P. falciparum* (strain K1) at 6 different preparations. SumFIC<sub>50</sub> and SumFIC<sub>90</sub> values have been calculated (SYN: synergy and ADD: additive)

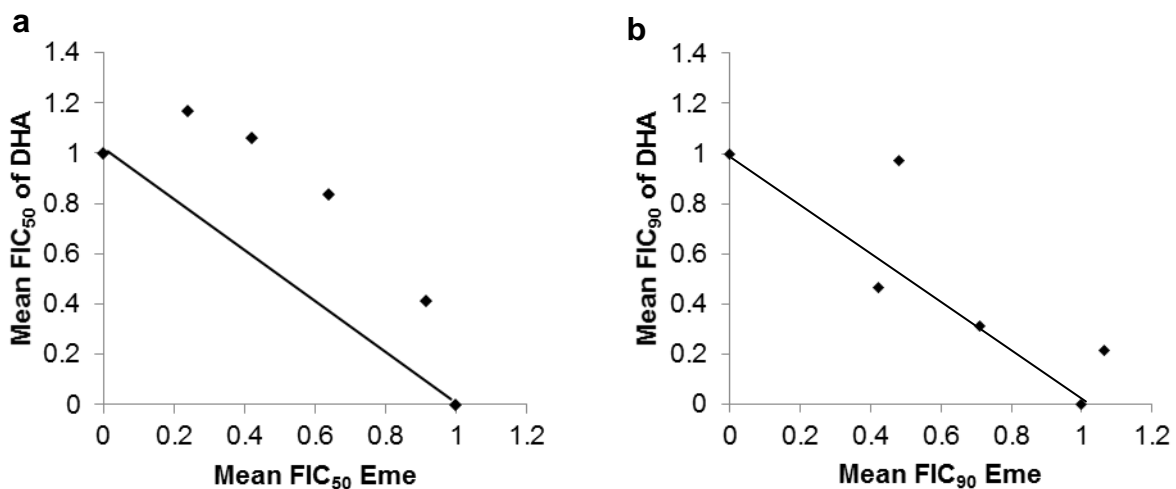


**Figure 6.3** Isobolograms showing the FIC<sub>50</sub> and FIC<sub>90</sub> interactions between dihydroartemisinin and emetine. The fixed ratio method was used to analyse the interaction between dihydroartemisinin and emetine dihydrochloride hydrate initiated against trophozoite stage parasites. Treatments were set up in duplicate for 48 hours and analysed using the SG-FCM. The mean FIC<sub>50</sub> (a) and mean FIC<sub>90</sub> (b) concentrations were determined and used to plot the isobolograms.

### 6.3.3 Analysis of the interaction between dihydroartemisinin and emetine using CalcuSyn

Median effect analysis of the dihydroartemisinin-emetine combination was also completed. Dose response curves were generated using the CalcuSyn software programme. Growth inhibition for the combination appeared comparable to that of the DHA treatment series (Figure 6.4). Good correlations coefficients of the median effect plot were reported for dihydroartemisinin ( $R=0.91135$ ), emetine ( $R=0.92543$ ) and the combination ( $R=0.88689$ ) indicating accurate data measurement and good conformity to the mass-action law (Fig 6.5.b). The fraction of affected cells in response to each treatment was thus utilised to perform interaction analysis where both drug potency and shape of the dose effect curve are considered. The CalcuSyn isobologram results were slightly above the line of additivity at the 50% growth inhibition level (Figure 6.4.c). In agreement, the

Combination Index (CI = 1.147) was also at the borderline of the nearly additive and slight antagonism classifications. However the CalcuSyn isobologram (Figure 6.4.c) and CI data indicated moderate antagonism and antagonism at the 75% (Combination index = 1.316) and 90% (Combination index = 1.526) levels of parasite inhibition respectively (see Table 6.7 for detailed criteria).

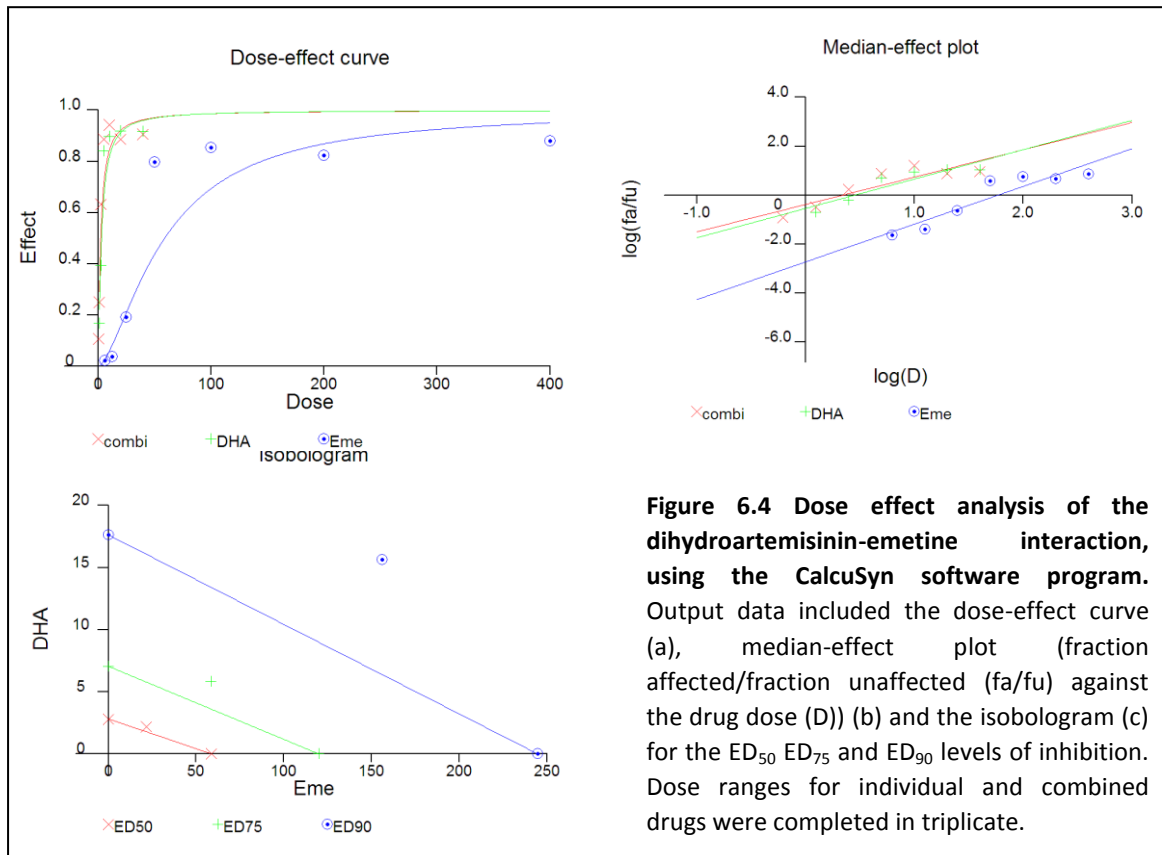


**Figure 6.4 Dose effect analysis of the dihydroartemisinin-emetine interaction, using the CalcuSyn software program.** Output data included the dose-effect curve (a), median-effect plot (fraction affected/fraction unaffected (fa/fu) against the drug dose (D)) (b) and the isobologram (c) for the ED<sub>50</sub> ED<sub>75</sub> and ED<sub>90</sub> levels of inhibition. Dose ranges for individual and combined drugs were completed in triplicate.

Range of CI	Symbol	Description
<0.1	+++++	Very strong synergism
0.1-0.3	++++	Strong synergism
0.3-0.7	+++	Synergism
0.7-0.85	++	Moderate synergism
0.85-0.90	+	Slight synergism
0.90-1.10	±	Nearly additive
1.10-1.20	–	Slight antagonism
1.20-1.45	– –	Moderate antagonism
1.45-3.3	– – –	Antagonism
3.3-10	– – – –	Strong antagonism
>10	– – – – –	Very strong antagonism

**Table 6.7 Recommended symbols and descriptions for defining synergism or antagonism using the combination index method.** The more broadly defined criteria suggests that the combination index, CI < 1, = 1, and >1 indicate synergism, additive effect and antagonism, respectively (Source: CalcuSyn manual, Biosoft).

Further interrogation of the treatment regime employed to permit interaction analysis via the CalcuSyn software program revealed basic empirical evidence of an additive (indifferent) interaction between dihydroartemisinin and emetine

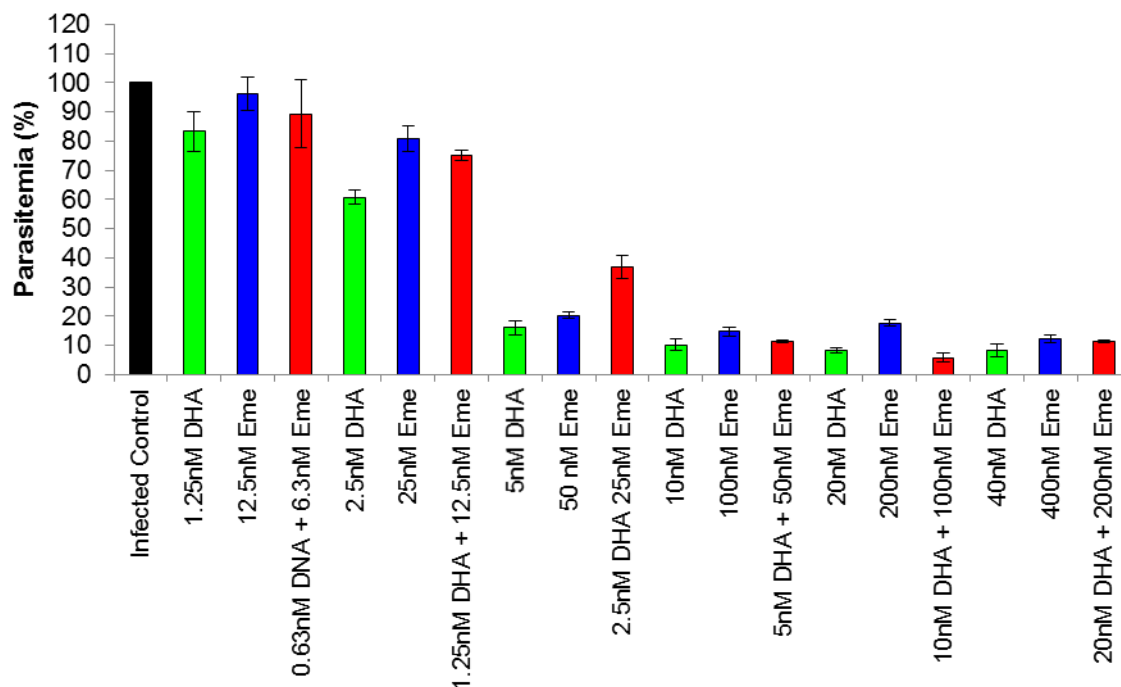


**Figure 6.5 Basic graphical representation of the interaction between dihydroartemisinin and emetine.** Comparable inhibitory concentrations of drugs A (DHA- Green bars) and B (Eme-Blue bars) are plotted against 0.5 A + 0.5 B (red bars) from 0.25x IC<sub>50</sub> up to 8x IC<sub>50</sub> values. Parasitaemia (%) was calculated relative to the infected control which was set at 100 %. Error bars are based on the SEM of duplicate data points.

In brief, the level of inhibition achieved by the administration of the single agents A (DHA) and B (Eme) was compared with the combination of the two compounds at half the respective dose (0.5 A + 0.5 B). The level growth inhibition incurred via the combination commonly fell between that of the compounds administered separately. Only at the 80 % inhibition level did growth in the combination sample exceed that of the single compound treatments (Figure 6.5).

#### 6.3.4 Validation of the CalcuSyn assay for malaria

##### 6.3.4.1 Optimisation of drug dosing and treatment period

The known synergists, atovaquone and proguanil, were analysed via the constant ratio combination method in order to establish whether CalcuSyn, using SG-FCM as a read out for parasite viability, can reliably determine the nature of an interaction between two compounds against erythrocytic stage malaria. The results of the initial combination experiment were inconclusive. Atovaquone failed to induce the expected response for the



dose series selected and a clear synergistic interaction was not apparent between the two compounds (Figure 6.6).

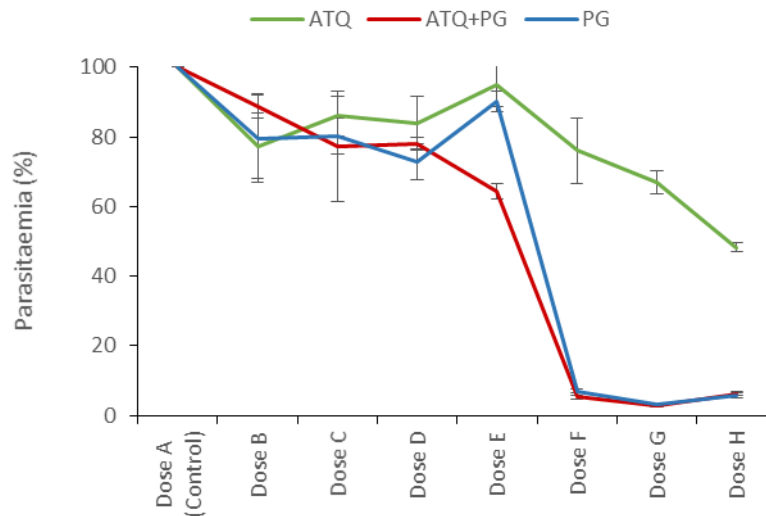


**Figure 6.6 Atovaquone-proguanil combination against *P. falciparum* malaria, strain K1.** Trophozoite stage parasites were treated with a dose series of Atovaquone (ATQ), Proguanil (PG) or a combination of the two (ATQ+PG). The 2-fold serial dilution ranged from 0.09-5.6 ng/ml for ATQ and 0.6-36.8 µg/ml for PG so that the mid-point (Dose E) equated to the previously determined IC<sub>50</sub> value for each drug. After a 48 hour incubation period samples were analysed using the SG-FCM method. Parasitaemia was determined relative to untreated controls which were set at 100 %. Error bars represent standard error of the mean (SEM) for triplicate data.

The second experiment aimed to increase the atovaquone dose to address the query as to whether its ineffectiveness was responsible for the lack of synergism observed. Although the dose shift permitted up to 80 % inhibition, a similar response pattern to the first experiment emerged. The dose response for the combination was in fact comparable to that of proguanil alone (Figure 6.7).

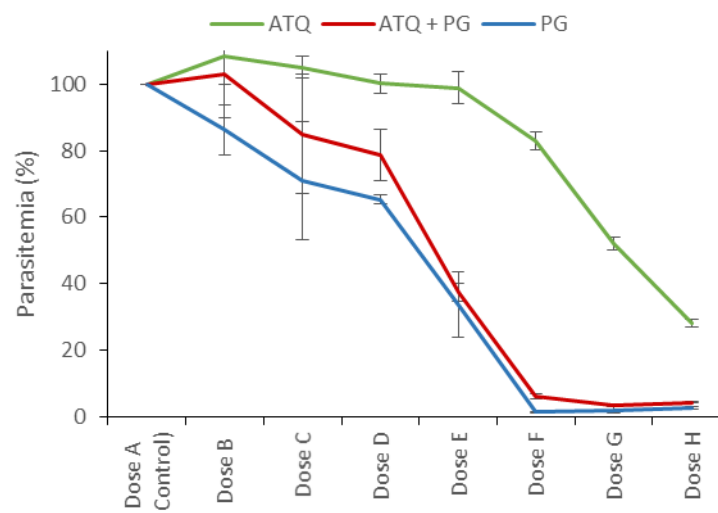


**Figure 6.7 Atovaquone-proguanil combination using a higher doses-series of atovaquone.** Trophozoite stage parasites (strain K1) were treated with a dose series of Atovaquone (ATQ), Proguanil (PG) or a constant ratio combination of both drugs (ATQ+PG). Doses ranged from 0.18-11.2 ng/ml and 0.6-36.8 µg/ml for ATQ and PG respectively. SG-FCM method was used to analyse parasite growth after 48 hours of treatment. The parasitaemia of drug treated samples was determined relative to untreated controls (100 % parasitaemia). Triplicate samples were used to derive error bars based on the standard error of the mean (SEM).

The next enquiry was concerned with drug order and addition as well as the length of the treatment period. The two parameters were adjusted in the same experiment. All controls were shown to be effective in the study. In particular, the Acetonitrile: water control indicated that the solvent was not inhibitory to the parasite the highest dose used. Confirming that the atovaquone and proguanil concentrations were responsible for any inhibition observed. Whether the compounds were added before the addition of parasitised culture (together) or after (separately) appeared to have no effect on drug potency or combinatory outcome (Fig 6.9).

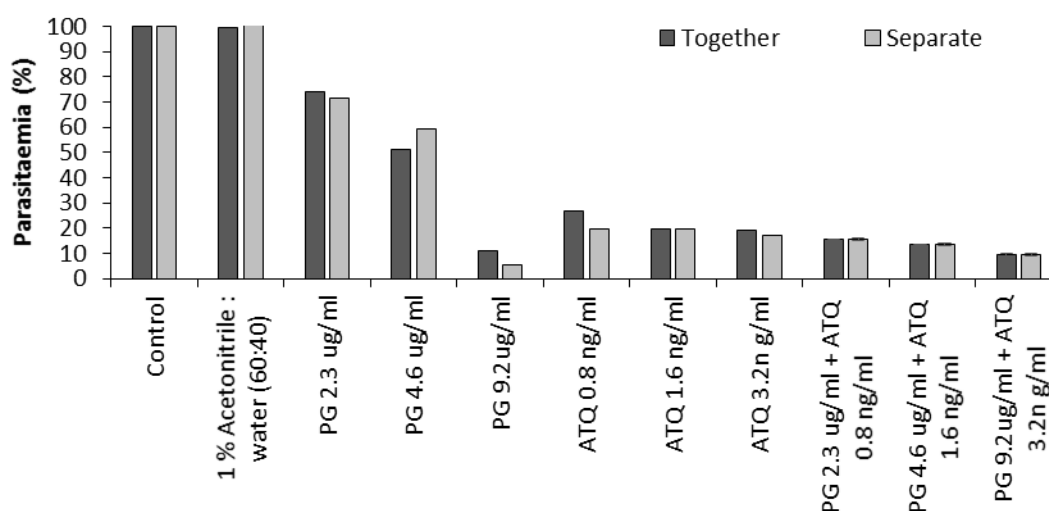


**Figure 6.8 The effect of drug addition method on combinatory outcome of the atovaquone-proguanil combination.** Ring stage parasites were treated for 72 hours with three doses of either atovaquone (ATQ), proguanil (PG) or a combination of the two. The drugs were either added to the 96 well plate prior to the addition of the diluted parasitised culture in the 'together' condition. In the 'separate' condition the culture was added to the plate first, followed by the addition of each drug individually (including the combination treatments). The inhibitory effect of an equivalent amount of the proguanil solvent, 1% acetonitrile: water (60:40) at the highest dose (PG 9.2  $\mu\text{g/ml}$ ) used in the study was also analysed. Parasite growth was determined by SG-FCM. Error bars representing the standard error of the mean are shown for samples with replicates.

The increase in treatment period from 48 to 72 hours, however, revealed a more potent atovaquone phenotype (Figure 6.9). It was also evident that there was slightly more inhibition incurred by the combination of atovaquone and proguanil than the drug alone comparisons. It appears that the effect may have been masked by the high potency of atovaquone that achieved ~80% inhibition for the lowest dose used in the study.

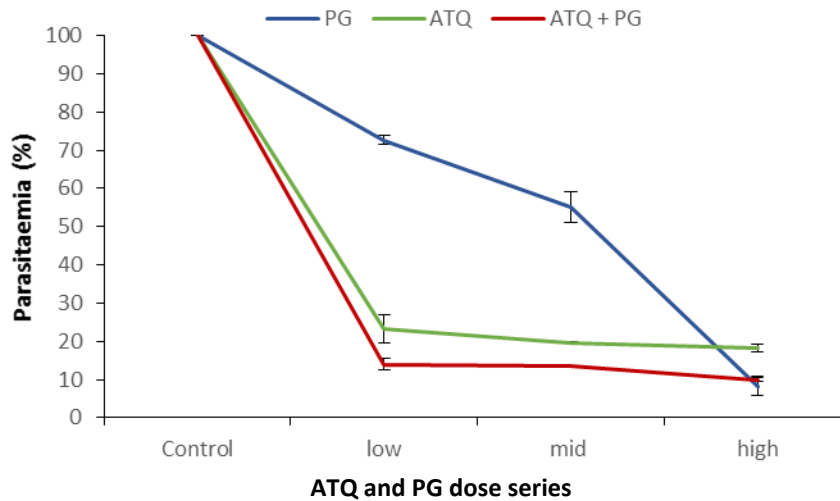


**Figure 6.9** The effect of incubation time on combinatory outcome of the atovaquone-proguanil combination. Ring stage parasites were treated for 72 hours with a 2-fold dose series of either atovaquone (ATQ, 0.8, 1.6 and 3.2 ng/ml), proguanil (PG 2.3, 4.6 and 9.2 µg/ml) or a combination of the two. SG-FCM was used to analyse parasite survival. Parasitaemia in drug treated samples was relative to untreated controls that were equated to 100%. Error bars are based on the SEM for quadruplicate samples.

Taken together the above data indicated that the constant ratio combination method may be used to accurately identify nature of the interaction between atovaquone and proguanil if the atovaquone dose is reduced and a 72 hour treatment regime is adopted. Including these alterations in the subsequent experiment did expose a dose response pattern that alluded to potential synergism (Fig 6.11) and most importantly provided sufficient data for CalcuSyn analysis. It should be noted that some inhibition was also incurred by the highest dose of acetonitrile: water included in the present study.

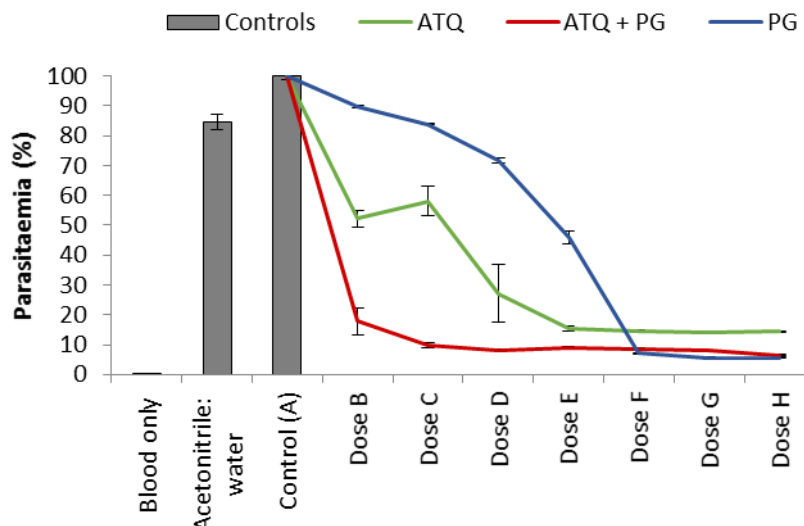
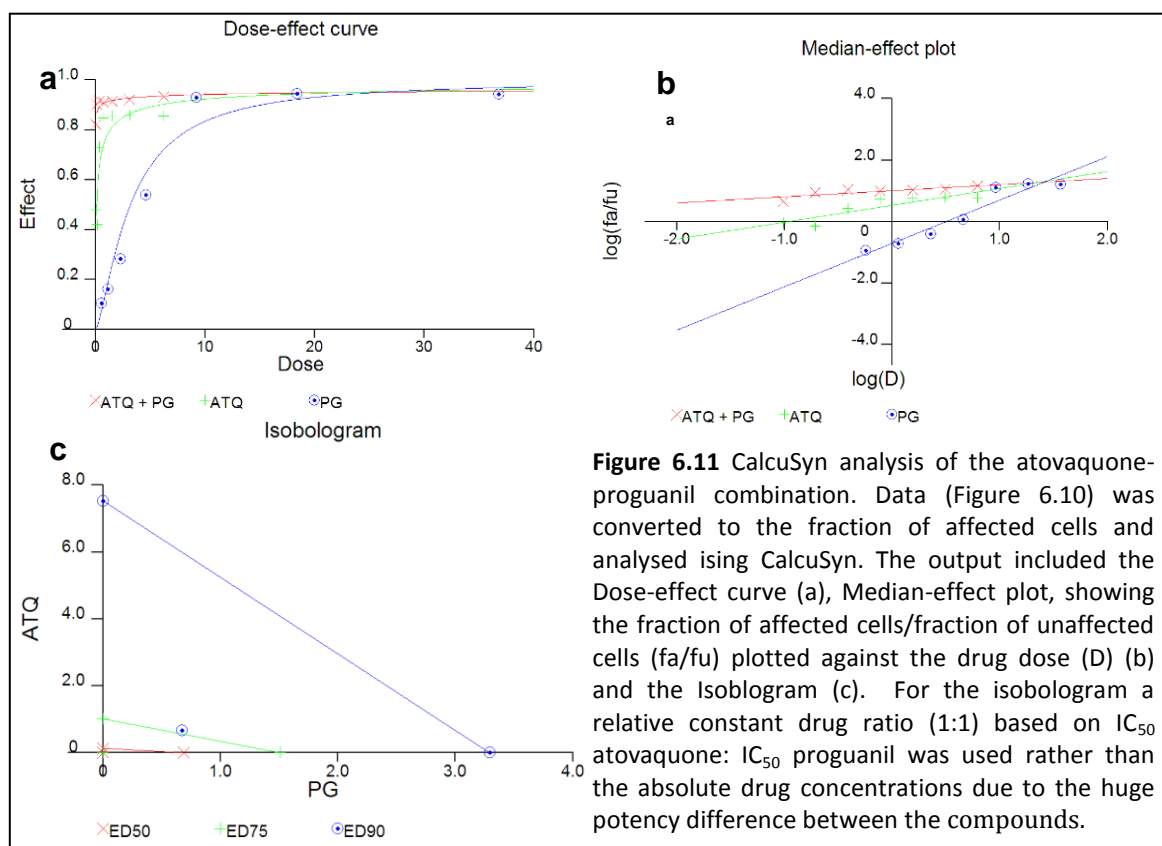


**Figure 6.10** Dose response curves for atovaquone (ATQ), proguanil (PG) and the constant ratio combination of the two drugs. The highest dose of the acetonitrile: water (60:40) solvent for proguanil was also included as a control. Ring stage parasites were treated for 72 hours and analysed using the SG-FCM method.

CalcuSyn analysis of the dose-effect data also confirmed that the combination was more potent than either ATQ or PG alone (6.12.a). The Median-effect plot (Figure 6.11 b) indicated that the drugs act *via* different modes of action due to the lack parallel lines which reflect a difference in the shape of the dose effect curve (hyperbolic/ sigmoidal). The isobologram showed synergy at the ED<sub>50</sub> and ED<sub>75</sub> levels but antagonism at the ED<sub>90</sub> level of inhibition (Figure 6.11 c).



The Combinatory index indicated that there was indeed very strong synergy for the atovaquone-proguanil combination at the ED<sub>50</sub> level of inhibition. However, at the ED<sub>75</sub> and ED<sub>90</sub> levels of inhibition the combinatory index and isobologram data defined the interaction as antagonism and very strong antagonism respectively (Table 6.8).

Drug	CI Values at					
	ED50	ED75	ED90	Dm	m	R
ATQ	N/A	N/A	N/A	0.10622	0.54763	0.87866
PG	N/A	N/A	N/A	3.18043	1.40769	0.96199
ATQ + PG (1:5897)	0.01490	1.74528	204.97422	7.9943e-006	0.19804	0.82530

**Table 6.8** The combinatory index values (CI) for the ATQ + PG constant ratio combination (1:15987) at the ED<sub>50</sub>, ED<sub>75</sub> and ED<sub>90</sub> levels of inhibition. The Dm, m and r values are also shown for all sets of data. Dm indicates potency and depicts the median effect dose at the ED<sub>50</sub> level of inhibition. The m value refers to the kinetic order and shape of the curve  $m = 1$ ,  $> 1$ , and  $< 1$  indicates hyperbolic, sigmoidal, and negative sigmoidal shape, respectively. The r values is the linear correlation coefficient for the median effect plot and indicates conformity to the mass action law.

## 6.3.4.2 Non-constant ratio of combination of Atovaquone and Proguanil

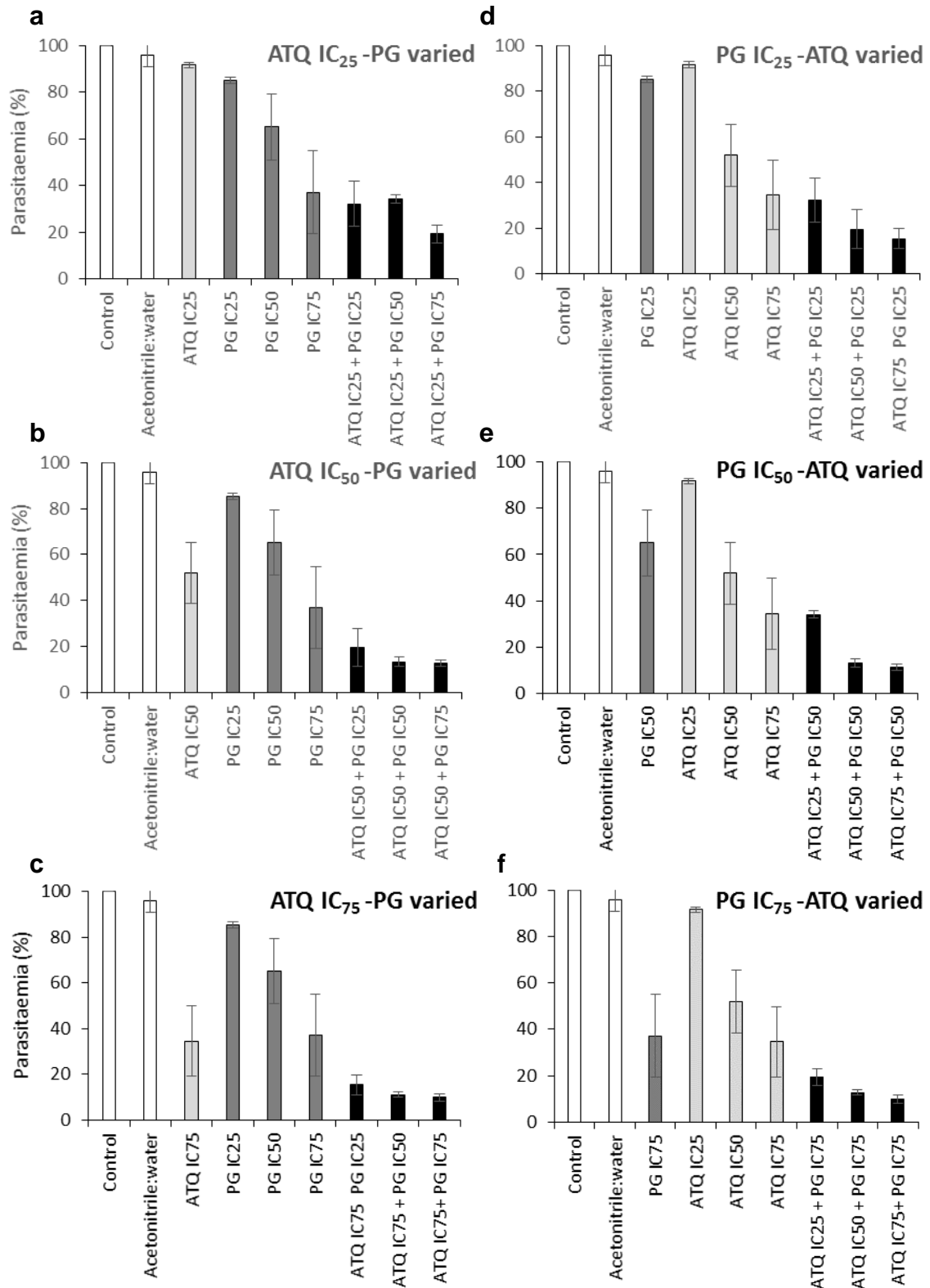


**Figure 6.12 The non-constant ratio combination of atovaquone and proguanil.** Ring stage parasites were treated for 72 hours with predetermined IC<sub>25</sub>, IC<sub>50</sub> and IC<sub>75</sub> doses of atovaquone and proguanil either alone or in combination. Combinations consisted of a constant dose of one drug with a varied dose range for the second drug and *vice versa*. Parasite growth was analysed using the SG-FCM method. Parasitaemia was calculated relative to the control (infected) which was equated to 100 %. Error bars represent the SEM of triplicate data from two separate experiments.

The data from the non-constant ratio design experiment consistently showed that when parasites were treated with one drug, no matter what the concentration, addition of a second drug induces further effects (Figure 6.12 a-f). Although the dose dependency effect was more obvious at lower doses, a dose response pattern was apparent for the second drug even under constant drug pressure of the IC<sub>75</sub> concentration for the first compound. The constant ratio design data (completed in parallel) was consistent with the dose response pattern observed in previous experiments (Figure 6.13). The atovaquone dose range used in the study did not achieve greater than 40% inhibition. However, the 72 hour treatment period permitted detection of additional suppression and possible synergy in the combination sufficient for re-growth analysis following removal of the drug in the second part of the experiment.

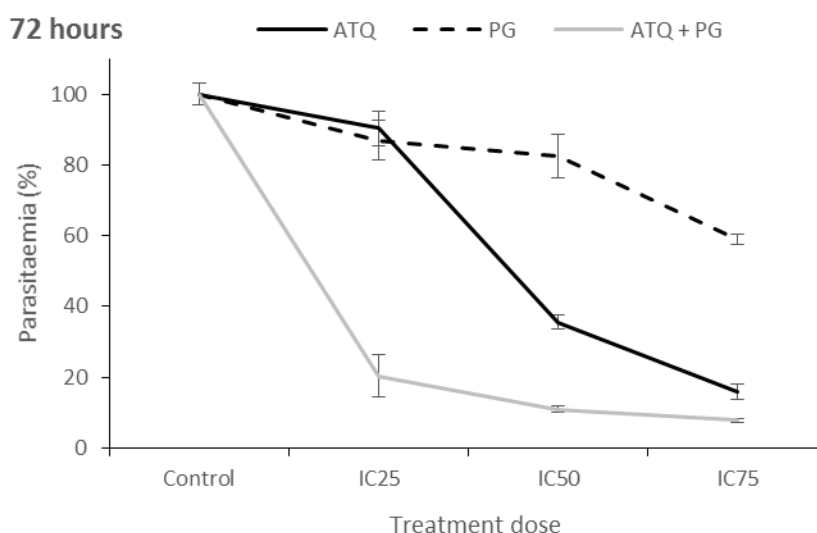


**Figure 6.13** Constant ratio data for the atovaquone proguanil combination after 72 hours. Ring stage parasites were treated with IC<sub>25</sub>, IC<sub>50</sub> and IC<sub>75</sub> dose of each drug or the corresponding combination at each level. Growth inhibition was analysed at 72 hours using the SG-FCM method. Triplicate data was used to construct error bars from the SEM.

#### 6.3.4.3 Recovery of parasites treated with the atovaquone-proguanil combination

The regrowth experiment showed that the combinations were more lethal than the drug alone treatments (Fig 6.15). Indeed, no growth was detected after 20 days in the IC<sub>50</sub> + IC<sub>50</sub> and IC<sub>75</sub> + IC<sub>75</sub> combinations. In fact only the IC<sub>25</sub> + IC<sub>25</sub> combination permitted the recovery of parasites. None of the Non-constant ratio combination supported parasite growth above that of the IC<sub>25</sub> + IC<sub>25</sub> combination (Appendix XI). A dose response pattern could be observed in the drug alone treatments after 20 days of incubation confirming the reliability of the data. Although there appears to be the same level of regrowth at the IC<sub>25</sub>, IC<sub>50</sub> and IC<sub>75</sub> levels of inhibition for proguanil (growth present in the first two dilutions for all concentrations) the parasitaemia showed a dose response pattern. First dilution

parasitaemias were 3.4 %, 2.2 % and 0.41 % and second dilution parasitaemias were 0.83 %, 0.46 % and 0.23 % for IC<sub>25</sub>, IC<sub>50</sub> and IC<sub>75</sub> doses respectively (control 4.4 first dilution 3.7 second dilution). Overall, the data inferred that the interaction between the two drugs was not antagonistic, recovery in all the combinations was less than even the highest doses of the drug alone counterparts. Therefore indicating, the background staining of dead parasites, or those committed to dying, had confounded the data at the higher doses.

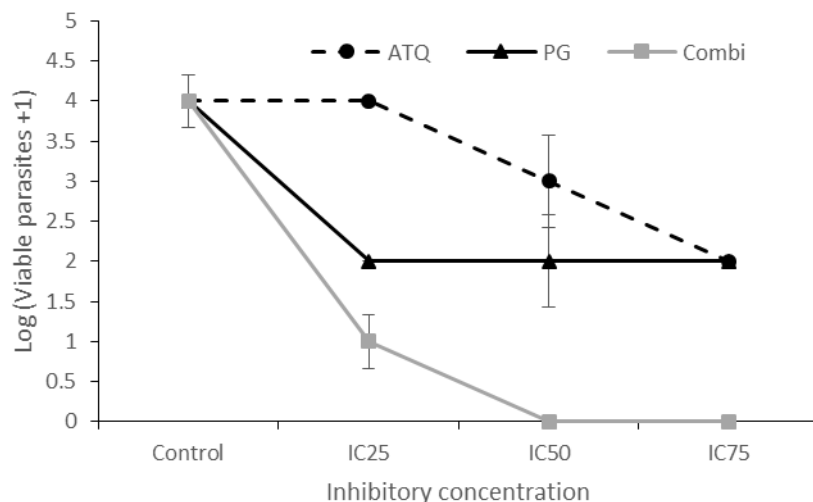


**Figure 6.14 Constant ratio data for the atovaquone-proguanil combination after 20 days.** The experiment was initiated with ring stage parasites in a 96 well plate format. Drug pressure was removed after 72 hours of treatment, parasites were subjected to 8, 10-fold limiting serial dilutions and incubated for a further 17 day. Spent media was replaced with fresh media and erythrocytes on day 7. The presence or absence of growth in wells was determined used the SYBR green methods (chapter 2). Error bars represent the SEM for 3 replica samples.

#### 6.3.5 Combination of emetine and existing antimalarials using the CalcuSyn constant ratio method

The combination of emetine and dihydroartemisin was reanalysed using the optimised 72 hour treatment regime. The constant ratio method was also used to analyse the interaction between emetine and chloroquine and emetine and atovaquone. Ratios were selected based of the respective predetermined IC<sub>50</sub> values for each compound. The data for all of the combinations showed good conformity to the mass action law ( $r = 0.85-0.97$  refer to Tables 6.9, 6.10 and 6.11). The DHA-Eme combination was classified as antagonistic for the 1:10 ratio at all inhibitory levels analysed in the current study (See isobologram (Figure 6.15 d) and combinatory indexes (Table 6.9). The interaction between CQ-Eme, for the 72 hour treatment period at a 4.6:1 ratio, was classified as antagonism, antagonism and mild antagonism for the ED<sub>50</sub>, ED<sub>75</sub> and ED<sub>90</sub> levels inhibition respectively (Figure 6.16 and Table 6.10). For the ATQ-Eme (ratio 1:46) combination the ED<sub>50</sub> level of inhibition was classified as synergism, the ED<sub>75</sub> moderate synergism and ED<sub>90</sub> moderate antagonism (Figure 6.17 and Table 6.11).

### Dihydroartemisinin Emetine combination

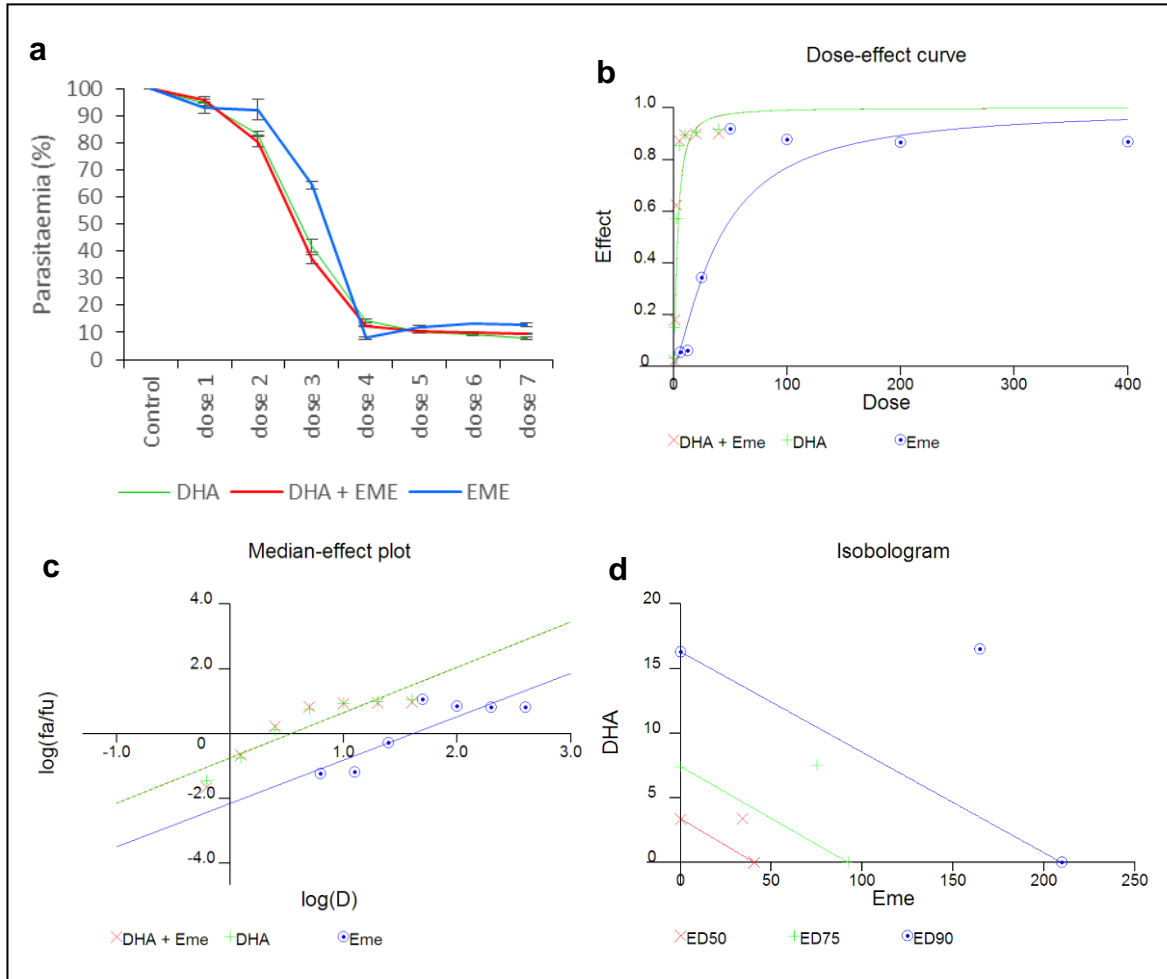


**Figure 6.15 The constant ratio combination of dihydroartemisinin and emetine.** Parasites were treated with dihydroartemisinin: emetine combination at a constant ratio of 1:10 for 72 hours. *P. falciparum* strain K1 parasite survival was determined using the SG-FCM method. The complied image shows the dose response curve based on the raw data (a) and the CalcuSyn output including: dose effect curve (b), median effect plot (fraction affected/fraction unaffected (fa/fu) against the drug dose (D)) (c) and isobologram (d).

Drug	CI Values at					
	ED50	ED75	ED90	Dm	m	r
DHA	N/A	N/A	N/A	3.07235	1.32229	0.92816
Eme	N/A	N/A	N/A	37.07047	1.26772	0.86364
DHA + Eme (1:10)	1.80297	1.80543	1.80847	3.02898	1.29514	0.89936

**Table 6.9 The combinatory index values (CI) for the dihydroartemisinin-emetine combination at a constant ratio of 1:10.** Determinants of potency at ED<sub>50</sub> (Dm), Shape of the curve ( $m = 1$ ,  $> 1$ , and  $< 1$  signify hyperbolic, sigmoidal, and flat sigmoidal respectively) and the linear correlation coefficient (r) are also presented in the table. Tabular data accompanies the CalcuSyn output presented in Figure 6.15 for the *P. falciparum*, strain K1 exposure to the dihydroartemisinin- emetine combination for 72 hours.



## Chloroquine Emetine combination

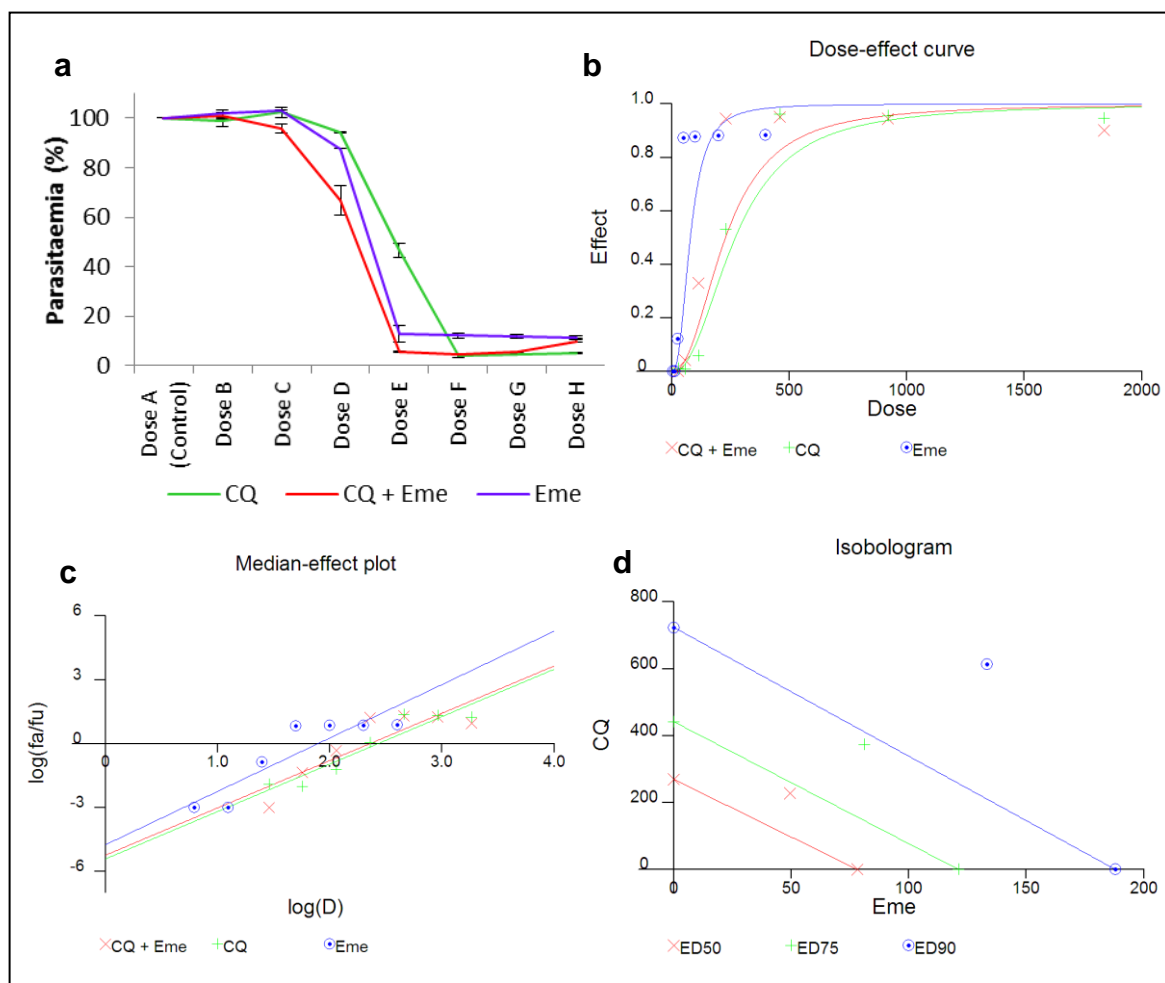


**Figure 6.16 The constant ratio combination of chloroquine and emetine.** The Chloroquine emetine combination was analysed using the constant ratio (4.6:1) design for CalcuSyn median-effect based analysis. The experiment was initiated at ring stage and parasite were exposed to drug alone and drug combination dose series for 72 hours. Growth inhibition was analysed using the SG-FCM method. The dose response curve (a) and CalcuSyn output curves: namely, dose effect (b), median effect (fraction affected/fraction unaffected ( $fa/fu$ ) against the drug dose ( $D$ )) (c) and isobologram (d) are shown.

Drug	CI Values at					
	ED50	ED75	ED90	Dm	m	r
CQ	N/A	N/A	N/A	391.33597	3.01961	0.91788
Eme	N/A	N/A	N/A	49.17856	1.55407	0.89619
CQ + Eme (4.6:1)	1.58798	1.47786	1.41581	227.64205	2.21787	0.86713

**Table 6.10 The dose effect parameters for the chloroquine-emetine combination.** The combinatory index values are shown for the combination at the ED<sub>50</sub>, ED<sub>75</sub> and ED<sub>90</sub> levels of inhibition. Dm, m and r values are also reported and indicate potency of the compounds tested, shape of the median effect curve and the correlation coefficient of the data to the mass action law, respectively.

Atovaquone Emetine combination

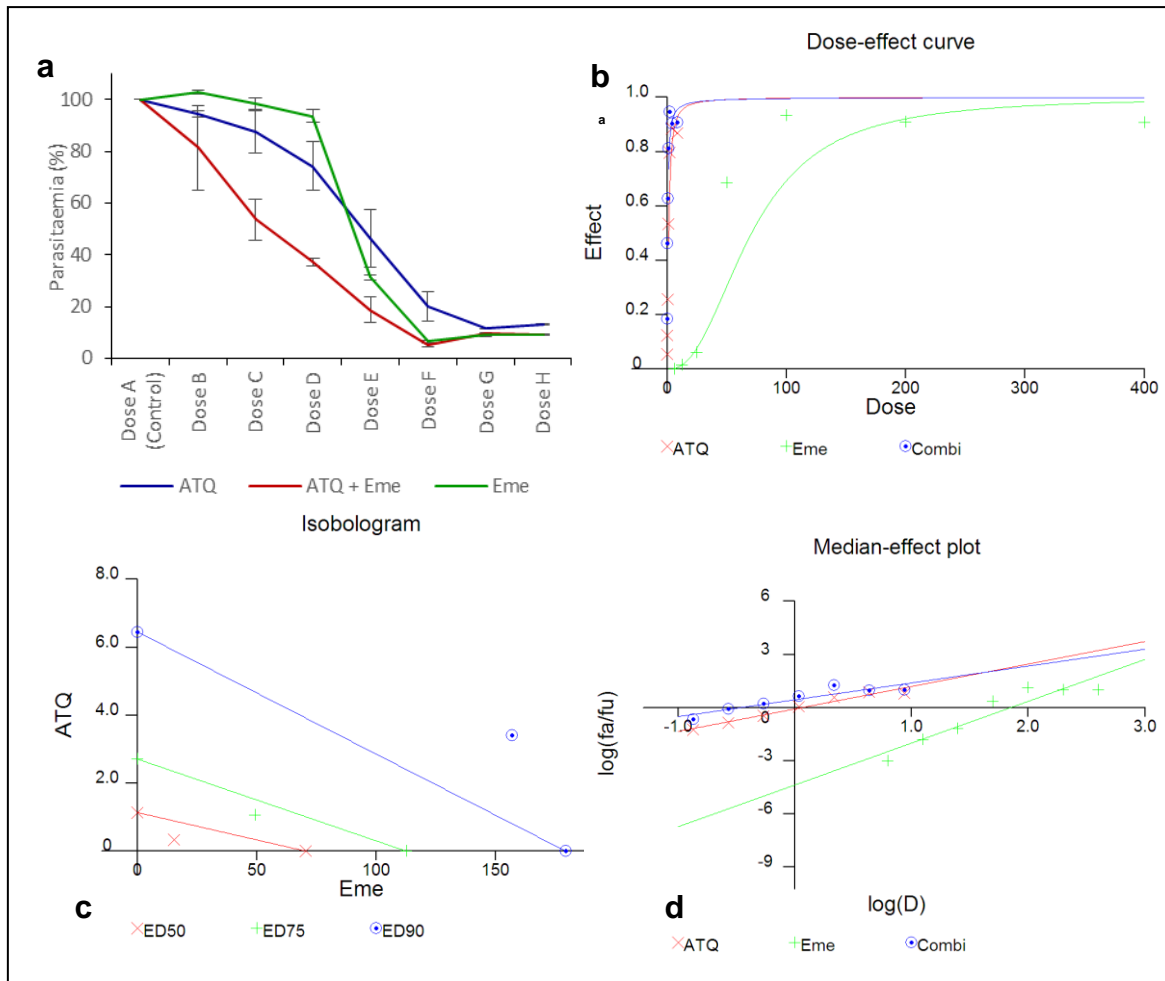


**Figure 6.17** The constant ratio (1:46) combination of atovaquone and emetine. Parasite viability was analysed after 72 hours using the SG-FCM method. A basic dose response curve is shown (a) as well as CalcuSyn dose effect curve, and median effect plot (fraction affected/fraction unaffected (fa/fu) against the drug dose (D)) which are based on the fraction of affected parasites. The isobologram is also shown and indicate the nature of the interaction between the two compounds at the ED<sub>50</sub> ED<sub>75</sub> and ED<sub>90</sub> levels of inhibition (Marker below the line = synergistic, on the line = additive and above the line antagonistic). The degree of the classification is indicated by the distance of the marker from the respective (colour coded) line.

Drug	CI Values at					
	ED50	ED75	ED90	Dm	m	r
ATQ	N/A	N/A	N/A	1.13857	1.26701	0.97767
Eme	N/A	N/A	N/A	70.64774	2.35775	0.93572
Combi (1:46)	0.51595	0.83394	1.40272	0.33735	0.94992	0.91194

**Table 6.11** The combinatory index (CI) values for the atovaquone emetine combination at the ED<sub>50</sub>, ED<sub>75</sub> and ED<sub>90</sub> levels of inhibition. Dm, m and r values (as described in table 6.8-10) are also displayed for the atovaquone-emetine combination at a 1:46 ratio against *P. falciparum* strain K1. Tabular data accompanies the CalcuSyn output plots presented in Figure 6.17.

## 6.4 DISCUSSION

It is now widely accepted that combination regimes have significant therapeutic advantages when compared to monotherapy (Fivelman *et al.*, 2004). The aim of this study was therefore to evaluate the combinatorial therapeutic potential of the novel antimalarial candidate, Emetine dihydrochloride hydrate with existing antimalarials. As an initial stepping stone to such investigations, *in vitro* interaction assays are used. Unfortunately, poor standardisation has meant that discrepancies have often appeared in the malaria literature (Canfield *et al.*, 1995; Fivelman *et al.*, 2004; Gorka *et al.*, 2013; Mariga *et al.*, 2005). For this reason, an automated interaction analysis programme, CalcuSyn, was optimised for use in malaria and employed to determine the nature of the interaction between emetine and three antimalarials: namely, dihydroartemisinin, chloroquine and atovaquone.

### 6.4.1 Comparison of the fixed ratio and CalcuSyn methods for drug interaction analysis

To provide a more in depth pharmacodynamic perspective of the dihydroartemisinin-emetine interaction detailed *in vitro* analyses were carried out. In the current climate the DHA-Eme interaction is of particular importance due to the worldwide dependence on the artemisinin class and the essentiality of preventing resistance development. As the active metabolite of all artemisinin derivatives, dihydroartemisinin, was used for all combinatorial investigations with emetine in the study. Initially, the fixed ratio method was employed in accordance with Bhattacharya *et al.* (2009). Dihydroartemisinin and emetine were combined at four fixed ratios and the dose response curves generated for each ratio were compared with those of the individual compounds. There are two indicators of the fixed ratio method that serve to clarify the nature of an interaction between two compounds. Firstly, the sum of the fractional inhibitory concentration ( $\Sigma$ FIC) is calculated and its value is integrated into predefined criteria that correspond to synergism, additivity or antagonism. Secondly, the isobologram plot where the FIC values at each ratio for drug 'A' are plotted against the FIC values at the corresponding ratios for drug 'B'. A concave curve represents a synergistic interaction while a convex curve indicates antagonism. Additivity is referred to as an indifferent interaction and represented by a straight line. Unfortunately, data representing the two read-outs from the fixed ratio method were in conflict. SumFIC<sub>50, 90</sub> values predicted that the drug ratios predominantly fell within the additive range when applying criteria used by Bhattacharya *et al.* (2009). At the  $\Sigma$ FIC<sub>90</sub> level of inhibition a single case of synergy was also reported (ratio 3:2).

However, while the  $FIC_{50}$  isobolograms showed an antagonistic trend, the  $FIC_{90}$  isobolograms followed an additive trend. Although variation between ratios is expected, different measures of the interaction at the same ratio should be in agreement. Such contradictions call into question the reliability of the methods of interpretation. Particularly when  $\Sigma FIC$  cut off values are not standardised in published literature. For example, Vivas et al., (2007) and other critiques of the method, interpret additivity as an indifferent interaction for which the  $\Sigma FIC$  values should strictly equal '1'. Anything below or above 1 should be defined as synergy and antagonism respectively (Canfield et al., 1995). As such narrow limits are difficult to achieve in biological systems others such as Abiodun et al., (2013) have selected broader categories to incorporate a region of error (ie.  $\Sigma FIC < 0.8$  = synergism,  $\Sigma FIC > 0.8-1.4$  = additive,  $\Sigma FIC > 1.4$  = antagonistic). Applied, to the current study these criteria would suggest that the interactions at both  $\Sigma FIC_{50}$  and  $\Sigma FIC_{90}$  would fall within the additive to mildly antagonistic range. However this is not the case for Bhattacharya and colleagues (2009) as the additive window they adopt is not around 1 but equal to or above 1. Furthermore, for their selection of interaction criteria they only on quote their previous work and a paper Odds (2003) which they seem to have misinterpreted. In fact Odds (2003) is actually making the point that broad criteria for defining drug interactions cannot be considered as an equivalent to experimental error or confidence intervals. They suggest that only extreme cases  $<0.5$  for and  $> 4$  of synergism and antagonism, respectively should be accepted, to encourage more conserved interpretations, rather than authors subjectively putting a positive spin on their data (Odds, 2003). The issue of selecting appropriate guidelines is avoided if the CalcuSyn method is employed as the cut-off criteria are clearly outlined. In order to permit automated analysis of the dihydroartemisinin-emetine combination with CalcuSyn, a constant ratio method was adopted. The data generated by the software focuses on the effective dose ( $ED_{50}$ ), a term that is often used interchangeably with the  $IC_{50}$ . The CalcuSyn output described the interaction between dihydroartemisinin and emetine borderline 'nearly additive'/'slightly antagonistic' at the  $ED_{50}$  level, 'slightly antagonistic' at the  $ED_{75}$  level and 'antagonistic' at the  $ED_{90}$  level. Combination index data and the isobologram plot were found to be in complete agreement using CalcuSyn analysis software demonstrating the superior accuracy of the method. Possibly owing to the more stringent guidelines and automation, the analysis prevents the user bias of selecting criteria to suit the desired outcome of an interaction. Indeed, if the criteria defined by Canfield and colleagues (1995) were applied to the fixed ratio analysis all ratios would be classified as antagonistic at the  $\Sigma FIC_{50}$  level,

while at the  $\Sigma\text{FIC}_{90}$  level, the ratios would vary from synergistic to antagonistic which is in better agreement with the isobolograms obtained for the same set of data. One would expect that more stringent guidelines should endorse more accurate data. However, achieving such narrow limits in biological systems is problematic and could result in the exclusion of potentially effective combinatory options. For example, visual scrutinisation of the DHE-Eme interaction under the constant drug ratio design (Figure 6.5) employed for its compatibility with CalcuSyn, indicated that drug doses could be halved when used in combination. Only at the 2.5 nM DHA + 25 nM Eme was this phenomenon not observed. This could potentially suggest that, a toxicity reduction advantage of combination therapy could be achieved by the dihydroartemisinin-emetine interaction despite its classification. This highlights, a significant advantage of combinations classified as additive, due to the obvious impact of delayed resistance acquisition. Nevertheless, it is evident that in order to obtain a standardised system stringent non-subjective criteria, like those defined by Chou-Talay for CalcuSyn should be adopted. It is therefore a separate issue that candidates with classification around the additive or mildly antagonistic window, like emetine, should not be disregarded. Particularly, since differences in *in vitro* and *in vivo* interactions are commonly reported (Fivelman *et al.*, 2004; Keiser *et al.*, 2012; Synder *et al.*, 2007). Indeed recent *in vivo* studies have demonstrated that weak antagonism does not necessarily translate to slower parasite clearance times when compared to individual compounds (Synder *et al.*, 2007). Furthermore, the RBx11160 (OZ277) and piperaquine interaction was in fact shown to be reduced from antagonistic *in vitro* to additive *in vivo* indicating that pharmacokinetics play an important role (Fivelman *et al.*, 2004; Synder *et al.*, 2007).

Due to the limited number of options available for malarial treatment, it is therefore evident that, the idealistic synergistic interaction between two drugs may need to be compromised if the benefits bestowed by a two pronged attack: namely toxicity reduction and a delay in the onset of resistance, outweigh the therapeutic disadvantage of a mere additive classification. Furthermore, given the complex nature of the parasite life cycle, including its stage and strain specific variations, other factors besides simplistic mechanistic deductions based on parasite clearance should be investigated (Bell, 2005). Interactions described as additive, verging on mildly antagonistic, should be analysed further before potential combinatory partners are discarded prior to *in vivo* studies (Vivas *et al.*, 2007).

However, the value of *in vitro* studies to refine the candidate list would be lost if every compound was considered for further *in vivo* investigations. One would expect that the classification of candidates as strongly synergistic or strongly antagonistic should not be misjudged, thus, studies should aim to rule out any strongly antagonistic combinations. A major issue with the DHA-Eme data is that although the application of more ridged criteria to the fixed ratio data meant that the ED<sub>50</sub> classification was in agreement with the CalcuSyn analysis (slightly antagonistic), for the EC<sub>90</sub> level they are completely contradictory. The data range from synergy to strong antagonism. Numerous factors may have affected the outcome of the classifications, such as, experimental conditions whether the interaction is ratio, dose or effect dependent (CalcuSyn manual 1996-2006; Bell, 2005). Indeed, different drug ratios were used for the fixed ratio and CalcuSyn methods. For the ED<sub>50</sub> level of inhibition this was not a problem as the same outcome was reported for all ratios used, but at the EC<sub>90</sub> level, variations are reported for the different ratios adopted in the fixed ratio method. Another foreseeable problem with the CalcuSyn study was that the parasitaemia was low, even in control samples; meaning at the highest levels of inhibition background interference was likely, particularly as the analysis takes into account the entire shape of the curve. As this data is inconclusive and the reliability of the CalcuSyn method cannot be confirmed, further work was focused on using antimalarial compounds with a known interaction outcome to validate the method.

#### 6.4.2 Validation of the CalcuSyn method for malaria using the malarone combination

The Atovaquone and proguanil combination was selected as known antimalarial synergists to validate the CalcuSyn method for malaria (Khositnithikul *et al.*, 2008; Radloff *et al.*, 1996). A constant ratio design, compatible with the CalcuSyn software, was set up in accordance with their previously determined IC<sub>50</sub> values (Chapter 3). In the first two experiments the combination failed to show a marked increase in growth suppression when compared with the drug alone counterparts (Figure 6.6 and 6.8). Initially, the low activity of atovaquone was thought to be responsible for the lack of synergism observed, possibly attributable to solubility issues of the compound also reported by Canfield and colleagues (1995). The dose increase in the second experiment achieved up to 80% inhibition yet no evidence of synergy could be observed. As the interaction is known to be synergistic there appeared to be a problem with the experiment set up and drug treatment regime. A preliminary experiment had shown some additional growth inhibition in a flask experiment where the compounds are added to the culture, as opposed to in the 96 well plate set up,

where plates were dosed prior to the addition of the parasitised culture, thus providing the opportunity for a physical interaction between the two compounds. Another possibility was that the 48 hour time-course is too short to detect an interaction between the two compounds particularly as atovaquone is known to be one of the slowest acting antimalarials available (Sanz *et al.*, 2012). Both parameters were tested in the subsequent experiment and the data confirmed that the treatment period was responsible for the lack synergism observed in the initial experiments. Had the effect not been masked by the higher potency of atovaquone at the 72 h time point, the observed increase in growth inhibition for the combination may have alluded to synergy. Accordingly, the reduction of the atovaquone dose in the subsequent experiment revealed the expected synergistic interaction.

Canfield *et al.* (1995) also reported differences between interaction classifications in their preliminary data (48 h) and their more detailed experiments (72 h). However, they attribute these differences to changes in the treatment regime and the solubility of atovaquone rather than the shift to a 72 hour treatment period. The findings presented here are contradictory to those of Fivelman *et al.*, (2004), who showed the atovaquone proguanil combination to be synergistic within a 48 hour treatment period using the hypoxanthine incorporation method, indicating that the problem was not related to the drug killing profile but the growth detection method used. Indeed Wein *et al.*, (2010) suggest that while the hypoxanthine incorporation method can be used at 48 h, the SYBR green-based methods require a 72 hour treatment period to obtain accurate data, suggesting that the read out is affected by drug mode of action. A further issue is that despite the correct identification of a synergistic interaction at the ED<sub>50</sub> level, at the ED<sub>75</sub> and ED<sub>90</sub> levels of inhibition the combination was deemed slightly antagonistic and antagonistic respectively. Such an outcome is unlikely considering the effectiveness of the combination in the field. Another variable must, therefore, be confounding the data at the higher doses. One possibility is that inhibition incurred by highest concentration of acetonitrile: water solvent influenced the interaction outcome. Notably, additional growth inhibition was not observed after dose point F which is in fact comparable with the highest dose used in the previous experiment where no inhibition was observed. Another possibility is that dead parasites, or those committed to dying, are being detected as live. It is likely that the amount of intact DNA, detected by the SG-FCM, is affected directly or indirectly by drug mechanism of action (Wein *et al.*, 2010). This notion is supported by the observations that no drug dose used in

the study achieved 100% inhibition and different drugs plateau at different levels of inhibition, with the combination mirroring the most DNA degrading of the two compounds. In order to determine whether the combination is in fact antagonistic at high doses, the parasites were treated with a high constant concentration of one drug in combination with a dose range for the second drug ( $IC_{25}$ ,  $IC_{50}$  and  $IC_{75}$ ). Lower constant doses were also included for comparison. Despite the finding that dose dependency effect was more pronounced in combinations with the lower constant concentrations, a trend was still apparent with the higher constant concentrations. The data consistently showed that further effects can be achieved by the addition of a second drug no matter what the concentration of the first. Although the effects are not huge they are not indicative of a strongly antagonistic interaction. Again inhibition did not exceed 90% indicating the possibility of 10% background effects. In order to determine whether the parasites are dead or committed to dying, parasite recovery and regrowth was monitored. In the replica experiment after 72 h of treatment the drugs were removed, parasites were subjected to a limiting serial dilution and allowed to recover for a further 17 days. The assumption being that if the drugs are antagonistic then recovery/growth should be higher in the combinations than in the singly treated controls. Interestingly, despite showing some remaining live parasites after 72 hours of treatment, none of the parasites recovered once the drug combination was removed during the regrowth period. Although after 72 hours the highest dose of proguanil achieved nearly the same level of inhibition as the combination singly treated parasites were able to recover (after 17 days) whilst those subjected to the combination were not. Taken together the data indicates that the combination is not antagonistic at high doses. Data from the SG-FCM assay at higher levels in inhibition should be viewed with caution as background interference likely. Furthermore, the variations at what level of inhibition each compound plateaus appear to be dependent on intrinsic mode of action, inferring that different drugs will affect the SG readout differently.

#### *6.4.3 CalcuSyn analysis of emetine with existing antimalarials*

Three existing antimalarials: dihydroartemisinin, chloroquine and atovaquone were investigated for their interaction with emetine. After 72 hours of incubation the DHA-Eme interaction was classified as antagonistic which is contradictory to the initial findings at 48 hours which were nearly additive/slight antagonism, moderate antagonism and antagonism. Given the slow killing profile of emetine (Chapter 5) it is likely that the 72



hour data is more accurate and the compound needed more time to antagonise the faster acting DHA component. A discrepancy also arose between the shape of the median effect curve as indicated by unparallel and parallel lines for each of the drugs at 48 and 72 hours respectively. Parallel lines are indicative of a similar killing profile inferring a similar mode of action. However this would be contradictory to the extensive killing profile data obtained for emetine in Chapter 5. The variation between the two time points presented here implies that a timing issue and the misinterpretation of dormant and dead parasites by SG-FCM may have confounded the current data. The suggestion that emetine has a similar killing profile to atovaquone and possibly a mitochondrial mode of action is corroborated by the interaction data presented here as artemisinin atovaquone combinations have also been defined as antagonistic elsewhere (Fivelman *et al.*, 2004; Vivas *et al.*, 2007). There is a possibility that the mode of action of these compounds overlap particularly as both emetine and artemisinin have been predicted to have multiple targets in malaria. Amongst numerous theories that have been put forward for the mechanistic actions of artemisinins one has implicated the involvement of the mitochondria electron transport chain as a source of reactive oxygen species (Haynes and Krishna, 2004; Mercer *et al.*, 2011; Krungkrai *et al.*, 2010; Wang *et al.*, 2010). It is evident that the predominant actions differ due to the differences in their speed of kill (chapter 5). The data infer that it is unlikely that emetine will be a good combinatorial candidate for ACT.

The interaction between chloroquine and emetine was shown to be antagonistic and antagonism between CQ-ATQ has been also reported elsewhere (Gorka *et al.*, 2013). Some authors suggest that antagonism implies action on the same target. However like emetine, chloroquine has also been used previously to treat amoebiasis and in this protozoan parasite the drugs were found to act on different parasite targets. Chloroquine was shown to inhibit DNA synthesis in the vegetative forms of the parasite while emetine killed the trophozoite stage by inhibiting protein synthesis (Bansal *et al.*, 2004). The lack of parallel trend lines on the median effect plot also infers a difference in mode of action. One possibility is that in both cases of antagonism (DHA-Eme and CQ-Eme combination) there is some overlap in the death progression phenotypes incurred by direct or indirect actions of the multiple-targeted compounds.

The interaction between atovaquone and emetine was classified as synergistic (ED<sub>50</sub>) and mildly antagonistic (ED<sub>75</sub> and ED<sub>90</sub>). Indeed other studies have reported sporadic cases of antagonism in combinations that are otherwise synergistic (Mariga *et al.*, 2005). Due to the

previous issues at high levels of inhibition it is however likely that background effects are responsible of the contrary classifications in the current investigation. Due to the pharmacokinetic matching of the compounds (Chapter 5), the synergistic outcome presents an exciting option for antimalarial therapy. The similarity in the killing profiles of atovaquone and emetine suggest both drug may be acting on different targets in the mitochondria, thus working together to potentiate drug action (Sanz *et al.*, 2102; Zimmermann *et al.*, 2007). For emetine the most likely mitochondrial target is protein synthesis in the mitochondrial ribosome. Such theories would require a more detailed inquiry and cannot be deduced from the data presented here. Clearly, further investigations will be needed to establish whether the combination will be efficacious *in vivo*.

#### 6.4.4 Conclusion and future directions

Taken together the data presented here provides support that the CalcuSyn constant ratio method offers a more standardised, simple, reliable user friendly alternative to the checkerboard and fixed ratio methods to analyse antimalarial drug interactions. One potential drawback is that in a single experiment only one ratio is analysed. However other studies have used the method to evaluate different fixed ratios (Corral *et al.*, 2014; Feng *et al.*, 2009). In the current study, drug ratios were based on pre-defined IC<sub>50</sub> values which presented huge ratio variations due to the differential potency of the different compounds. Some studies base ratios on mass while others use IC<sub>50</sub> information (Keiser *et al.*, 2011; Hu *et al.*, 2010). The ratio of the compounds *in vivo* will most likely be affected by pharmacokinetics and pharmacodynamic aspects of the individual compound, making the selection of an appropriate ratio at the *in vitro* level difficult. For this reason, either a wide range of ratios should be tested or basic interaction data could be obtained initially, then further characterised once more detailed information on *in vivo* pharmacokinetic profile of a drug candidate becomes available. In most cases different ratios present different interaction classifications (Harasym *et al.*, 2010), however, the value of identifying desirable interactions is redundant if such ratios cannot be achieved in the *in vivo* situation. Despite being validated as reliable (Co *et al.*, 2009), the current study also highlighted issues with the SG-based methods for analysing drug interactions, particularly at high levels of inhibition. It is likely that other viability assays are also affected by drug mode of action and as a result attribute erroneous classification to drug combinations. It is probable that such issues are responsible variations in interaction classifications reported in the literature. For this reason, it may be a better option to analyse drug interactions based on

lethal dose inhibition. This could be achieved by removing the drug after 72 hours of exposure and analysing parasite re-growth after an extended recovery period (Gorka *et al.*, 2013; Painter *et al.*, 2010; Sanz *et al.*, 2012). As parasite killing is the ultimate goal, such modifications to the current protocols should provide better *in vitro* to *in vivo* translation.

Overall findings of the current study indicate that emetine dihydrochloride hydrate should be considered as a viable antimalarial candidate and should be progressed for more detailed *in vitro* and *in vivo* analyses. Further work is needed to establish whether the compound is suitable for use as a partner drug with atovaquone. Failing that, other combinatory options with other repositioned compounds could be explored. Further work should aim to evaluate the combinatorial potential of less toxic derivatives of the molecule, such as dehydroemetine, providing the antimalarial potency is comparable. In the current climate of malaria drug discovery it is vital that such potentially valuable candidates are taken forward and not overlooked or summarily discarded.

## CHAPTER 7

---

### GENERAL DISCUSSION

This study has investigated drug repositioning as a fast-track option for antimalarial drug discovery. In doing so, the work has provided information in greater detail regarding the use of SYBR Green methods for antimalarial drug susceptibility and characterisation assays. The findings of this work have further highlighted the issues concerning current *in vitro* practises for antimalarial drug development, to which alternatives, that may offer better *in vitro* to *in vivo* translation, have been proposed. Drug repositioning, as an option for antimalarial drug discovery, shows promise. From a screen of ~700 bioactive compounds, novel antimalarial drug classes inhibitory towards the multidrug resistant strain K1, have been identified. Additionally, the work has added to the understanding of the selected hit compound, emetine dihydrochloride hydrate, and its action against the malaria parasite, through characterisation of its killing profile and drug interaction analyses. One issue with the antimalarial development of the compound was the concern regarding dose-related toxicity. Data from the current study has presented a solution to the problem through combination with atovaquone. In addition to the other benefits of combination therapy, such as an obstacle to resistance development, the synergistic interaction between emetine and atovaquone, revealed here, would permit further dose reductions of the repositioned compound. Some preliminary indications about the parasite targets of the emetine have also been ascertained.

#### *7.1 SYBR Green-based methods for antimalarial drug screening and development*

##### *7.1.1 SYBR Green-based methods for drug susceptibility*

Since 2009 there has been a growing body of evidence implicating the use the DNA stain, SYBR Green 1, for determining malarial parasite viability in response to drug treatment (Bacon *et al.*, 2007; Johnson *et al.*, 2007; Karl *et al.* 2009; Vossen *et al.*, 2010). The reliability of the SG-based methods was confirmed in the current study, by good conformity with the traditional Giemsa microscopic test. Corroborating the findings of Wein *et al.* (2010), further interrogation revealed that it is important to monitor and control the parasite stage in relation to the drug treatment time-course. Although Wein *et al.* (2010) suggest a 72 hour treatment period is required to obtain reliable results with the SG assays, we show that a 48 hour treatment may also be used, providing that, it spans schizont rupture, re-invasion and entry into the subsequent erythrocytic cycle. However,

when drug action and speed of kill is unknown, a 72 hour treatment period, initiated at ring and analysed at trophozoite stages, may be the best option to permit the action of slower acting antimalarials and ensure that parasites are fully established in the subsequent erythrocytic cycle at the time of analysis.

In the current study, issues also arose concerning background fluorescence in the SG-MicroPlate method, for which complete media, containing albumin, was found to be responsible. This issue has not been commonly reported in the literature and was not particularly problematic for dose response curves where staining is relative and a trend, rather than absolute values, is expected to be observed. However, washing steps to remove to complete media were necessary to obtain reliable results from the screening of drug libraries, where parasitaemia can be reduced to minimal amounts and thus, is easily confounded by background effects. Whether this issue is specific to the Albumax used in the current study is unknown. Plouffe *et al.* (2008) also briefly mention issues with Albumax that result in a small protein shift of fluorescence. Yet other studies that have used human serum to supplement the media, have reported the dilution SYBR Green with complete media (Gorka *et al.*, 2013).

#### 7.1.2 SYBR Green-based methods for drug interaction analysis

The use of SYBR Green 1 for drug interaction analysis has also been evaluated more recently in the literature (Co *et al.*, 2009; Gorka *et al.*, 2013). These studies adopted a 96-well plate reader method for the analysis, and reported no issues with background effects. Using an unsynchronised culture Gorka and colleagues adopted a 48 hour treatment regime, and analysed the IC<sub>50</sub> and LD<sub>50</sub> levels of inhibition to consider cytostatic and cytotoxic effects respectively. The study did not include analysis of known antimalarial drug combinations, making it difficult to determine reliability and draw comparisons with the current data. In contrast, Co *et al.* (2009) used a 72 hour treatment period and replicated antimalarial drug combinations with known interaction outcomes. This showed that such classification could be obtained using the SYBR Green method. As interaction data for the ED<sub>75</sub> and ED<sub>90</sub> levels of inhibition are not presented by Co *et al.* (2009) the ED<sub>50</sub> classification reported here, using the more accurate SG-FCM method and the interaction analysis software CalcuSyn, was in agreement with their findings at the IC<sub>50</sub> level of inhibition. This, and the correct assignment of synergy to the known atovaquone-proguanil combination in the current study, served to validate the use of CalcuSyn as a reliable automated determinant of antimalarial drug interaction classifications.

Unfortunately, the value of using such as system was slightly concealed in the current study by interference of inherent drug-mode-of-action factors with the SYBR Green detection of live parasites. Firstly, a 72 hour time-course was necessary to detect synergy between atovaquone and proguanil using SG-FCM. Secondly, antagonism was incorrectly assigned to interactions at ED<sub>75</sub> and ED<sub>90</sub> levels of inhibition (not considered in the previous studies), as confirmed by an extended regrowth assay. It is likely that this issue is not limited to the SYBR green assay, and is probably common to all drug susceptibility assays. Indeed, readouts such as the measurement of metabolic parameters can commonly be uncoupled from parasite viability and are differentially affected by drug mode of action (Sanz *et al.*, 2012 and Wein *et al.*, 2010). In these cases two inverse misinterpretations may arise: (1) cytostatic parasites may be considered dead, even though they are capable of resuming productive growth once the drug has been removed, (2) parasites may be considered alive, although already committed to death, after exposure to a cytotoxic compound that induces a delayed death profile (Sanz *et al.*, 2012).

### 7.1.3 Conclusions and future directions for drug susceptibility assays

Taken together, the data presented here provides a greater understanding of SYBR Green determination of parasite viability and how the readout can be affected by drug mode of action. Clearly, appropriate treatment regimens for the different drug susceptibility assays available, should be adopted and standardised between groups using the same assay, so that reliable comparisons can be drawn. Although the currently available *in vitro* assays are sufficient for identifying compounds with antimalarial activity, drug mode of action and, particularly, speed-of-kill should be considered during more detailed *in vitro* characterisations. The necessity of combination therapy has meant that underlying issues with current *in vitro* drug susceptibility assessment practises have transposed into the interaction assays where, as highlighted by the current study, the relationship between drug mode of action and viability readout becomes more problematic.

Inconsistent definitions in the literature call in to question the reliability of the available drug interaction data and provide a possible explanation of poor *in vitro* to *in vivo* translation (Abiodun *et al.*, 2013; Bhattacharya *et al.*, 2009; Fivelman *et al.*, 2004; Keiser *et al.*, 2012; Synder *et al.*, 2007). For this reason, it may be necessary to reevaluate assay design for determining antimalarial drug interactions. Evidently, investigations using the SG-based methods for drug interaction analysis should adopt a 72 treatment regime. Such screening assays should be considered preliminary interaction data and ED<sub>75</sub> and ED<sub>90</sub> data

in particular should be viewed with caution. As the killing of parasites is the ultimate goal, future work should explore the possibility of adopting an interaction assay based on the cytocidal effects of drugs. Gorka *et al.* (2013) considered drug interactions based on cytocidal activity, however, the analysis was completed after 48 hours. The current data suggest that these outcomes may have been differentially conflicted by drug mode of action. Analysing parasite viability following a longer regrowth period (limiting serial dilution), in the absence of drug pressure, would serve to eliminate the disconnection between the susceptibility assays and parasite viability. This design may provide better predictions about *in vivo* drug interaction outcomes. Such intensive investigations may limit the practical number of testable drug ratios. Indeed, one limitation of the CalcuSyn method is that repeated experiments are needed to test different drug ratios, as the software is compatible only with the input of a single fixed ratio dose series. Non-constant ratios can be inputted manually, but the procedure is time consuming. Undoubtedly, the current situation, where different groups report different classifications justified by the use of different drug ratios, is not acceptable and poorly serves the goal of prioritising candidates for further development. Selecting the optimum ratio that would be achievable *in vivo* may be better informed by *in vivo* pharmacokinetic data. This idea is in agreement with the most recent proposal of the antimalarial drug development pipeline. Indeed, rather than being linear, the ideal lead optimisation phase involves a feedback loop between *in vitro*, *in vivo*, toxicology and pharmacokinetic studies (Figure 7.1).

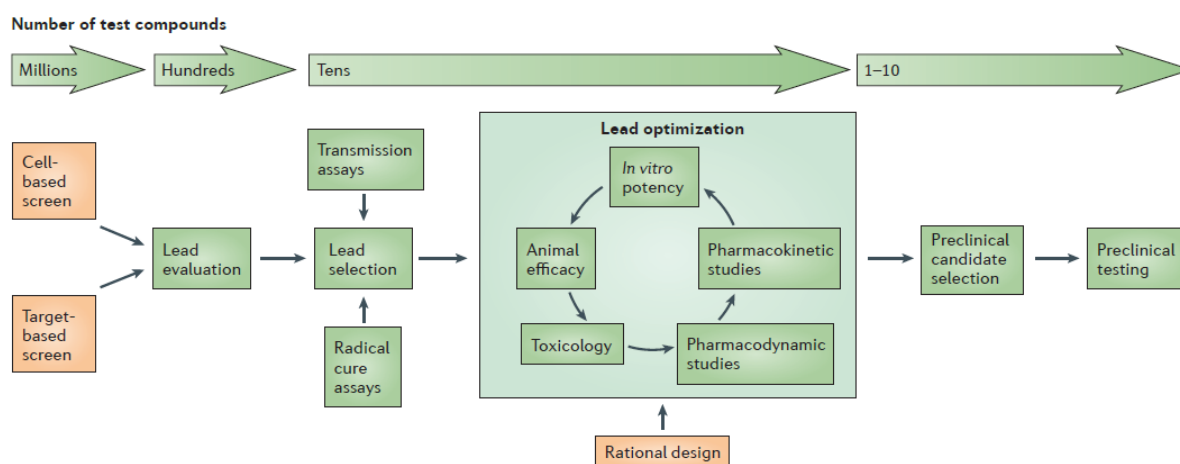


Figure 7.1 Drug development strategy for novel antimalarial drugs (Source Flannery *et al.*, 2013)

## 7. 2 Drug repositioning for malaria

A more systematic version of the traditional serendipitous approach to drug discovery was used in the current study to identify novel antimalarial leads (Medina-Franco *et al.*, 2013). Compound libraries (ENZO and LOPAC), with known bioactivities and a high degrees of drug likeness, were phenotypically screened against *Plasmodium falciparum* red blood cell stage malaria. From the screen of < 700 compounds more than 50 were shown to inhibit parasite growth by 50% at a concentration of 2.5  $\mu$ M. A particularly high hit rate (9.5 %) when compared with other, less focused, library screens. Corroborating the growing body of literature on similar screening initiatives, MeSH categories, namely: anticancer, antipsychotic and antibiotics were the most commonly re-identified antimalarial inhibitors in the screen (Gamo *et al.*, 2010; Lotharius *et al.*, 2014; Plouffe *et al.*, 2008; Weisman *et al.*, 2006). Identification of existing antimalarials and other previously reported hits such as emetine and propafenone, further confirmed the reliability of the results obtained. As the ENZO library was screened blindly, the compound overlap, particularly, with a liver-stage screen completed by Derbyshire *et al.* (2012) was initially unknown, but served to validate commonly identified hits as multi-stage, multi-strain inhibitors. Indeed, in addition to the activity of clemastine (over-the-counter anti-histamine) reported against liver-stage parasites Derbyshire *et al.* (2012) also reported activity of the compound in blood-stage screens against *P. falciparum* strains 3D7 and Dd2. The current study provided further corroboration, and demonstrated activity (< 500nM) against the multidrug resistant K1 strain. Other liver stage-active compounds, telmisartan (Angiotensin receptor blocker) and ketanserin (Serotonin receptor antagonist), were also identified as K1 inhibitors. Conversely, Derbyshire *et al.* (2012) showed telmisartan to be inactive against 3D7 and Dd2 erythrocytic stages at a concentration of 5  $\mu$ M. Interestingly, the group also showed that analogues more specific for the human angiotensin II receptor target than telmisartan, were less active against the parasite. This suggests that off-target effects may be responsible for the activity of repositioned compounds in their novel indication (Derbyshire *et al.* 2012). The current study, therefore further validated the MeSH categories detailed above, specifically the antihistamines and antiarrhythmic compounds, as potential starting points for novel antimalarial drug classes. Furthermore, antimalarial potencies against the multi drug resistant K1 strain were consistent with the criteria (< 1  $\mu$ M) outlined by MMV (Lotharius *et al.*, 2014). This provides evidence that small-scale focused screens against the whole parasite can identify valuable antimalarial hits. These



hits, through their occupation of diverse chemical space compared to existing therapies, offer the potential of much needed novel antimalarial targets.

### 7.2.1 Conclusions and future directions for antimalarial drug repositioning

This study along with the fast pace of development of some of the early identified candidates supports drug-repositioning as a valuable strategy of antimalarial drug discovery (Guiguemde *et al.*, 2010; Guiguemde *et al.*, 2012). The whole parasite, phenotypic screen presented here has permitted the identification of antimalarials with, potentially, multiple parasite targets. Furthermore, the compound classes that have been shown to be active against liver-stage parasites (Derbyshire *et al.*, 2012) and have been re-confirmed, by the current study, as inhibitors of blood-stage, K1, multiple drug resistant parasites, would be valuable assets to the eradication agenda. Future work should therefore focus on lead optimisation of the novel antimalarial classes identified in the current screen and elsewhere. The expansion of publically available antimalarial screening data should permit wide scale *in silico* analysis to determine structure activity relations and therefore help further inform structural modifications.

### 7.3 Antimalarial activity of emetine dihydrochloride hydrate

Before this study, the antimalarial activity of emetine had been established (Andrews *et al.*, 2014; Lucumi *et al.*, 2010; Plouffe *et al.*, 2008) but, hindered by concerns over possible toxicity and the identification of other attractive options, the compound was not considered for further development. However, a literature survey revealed the potential of a clinically more promising dose-related toxicity profile when antimalarial potency was compared with *in vitro* *Entamoeba histolytica* inhibitory concentrations (Bansal *et al.*, 2004). Furthermore, the existence of the safer dehydroemetine alternative and the informative structural activity relationships between emetine and its natural analogs, shown here by shifts in antimalarial potency and HepG2 cellular toxicity of emetine and cephaeline, provide a good platform for derivatisation of the compound. Taken together with its high potency against the multiple drug resistant *P. falciparum* K1 strain the antimalarial potential of the compound warranted further investigation.

Detailed characterisation of emetine revealed a similar killing profile to the existing antimalarial atovaquone (Sanz *et al.*, 2012). Like atovaquone, emetine displayed initial cytostatic activity during a 48 hour lag phase. Once parasite killing was initiated, at which point the drug induced effects have become irreversible, the PRR (the decrease in viable

parasite over 48 hours) and PCT (the time taken to clear 99.9% of a parasite population) were also similar to atovaquone. Compounds with similar killing profiles, it is suggested, have similar modes of action (Sanz *et al.*, 2012). As atovaquone acts *via* the parasite mitochondria (Srivastava and Viaidya, 1999), mitochondrial depolarization in response to both compounds was evaluated. Again, parasites responded similarly to emetine and atovaquone drug pressure, but both compounds were not as effective at inducing loss of mitochondrial membrane potential as the CCCP positive control. This may be attributable to the assaying time-course. A notable difference was that parasitaemia, as determined by SG staining, was slightly reduced in the emetine treated sample but not the atovaquone sample. As emetine has also been shown to bind to the cytosolic 80s ribosome, predicted to be a fast-acting drug target (Wong *et al.*, 2014), it is likely that the mitochondrion is not the only target of emetine in the parasite. Indeed, a rather broad spectrum of biological activities has been reported in the literature (Akinboye and Bakare, 2011). Although the mitochondrial action of atovaquone has not been associated with parasite apoptosis, emetine has been linked to the induction of apoptosis phenotypes in both trypanosomes and cancer cells (Boon-Unge *et al.*, 2007; Rosenkranz and Wink, 2008). Despite the fact it is more difficult to define the mode of action of multiple-targeted drugs, the potential of such a compound to help circumvent resistance development is obviously advantageous for antimalarial therapy.

Through drug interaction analysis with CalcuSyn, optimised for malaria in the current study using SG-FCM, the ED<sub>50</sub> level interactions between emetine-dihydroartemisinin, emetine-chloroquine and emetine-atovaquone were classified as antagonism, antagonism and synergism respectively. Data from the ED<sub>75</sub> and ED<sub>90</sub> levels of inhibition were not considered reliable due to background interference and possible misidentification of live parasites differentially affected by an intrinsic drug mode of action, as discussed above. However, the synergistic interaction between the pharmacokinetically similar atovaquone and emetine compounds provides an exciting opportunity for antimalarial therapy. If the combination is found to be efficacious *in vivo*, the other advantages of combination therapy, such as prolongation of use before resistance development and the potential for a reduction in the required emetine dose, will have beneficial implications for the toxicity profile of the drug.

### 7.3.1 Conclusions and future directions for the antimalarial development of emetine

The preliminary indication of a synergistic interaction between atovaquone and emetine is presented here for a single drug ratio of (IC<sub>50</sub>: IC<sub>50</sub> dose ratio ATQ: Eme= 1: 46) at the ED<sub>50</sub> level of inhibition and would need to be clarified for other ratios. Given the potentially infinite number of ratios that could be tested in further *in vitro* investigations, this could be considered following additional *in vivo* pharmacokinetic data being made available about the compound, as was proposed above.

Most importantly, to further progress the evaluation of emetine and its related analogues as a novel antimalarial class, the compound or its derivatives need to be defined as being safe antimalarial options. In terms of the common emesis issue, drug formulation and novel delivery systems may help avoid irritating side effects (Allen and Cullis, 2004). To alleviate the more serious, yet less common cardiotoxic adverse events, cardiotoxicity should be evaluated using modern techniques. Information about cardiotoxicity should be gathered for natural and synthetic emetine derivatives, in particular dehydroemetine, alongside antimalarial potency evaluation, to inform useful structural modifications of the compound. Advances in *in vitro* cardiotoxic assessment assays has meant that patch clamp techniques, to determine the electrophysiology of cells in response to drug treatment, can be used for single ion channel analysis (Kang, 2001). One important channel, encoded by the human ether a-go-go related gene (hERG), is a common attrition hurdle for a number cardiotoxic compounds and would therefore serve as a good starting point for cardiotoxic evaluation (Recanatini *et al.*, 2005). Subsequently, more intensive *in vitro* investigations, such as the microelectrode array (MEA) which is considered the *in vitro* ECG equivalent could be used to evaluate whole-cell ion channel effects (Kang, 2001). Other *in vitro* tests use biomarkers to determine cardiac hypertrophy or cardiac damage (Dinh *et al.*, 2011). The results of these evaluations might be used to select or engineer an optimised form of emetine.

In parallel to drug development, the mode of action of the drug should be further investigated. In addition to further work on mitochondrial depolarization, other features of parasite apoptosis in response to emetine treatment might usefully be evaluated. Cryo-EM and structural modelling could be employed to confirm whether a binding site in the mitochondrial ribosome is an emetine target. Indeed, the mitochondrial toxicity in the parasite may be accompanied by cardiotoxicity in the mitochondria-dense heart muscle (Montaigne *et al.*, 2012). Thus, selectivity for parasite mitochondria should be determined.

The resulting optimised emetine derivative should then be re-combined with atovaquone to evaluate whether the moiety responsible for synergy has been retained. Furthering that, other combinatory options should be explored. In order to predict improved *in vitro* to *in vivo* translation, and overcome mode-of-action interference with existing susceptibility assays the results of the current study strongly suggests that interaction evaluation should be based on lethal dose concentrations, evaluated after an extended recovery period, as has been discussed above.

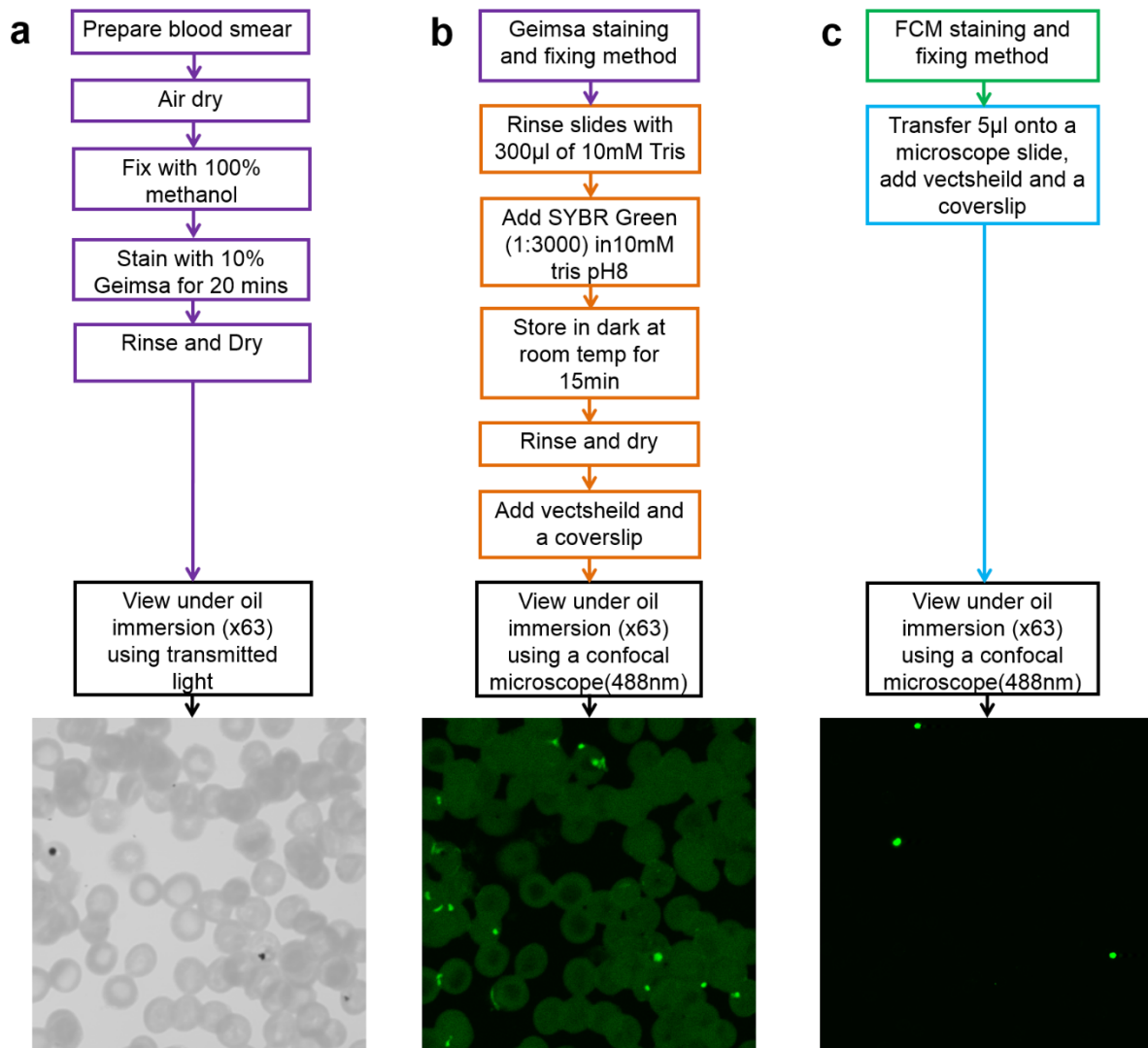
Given that the trajectory of artemisinin resistance is following the route of the previous antimalarial drug classes, and has already reached the Indian border (Tun *et al.*, 2015), it is imperative that repositioned hit candidates are taken forward to provide the much needed fast-track option to antimalarial drug development. The main successes of antimalarial chemotherapy has largely been reliant on natural products. Along with the two most effective drugs, quinine and artemisinin, the most recent compound to present a novel antimalarial drug target, atovaquone, is a synthetic version of the natural product lapichol (Flannery *et al.*, 2013). In emetine, we have yet another compound of natural origin with potent antimalarial activity and the possibility of multiple parasite targets. The antimalarial development of the compound is further supported by its potential for derivatisation and the pharmacokinetically-matched synergistic combination with atovaquone.

## APPENDIX

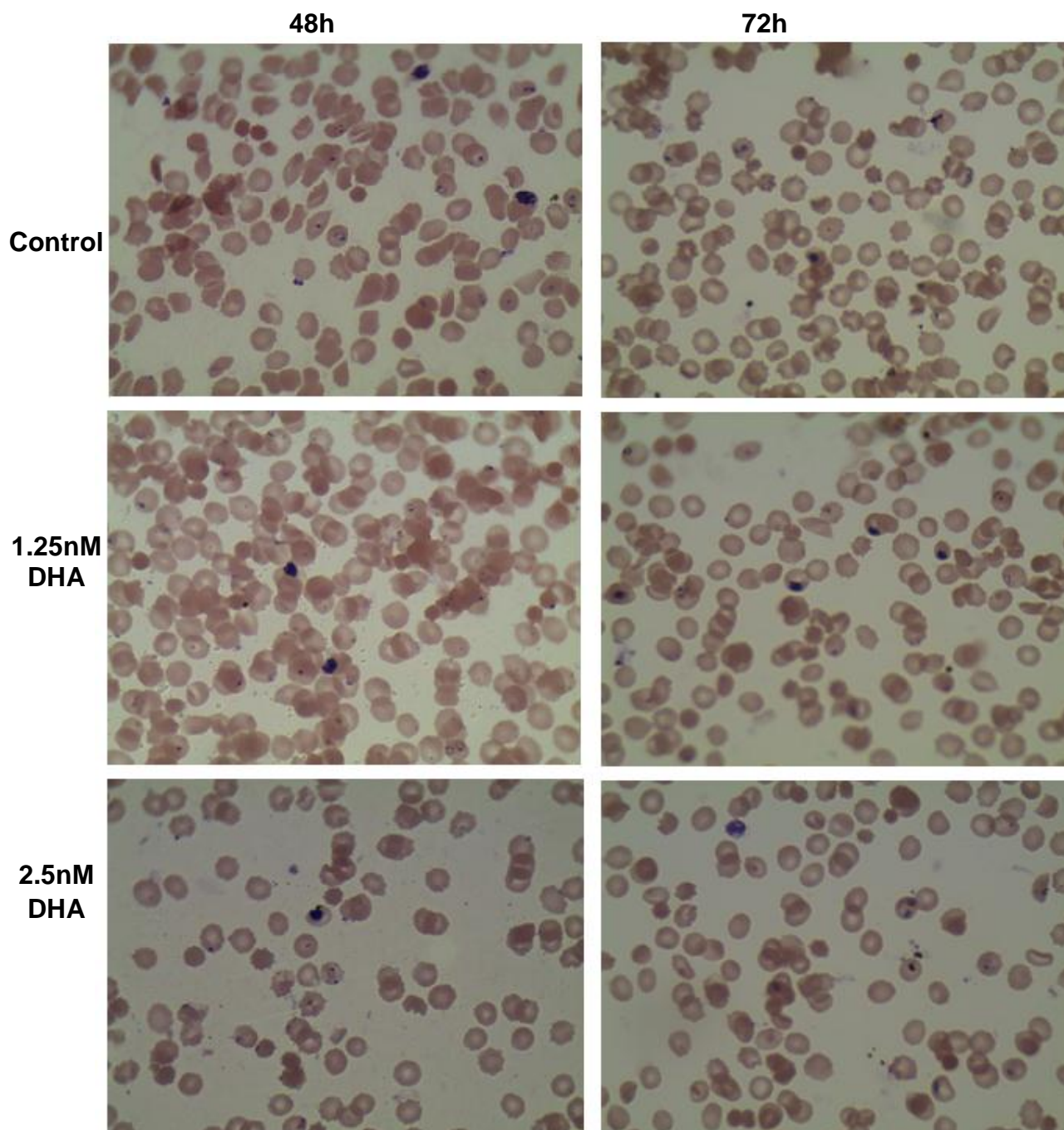
---

**Appendix I: SYBR Green staining of *P. falciparum* for fluorescence confocal microscopy.**

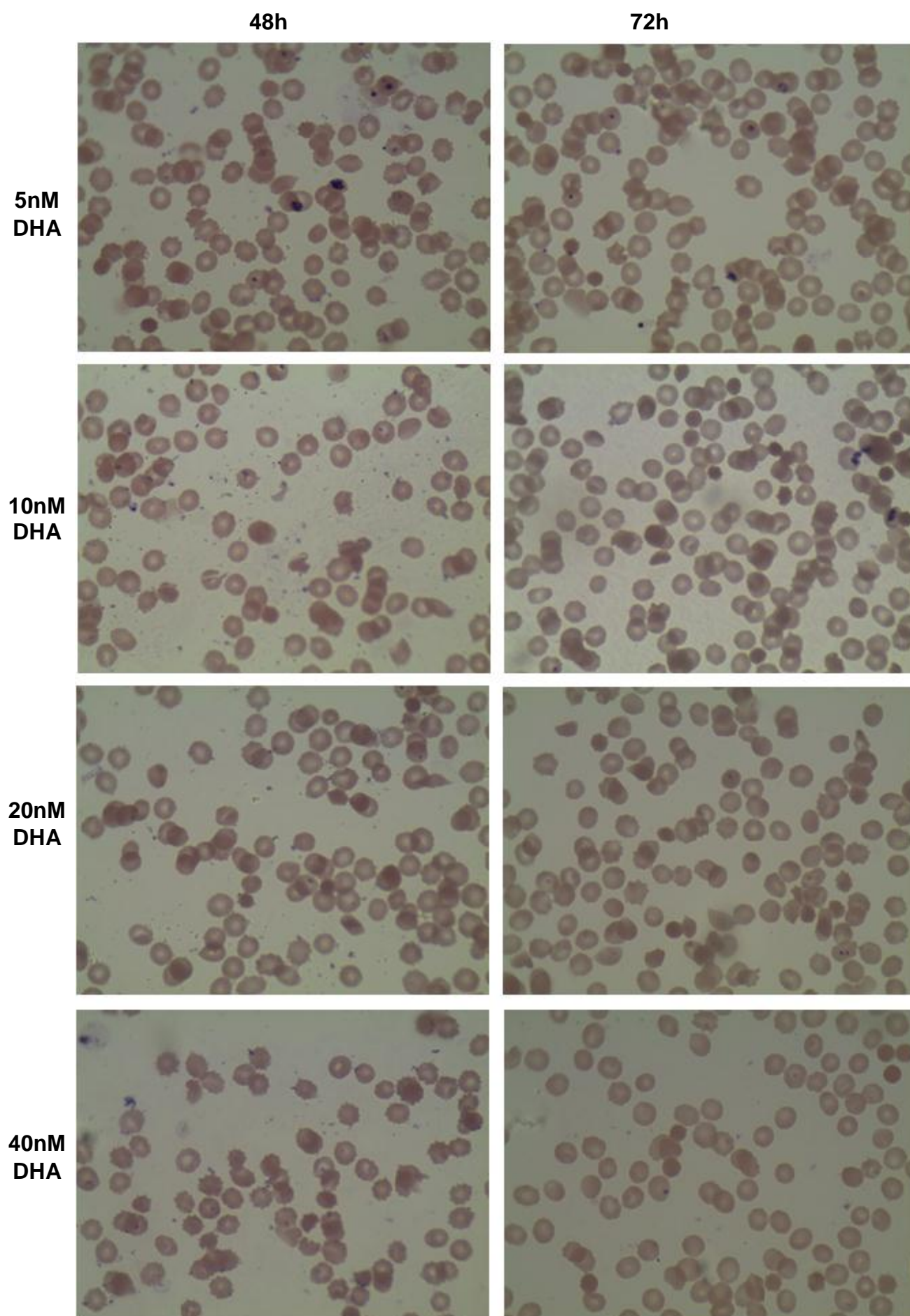
Shows three different methods used to stain and unsynchronised culture of *P. falciparum* (a-c) ; The traditional geimsa method (a) the traditional Giemsa method followed by SYBR Green 1 staining (Guy *et al.*, 2007) (b) and a novel FCM staining procedure. An example of the image produced by the each respective method is shown. Method (c) was most successful in reducing background fluorescence and was therefore selected for future experiments.



**Appendix II: An example of Giemsa stained *P. falciparum* parasites (strain K1) following treatment with dihydroartemisinin (DHA).** Images were taken for the control sample and each DHA dose used (from 1.25nM - 40nM DHA) to generate the dose response curve. Examples of both the 48 and 72h time points are included.



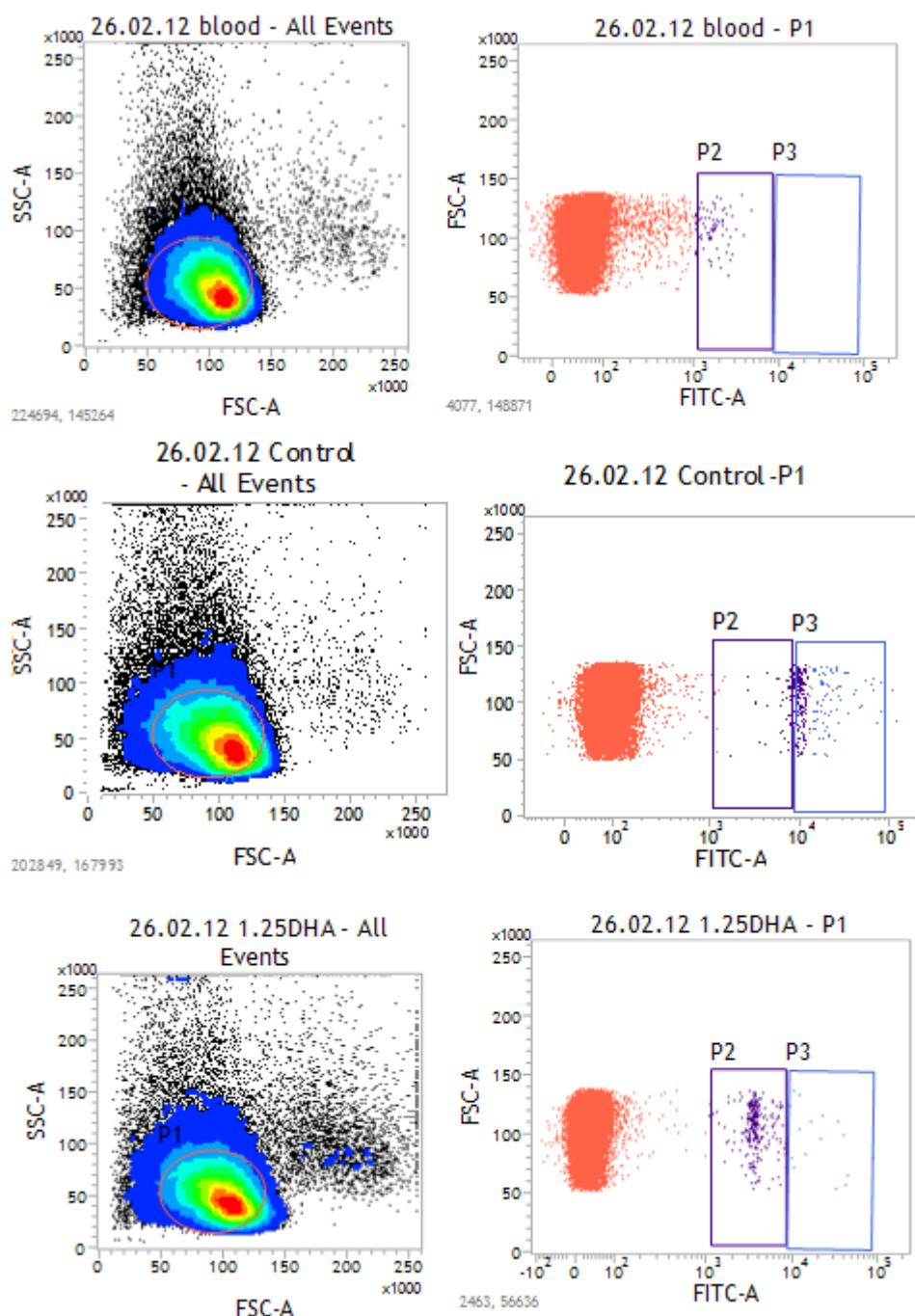


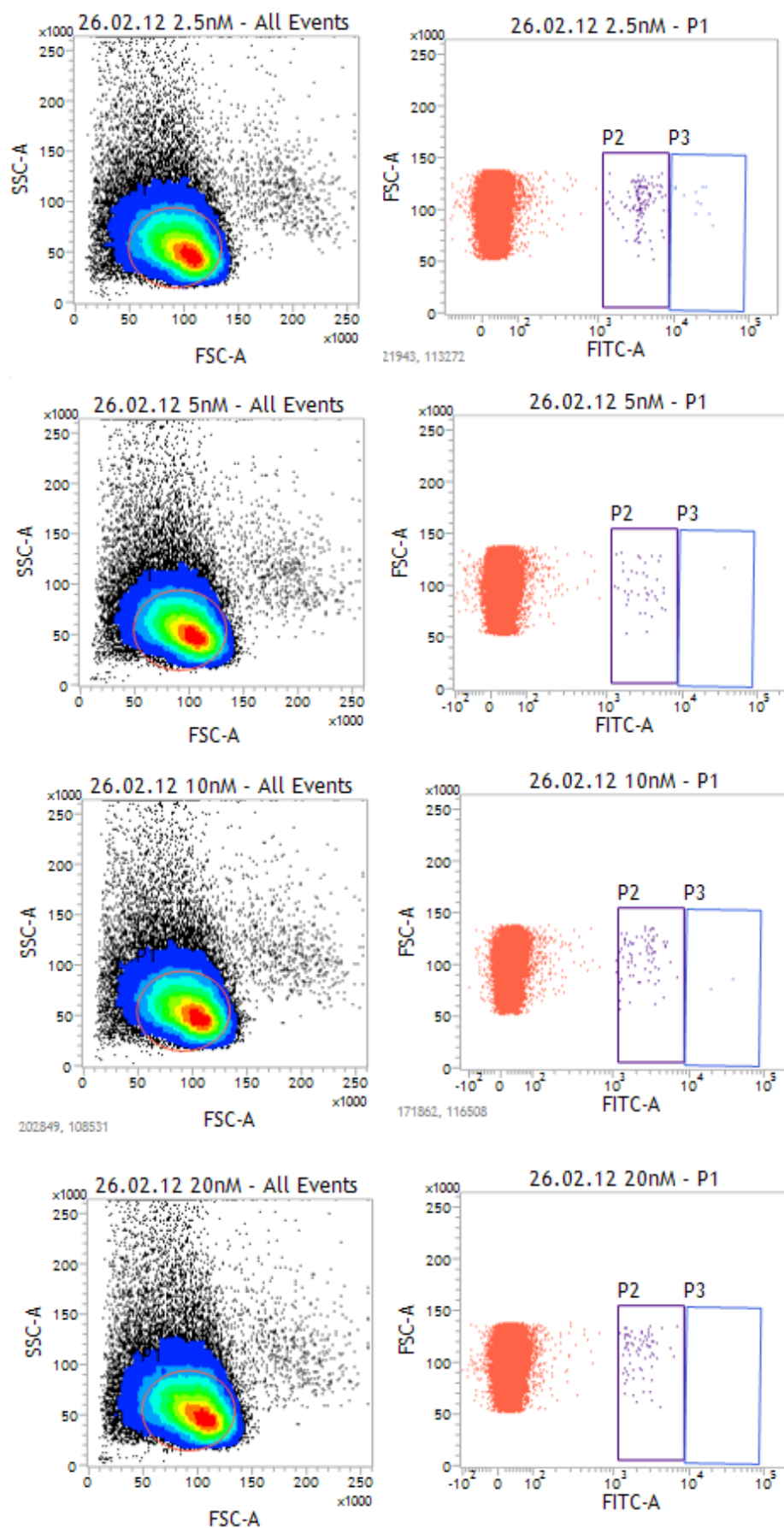




**Appendix III: An example of the flow cytometer output obtained during the generation of dose response curves, for dihydroartemisinin against *P. falciparum* strain K1, using the SYBR Green-based Flow cytometer method.** Images show density plots of forward scatter (size) against side scatter (granularity) and dot plots of FITC (SG fluorescence) against forward scatter. Tables show the statistical information recorded for each experimental condition. Data is shown for blood only (uninfected) and infected controls alongside each DHA dose used (1.25nM - 40nM DHA) for both the 48 and 72 h time points.

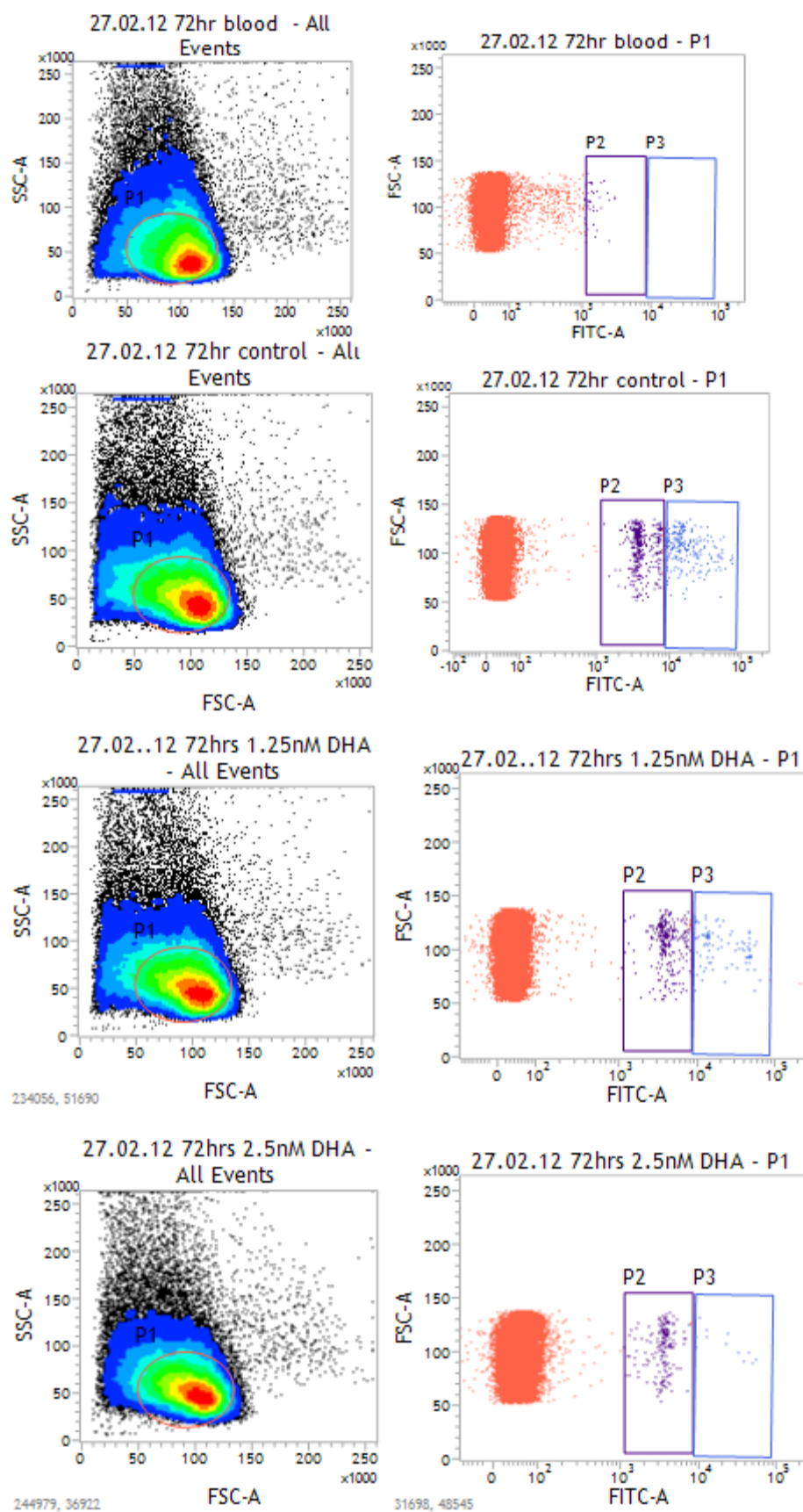
## 48 h

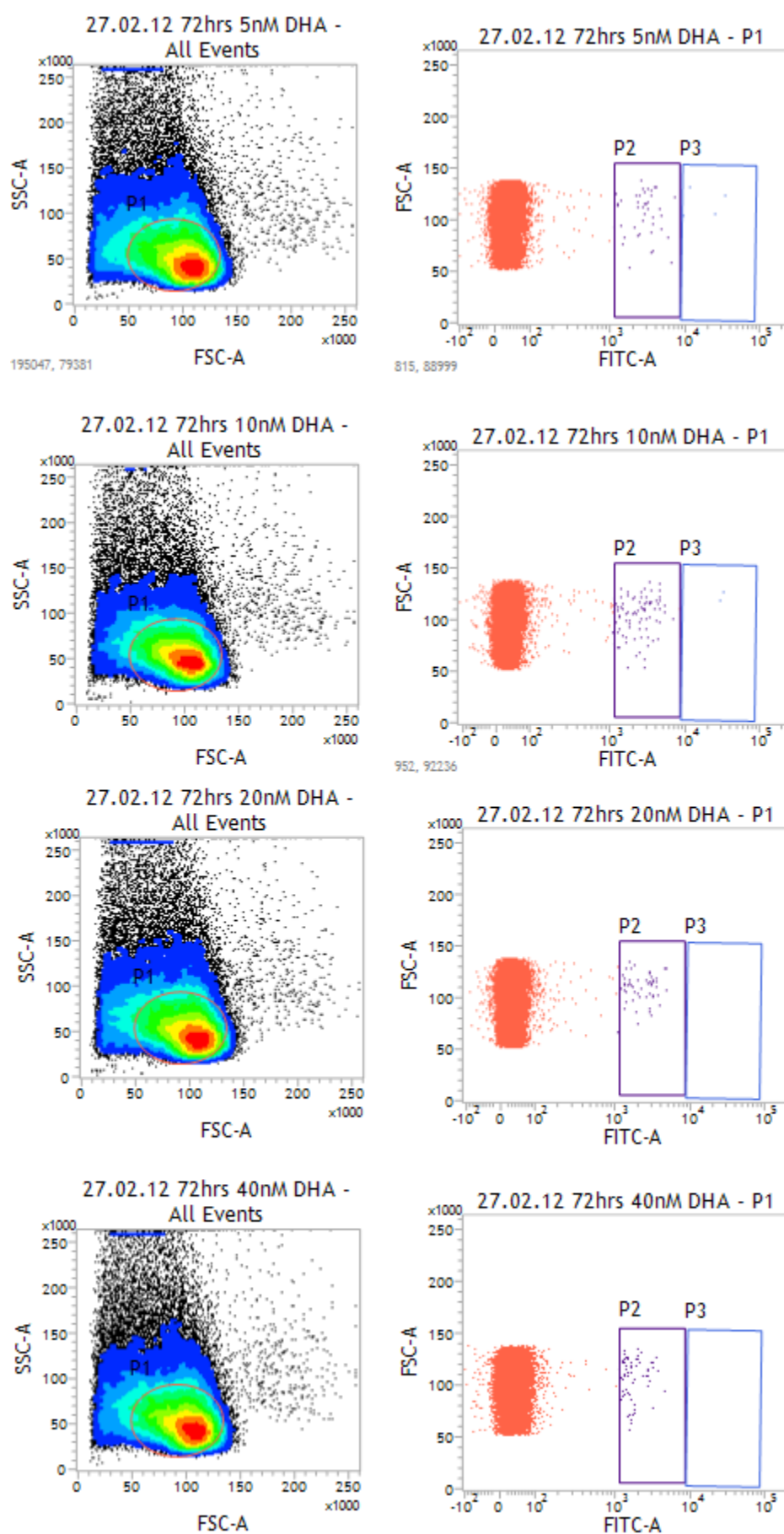




Population View				
✓ Show Population Statistics				
Name	Events	% Parent	% Grandparent	% Total
26.02.12 Control				
All Events	50,000	***	***	100.00
P1	36,355	72.71	***	72.71
P2	245	0.67	0.49	0.49
P3	72	0.20	0.14	0.14
26.02.12 blood				
All Events	50,000	***	***	100.00
P1	41,064	82.13	***	82.13
P2	83	0.20	0.17	0.17
P3	0	0.00	0.00	0.00
26.02.12 1.25DHA				
All Events	50,000	***	***	100.00
P1	37,262	74.52	***	74.52
P2	274	0.74	0.55	0.55
P3	18	0.05	0.04	0.04
26.02.12 2.5nM				
All Events	50,000	***	***	100.00
P1	39,267	78.53	***	78.53
P2	122	0.31	0.24	0.24
P3	13	0.03	0.03	0.03
26.02.12 5nM				
All Events	50,000	***	***	100.00
P1	40,383	80.77	***	80.77
P2	41	0.10	0.08	0.08
P3	1	0.00	0.00	0.00
26.02.12 10nM				
All Events	50,000	***	***	100.00
P1	39,798	79.60	***	79.60
P2	76	0.19	0.15	0.15
P3	2	0.01	0.00	0.00
26.02.12 20nM				
All Events	50,000	***	***	100.00
P1	38,551	77.10	***	77.10
P2	75	0.19	0.15	0.15
P3	0	0.00	0.00	0.00
26.02.12 40nM				
All Events	50,000	***	***	100.00
P1	38,192	76.38	***	76.38
P2	81	0.21	0.16	0.16
P3	0	0.00	0.00	0.00

72 h





Show Statistical Gates/Populations				
Gate Hierarchy				
<div> <div>All Events</div> <div> <div>P1</div> <div>P2</div> <div>P3</div> </div> </div>				
Population View				
Show Population Statistics				
Name	Events	% Parent	% Grandparent	% Total
27.02.12 72hr blood				
All Events	50,000	***	***	100.00
P1	32,890	65.78	***	65.78
P2	39	0.12	0.08	0.08
P3	0	0.00	0.00	0.00
27.02.12 72hr control				
All Events	50,000	***	***	100.00
P1	31,679	63.36	***	63.36
P2	368	1.16	0.74	0.74
P3	228	0.72	0.46	0.46
27.02.12 72hrs 1.25nM DHA				
All Events	50,000	***	***	100.00
P1	32,635	65.27	***	65.27
P2	276	0.85	0.55	0.55
P3	95	0.29	0.19	0.19
27.02.12 72hrs 2.5nM DHA				
All Events	50,000	***	***	100.00
P1	35,721	71.44	***	71.44
P2	172	0.48	0.34	0.34
P3	12	0.03	0.02	0.02
27.02.12 72hrs 5nM DHA				
All Events	50,000	***	***	100.00
P1	31,004	62.01	***	62.01
P2	45	0.15	0.09	0.09
P3	4	0.01	0.01	0.01
27.02.12 72hrs 10nM DHA				
All Events	50,000	***	***	100.00
P1	34,286	68.57	***	68.57
P2	83	0.24	0.17	0.17
P3	2	0.01	0.00	0.00
27.02.12 72hrs 20nM DHA				
All Events	50,000	***	***	100.00
P1	31,683	63.37	***	63.37
P2	55	0.17	0.11	0.11
P3	0	0.00	0.00	0.00
27.02.12 72hrs 40nM DHA				
All Events	50,000	***	***	100.00
P1	32,391	64.78	***	64.78
P2	64	0.20	0.13	0.13
P3	0	0.00	0.00	0.00

**Appendix IV: Percentage inhibition table for each compound from the ENZO library against *P. falciparum* strain K1 at a concentration of 2.5  $\mu$ M.** The SYBR Green-MicroPlate method was used to analyse parasite growth in response to drug treatment. Each estimate represents duplicate data. Background fluorescence from uninfected blood was deducted accordingly and % inhibition was calculated relative to untreated controls. The 56 most potent compounds are excluded from the table as they are shown in Chapter 4, Table 4.1.

Name	% inhibition <i>P. falciparum</i> strain K1
Triamcinolone	50.79
Levallorphan	50.64
Propranolol	50.30
Butoconazole nitrate	50.21
Manidipine	49.55
Fluperlapine	49.26
Naltriben methanesulfonate hydrate	48.81
Dihydroergotamine mesylate	48.73
Stanozolol	48.63
Oxatomide	48.57
Troglitazone	48.40
Diphenhydramine·HCl	48.28
Strychnine·HCl	47.83
Cinanserin	47.73
Alprenolol·HCl	47.57
Topotecan·HCl	47.31
Lapatinib ditosylate	47.24
Flecainide acetate	47.13
Gestrinone	46.35
Buphenine·HCl	46.27
Promethazine·HCl	46.02
amrinone	45.95
Bepridil·HCl	45.81
(R)-(-)-Apomorphine·HCl	45.80
Fluphenazine·2HCl	45.77
Etoposide	45.24
Clozapine	45.14
Pentamidine	44.97
Vardenafil	44.23
Astemizole	43.48
Sulbactam	43.44
Tylosin	43.40
Bupivacaine	43.16
Oxibendazole	43.00
Telenzepine·2HCl	42.91
Trans-triprolidine·HCl	42.88
Memantine·HCl	42.82
Tosufloxacin	42.81
Ifenprodil tartrate	42.43
Spiperone·HCl	42.17
Cimaterol	42.12
Tamsulosin	41.97
Mepyramine maleate	41.97
Olanzapine	41.97

Harmine	41.62
Tenoxicam	41.53
Ketotifen	41.06
Amantadine·HCl	41.01
Lidocaine·HCl·H <sub>2</sub> O	40.60
Tioconazole	40.55
(+)-Butaclamol·HCl	40.47
Terazosin	40.38
Auranofin	40.37
Amoxapine	40.17
Captopril	40.13
Tolbutamide	40.08
Dobutamine·HCl	39.93
Amoxicillin	39.91
Vidarabine	39.82
Atazanavir	39.40
Dipyridamole	39.37
Mianserin·HCl	39.25
Flufenamic acid	39.13
Alfuzosin	38.89
Acetylsalicylic Acid	38.42
Canthaxanthin	38.06
Chlorpromazine·HCl	37.67
Procainamide·HCl	37.25
Ramipril	36.94
Pentoxifylline	36.75
Cyproheptadine	36.74
Citalopram	36.59
Aripiprazole	36.55
Tetracycline	36.46
Spectinomycin·2HCl	36.37
Pergolide mesylate	36.19
Anagrelide	36.16
Tramadol	35.82
Rosiglitazone maleate	35.79
Glipizide	35.67
Succinylcholine	35.55
Remoxipride	35.00
Vecuronium	34.61
Nalbuphine	34.59
Phenytoin	34.38
Delavirdine mesylate	34.18
Phentolamine	34.14
Clonidine·HCl	34.03
Pilocarpine·HCl	33.82
Quetiapine Fumarate	33.51
Sparfloxacin	33.22
Ketoconazole	33.16
Nialamide	33.02
Clothiapine	32.73
Venlafaxine	32.69
Primaquine	32.67



Lincomycin	32.58
Loratadine	32.26
Pinacidil	32.08
Vitamin A acetate	32.07
Levocabastine·HCl	32.01
Dexamethasone	31.59
Sotalol·HCl	31.31
Naloxonazine	30.92
Imipramine·HCl	30.81
Tropicamide	30.79
Linezolid	30.53
Sulfadimethoxine	30.43
(R)-(-)-Deprenyl·HCl	30.34
Ethacrynic Acid	30.17
Calcitriol	30.15
Disodium Cromoglycate	29.76
Tolmetin	29.28
Bezafibrate	29.23
Oxacillin	28.86
Propranolol S(-)	28.71
Domperidone	28.63
Thalidomide	28.50
Xylazine	28.18
Guanabenz	28.18
Tobramycin (free base)	28.09
Leflunomide	27.95
Pancuronium·2Br	27.92
Enalaprilat	27.90
Temozolomide	27.79
Nelfinavir mesylate	27.61
Donepezil·HCl	27.60
Lacidipine	27.29
Prazosin·HCl	27.22
Propofol	27.00
Metoclopramide	26.78
Fosinopril	26.77
Cefepime	26.67
Pregnenolone	26.60
Amfebutamone	26.50
Zolmitriptan	26.16
Lovastatin	26.03
Iproniazid	25.92
Clindamycin·HCl	25.82
Amorolfine	25.82
Acitretin	25.70
Mecamylamine	25.63
Levamisole	25.62
Novobiocin·Na	25.41
Pantothenic acid	25.40
Isoniazid	25.23
Lobeline	25.21
Sildenafil	25.07

Amisulpride	24.89
Nimesulide	24.82
Oxiconazole	24.65
Oxotremorine	24.46
Physostigmine sulfate	24.45
Naloxone	24.42
Naltrindole-HCl	24.24
Indomethacin	23.97
Benzamil	23.91
Docetaxil	23.83
Tenatoprazole	23.80
Entacapone	23.58
Imipenem	23.45
Lorglumide	23.43
Latanoprost	23.24
Prothionamide	23.16
Cimetidine	23.12
Didanosine	22.90
Camptothecin	22.83
Escitalopram	22.60
Rimantadine	22.55
Metoprolol	22.51
Mifepristone	22.22
Decamethonium	22.08
Clopidogrel	22.06
Clodronic acid	22.06
Toremifene	21.95
Abamectin	21.91
Climbazole	21.89
Aceclofenac	21.77
Acipimox	21.72
Methimazole	21.61
Piribedil-2HCl	21.59
Pindolol	21.01
Carbamyl-beta-methylcholine	20.94
Rebamipide	20.92
Methylprednisolone	20.88
Amlodipine	20.58
Neomycin	20.56
Carvedilol	20.54
Tiotidine	20.49
Clenbuterol	20.47
Guanfacine-HCl	20.36
Olmesartan	20.34
Levetiracetam	19.88
Dofetilide	19.83
Fluvastatin	19.82
Octreotide	19.80
Clomiphene	19.54
Dilazep	19.44
Methyl salicylate	19.44
Naftopidil-2HCl	19.30

Tropisetron	19.19
3'-Azido-3'-deoxythymidine	19.17
Sulfadoxine	19.16
Oxfendazole	19.04
Methysergide maleate	18.92
Norfloxacin	18.91
Thiamphenicol glycinate	18.79
Esmolol	18.72
Procarbazine	18.30
Moroxydine·HCl	18.12
Yohimbine·HCl	18.12
Calcifediol	17.71
Tolfenamic acid	17.49
Ibutilast	17.48
Nisoldipine	17.04
Riluzole·HCl	16.85
Roxatidine acetate·HCl	16.72
Fenretinide	16.68
Prednisone	16.57
Norethindrone	16.37
Acycloguanosine	16.35
Picotamide	16.35
Lomofungin	16.23
Butenafine	16.20
Diltiazem	16.20
Tolcapone	15.83
Salbutamol hemisulfate	15.73
Naproxen	15.72
Losartan potassium	15.69
Nicergoline	15.57
Candesartan	15.52
Ticlopidine	15.40
Felbamate	15.13
Furafylline	15.11
FAMOTIDINE	14.93
Scopolamine	14.81
Idazoxan·HCl	14.77
Risperidone	14.75
Nicorandil	14.68
Atropine	14.62
Aminophylline	14.53
Lamotrigine	14.50
Ouabain	14.33
Azathioprine	14.32
Gallamine	14.31
Orphenadrine citrate	14.10
Pencillin V	14.05
HA1077	14.03
Nateglinide	14.00
Mycophenolate mofetil	13.79
Naltrexone·HCl	13.68
Mesulergine	13.64

Lofexidine·HCl	13.56
Myclobutanil	13.53
Piroxicam	13.48
Nystatin	13.46
Nadifloxacin	13.43
Gemcitabine	13.28
Lisinopril	13.20
Mevastatin	13.05
Olopatadine	12.97
Etoricoxib	12.94
Oxymetazoline·HCl	12.57
Cabergoline	12.54
Tibolone	12.53
Pirenzepine·2HCl	12.46
DL-Isoproterenol	12.40
S(-)-Raclopride	12.34
Ozagrel	12.11
Granisetron	12.11
Troleandomycin	12.10
Raloxifene	12.06
Amiloride	12.04
2',3' - Dideoxycytidine	11.94
Ipratropium·Br	11.77
Chlorpheniramine	11.71
Terbinafine	11.69
Rilmenidine phosphate	11.62
Bumetanide	11.58
L-thyroxine	11.53
Lomerizine	11.39
Desloratadine	11.30
Ranolazine·2HCl	11.29
Progesterone	11.26
(+)-Tubocurarine chloride	11.25
Streptomycin	11.22
Dorzolamide·HCl	10.98
Ampicillin	10.86
4-Aminosalicylic acid	10.85
Galanthamine	10.52
Sibutramine	9.74
Clinafloxacin	9.64
Zonisamide	9.55
Ranitidine·HCl	9.08
Guaiacol	9.01
Erlotinib	8.66
Nedaplatin	8.48
Aniracetam	8.01
Ampiroxicam	7.94
Molsidomine	7.92
Sodium Phenylacetate	7.88
Hydroxytacrine	7.77
Norepinephrine-(+)-tartrate L (-)	7.33
Pravadoline	7.25

Ciprofloxacin	7.22
Quinapril	7.02
Ibuprofen	6.73
Dolasetron	6.72
Sulfasalazine	6.66
Piperacillin	6.64
Tinidazole	6.60
5-Aminosalicylic acid	6.59
Verapamil	6.56
Ginkgolide A	6.53
Vatalanib	6.50
Benzydamine	6.44
Melatonin	6.41
Praziquantel	6.37
Anethole, trans-	6.34
Bosentan	6.22
Ambroxol	6.07
Ibandronate	6.05
Apramycin	5.96
Chlormadinone Acetate	5.94
(S)-Timolol maleate	5.55
Lomustine	5.51
Adapalene	5.45
Levonorgestrel	5.34
Nimodipine	5.15
Phenylbutazone	5.13
Ribavirin	5.03
Nabumetone	4.99
(S)-(-)-Sulpiride	4.64
Carbamylcholine	4.36
Carbidopa	4.12
Metronidazole	4.05
Trichloromethiazide	4.04
DL-Aminoglutethimide	4.01
Roxithromycin	3.92
Vinpocetine	3.91
Benserazide	3.87
Acetylcholine	3.82
Suramin	2.89
Actarit	2.74
Bicalutamide	2.71
Dinoprost	2.19
Docebenone	1.94
Enoxacin	1.79
Moxifloxacin-HCl	1.73
Flumazenil	1.60
Atracurium besylate	1.31
Fenbendazole	1.12
Clarithromycin	1.07
Fumagillin	0.75
Capsaicin	0.63
Lomefloxacin	0.54

Diclofenac	0.44
Sodium Phenylbutyrate	0.43
Chlorambucil	0.33
Cetirizine 2HCl	0.18
Doxazosin	-0.03
Sarafloxacin	-0.05
Salmeterol xinafoate	-0.21
Debrisoquin	-0.21
Idebenone	-0.44
Flunarizine·2HCl	-0.51
Minocycline	-0.57
Diethylstilbestrol	-0.62
Procaterol·HCl	-0.71
Diflunisal	-0.80
Cyproterone Acetate	-0.94
Doxifluridine	-1.00
Exemestane	-1.03
Naphazoline	-1.05
Levofloxacin	-1.06
Paroxetine	-1.18
Dehydroepiandrosterone	-1.44
Zoledronic acid	-1.47
Amifostine	-1.55
Clofibrate	-1.75
Azithromycin	-1.80
Ethisterone	-1.92
Crotamiton	-1.96
Azaperone	-2.02
Famciclovir	-2.33
Meropenem	-2.43
Doxofylline	-2.48
Betaxolol·HCl	-2.59
Clofarabine	-2.63
Estriol	-2.71
Eprosartan mesylate	-2.82
Imatinib	-2.85
Neostigmine	-2.86
Enalapril	-3.11
L-(+)-Epinephrine tartrate	-3.15
Altretamine	-3.18
Estradiol	-3.19
Oltipraz	-3.24
Prednisolone	-3.35
Nifedipine	-3.43
Danazol	-3.52
Dextromethorphan	-3.65
Enrofloxacin	-3.72
Doxycycline	-3.74
Amprenavir	-3.80
Retinoic Acid	-3.92
Esomeprazole	-3.95
Albendazole	-3.99

Cyclocytidine	-4.06
Etretinate	-4.13
Canrenone	-4.59
Allopurinol	-4.79
Clopamide	-4.91
Emtricitabine	-4.93
Scopolamine N-butyl	-4.97
Etidronate	-5.01
Meglumine	-5.04
Tamoxifen	-5.12
Alprostadiol	-5.19
Tranlycypromine	-5.24
Corticosterone	-5.33
Secnidazole	-5.47
Oxaliplatin	-5.56
Trequinsin-HCl	-5.64
Omeprazole	-5.68
Rufloxacin	-5.96
Gefitinib	-6.09
Disulfiram	-6.16
Sumatriptan Succinate	-6.59
Aprepitant	-6.66
Simvastatin	-6.67
Niflumic acid	-6.71
Cytarabine	-6.74
Chloramphenicol	-6.93
Atenolol	-7.06
Cyclophosphamide	-7.10
Estrone	-7.13
Dacarbazine	-7.34
Racecadotril	-7.56
Siguazodan	-7.56
Alendronate	-7.61
Acemetacin	-8.08
Zaprinast	-8.17
Bleomycin	-8.62
Aztreonam	-8.66
Butyrylcholine	-8.67
Clobetasol Propionate	-8.90
Vinorelbine	-9.16
Efavirenz	-9.19
Gabapentin	-9.47
Nifekalant	-9.67
Buspirone	-9.80
Metformin	-10.09
Montelukast	-10.38
Tulobuterol	-10.66
Tizanidine-HCl	-10.68
Levodopa	-12.01
Rolipram	-12.29
Oseltamivir	-12.58
Taurocholic acid	-12.99

Pamidronate·2Na·5H <sub>2</sub> O	-13.04
Ofloxacin	-13.07
Pioglitazone	-13.28
Tacrine	-13.85
Xamoterol hemifumarate	-14.32
Oxcarbazepine	-14.51
Capecitabine	-14.52
Vinblastine	-14.92
Goserelin	-15.17
Pazufloxacin	-15.52
Minoxidil	-15.58
Penciclovir	-15.59
17- Hydroxyprogesterone	-15.66
Ceftazidime	-15.68
Fenofibrate	-16.65
Megestrol Acetate	-16.88
Melengestrol Acetate	-17.28
Pantoprazole	-17.50
Meloxicam	-17.86
Alfacalcidol	-18.10
Ketoprofen	-18.26
Nefazodone	-18.34
Fentiazac	-18.41
Finasteride	-18.56
Vindesine sulfate	-18.61
Caffeine	-18.75
Pefloxacin mesylate dihydrate	-18.81
Phenylpropanolamine	-19.16
Felodipine	-19.62
Anastrozole	-20.47
Miconazole	-20.62
Fenoldopam·HCl	-20.69
Cerivastatin	-21.34
Fenbufen	-21.42
Cefoperazone acid	-22.30
Trifluoperazine·2HCl	-22.72
Dinoprostone	-22.91
Sulindac	-23.00
Cilastatin	-23.47
Carbadox	-24.42
Cilnidipine	-24.58
Nitrendipine	-24.73
Phenoxybenzamine·HCl	-24.80
Denbufylline	-24.89
Miltefosine	-24.94
Bifonazole	-24.96
Pranoprofen	-25.50
Fenoprofen	-25.54
Zardaverine	-25.80
Hydrocortisone 21-acetate	-27.04
(S)-(+)-Ketoprofen	-27.07
Misoprostol	-27.20



Letrozole	-28.15
Vincristine sulfate	-28.29
Clindamycin palmitate·HCl	-28.71
Tranilast	-29.27
5-Fluorouracil	-29.52
Imiquimod	-29.55
Celecoxib	-29.69
Cefotaxime Acid	-29.75
Carbamazepine	-29.80
Ergothioneine	-30.17
Itopride	-30.46
Tranexamic acid	-30.52
Mefenamic acid	-31.07
RIFAMYCIN SV	-31.28
Milrinone	-31.64
Melphalan	-31.97
Pravastatin Lactone	-32.80
Hydrocortisone	-32.81
Argatroban	-32.92
Fluconazole	-33.47
Pranlukast	-34.94
Fluocinolone acetonide	-35.37
Pyrantel Pamoate	-35.46
Bexarotene	-35.65
Tolazamide	-35.73
Gentamycin	-36.03
Medroxyprogesterone 17-Acetate	-36.34
Flurbiprofen	-36.50
Mephenytoin	-36.76
Gemfibrozil	-37.66
Ifosfamide	-38.02
Gliclazide	-38.48
Methyldopa	-39.09
Anethole-trithione	-39.84
Itraconazole	-39.87
Furosemide	-40.87
Hexestrol	-41.88
Betamethasone	-42.56
Amitriptyline·HCl	-43.36
Idoxuridine	-44.31
Bromhexine	-44.84
Mebendazol	-44.96
Glimepiride	-46.25
Formestane	-46.73
Guaifenesin	-47.19
Indapamide	-47.85
Gatifloxacin	-48.27
Flutamide	-48.38
Fleroxacin	-48.67
Ftorafur	-49.12
Floxuridine	-50.01
Valproic acid	-51.11

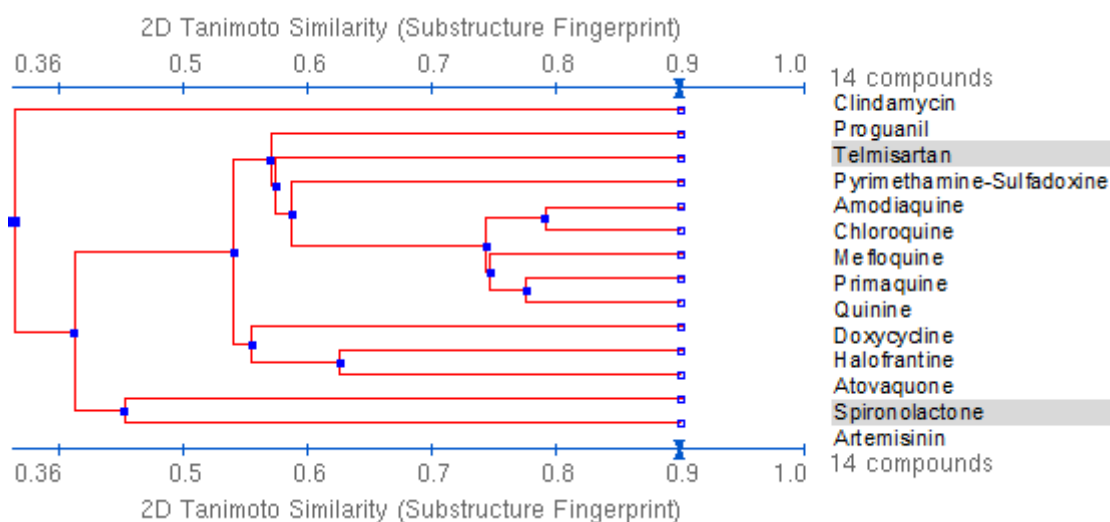
---

Flubendazole	-51.21
Bisacodyl	-51.98
Carboplatin	-54.28
Glyburide	-55.75
Ganciclovir	-56.89
Pramipexole	-57.83
Rofecoxib	-58.53
Diazoxide	-60.78
Rivastigmine	-67.33
Risedronic acid	-68.01
Bambuterol	-69.90
Zafirlukast	-72.88
Taxol	-75.10
Triptorelin	-77.68
Miglustat	-77.71
Fulvestrant	-79.41
Rocuronium bromide	-83.32
Ricobendazole	-88.62
Calcipotriene	-99.29
Zileuton	-112.80

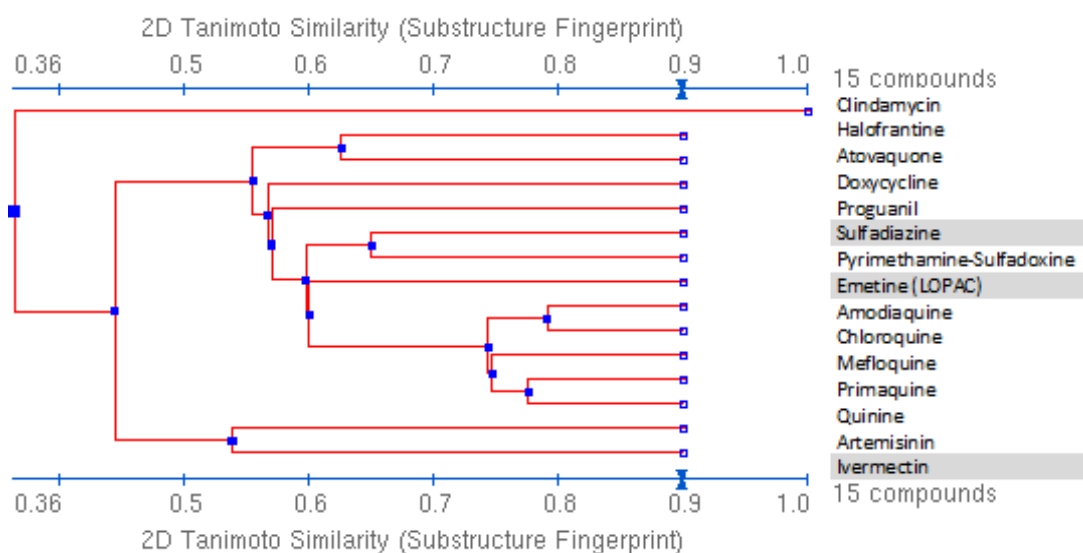
## Appendix V: Tanimoto similary fingerprints for identified LOPAC and ENZO library hits

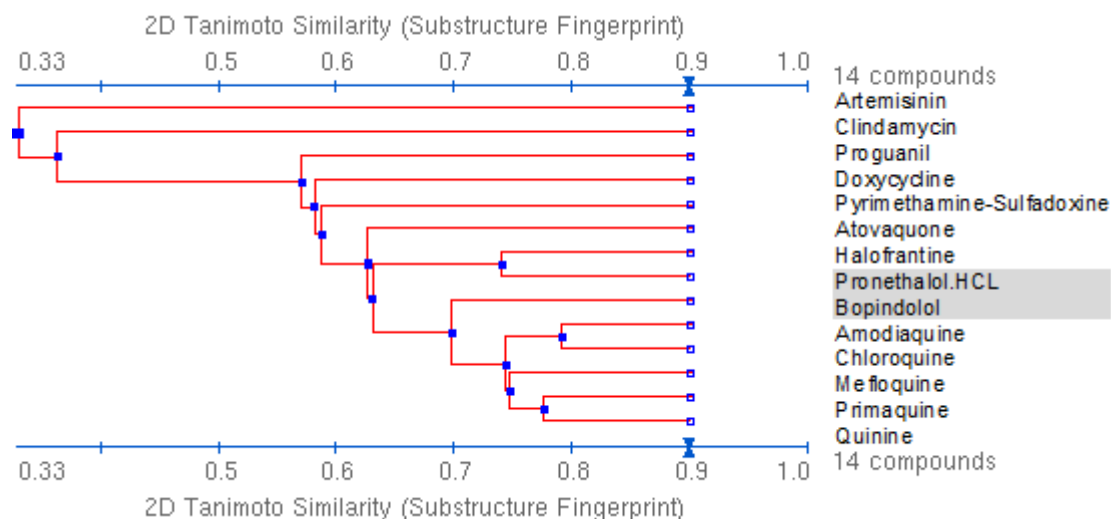
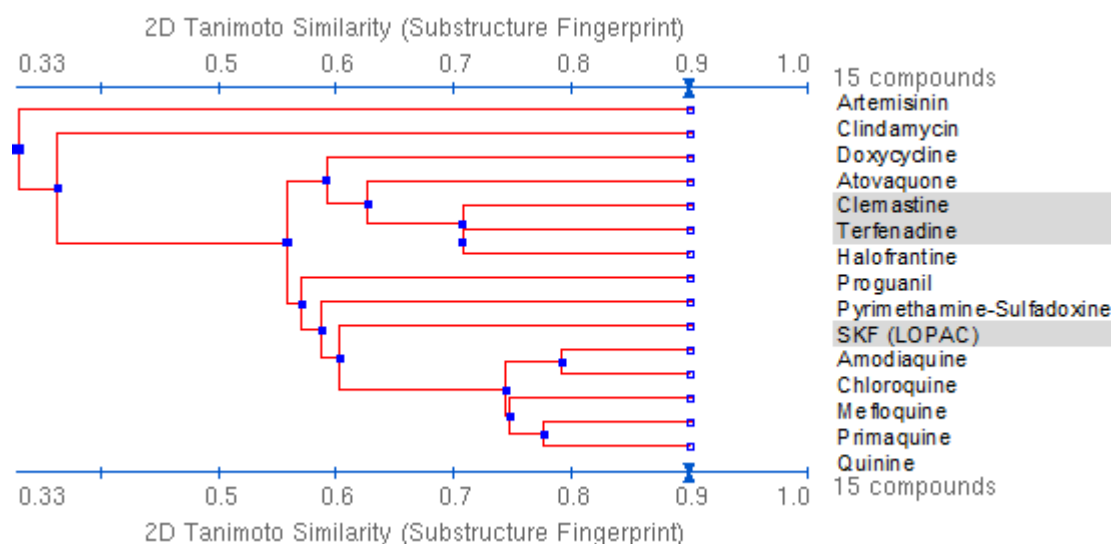
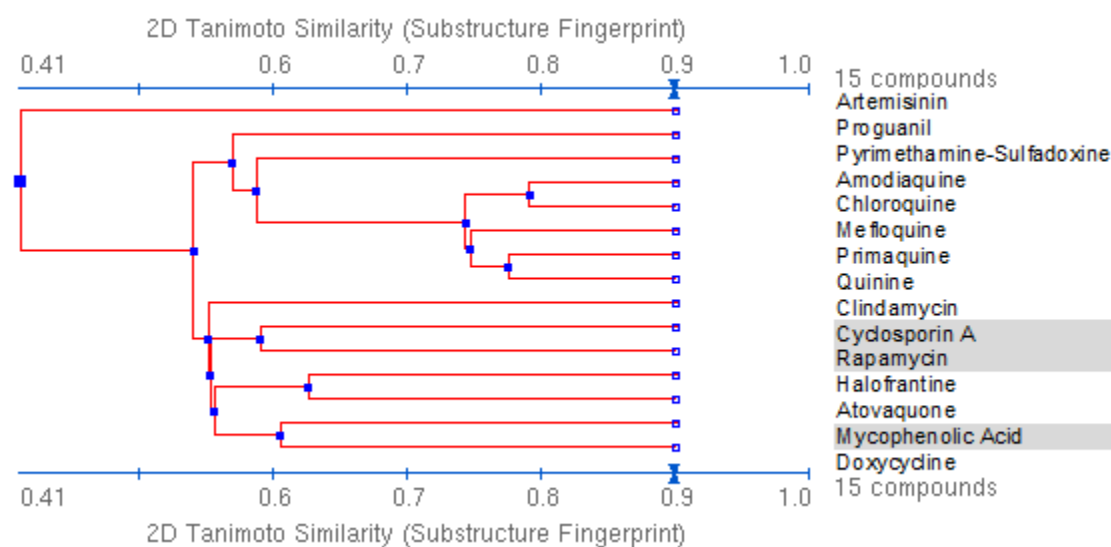
**with existing antimalarials.** ENZO library compounds were grouped in accordance with their previously defined medical subject heading (MeSH) category and analysed for Tanimoto similarity with representatives of existing antimalarial classes. Individual compound CIDs were determined and inputted into PubChem structural clustering for 2D similarity determination. Compounds with a score > 0.85 were consider to be structural similar and therefore likely to have the same mode of action. Three LOPAC of the compounds were also included and aligned well the identified MeSH catagories.

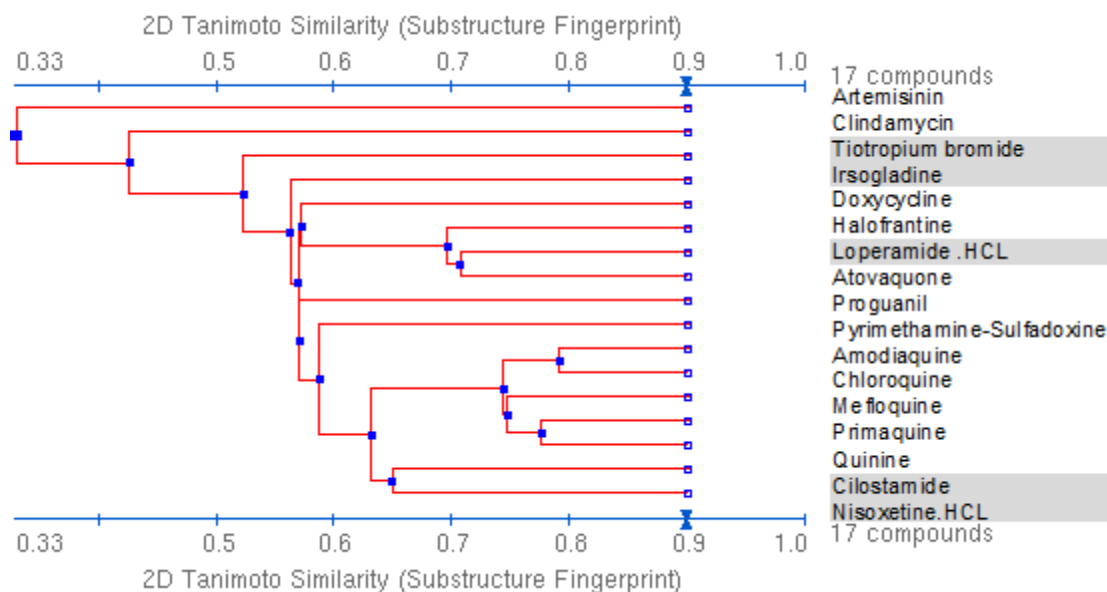
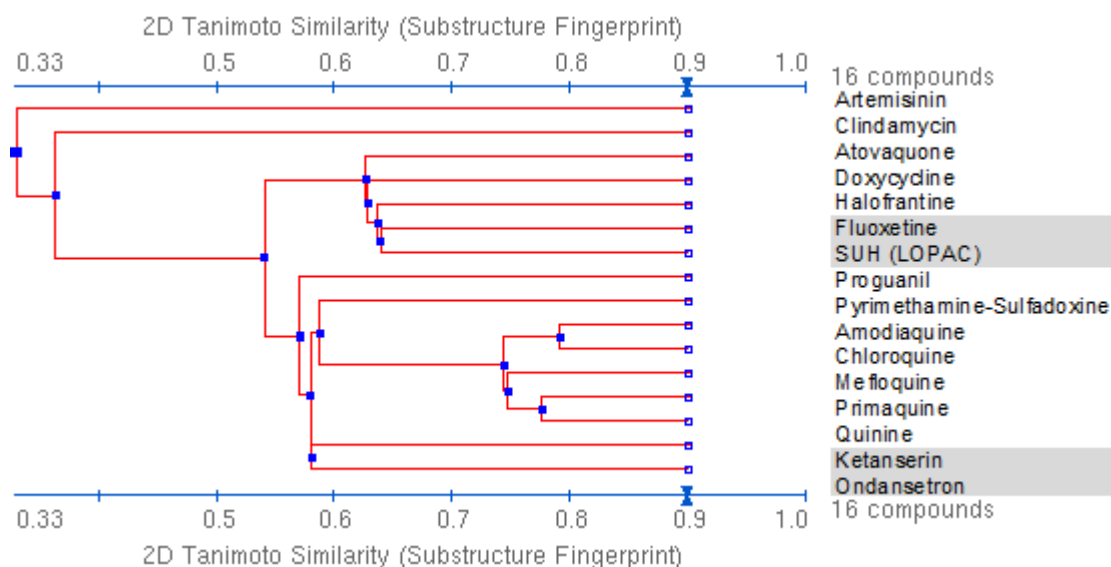
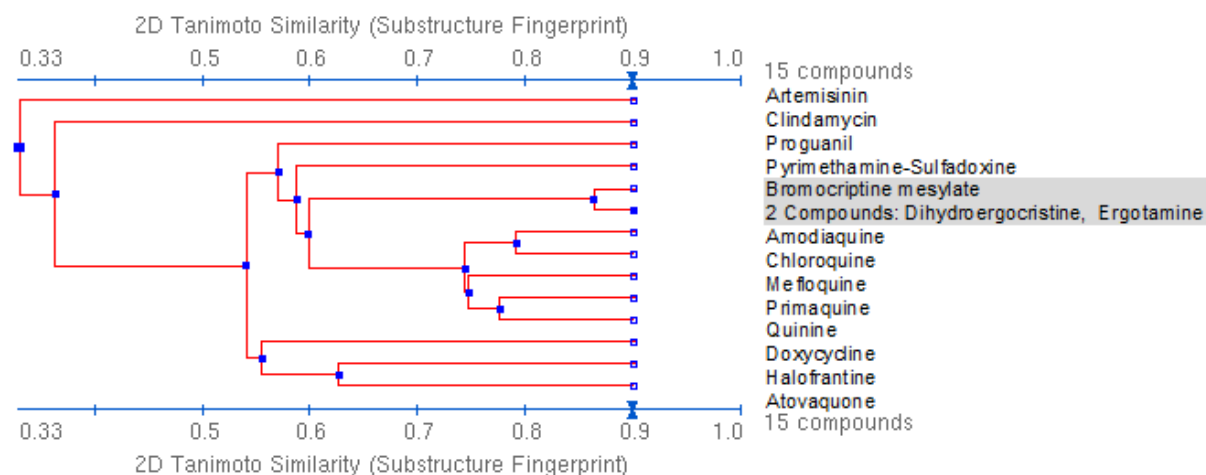
### Angiotensin receptor antagonist



### Antiparasitic

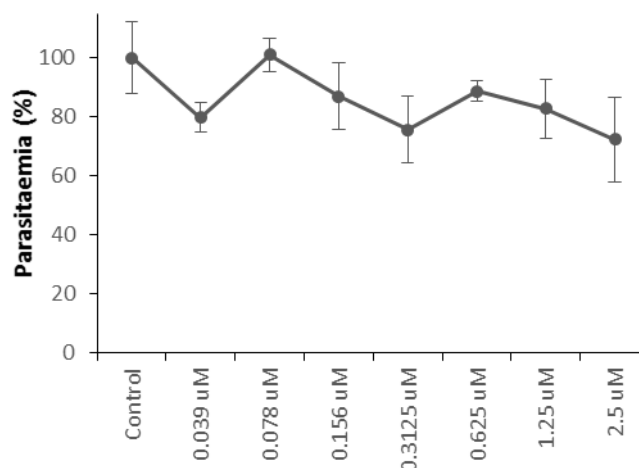
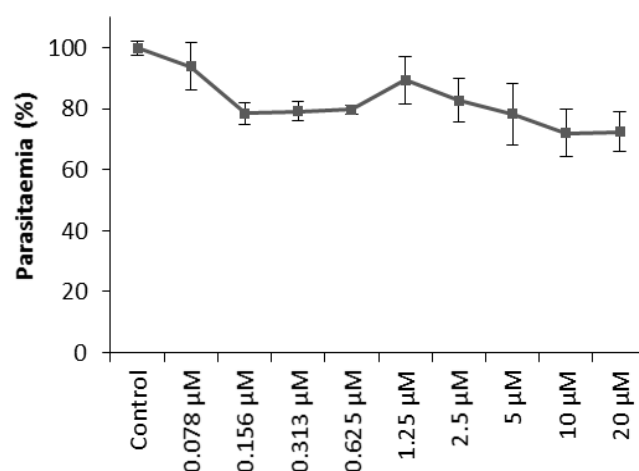
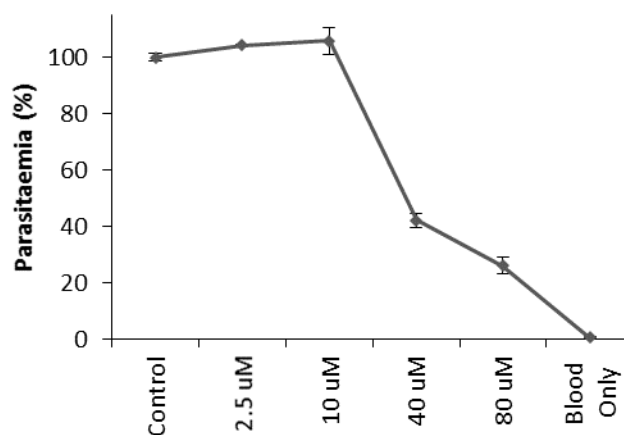


**Beta blockers****Histamine receptor antagonist****Immunosuppressant**

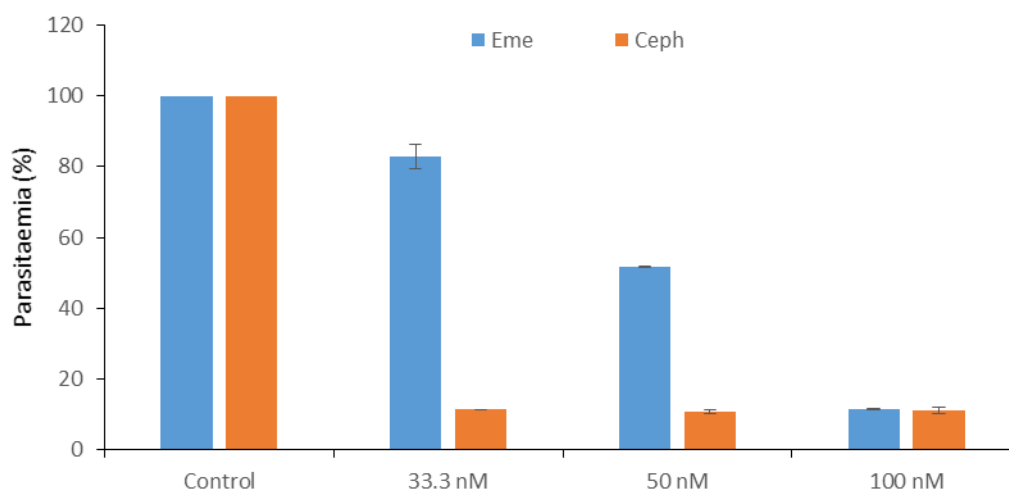
**Phosphodiesterase and other****Serotonin receptor antagonist****Vasodilator**

**Appendix VI: Optimisation of the ondansetron dose response against *P. falciparum*, strain**

**K1.** Despite showing ~60 % inhibition during the preliminary screen using a single 2.5  $\mu\text{M}$  dose point, Ondansetron (anti-emetic compound) failed to show a clear dose response pattern using the SG-MicroPlate method with concentrations up to 2.5  $\mu\text{M}$  (a). A new powder stock was purchased and the dose series was shifted up to 10  $\mu\text{M}$  and subsequently 20  $\mu\text{M}$  (b). Data was analysed using the more accurate SG-FCM method. A clear dose response pattern was not visible until a 2.5  $\mu\text{M}$ - 80  $\mu\text{M}$  dose series was employed (c).

**a. SG-MicroPlate****b. Ondansetron new stock analysed by SG-FCM****c. Ondansetron new stock analysed by SG-FCM**

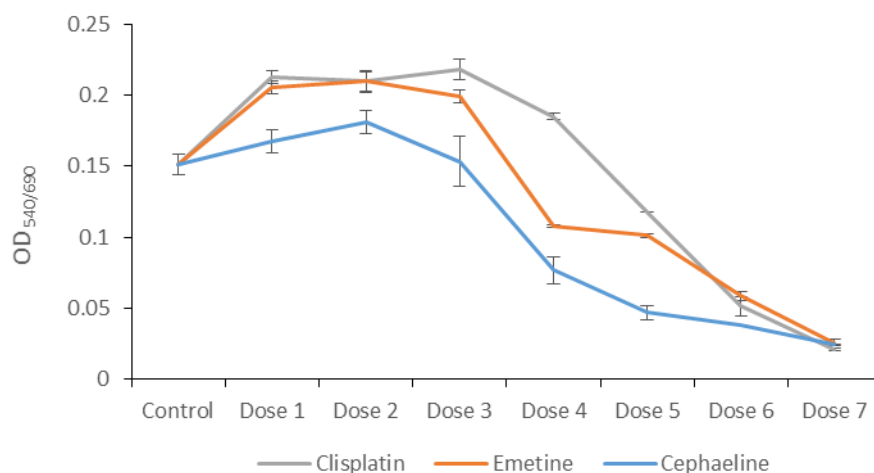
**Appendix VII: Preliminary screen of cephaeline compared with emetine against strain K1, *P. falciparum*.** Parasites were incubated for 72 hours under conditions described previously and analysed using SG-FCM. The emetine (Eme) 3-point dose response achieved the expected level of inhibition (previously determined  $IC_{50}$  achieved 49.3% inhibition). Cephaeline (Ceph) was shown to be more potent than emetine against the parasite.



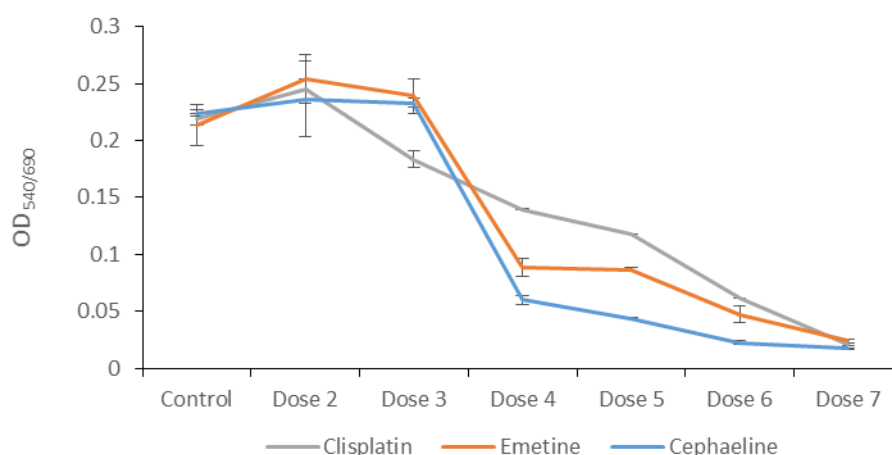
**Appendix VIII Preliminary investigation of the comparison between the cellular toxicity of emetine and cephaeline against the HepG2 cell line.** A wide dose range was selected (across two plates-14 doses in total) and analysed after either 48 or 120 hours incubation using the MTT assay. Cephaeline was consistently more toxic than emetine at the lower dose range for both time points. For the high dose range both compounds were inhibitory at the first dose used. For this reason, future replicates were based on the lower dose range to determine cephaeline and emetine IC<sub>50</sub> against HepG2. The positive control, cisplatin, was shown to be effective on each plate used.

Low doses	Cisplatin ( $\mu$ M)	Emetine (nM)	Cephaeline (nM)
Dose 1	0.39	3.05	3.05
Dose 2	0.78	6.10	6.10
Dose 3	1.56	12.21	12.21
Dose 4	3.13	24.41	24.41
Dose 5	6.25	48.83	48.83
Dose 6	12.5	97.66	97.66
Dose 7	25	195.3	195.3

Low doses 48 hrs

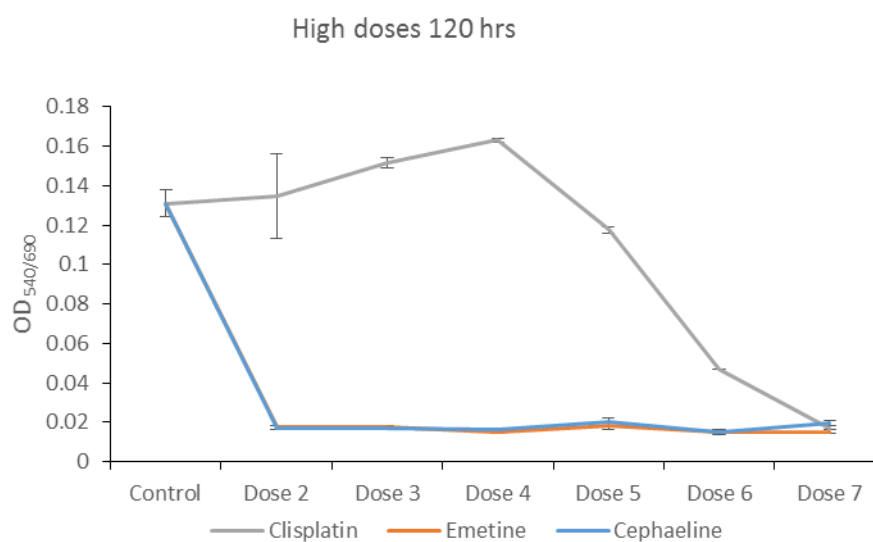
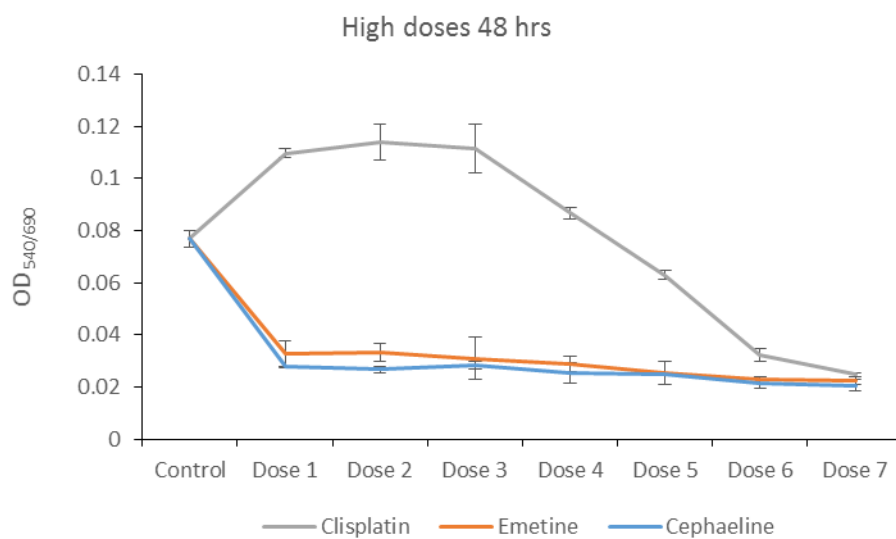


Low doses 120 hrs

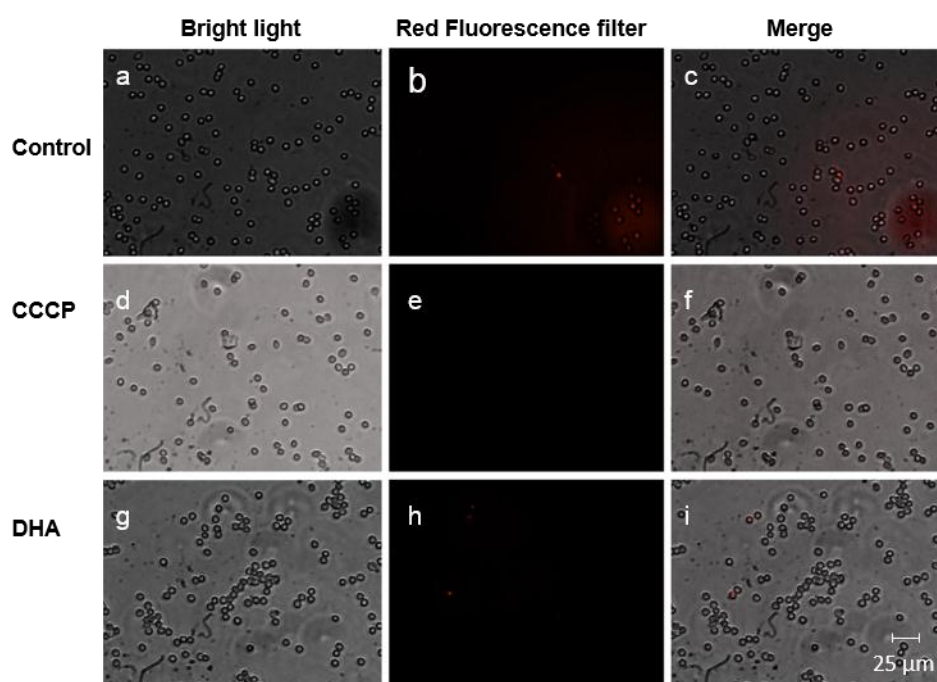




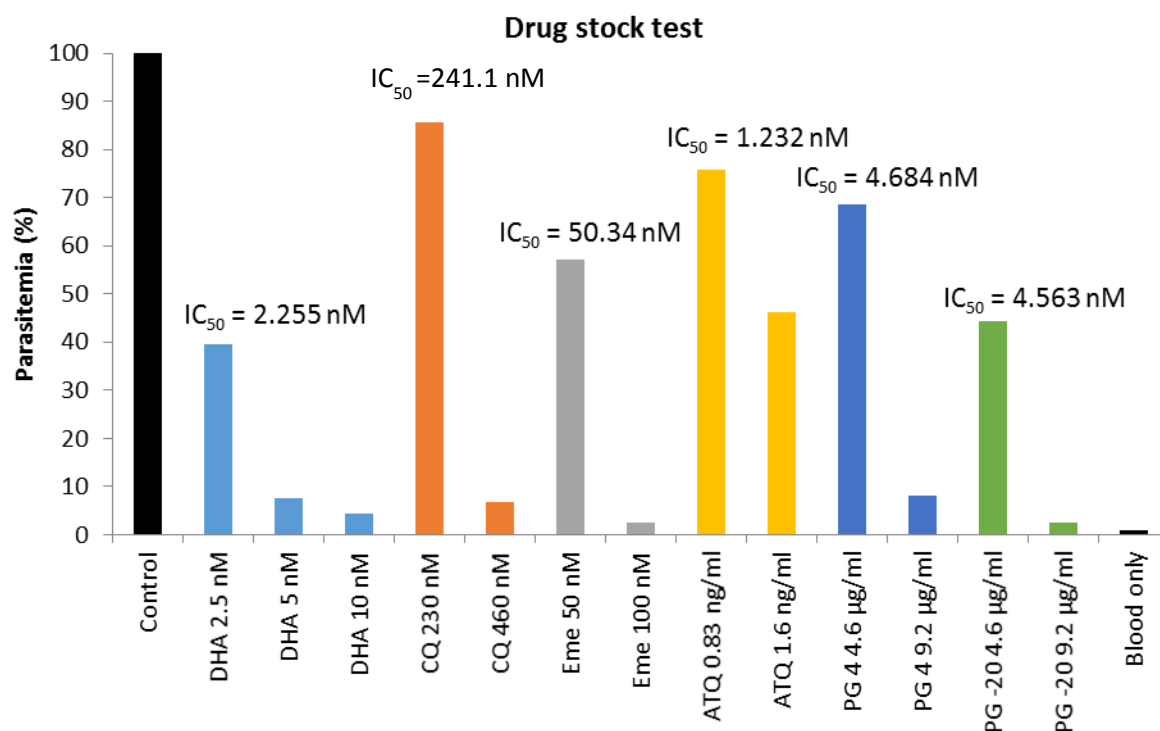
High doses	Cisplatin ( $\mu\text{M}$ )	Emetine ( $\mu\text{M}$ )	Cephaeline ( $\mu\text{M}$ )
Dose 1	0.39	0.39	0.39
Dose 2	0.78	0.78	0.78
Dose 3	1.56	1.56	1.56
Dose 4	3.13	3.13	3.13
Dose 5	6.25	6.25	6.25
Dose 6	12.5	12.5	12.5
Dose 7	25	25	25



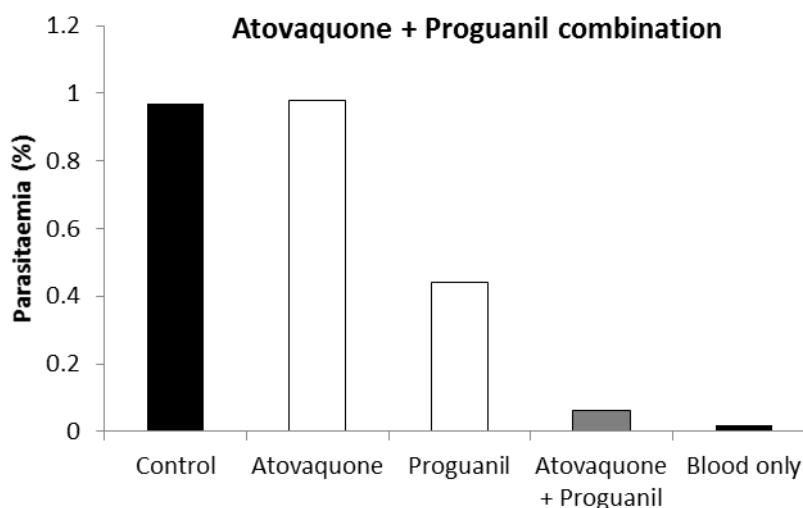
**Appendix IX: Fluorescence microscopy of JC-1 stained malaria parasites.** Parasites were treated with either CCCP (positive inducer of loss of mitochondrial membrane potential) or DHA as described in chapter 5 (section 5.2.5). Untreated parasite served as controls. Following treatment parasites were stained with JC-1 and viewed under the red fluorescence filter using Nikon Eclipse TE2000-S fluorescence microscope. Live parasites, with intact mitochondria, were stained red in the control (a-c) and DHA (g-i) treated sample. Staining was not visible in parasites that had been exposed to CCCP and thus confirmed loss of mitochondrial membrane potential (d-f).



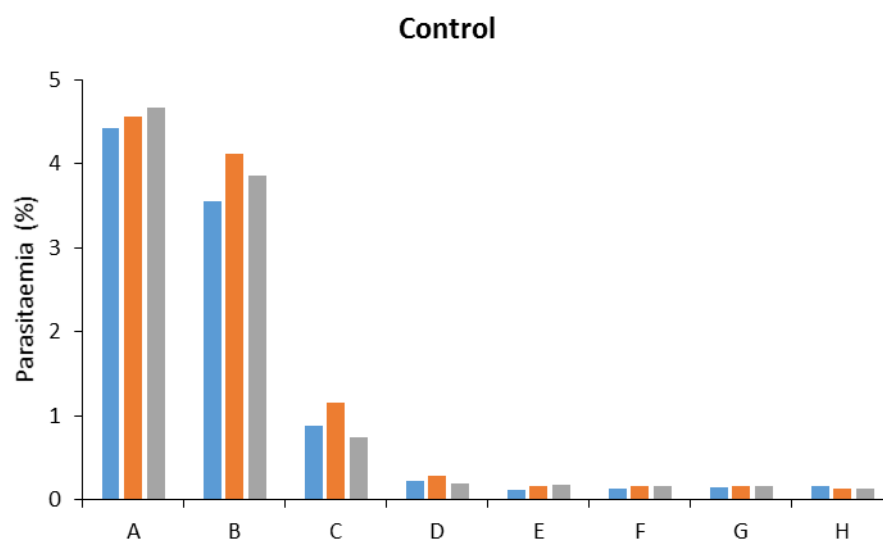
**Appendix X: Optimisation of the atovaquone proguanil combination against *P. falciparum* strain K1.** (a) Three point or two-point dose series were set up to check the activity of dihydroartemisinin (DHA), chloroquine (CQ), emetine (Eme), atovaquone (ATQ), and proguanil (PG) stock solutions against *P. falciparum* strain K1 (ring stage parasite, 72 hr incubation). For proguanil two stock solutions, stored at either 4°C or -20°C, were tested. SG-FCM analysis was employed as described previously. IC<sub>50</sub> estimates (GraphPad Prism) were consistent with those obtained previously although the ATQ IC<sub>50</sub> was slightly higher than the preliminary experiment it was consistent with more recent data.

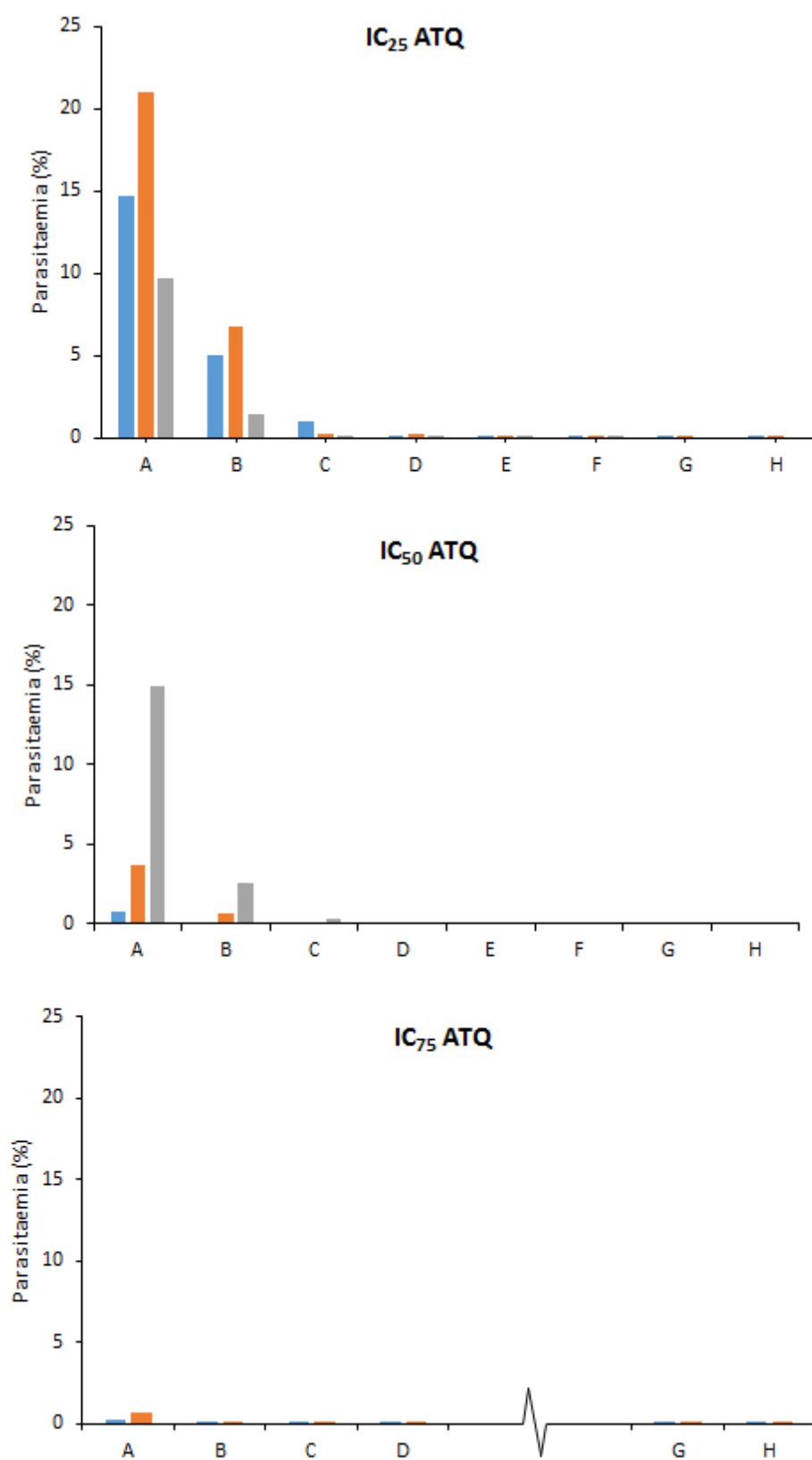


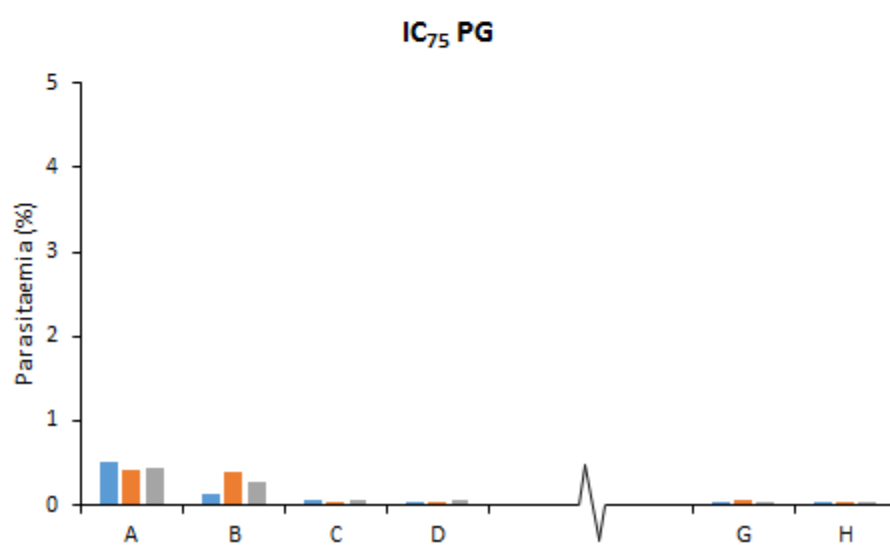
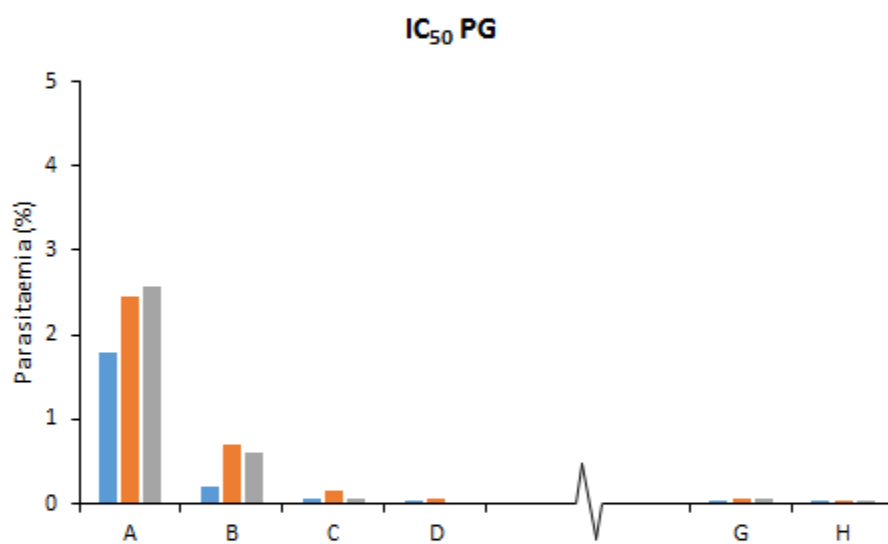
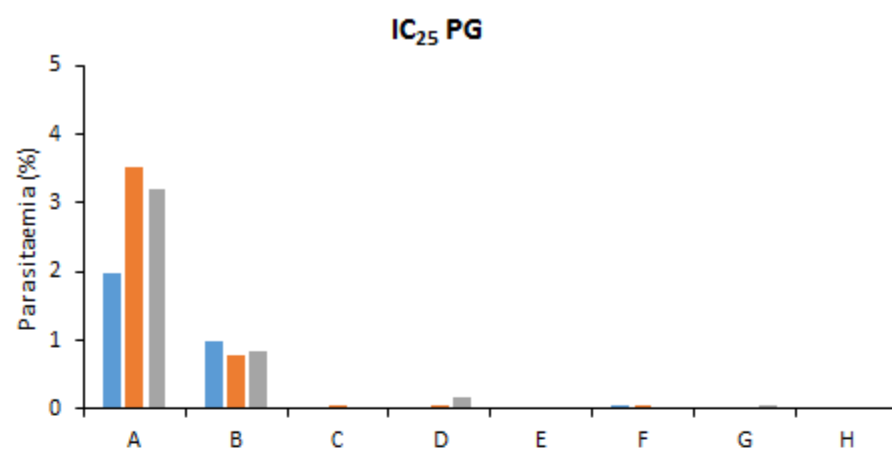
(b) Shows data from a flask experiment when the culture was diluted (trophozoite stage parasites, 48 hr incubation) and then compounds were subsequently added the culture separately (doses: ATQ 1.6 ng/ ml and PG 4.6 µg/ml). Analysed using the SG-FCM method the data showed that although ATQ failed to reduce parasite growth, the ATQ-PG combination show additional suppression when compared with the drug alone treatments.

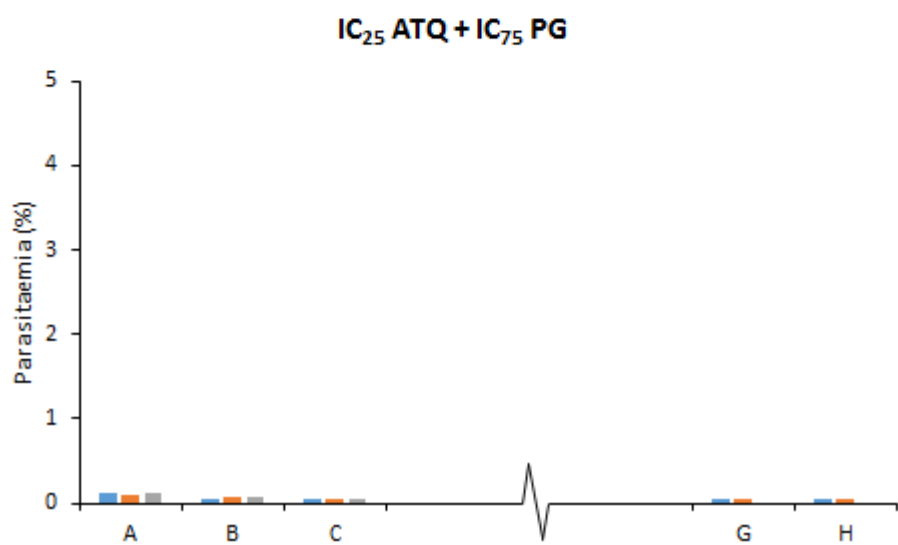
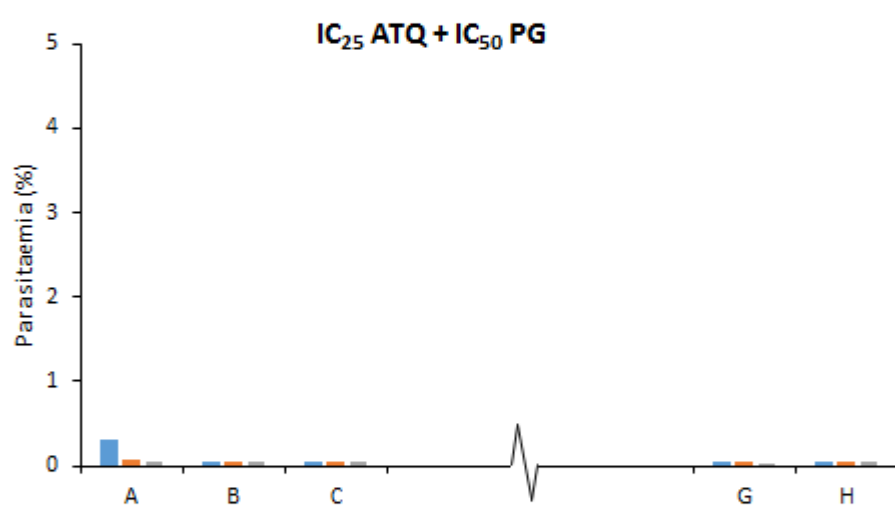
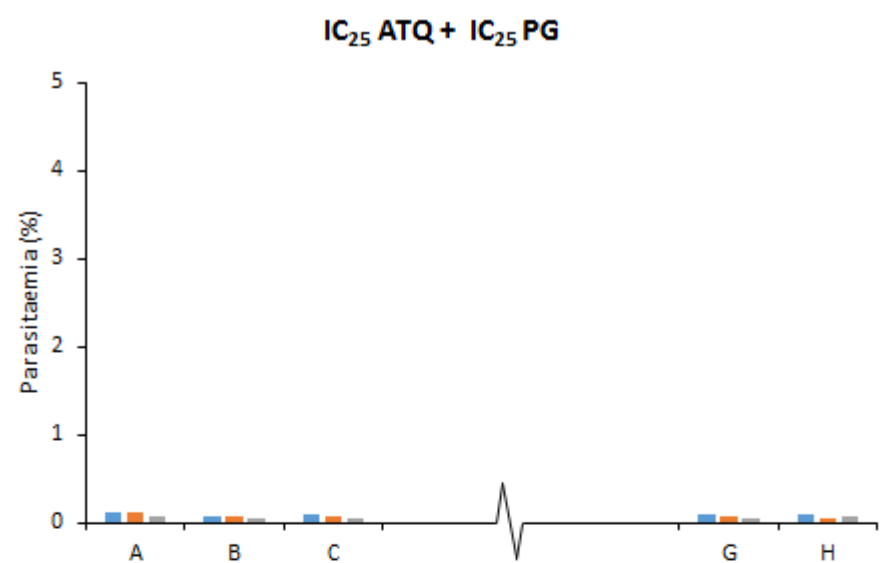


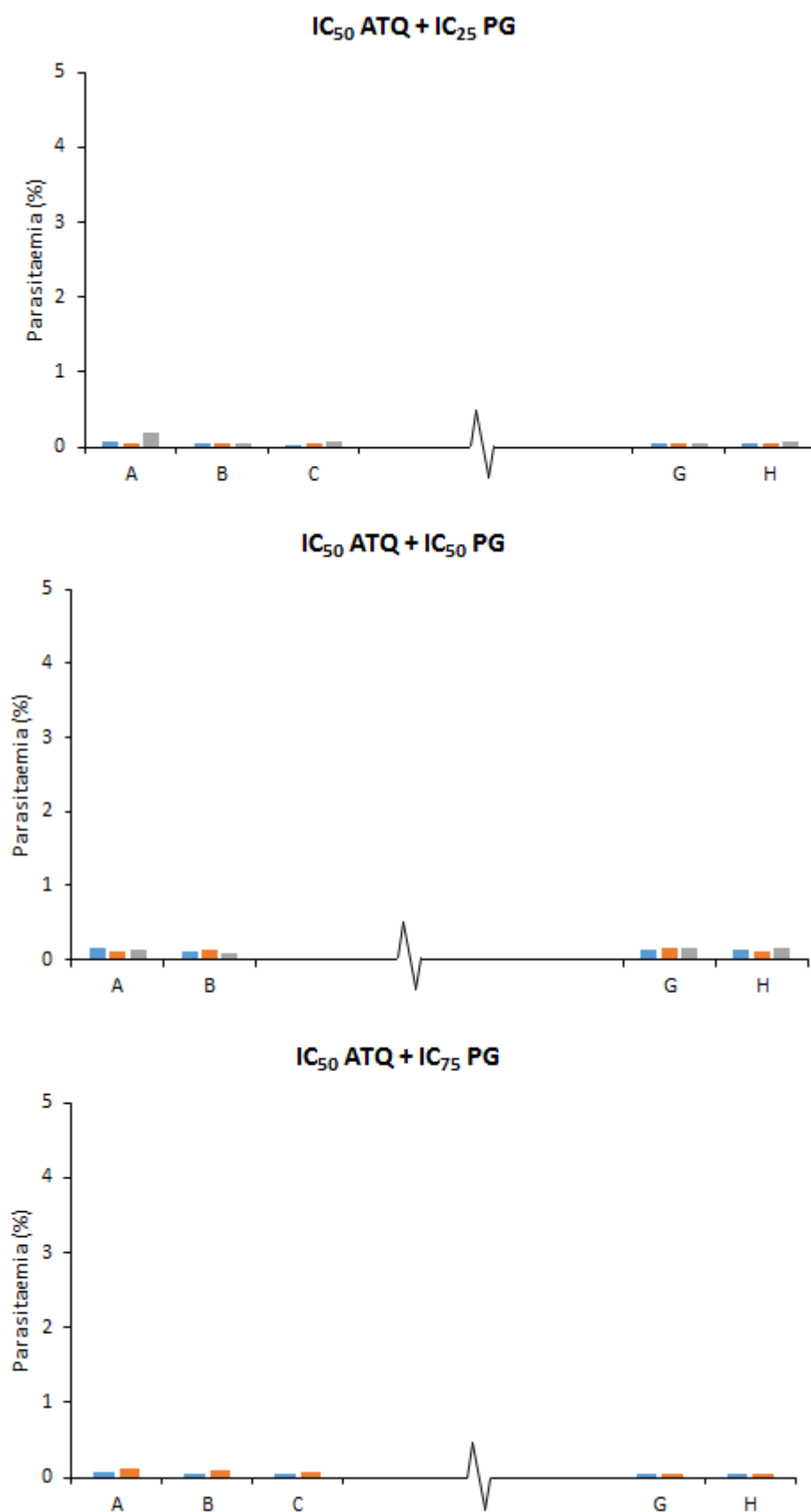
**Appendix XI: Recovery of *P. falciparum* strain K1 parasite after exposure to atovaquone or proguanil, either alone or at a non-constant ratio combination.** Parasites were treated with a non-constant ratio combination of atovaquone and proguanil. IC<sub>25</sub>, IC<sub>50</sub> and IC<sub>75</sub> doses were selected (0.05, 0.2 and 0.8 ng/ml for atovaquone and 2.4, 4.6 and 9.2 µg/ml for proguanil respectively). Each dose of atovaquone was combined with every dose of proguanil (15 combinations). Untreated control and drug alone treatments served as controls. After 72 hours of treatment each sample (triplicate) was washed 3 x in complete media and suspended at double the original volume so that the haematocrit was reduced from 2.5 to 1.25 %. A 1: 10 limiting serial dilution was performed in a 96 well plate (prepared with 200 µl of fresh blood in complete media) so that there were 8 dilutions (A-H) for each sample. After 7 days, spent media was discarded and replaced with 1% haematocrit blood in complete media. On day 20 parasite growth at each dilution was determined using the SG-FCM method. Each control and test combination was displayed separately and bar graphs indicate the % parasitaemia at each dilution. Triplicate data was shown separately to permit accurate determination of growth at each dilution in a presence or absence manner (differently coloured bars). Growth was observed in the control sample up to dilution C. The atovaquone alone samples followed a dose response pattern with growth present up to dilutions C, B and A for IC<sub>25</sub>, IC<sub>50</sub> and IC<sub>75</sub> doses respectively. Although the proguanil parasitaemia followed a dose response pattern growth was detected in dilutions A and B for all doses. No growth was observed at any dilution for the any of the combination treatments. Axis breaks indicate where data was not collected due to the consistency of surrounding data.



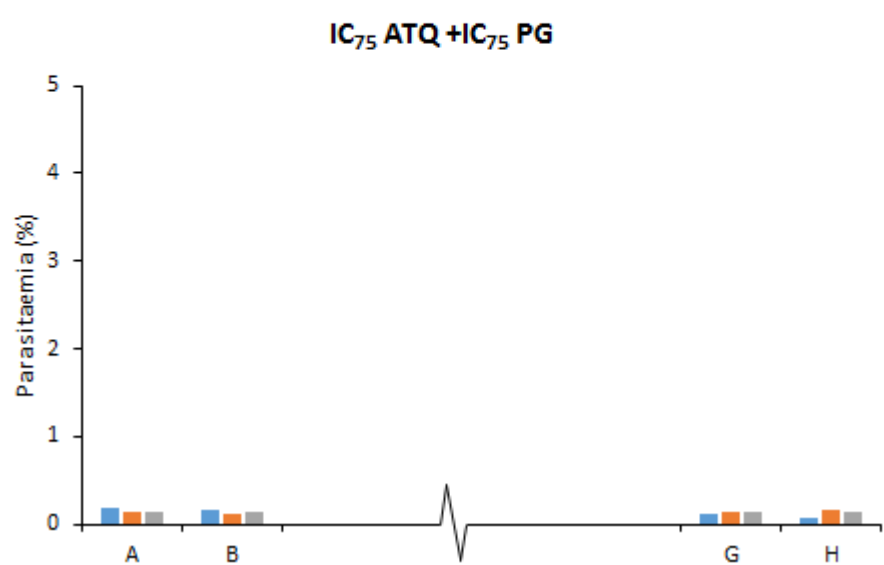
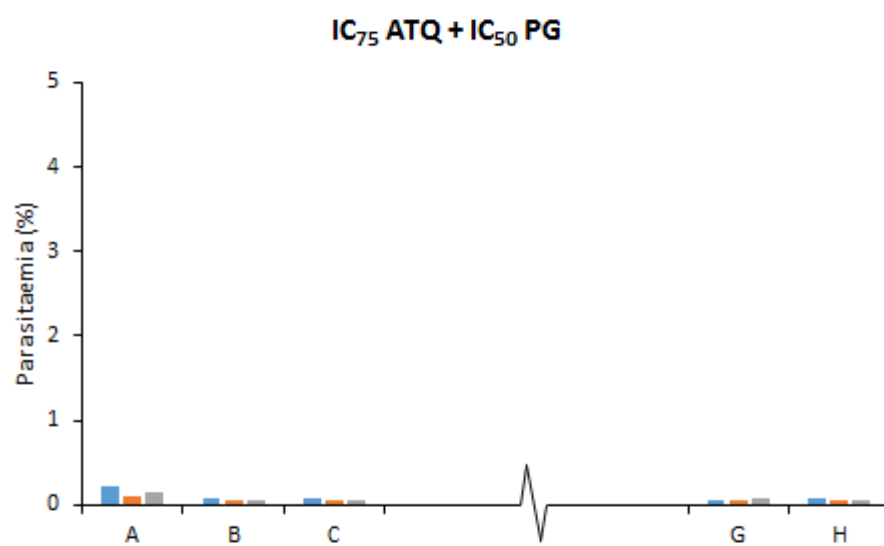
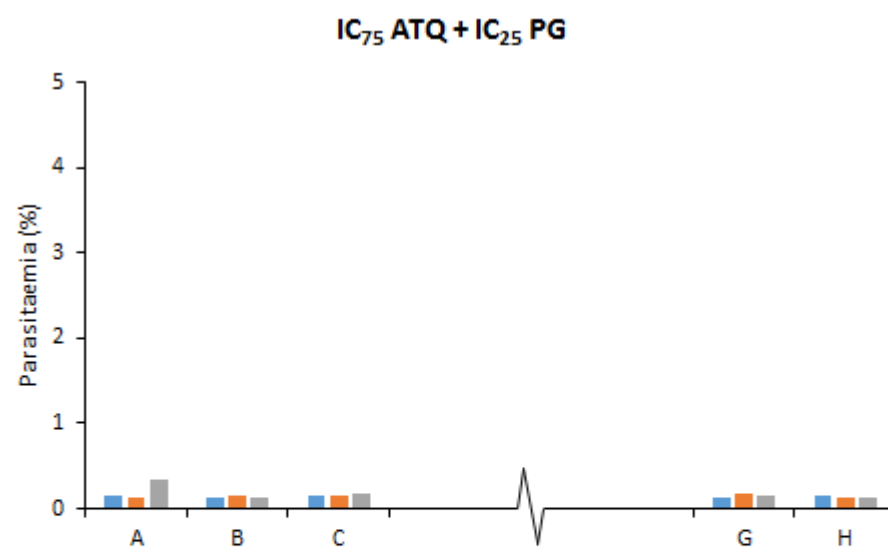












## REFERENCES

---

- Abiodun Oyindamola, O., Brun, R. and Wittlin, S. (2013) 'In vitro interaction of artemisinin derivatives or the fully synthetic peroxidic anti- malarial OZ277 with thapsigargin in *Plasmodium falciparum* strains', *Malaria Journal*, 12(1), 43.
- Achan, J., Talisuna, A. O., Erhart, A., Yeka, A., Tibenderana, J. K., Baliraine, F. N., Rosenthal, P. J. and Alessandro, U. (2011) 'Quinine, an old anti- malarial drug in a modern world: role in the treatment of malaria', *Malaria journal*, 10, 144.
- Akinboye, E. S., Rosen, M. D., Denmeade, S. R., Kwabi-addo, B. and Bakare, O. (2012) 'Design, Synthesis, and Evaluation of pH- Dependent Hydrolyzable Emetine Analogues as Treatment for Prostate Cancer', *Journal of Medicinal Chemistry*, 55(17), 7450-7459.
- Akinboye, E. S. and Bakare, O. (2011) 'Biological Activities of Emetine', *The Open Natural Products Journal*, 4, 8-15.
- Ali, M., Al-Olayan, E. M., Lewis, S., Matthews, H. and Hurd, H. (2010) 'Naturally Occurring Triggers that Induce Apoptosis-Like Programmed Cell Death in *Plasmodium berghei* Ookinetes', *PLoS ONE*, 5(9), e12634.
- Alker, A. P., Lim, P., Sem, R., Shah, N. K., YI, P., Bouth, D. M., Tsuyuoka, R., Maguire, J. D., Fandeur, T., Arie, F., Wongsrichanalai, C. and Mesnick, S. R. (2007) 'PFMDR1 and *in vivo* resistance to artesunate-mefloquine in *falciparum* malaria on the Cambodian-Thai border', *The American Journal of Tropical Medicine and Hygiene*, 76(4), 641-647.
- Allen, T.M. and Cullis, P.R. (2004) Drug Delivery Systems: Entering the Mainstream, *Science*, 303(5665), 1818-1822.
- Andrews, K. T., Fisher, G. and Skinner-Adams, T. S. (2014) 'Drug repurposing and human parasitic protozoan diseases', *International Journal for Parasitology: Drugs and Drug Resistance*, 4(2), 95-111.
- Asano, T., Sadakane, C., Ishihara, K., Yanagisawa, T., Kimura, M. and Kamei, H. (2001) 'High- performance liquid chromatographic assay with fluorescence detection for the determination of cephaeline and emetine in human plasma and urine', *Journal of Chromatography B: Biomedical Sciences and Applications*, 757(2), 197-206.
- Ashburn, T. T. and Thor, K. B. (2004) 'Drug repositioning: identifying and developing new uses for existing drugs', *Nat Rev Drug Discov*, 3(8), 673-683.
- Bacon, D. J., Latour, C., Lucas, C., Colina, O., Ringwald, P. and Picot, S. (2007) 'Comparison of a SYBR green I-based assay with a histidine-rich protein II enzyme-linked immunosorbent assay for in vitro antimalarial drug efficacy testing and application to clinical isolates', *Antimicrob Agents Chemother*, 51(4), 1172-8.
- Balint, G. A. (2001) 'Artemisinin and its derivatives: an important new class of antimalarial agents', *Pharmacology & Therapeutics*, 90(2-3), 261-265.

- Baniecki, M. L., Wirth, D. F. and Clardy, J. (2007) 'High-throughput *Plasmodium falciparum* growth assay for malaria drug discovery', *Antimicrob Agents Chemother*, 51(2), 716-23.
- Bansal, D., Sehgal, R., Chawla, Y., Mahajan, R. C. and Malla, N. (2004) 'In vitro activity of antiamebic drugs against clinical isolates of *Entamoeba histolytica* and *Entamoeba dispar*', *Ann Clin Microbiol Antimicrob*, 3, 27.
- Basco, L. K. (2007) *Field application of in vitro assays for the sensitivity of human malaria parasites to antimalarial drugs*. Geneva: World Health Organization Press.
- Bei, A. K., Desimone, T. M., Badiane, A. S., Ahouidi, A. D., Dieye, T., Ndiaye, D., Sarr, O., Ndir, O., Mboup, S. and Duraisingh, M. T. (2010) 'A flow cytometry-based assay for measuring invasion of red blood cells by *Plasmodium falciparum*', *Am J Hematol*, 85(4), 234-7.
- Bell, A. (2005) 'Antimalarial drug synergism and antagonism: mechanistic and clinical significance', *FEMS Microbiol Lett*, 253(2), 171-84.
- Bell, A., Wernli, B. and Franklin, R. M. (1994) 'Roles of peptidyl- prolyl CIS- trans isomerase and calcineurin in the mechanisms of antimalarial action of cyclosporin a, FK506, and rapamycin', *Biochemical Pharmacology*, 48(3), 495-503.
- Bhattacharya, A., Mishra, L. C., Sharma, M., Awasthi, S. K. and Bhasin, V. K. (2009) 'Antimalarial pharmacodynamics of chalcone derivatives in combination with artemisinin against *Plasmodium falciparum* in vitro', *European Journal of Medicinal Chemistry*, 44(9), 3388-3393.
- Bhattarai, A., Ali, A. S., Kachur, S. P., Mårtensson, A., Abbas, A. K., Khatib, R., Al-mafazy, A.-w., Ramsan, M., Rotllant, G., Gerstenmaier, J. F., Molteni, F., Abdulla, S., Montgomery, S. M., Kaneko, A. and Björkman, A. (2007) 'Impact of Artemisinin-Based Combination Therapy and Insecticide-Treated Nets on Malaria Burden in Zanzibar', *PLoS Med*, 4(11), e309.
- Biamonte, M. A., Wanner, J. and Le Roch, K. G. (2013) 'Recent advances in malaria drug discovery', *Bioorg Med Chem Lett*, 23(10), 2829-43.
- Bianco, A. E., Battye, F. L. and Brown, G. V. (1986) '*Plasmodium falciparum*: rapid quantification of parasitemia in fixed malaria cultures by flow cytometry', *Exp Parasitol*, 62(2), 275-282.
- Blaazer, A. R., Orrling, K. M., Shanmugham, A., Jansen, C., Maes, L., Edink, E., Sterk, G. J., Siderius, M., England, P., Bailey, D., de Esch, I. J. P. and Leurs, R. (2014) 'Fragment-Based Screening in Tandem with Phenotypic Screening Provides Novel Antiparasitic Hits', *Journal of Biomolecular Screening*, 20(1), 131-140.
- Bobbala, D., Koka, S., Lang, C., Boini, K. M., Huber, S. M. and Lang, F. (2008) 'Effect of cyclosporine on parasitemia and survival of *Plasmodium berghei* infected mice', *Biochemical and Biophysical Research Communications*, 376(3), 494-498.

- Boguski, M. S., Mandl, K. D. and Sukhatme, V. P. (2009) 'Repurposing with a Difference', *Science*, 324(5933), 1394-1395.
- Boon-Unge, K., Yu, Q., Zou, T., Zhou, A., Govitrapong, P. and Zhou, J. (2007) 'Emetine Regulates the Alternative Splicing of Bcl- x through a Protein Phosphatase 1-Dependent Mechanism', *Chemistry & Biology*, 14(12), 1386-1392.
- Burger, A. (1983) *A guide the the chemical basis of drug design*, New York, Chichester, Brisbane, Toronto, Singapore: John Wiley and Sons Inc.
- Burrows, J., Kowalczyk, P., McDonald, S., Spangenberg, T., Wells, T. and Willis, P. (2012) 'The Malaria Box: a catalyst for drug discovery', *Malar J*, 11(Suppl 1), 136.
- Canfield, C. J., Pudney, M. and Gutteridge, W. E. (1995) 'Interactions of Atovaquone with Other Antimalarial Drugs against *Plasmodium falciparum* in Vitro', *Exp Parasitol*, 80(3), 373-381.
- Carter, R. and Mendis, K. N. (2002) 'Evolutionary and historical aspects of the burden of malaria', *Clinical microbiology reviews*, 15(4), 564.
- Cavin, J. C., Krassner, S. M. and Rodriguez, E. (1987) 'Plant- derived alkaloids active against *Trypanosoma cruzi*', *Journal of Ethnopharmacology*, 19(1), 89-94.
- Cerutti Junior, C., Marques, C., Alencar, F. E., Durlacher, R. R., Alween, A., Segurado, A. A., Pang, L. W. and Zalis, M. G. (1999) 'Antimalarial drug susceptibility testing of *Plasmodium falciparum* in Brazil using a radioisotope method', *Mem Inst Oswaldo Cruz*, 94(6), 803-9.
- Ch'ng, J. H., Kotturi, S. R., Chong, A. G., Lear, M. J. and Tan, K. S. (2010) 'A programmed cell death pathway in the malaria parasite *Plasmodium falciparum* has general features of mammalian apoptosis but is mediated by clan CA cysteine proteases', *Cell Death Dis*, 1, e26.
- Chakrabarti, R., Rawat, P.S., Cooke, B.M., Coppel, R.L., Patankar, S. (2013) 'Cellular effects of curcumin on *Plasmodium falciparum* include disruption of microtubules', *PLoS ONE*, 8(3): e57302.
- Chatterjee, A. K. and Yeung, B. K. S. (2012) 'Back to the Future: Lessons Learned in Modern Target-based and Whole-Cell Lead Optimization of Antimalarials', *Current Topics in Medicinal Chemistry*, 12(5), 473-483.
- Chong, C. R., Chen, X., Shi, L., Liu, J. O. and Sullivan, D. J., Jr. (2006) 'A clinical drug library screen identifies astemizole as an antimalarial agent', *Nat Chem Biol*, 2(8), 415-6.
- Chou, T.-C. (2006) 'Theoretical basis, experimental design, and computerized simulation of synergism and antagonism in drug combination studies', *Pharmacological reviews*, 58(3), 621.

- Chou, T. C. (2010) 'Drug combination studies and their synergy quantification using the Chou-Talalay method', *Cancer Res*, 70(2), 440-6.
- Co, E. M. A., Dennull, R. A., Reinbold, D. D., Waters, N. C. and Johnson, J. D. (2009) 'Assessment of malaria in vitro drug combination screening and mixed- strain infections using the malaria Sybr green I- based fluorescence assay', *Antimicrobial agents and chemotherapy*, 53(6), 2557.
- Co, E. M. A., Johnson, S.M., Murthy, T., Talwar, M., Hickman, M.R. and Johnson, J.D. (2010) 'Recent Methods in Antimalarial Susceptibility Testing', *Anti-Infective Agents in Medicinal Chemistry*, 9, 148-160.
- Coatney, G. R. (1963) 'Pitfalls in a Discovery: The Chronicle of Chloroquine', *The American Journal of Tropical Medicine and Hygiene*, 12(2), 121-128.
- Corral, M. J., González-Sánchez, E., Cuquerella, M. and Alunda, J. M. (2014) 'In vitro synergistic effect of amphotericin B and allicin on *Leishmania donovani* and *L. infantum*', *Antimicrobial agents and chemotherapy*, 58(3), 1596.
- Cox, F. (2010) 'History of the discovery of the malaria parasites and their vectors', *Parasites & Vectors*, 3(5), 1-9.
- Cox, F. E. G. (2002) 'History of human parasitology', *Clinical microbiology reviews*, 15(4), 595.
- Craft, J. C. (2008) 'Challenges facing drug development for malaria', *Curr Opin Microbiol*, 11(5), 428-33.
- Croft, A. M. (2007) 'A lesson learnt: the rise and fall of Lariam and Halfan', *Journal of the Royal Society of Medicine*, 100(4), 170.
- Delves, M., Plouffe, D., Scheurer, C., Meister, S., Wittlin, S., Winzeler, E. A., Sinden, R. E. and Leroy, D. (2012) 'The activities of current antimalarial drugs on the life cycle stages of *Plasmodium*: a comparative study with human and rodent parasites', *PLoS Med*, 9(2), e1001169.
- Dempsey, J. J. and Salem, H. H. (1966) 'An enzymatic electrocardiographic study on toxicity of dehydroemetine', *British Heart Journal*, 28(4), 505-511.
- Deng, X., Nagle, A., Wu, T., Sakata, T., Henson, K., Chen, Z., Kuhen, K., Plouffe, D., Winzeler, E., Adrian, F., Tuntland, T., Chang, J., Simerson, S., Howard, S., Ek, J., Isbell, J., Tully, D. C., Chatterjee, A. K. and Gray, N. S. (2010) 'Discovery of novel 1H- imidazol- 2- yl- pyrimidine- 4,6- diamines as potential antimalarials', *Bioorganic & Medicinal Chemistry Letters*, 20(14), 4027-4031.
- Derbyshire, E. R., Mota, M. M. and Clardy, J. (2011) 'The Next Opportunity in Anti-Malaria Drug Discovery: The Liver Stage', *PLoS Pathogens*, 7(9), e1002178.

- Derbyshire, E. R., Prudêncio, M., Mota, M. M. and Clardy, J. (2012) 'Liver-stage malaria parasites vulnerable to diverse chemical scaffolds', *Proceedings of the National Academy of Sciences*, 109(22), 8511-8516.
- Desjardins, R. E., Canfield, C. J., Haynes, J. D. and Chulay, J. D. (1979) 'Quantitative assessment of antimalarial activity *in vitro* by a semiautomated microdilution technique', *Antimicrob Agents Chemother*, 16(6), 710-8.
- Dinh, W., Nickl, W., amp, Th, R., Lankisch, M., Hess, G., Zdunek, D., Scheffold, T., Barroso, M., Tiroch, K., Ziegler, D. and Seyfarth, M. (2011) 'High sensitive troponin T and heart fatty acid binding protein: Novel biomarker in heart failure with normal ejection fraction?: A cross-sectional study', *BMC Cardiovascular Disorders*, 11(1), 41.
- Djimdé, A., Doumbo, O. K., Cortese, J. F., Kayentao, K., Doumbo, S., Diourté, Y., Coulibaly, D., Dicko, A., Su, X.-z., Nomura, T., Fidock, D. A., Wellems, T. E. and Plowe, C. V. (2001) 'A Molecular Marker for Chloroquine-Resistant *Falciparum* Malaria', *New England Journal of Medicine*, 344(4), 257-263.
- Dondorp, A. M., Yeung, S., White, L., Nguon, C., Day, N. P. J., Socheat, D. and von Seidlein, L. (2010) 'Artemisinin resistance: current status and scenarios for containment', *Nat Rev Micro*, 8(4), 272-280.
- Drews, J. (2000) 'Drug discovery: a historical perspective', *Science (New York, N.Y.)*, 287(5460), 1960.
- Druilhe, P., Moreno, A., Blanc, C., Brasseur, P. H. and Jacquier, P. (2001) 'A colorimetric *in vitro* drug sensitivity assay for *Plasmodium falciparum* based on a highly sensitive double-site lactate dehydrogenase antigen-capture enzyme-linked immunosorbent assay', *Am J Trop Med Hyg*, 64(5-6), 233-41.
- Duffy, P. E. and Sibley, C. H. (2005) 'Are we losing artemisinin combination therapy already?', *The Lancet*, 366(9501), 1908-1909.
- Ekins, S., Williams, A. J., Krasowski, M. D. and Freundlich, J. S. (2011) 'In silico repositioning of approved drugs for rare and neglected diseases', *Drug Discov Today*, 16(7-8), 298-310.
- Ekland, E. H. and Fidock, D. A. (2008) 'In vitro evaluations of antimalarial drugs and their relevance to clinical outcomes', *International Journal for Parasitology*, 38(7), 743-747.
- Elabbadi, N., Ancelin, M. L. and Vial, H. J. (1992) 'Use of radioactive ethanolamine incorporation into phospholipids to assess in vitro antimalarial activity by the semiautomated microdilution technique', *Antimicrob Agents Chemother*, 36(1), 50-5.
- Feng, J., Ly, J., Myrick, F., Goodman, D., White, K., Svarovskaia, E., Borroto-Esoda, K. and Miller, M. (2009) 'The triple combination of tenofovir, emtricitabine and

- efavirenz shows synergistic anti- HIV- 1 activity in vitro: a mechanism of action study', *Retrovirology*, 6(1), 44.
- Fidock, D. A., Eastman, R. T., Ward, S. A. and Meshnick, S. R. (2008) 'Recent highlights in antimalarial drug resistance and chemotherapy research', *Trends Parasitol*, 24(12), 537-44.
- Fidock, D. A., Rosenthal, P. J., Croft, S. L., Brun, R. and Nwaka, S. (2004) 'Antimalarial drug discovery: efficacy models for compound screening', *Nat Rev Drug Discov*, 3(6), 509-20.
- Fink, H. A., Mac Donald, R., Rutks, I. R., Nelson, D. B. and Wilt, T. J. (2002) 'Sildenafil for male erectile dysfunction: A systematic review and meta-analysis', *Archives of Internal Medicine*, 162(12), 1349-1360.
- Fivelman, Q. L., Adagu, I. S. and Warhurst, D. C. (2004) 'Modified fixed- ratio isobologram method for studying *in vitro* interactions between atovaquone and proguanil or dihydroartemisinin against drug- resistant strains of *Plasmodium falciparum*', *Antimicrobial agents and chemotherapy*, 48(11), 4097.
- Fivelman, Q. L., Adagu, I. S. and Warhurst, D. C. (2007) 'Effects of piperazine, chloroquine, and amodiaquine on drug uptake and of these in combination with dihydroartemisinin against drug- sensitive and -resistant *Plasmodium falciparum* strains', *Antimicrobial agents and chemotherapy*, 51(6), 2265.
- Flannery, E. L., Chatterjee, A. K. and Winzeler, E. A. (2013) 'Antimalarial drug discovery - approaches and progress towards new medicines', *Nature reviews. Microbiology*, 11(12), 849.
- Frearson, J. A., Wyatt, P. G., Gilbert, I. H. and Fairlamb, A. H. (2007) 'Target assessment for antiparasitic drug discovery', *Trends Parasitol*, 23(12), 589-95.
- Fügi, M. A., Wittlin, S., Dong, Y. and Vennerstrom, J. L. (2010) 'Probing the Antimalarial Mechanism of Artemisinin and OZ277 (Arterolane) with Nonperoxidic Isosteres and Nitroxyl Radicals', *Antimicrob Agents Chemother*, 54(3), 1042-1046.
- Gamo, F. J., Sanz, L. M., Vidal, J., de Cozar, C., Alvarez, E., Lavandera, J.-L., Vanderwall, D. E., Green, D. V. S., Kumar, V., Hasan, S., Brown, J. R., Peishoff, C. E., Cardon, L. R. and Garcia-Bustos, J. F. (2010) 'Thousands of chemical starting points for antimalarial lead identification', *Nature*, 465(7296), 305.
- Ganguli, C. (2002) *A Handbook of Medical Treatment*, Calcutta: Academic Publishers.
- Gardner, M. J., Hall, N., Fung, E., White, O., Berriman, M., Hyman, R. W., Carlton, J. M., Pain, A., Nelson, K. E., Bowman, S., Paulsen, I. T., James, K., Eisen, J. A., Rutherford, K., Salzberg, S. L., Craig, A., Kyes, S., Chan, M.-S., Nene, V., Shallom, S. J., Suh, B., Peterson, J., Angiuoli, S., Pertea, M., Allen, J., Selengut, J., Haft, D., Mather, M. W., Vaidya, A. B., Martin, D. M. A., Fairlamb, A. H., Fraunholz, M. J., Roos, D. S., Ralph, S. A., McFadden, G. I., Cummings, L. M.,



- Subramanian, G. M., Mungall, C., Venter, J. C., Carucci, D. J., Hoffman, S. L., Newbold, C., Davis, R. W., Fraser, C. M. and Barrell, B. (2002) 'Genome sequence of the human malaria parasite *Plasmodium falciparum*', *Nature*, 419(6906), 498.
- Gelb, M. H. (2007) 'Drug discovery for malaria: a very challenging and timely endeavor', *Curr Opin Chem Biol*, 11(4), 440-5.
- Gesase, S., Gosling, R. D., Hashim, R., Ord, R., Naidoo, I., Madebe, R., Mosha, J. F., Joho, A., Mandia, V., Mrema, H., Mapunda, E., Savael, Z., Lemnge, M., Mosha, F. W., Greenwood, B., Roper, C. and Chandramohan, D. (2009) 'High Resistance of *Plasmodium falciparum* to Sulphadoxine/Pyrimethamine in Northern Tanzania and the Emergence of dhps Resistance Mutation at Codon 581', *PLoS ONE*, 4(2), e4569.
- Gilbert, I. H. (2013) 'Drug Discovery for Neglected Diseases: Molecular Target-Based and Phenotypic Approaches Miniperspectives Series on Phenotypic Screening for Antiinfective Targets', *Journal of Medicinal Chemistry*, 56(20), 7719-7726.
- Gorka, A. P., Jacobs, L. M. and Roepe, P. D. (2013) 'Cytostatic versus cytotoxic profiling of quinoline drug combinations via modified fixed-ratio isobologram analysis', *Malaria journal*, 12, 332.
- Grandesso, F., Bachy, C., Donam, I., Ntambi, J., Habimana, J., D'Alessandro, U., Maikere, J., Vanlerberghe, V., Kera, C. H. and Guthmann, J. P. (2006) 'Efficacy of chloroquine, sulfadoxine-pyrimethamine and amodiaquine for treatment of uncomplicated *Plasmodium falciparum* malaria among children under five in Bongor and Koumra, Chad', *Trans R Soc Trop Med Hyg*, 100(5), 419-26.
- Greenwood, B. M., Fidock, D. A., Kyle, D. E., Kappe, S. H. I., Alonso, P. L., Collins, F. H. and Duffy, P. E. (2008) 'Malaria: progress, perils, and prospects for eradication', *The Journal of Clinical Investigation*, 118(4), 1266-1276.
- Gregson, A. and Plowe, C. V. (2005) 'Mechanisms of Resistance of Malaria Parasites to Antifolates', *Pharmacological Reviews*, 57(1), 117-145.
- Grimberg, B. T. (2011) 'Methodology and application of flow cytometry for investigation of human malaria parasites', *J Immunol Methods*, 367(1-2), 1-16.
- Grollman, A. P. (1966) 'Structural basis for inhibition of protein synthesis by emetine and cycloheximide based on an analogy between ipecac alkaloids and glutarimide antibiotics', *Proceedings of the National Academy of Sciences of the United States of America*, 56(6), 1867.
- Guerin, P. J., Olliaro, P., Nosten, F., Druilhe, P., Laxminarayan, R., Binka, F., Kilama, W. L., Ford, N. and White, N. J. (2002) 'Malaria: current status of control, diagnosis, treatment, and a proposed agenda for research and development', *The Lancet Infectious Diseases*, 2(9), 564-573.

- Guiguemde, W. A., Shelat, A. A., Bouck, D., Duffy, S., Crowther, G. J., Davis, P. H., Smithson, D. C., Connelly, M., Clark, J., Zhu, F., Jiménez-Díaz, M. B., Martinez, M. S., Wilson, E. B., Tripathi, A. K., Gut, J., Sharlow, E. R., Bathurst, I., El Mazouni, F., Fowble, J. W., Forquer, I., McGinley, P. L., Castro, S., Angulo-Barturen, I., Ferrer, S., Rosenthal, P. J., Derisi, J. L., Sullivan, D. J., Lazo, J. S., Roos, D. S., Riscoe, M. K., Phillips, M. A., Rathod, P. K., Van Voorhis, W. C., Avery, V. M. and Guy, R. K. (2010) 'Chemical genetics of *Plasmodium falciparum*', *Nature*, 465(7296), 311.
- Guiguemde, W. A., Shelat, A. A., Garcia-Bustos, J. F., Diagana, T. T., Gamo, F. J. and Guy, R. K. (2012) 'Global phenotypic screening for antimalarials', *Chemistry & biology*, 19(1), 116.
- Gupta, S., Thapar, M. M., Mariga, S. T., Wernsdorfer, W. H. and Björkman, A. (2002) '*Plasmodium falciparum*: in vitro Interactions of Artemisinin with Amodiaquine, Pyronaridine, and Chloroquine', *Experimental Parasitology*, 100(1), 28-35.
- Harasym, T., Liboiron, B. and Mayer, L. (2010) 'Drug Ratio-Dependent Antagonism: A New Category of Multidrug Resistance and Strategies for Its Circumvention' in Zhou, J., ed., *Multi-Drug Resistance in Cancer*, Humana Press, 291-323.
- Hare, J. D. and Bahler, D. W. (1986) 'Analysis of *Plasmodium falciparum* growth in culture using acridine orange and flow cytometry', *Journal of Histochemistry & Cytochemistry*, 34(2), 215-220.
- Harrison, G. (1978) *Mosquitoes malaria and man: a history of hostilities since 1880*, London: John Murray.
- Hay, S. I., Guerra, C. A., Tatem, A. J., Noor, A. M. and Snow, R. W. (2004) 'The global distribution and population at risk of malaria: past, present, and future', *The Lancet Infectious Diseases*, 4(6), 327-336.
- Haynes, R. K. and Krishna, S. (2004) 'Artemisinins: activities and actions', *Microbes and Infection*, 6(14), 1339-1346.
- Heppner, D. G. (2013) 'The malaria vaccine-- status quo 2013', *Travel medicine and infectious disease*, 11(1), 2.
- Hill, A. V. S. (2011) 'Vaccines against malaria', *Philosophical Transactions of the Royal Society B*, 366(1579), 2806-2814.
- Hu, Y., Platzer, E. G., Bellier, A. and Aroian, R. V. (2010) 'Discovery of a highly synergistic anthelmintic combination that shows mutual hypersusceptibility', *Proceedings of the National Academy of Sciences of the United States of America*, 107(13), 5955.
- Hyde, J. E. (2005) 'Exploring the folate pathway in *Plasmodium falciparum*', *Acta Trop*, 94(3), 191-206.
- Hyde, J. E. (2007) 'Drug-resistant malaria - an insight', *FEBS J*, 274(18), 4688-98.

- Ioset, J. R. and Kaur, H. (2009) 'Simple field assays to check quality of current artemisinin-based antimalarial combination formulations', *PLoS ONE*, 4(9), e7270.
- Izumiyama, S., Omura, M., Takasaki, T., Ohmae, H. and Asahi, H. (2009) '*Plasmodium falciparum*: development and validation of a measure of intraerythrocytic growth using SYBR Green I in a flow cytometer', *Exp Parasitol*, 121(2), 144-50.
- Jackson, P. R., Winkler, D. G., Kimzey, S. L. and Fisher, F. M. (1977) 'Cytofluorograf detection of *Plasmodium yoelii*, *Trypanosoma gambiense*, and *Trypanosoma equiperdum* by laser excited fluorescence of stained rodent blood', *The Journal of parasitology*, 63(4), 593-598.
- Jambou, R., Le Bras, J. and Randrianarivelosoa, M. (2011) 'Pitfalls in new artemisinin-containing antimalarial drug development', *Trends in Parasitology*, 27(2), 82-90.
- Jana, S. and Paliwal, J. (2007) 'Novel molecular targets for antimalarial chemotherapy', *International Journal of Antimicrobial Agents*, 30(1), 4-10.
- Jensen, M. and Mehlhorn, H. (2009) 'Seventy-five years of Resochin in the fight against malaria', *Parasitology Research*, 105(3), 609-627.
- Johnson, J. D., Dennull, R. A., Gerena, L., Lopez-Sanchez, M., Roncal, N. E. and Waters, N. C. (2007) 'Assessment and continued validation of the malaria SYBR green I-based fluorescence assay for use in malaria drug screening', *Antimicrob Agents Chemother*, 51(6), 1926-33.
- Jones, D. C., Hallyburton, I., Stojanovski, L., Read, K. D., Frearson, J. A. and Fairlamb, A. H. (2010) 'Identification of a  $\kappa$ -opioid agonist as a potent and selective lead for drug development against human African trypanosomiasis', *Biochemical pharmacology*, 80(10), 1478.
- Kaddouri, H., Nakache, S., Houzé, S., Mentré, F. and Le Bras, J. (2006) 'Assessment of the drug susceptibility of *Plasmodium falciparum* clinical isolates from africa by using a *Plasmodium* lactate dehydrogenase immunodetection assay and an inhibitory maximum effect model for precise measurement of the 50-percent inhibitory concentration', *Antimicrob Agents Chemother*, 50(10), 3343-9.
- Kang, Y. J. (2001) 'Molecular and cellular mechanisms of cardiotoxicity', *Environmental Health Perspectives*, 109(Suppl 1), 27-34.
- Karl, S., Wong, R. P., St Pierre, T. G. and Davis, T. M. (2009) 'A comparative study of a flow-cytometry-based assessment of *in vitro Plasmodium falciparum* drug sensitivity', *Malar J*, 8, 294.
- Katrak, S., Gasasira, A., Arinaitwe, E., Kakuru, A., Wanzira, H., Bigira, V., Sandison, T. G., Homsy, J., Tappero, J. W., Kanya, M. R. and Dorsey, G. (2009) 'Safety and tolerability of artemether-lumefantrine versus dihydroartemisinin-piperaquine for malaria in young HIV-infected and uninfected children', *Malar J*, 8, 272.

- Keiser, J., Manneck, T. and Vargas, M. (2011) '*Schistosoma mansoni in vitro* Interactions of mefloquine with praziquantel in the *Schistosoma mansoni* mouse model and *in vitro*', *Journal of Antimicrobial Chemotherapy*, 66(8), 1791-1797.
- Keiser, J., Tritten, L., Adelfio, R. and Vargas, M. (2012) 'Effect of combinations of marketed human anthelmintic drugs against *Trichuris muris in vitro* and *in vivo*', *Parasites & Vectors*, 5(1), 292.
- Khositnithikul, R., Tan-Ariya, P. and Mungthin, M. (2008) 'In vitro atovaquone/proguanil susceptibility and characterisation of the cytochrome b gene of *Plasmodium falciparum* from different endemic regions of Thailand', *Malaria Journal*, 7(1), 23.
- Kitchen, L. W., Vaughn, D. W. and Skillman, D. R. (2006) 'Role of US military research programs in the development of US Food and Drug Administration-- approved antimalarial drugs', *Clinical infectious diseases : an official publication of the Infectious Diseases Society of America*, 43(1), 67.
- Klonis, N., Crespo-Ortiz, M. P., Bottova, I., Abu-Bakar, N., Kenny, S., Rosenthal, P. J. and Tilley, L. (2011) 'Artemisinin activity against *Plasmodium falciparum* requires hemoglobin uptake and digestion', *Proceedings of the National Academy of Sciences*, 108(28), 11405–11410.
- Koram, K. A., Abuaku, B., Duah, N. and Quashie, N. (2005) 'Comparative efficacy of antimalarial drugs including ACTs in the treatment of uncomplicated malaria among children under 5 years in Ghana', *Acta Trop*, 95(3), 194-203.
- Kotz, J. (2012) 'Phenotypic screening, take two', *SciBX*, 5(15), 1-3.
- Krafts, K., Hempelmann, E. and Skórska-Stania, A. (2012) 'From methylene blue to chloroquine: a brief review of the development of an antimalarial therapy', *Founded as Zeitschrift für Parasitenkunde*, 111(1), 1-6.
- Kremsner, P. G. and Krishna, S. (2004) 'Antimalarial combinations', *Lancet*, 364(9430), 285-94.
- Krishna, S., Uhlemann, A.-C. and Haynes, R. K. (2004) 'Artemisinins: mechanisms of action and potential for resistance', *Drug Resistance Updates*, 7(4–5), 233-244.
- Krungkrai, J., Imprasittichai, W., Ojungeed, S., Pongsabut, S. and Krungkrai, S. R. (2010) 'Artemisinin resistance or tolerance in human malaria patients', *Asian Pacific Journal of Tropical Medicine*, 3(9), 748-753.
- Lalremruata, A., Ball, M., Bianucci, R., Welte, B., Nerlich, A. G., Kun, J. F. J. and Pusch, C. M. (2013) 'Molecular identification of *falciparum* malaria and human tuberculosis co- infections in mummies from the Fayum depression (Lower Egypt)', *PloS one*, 8(4), e60307.
- Lotharius, J., Gamo-Benito, F. J., Angulo-Barturen, I., Clark, J., Connelly, M., Ferrer-Bazaga, S., Parkinson, T., Viswanath, P., Bhandodkar, B., Rautela, N., Bharath, S.,

- Duffy, S., Avery, V. M., Möhrle, J. J., Guy, R. K. and Wells, T. (2014) 'Repositioning: the fast track to new anti- malarial medicines?', *Malaria journal*, 13, 143.
- Lowes, D. J., Guiguemde, W. A., Connelly, M. C., Zhu, F., Sigal, M. S., Clark, J. A., Lemoff, A. S., Derisi, J. L., Wilson, E. B. and Guy, R. K. (2011) 'Optimization of Propafenone Analogues as Anti-Malarial Leads', *Journal of medicinal chemistry*, 54(21), 7477-7485.
- Lucumi, E., Darling, C., Jo, H., Napper, A. D., Chandramohanadas, R., Fisher, N., Shone, A. E., Jing, H., Ward, S. A., Biagini, G. A., DeGrado, W. F., Diamond, S. L. and Greenbaum, D. C. (2010) 'Discovery of potent small-molecule inhibitors of multidrug-resistant *Plasmodium falciparum* using a novel miniaturized high-throughput luciferase-based assay', *Antimicrob Agents Chemother*, 54(9), 3597-604.
- Mackey, Z. B., Baca, A. M., Mallari, J. P., Apsel, B., Shelat, A., Hansell, E. J., Chiang, P. K., Wolff, B., Guy, K. R., Williams, J. and McKerrow, J. H. (2006) 'Discovery of Trypanocidal Compounds by Whole Cell HTS of *Trypanosoma brucei*', *Chemical Biology & Drug Design*, 67(5), 355-363.
- Major, L. L. and Smith, T. K. (2011) 'Screening the MayBridge Rule of 3 Fragment Library for Compounds That Interact with the *Trypanosoma brucei* myo- Inositol-3- Phosphate Synthase and/or Show Trypanocidal Activity', *Molecular Biology International*, 2011, 389364.
- Makler, M. T., Lee, L.G. and Recktenwald, D (1987) 'Thiazole Orange: A New Dye for *Plasmodium* Species Analysis', *Cytometry Part A*, 8, 568-570.
- Makler, M. T., Piper, R. C. and Milhous, W. K. (1998) 'Lactate Dehydrogenase and the Diagnosis of Malaria', *Parasitology Today*, 14(9), 376-377.
- Malleret, B., Claser, C., Ong, A. S., Suwanarusk, R., Sriprawat, K., Howland, S. W., Russell, B., Nosten, F. and Renia, L. (2011) 'A rapid and robust tri-color flow cytometry assay for monitoring malaria parasite development', *Sci Rep*, 1, 118.
- Mariga, S. T., Gil, J. P., Wernsdorfer, W. H. and Björkman, A. (2005) 'Pharmacodynamic interactions of amodiaquine and its major metabolite desethylamodiaquine with artemisinin, quinine and atovaquone in *Plasmodium falciparum* in vitro', *Acta Tropica*, 93(3), 221-231.
- Matthews, H., Ali, M., Carter, V., Underhill, A., Hunt, J., Szor, H. and Hurd, H. (2012) 'Variation in apoptosis mechanisms employed by malaria parasites: the roles of inducers, dose dependence and parasite stages', *Malaria Journal*, 11(1), 297.
- Matthews, H., Usman-Idris, M., Khan, F., Read, M. and Nirmalan, N. J. (2013) 'Drug repositioning as a route to anti-malarial drug discovery: preliminary investigation of the *in vitro* anti-malarial efficacy of emetine dihydrochloride hydrate'. *Malaria Journal*, 12, 359.

- McAlpine, J. A., Lu, H.-T., Wu, K. C., Knowles, S. K. and Thomson, J. A. (2014) 'Down-regulation of argininosuccinate synthetase is associated with cisplatin resistance in hepatocellular carcinoma cell lines: implications for PEGylated arginine deiminase combination therapy', *BMC cancer*, 14, 621.
- Medina-Franco, J. L., Giulianotti, M. A., Welmaker, G. S. and Houghten, R. A. (2013) 'Shifting from the single to the multitarget paradigm in drug discovery', *Drug Discovery Today*, 18(9-10), 495-501.
- Meister, S., Plouffe, D. M., Kuhen, K. L., Bonamy, G. M. C., Wu, T., Barnes, S. W., Bopp, S. E., Borboa, R., Bright, A. T., Che, J., Cohen, S., Dharia, N. V., Gagaring, K., Gettayacamin, M., Gordon, P., Groessl, T., Kato, N., Lee, M. C. S., McNamara, C. W., Fidock, D. A., Nagle, A., Nam, T.-g., Richmond, W., Roland, J., Rottmann, M., Zhou, B., Froissard, P., Glynne, R. J., Mazier, D., Sattabongkot, J., Schultz, P. G., Tuntland, T., Walker, J. R., Zhou, Y., Chatterjee, A., Diagana, T. T. and Winzeler, E. A. (2011) 'Imaging of *Plasmodium* Liver Stages to Drive Next-Generation Antimalarial Drug Discovery', *Science*, 334(6061), 1372-1377.
- Mercer, A. E., Copple, I. M., Maggs, J. L., O'Neill, P. M. and Park, B. K. (2011) 'The Role of Heme and the Mitochondrion in the Chemical and Molecular Mechanisms of Mammalian Cell Death Induced by the Artemisinin Antimalarials', *Journal of Biological Chemistry*, 286(2), 987-996.
- Merschjohann, K., Sporer, F., Steverding, D. and Wink, M. (2001) 'In vitro effect of alkaloids on bloodstream forms of *Trypanosoma brucei* and *T. congolense*', *Planta Medica*, 67(7), 623-627.
- Meshnick, S. R. (2002) 'Artemisinin: mechanisms of action, resistance and toxicity', *International Journal for Parasitology*, 32(13), 1655-1660.
- Mesnick, S. R., Taylor, T.E. AND Kamchonwongpaisan, S (1996) 'Artemisinin and the Antimalarial Endoperoxides: from Herbal Remedy to Targeted Chemotherapy', *Microbiological Reviews*, 60(2), 301-315.
- Miller, L. H. and Su, X. (2011) 'Artemisinin: discovery from the Chinese herbal garden', *Cell*, 146(6), 855-8.
- Moneriz, C., Marin-Garcia, P., Bautista, J. M., Diez, A. and Puyet, A. (2009) 'Haemoglobin interference and increased sensitivity of fluorimetric assays for quantification of low-parasitaemia *Plasmodium* infected erythrocytes', *Malar J*, 8, 279.
- Montaigne, D., Hurt, C. and Nevriere, R. (2012) 'Mitochondria Death/ Survival Signaling Pathways in Cardiotoxicity Induced by Anthracyclines and Anticancer- Targeted Therapies', *Biochemistry Research International*, 2012, 951539.
- Muhammad, I., Dunbar, D. C., Khan, S. I., Tekwani, B. L., Bedir, E., Takamatsu, S., Ferreira, D. and Walker, L. A. (2003) 'Antiparasitic alkaloids from *Psychotria klugii*', *Journal of natural products*, 66(7), 962.

- Musonda, C. C., Whitlock, G. A., Witty, M. J., Brun, R. and Kaiser, M. (2009) 'Chloroquine- astemizole hybrids with potent *in vitro* and *in vivo* antiplasmodial activity', *Bioorganic & medicinal chemistry letters*, 19(2), 481.
- Muthyala, R. (2011) 'Orphan/ rare drug discovery through drug repositioning', *Drug Discovery Today: Therapeutic Strategies*, 8(3-4), 71-76.
- Na-Bangchang, K. and Karbwang, J. (2009) 'Current status of malaria chemotherapy and the role of pharmacology in antimalarial drug research and development', *Fundam Clin Pharmacol*, 23(4), 387-409.
- Nandakumar, D. N., Nagaraj, V. A., Vathsala, P. G., Rangarajan, P. and Padmanaban, G. (2006) 'Curcumin-artemisinin combination therapy for malaria', *Antimicrob Agents Chemother*, 50(5), 1859-60.
- Ng, R. (2009) *Drugs: From Discovery to Approval*, 2<sup>nd</sup> Ed. USA: John Wiley and Sons, Inc.
- Noedl, H., Bronnert, J., Yingyuen, K., Attlmayr, B., Kollaritsch, H. and Fukuda, M. (2005) 'Simple histidine-rich protein 2 double-site sandwich enzyme-linked immunosorbent assay for use in malaria drug sensitivity testing', *Antimicrob Agents Chemother*, 49(8), 3575-7.
- Noedl, H., Se, Y., Schaecher, K., Smith, B. L., Socheat, D. and Fukuda, M. M. (2008) 'Evidence of Artemisinin-Resistant Malaria in Western Cambodia', *New England Journal of Medicine*, 359(24), 2619-2620.
- Noedl, H., Wernsdorfer, W. H., Miller, R. S. and Wongsrichanalai, C. (2002) 'Histidine-rich protein II: a novel approach to malaria drug sensitivity testing', *Antimicrob Agents Chemother*, 46(6), 1658-64.
- Nozaki, T. and Bhattacharya, A. (2014) *Amebiasis: Biology and Pathogenesis of Entamoeba*, Japan: Springer.
- Nwaka, S., Riopel, L., Ubben, D. and Craft, J. C. (2004) 'Medicines for Malaria Venture new developments in antimalarials', *Travel Med Infect Dis*, 2(3-4), 161-70.
- Nzila, A. (2006) 'The past, present and future of antifolates in the treatment of *Plasmodium falciparum* infection', *Journal of Antimicrobial Chemotherapy*, 57(6), 1043-1054.
- Nzila, A., Ma, Z. and Chibale, K. (2011) 'Drug repositioning in the treatment of malaria and TB', *Future Med Chem*, 3(11), 1413-26.
- Nzila, A., Okombo, J., Becker, R. P., Chilengi, R., Lang, T. and Niehues, T. (2010) 'Anticancer agents against malaria: time to revisit?', *Trends Parasitol*, 26(3), 125-9.

- Obonyo, C. O. and Juma, E. A. (2012) 'Clindamycin plus quinine for treating uncomplicated *falciparum* malaria: a systematic review and meta-analysis', *Malar J*, 11, 2.
- Obua, C., Gustafsson, L. L., Aguttu, C., Anokbonggo, W. W., Ogwal-Okeng, J. W., Chiria, J. and Hellgren, U. (2006) 'Improved efficacy with amodiaquine instead of chloroquine in sulfadoxine/pyrimethamine combination treatment of *falciparum* malaria in Uganda: experience with fixed-dose formulation', *Acta Trop*, 100(1-2), 142-50.
- Odds, F.C. (2003) 'Synergy and antagonism and what the checkerboard puts between them', *Journal of Antimicrobial Chemotherapy*, 52:1.
- Oksman-Caldentey, K.-M. and Inzé, D. (2004) 'Plant cell factories in the post- genomic era: new ways to produce designer secondary metabolites', *Trends in Plant Science*, 9(9), 433-440.
- Oprea, T. I., Bauman, J. E., Bologa, C. G., Buranda, T., Chigaev, A., Edwards, B. S., Jarvik, J. W., Gresham, H. D., Haynes, M. K., Hjelle, B., Hromas, R., Hudson, L., Mackenzie, D. A., Muller, C. Y., Reed, J. C., Simons, P. C., Smagley, Y., Strouse, J., Surviladze, Z., Thompson, T., Ursu, O., Waller, A., Wandinger-Ness, A., Winter, S. S., Wu, Y., Young, S. M., Larson, R. S., Willman, C. and Sklar, L. A. (2011) 'Drug repurposing from an academic perspective', *Drug Discovery Today: Therapeutic Strategies*, 8(3-4), 61-69.
- Painter, H. J., Morrissey, J. M. and Vaidya, A. B. (2010) 'Mitochondrial electron transport inhibition and viability of intraerythrocytic *Plasmodium falciparum*', *Antimicrobial agents and chemotherapy*, 54(12), 5281.
- Pasini, E. M., van den Ierssel, D., Vial, H. J. and Kocken, C. H. M. (2013) 'A novel live-dead staining methodology to study malaria parasite viability', *Malaria Journal*, 12, 190-190.
- Payne, D. (1987) 'Spread of chloroquine resistance in *Plasmodium falciparum*', *Parasitology Today*, 3(8), 241-246.
- Payne, D. and Wernsdorfer, W. H. (1989) 'Development of a blood culture medium and a standard *in vitro* microtest for field-testing the response of *Plasmodium falciparum* to antifolate antimalarials', *Bull World Health Organ*, 67(1), 59-64.
- Peters, W. (1999) 'The evolution of tafenoquine-- antimalarial for a new millennium?', *Journal of the Royal Society of Medicine*, 92(7), 345.
- Pina, A., Hussain, A. and Roque, A. (2010) 'An Historical Overview of Drug Discovery' in Roque, A. C. A., ed., *Ligand-Macromolecular Interactions in Drug Discovery*, Humana Press, 3-12.
- Plouffe, D., Brinker, A., McNamara, C., Henson, K., Kato, N., Kuhen, K., Nagle, A., Adrián, F., Matzen, J. T., Anderson, P., Nam, T.-G., Gray, N. S., Chatterjee, A., Janes, J., Yan, S. F., Trager, R., Caldwell, J. S., Schultz, P. G., Zhou, Y. and



- Winzeler, E. A. (2008) '*In silico* activity profiling reveals the mechanism of action of antimalarials discovered in a high- throughput screen', *Proceedings of the National Academy of Sciences of the United States of America*, 105(26), 9059.
- Plowe, C. V. (2009) 'The evolution of drug-resistant malaria', *Transactions of the Royal Society of Tropical Medicine and Hygiene*, 103(Suppl 1), S11-S14.
- Poinar, G., Jr. (2005) '*Plasmodium dominicana* n. sp. (Plasmodiidae: Haemospororida) from Tertiary Dominican amber', *Systematic Parasitology*, 61(1), 47-52.
- Radloff, P. D., Philips, J., Nkeyi, M., Kremsner, P. G. and Hutchinson, D. (1996) 'Atovaquone and proguanil for *Plasmodium falciparum* malaria', *The Lancet*, 347(9014), 1511-1514.
- Ramharter, M., Noedl, H., Winkler, H., Graninger, W., Wernsdorfer, W. H., Kremsner, P. G. and Winkler, S. (2003) '*In Vitro* Activity and Interaction of Clindamycin Combined with Dihydroartemisinin against *Plasmodium falciparum*', *Antimicrob Agents Chemother*, 47(11), 3494-3499.
- Randrianarivelojosa, M., Raveloson, A., Randriamanantena, A., Juliano, J. J., Andrianjafy, T., Raharimalala, L. A. and Robert, V. (2009) 'Lessons learnt from the six decades of chloroquine use (1945-2005) to control malaria in Madagascar', *Trans R Soc Trop Med Hyg*, 103(1), 3-10.
- Rason, M. A., Randrianatsoa, T., Andrianantenaina, H., Ratsimbaoa, A. and Menard, D. (2008) 'Performance and reliability of the SYBR Green I based assay for the routine monitoring of susceptibility of *Plasmodium falciparum* clinical isolates', *Trans R Soc Trop Med Hyg*, 102(4), 346-51.
- Ratcliff, A., Siswantoro, H., Kenangalem, E., Wuwung, M., Brockman, A., Edstein, M. D., Laihad, F., Ebsworth, E. P., Anstey, N. M., Tjitra, E. and Price, R. N. (2007) 'Therapeutic response of multidrug-resistant *Plasmodium falciparum* and *P. vivax* to chloroquine and sulfadoxine-pyrimethamine in southern Papua, Indonesia', *Trans R Soc Trop Med Hyg*, 101(4), 351-9.
- Read, M. and Hyde, J. E. (1993) 'Simple *In Vitro* Cultivation of the Malaria Parasite *Plasmodium falciparum* (Erythrocytic Stages) Protocols in Molecular Parasitology' in Hyde, J. E., ed., Humana Press, 43-55.
- Reaume, A. G. (2011) 'Drug repurposing through nonhypothesis driven phenotypic screening', *Drug Discovery Today: Therapeutic Strategies*, 8(3-4), 85-88.
- Recanatini, M., Poluzzi, E., Masetti, M., Cavalli, A. and De Ponti, F. (2005) 'QT prolongation through hERG K + channel blockade: Current knowledge and strategies for the early prediction during drug development', 25, 133-166.
- Renneberg, J. and Walder, M. (1989) 'Postantibiotic effects of imipenem, norfloxacin, and amikacin in vitro and in vivo', *Antimicrobial agents and chemotherapy*, 33(10), 1714.

- Ridley, R. G. (2002) 'Medical need, scientific opportunity and the drive for antimalarial drugs', *Nature*, 415, 686-693.
- Rieckmann, K. H., Campbell, G. H., Sax, L. J. and Mrema, J. E. (1978) 'Drug sensitivity of *Plasmodium falciparum*. An *in-vitro* microtechnique', *Lancet*, 1(8054), 22-3.
- Roman, G., Crandall, I. E. and Szarek, W. A. (2013) 'Synthesis and anti- *Plasmodium* activity of benzimidazole analogues structurally related to astemizole', *ChemMedChem*, 8(11), 1795.
- Rosenkranz, V. a. W., Michael (2008) 'Alkaloids Induce Programmed Cell Death in Bloodstream Forms of Trypanosomes (*Trypanosoma b. brucei*)', *Molecules*, 13(10), 2462.
- Rosenthal, P. J. (2003) 'Antimalarial drug discovery: old and new approaches', *The Journal of experimental biology*, 206(21), 3735.
- Rosenthal, P. J. (2008) 'Artesunate for the Treatment of Severe *Falciparum* Malaria', *The New England Journal of Medicine*, 358(1), 1829-1836.
- Rottmann, M., McNamara, C., Yeung, B. K. S., Lee, M. C. S., Zou, B., Russell, B., Seitz, P., Plouffe, D. M., Dharia, N. V., Tan, J., Cohen, S. B., Spencer, K. R., González-Páez, G. E., Lakshminarayana, S. B., Goh, A., Suwanarusk, R., Jegla, T., Schmitt, E. K., Beck, H.-P., Brun, R., Nosten, F., Renia, L., Dartois, V., Keller, T. H., Fidock, D. A., Winzeler, E. A. and Diagana, T. T. (2010) 'Spiroindolones, a new and potent chemotype for the treatment of malaria', *Science (New York, N.Y.)*, 329(5996), 1175-1180.
- Rubin, R. P. (2007) 'A brief history of great discoveries in pharmacology: in celebration of the centennial anniversary of the founding of the American Society of Pharmacology and Experimental Therapeutics', *Pharmacological reviews*, 59(4), 289.
- Sadasivaiah, S., Tozan, Y. and Breman, J. G. (2007) 'Dichlorodiphenyltrichloroethane (DDT) for indoor residual spraying in Africa: how can it be used for malaria control?', *The American journal of tropical medicine and hygiene*, 77(Suppl 6), 249.
- Saito-Ito, A., Akai, Y., He, S., Kimura, M. and Kawabata, M. (2001) 'A rapid, simple and sensitive flow cytometric system for detection of *Plasmodium falciparum*', *Parasitol Int*, 50(4), 249-57.
- Sanz, L. M., Crespo, B., De-Cózar, C., Ding, X. C., Llergo, J. L., Burrows, J. N., García-Bustos, J. F. and Gamó, F.-J. (2012) 'P. falciparum *In Vitro* Killing Rates Allow to Discriminate between Different Antimalarial Mode-of- Action (*In Vitro* Killing Rates for Antimalarials)', *PLoS ONE*, 7(2), e30949.
- Satou, T., Akao, N., Matsushashi, R., Koike, K., Fujita, K. and Nikaido, T. (2002) 'Inhibitory Effect of Isoquinoline Alkaloids on Movement of Second- Stage

- Larvae of *Toxocara canis*', *Biological and Pharmaceutical Bulletin*, 25(12), 1651-1654.
- Sauvain, M., Moretti, C., Bravo, J. a., Callapa, J., Muñoz, V., Ruiz, E., Richard, B. and Le Men-olivier, L. (1996) 'Antimalarial Activity of Alkaloids from *Pogonopus tubulosus*', *Phytotherapy Research*, 10(3), 198-201.
- Schlitzer, M. (2007) 'Malaria Chemotherapeutics. Part 1. History of Antimalarial Drug Development, Currently Used Therapeutics, and Drugs in Clinical Development', *ChemMedChem*, 2(7), 944-86.
- Seidlein, L. v. and Bejon, P. (2013) 'Malaria vaccines: past, present and future', *Archives of Disease in Childhood*, 98(12), 981.
- Shapiro, H. M. and Mandy, F. (2007) 'Cytometry in malaria: Moving beyond Giemsa', *Cytometry Part A*, 71A(9), 643-645.
- Smilkstein, M., Sriwilaijaroen, N., Kelly, J. X., Wilairat, P. and Riscoe, M. (2004) 'Simple and inexpensive fluorescence-based technique for high-throughput antimalarial drug screening', *Antimicrob Agents Chemother*, 48(5), 1803-6.
- Smith, D. C. and Sanford, L. B. (1985) 'Laveran's Germ: The Reception and Use of a Medical Discovery', *The American Journal of Tropical Medicine and Hygiene*, 34(1), 2-20.
- Snyder, C., Chollet, J., Santo-Tomas, J., Scheurer, C. and Wittlin, S. (2007) 'In vitro and in vivo interaction of synthetic peroxide RBx11160 (OZ277) with piperaquine in *Plasmodium* models', *Exp Parasitol*, 115(3), 296-300.
- Spangenberg, T., Burrows, J. N., Kowalczyk, P., McDonald, S., Wells, T. N. C. and Willis, P. (2013) 'The open access malaria box: a drug discovery catalyst for neglected diseases', *PloS one*, 8(6), e62906.
- Srivastava, I. K. and Vaidya, A. B. (1999) 'A mechanism for the synergistic antimalarial action of atovaquone and proguanil', *Antimicrobial agents and chemotherapy*, 43(6), 1334.
- Sutherland, C. J., Tanomsing, N., Nolder, D., Oguike, M., Jennison, C., Pukrittayakamee, S., Dolecek, C., Hien, T. T., Do Rosário, V. E., Arez, A. P., Pinto, J., Michon, P., Escalante, A. A., Nosten, F., Burke, M., Lee, R., Blaze, M., Otto, T. D., Barnwell, J. W., Pain, A., Williams, J., White, N. J., Day, N. P. J., Snounou, G., Lockhart, P. J., Chiodini, P. L., Imwong, M. and Polley, S. D. (2010) 'Two nonrecombining sympatric forms of the human malaria parasite *Plasmodium ovale* occur globally', *The Journal of infectious diseases*, 201(10), 1544.
- Trager, W. and Jensen, J. B. (1976) 'Human malaria parasites in continuous culture', *Science*, 193(4254), 673-5.
- Tun, M, K., Imwong, Mallika, Lwin, M, K., Win, A, A., Hlaing, M, T., Hlaing, Thaung, Lin, Khin, Kyaw, P, M., Plewes, Katherine, Faiz, Abul, M., Dhorda, Mehul,

- Cheah, Yeong, P., Pukrittayakamee, Sasithon, Ashley, A. E., Anderson, C. T. J., Nair, Shalini, McDew-White, Marina, Flegg, A. J., Grist, M. E. P., Guerin, Philippe, Maude, J. R., Smithuis, Frank, Dondorp, M. A., Day, J. N. P., Nosten, François, White, J. N., Woodrow and J. C. (2015) 'Spread of artemisinin-resistant *Plasmodium falciparum* in Myanmar: a cross-sectional survey of the K13 molecular marker', *The Lancet Infectious Diseases* 15(4), 415-421.
- Valderramos, S. G., Scanfeld, D., Uhlemann, A.-C., Fidock, D. A. and Krishna, S. (2010) 'Investigations into the Role of the *Plasmodium falciparum* SERCA (PfATP6) L263E Mutation in Artemisinin Action and Resistance', *Antimicrob Agents Chemother*, 54(9), 3842-3852.
- Valecha, N., Joshi, H., Mallick, P. K., Sharma, S. K., Kumar, A., Tyagi, P. K., Shahi, B., Das, M. K., Nagpal, B. N. and Dash, A. P. (2009) 'Low efficacy of chloroquine: time to switchover to artemisinin-based combination therapy for *falciparum* malaria in India', *Acta Trop*, 111(1), 21-8.
- Van Vianen, P. H., Van Engen, A., Thaithong, S., Van der Keur, M., Tanke, H.J., Van der Kaay, H.J., Mons, B. and Janse, C.J. (1993) 'Flow Cytometric Screening of Blood Samples for Malaria Parasites', *Cytometry Part A*, 14, 276-280.
- Vivas, L., Rattray, L., Stewart, L. B., Robinson, B. L., Fugmann, B., Haynes, R. K., Peters, W. and Croft, S. L. (2007) 'Antimalarial efficacy and drug interactions of the novel semi-synthetic endoperoxide artemisone *in vitro* and *in vivo*', *Journal of Antimicrobial Chemotherapy*, 59(4), 658-665.
- Vossen, M. G., Pferschy, S., Chiba, P. and Noedl, H. (2010) 'The SYBR Green I malaria drug sensitivity assay: performance in low parasitemia samples', *Am J Trop Med Hyg*, 82(3), 398-401.
- Vythilingam, I., Noorazian, Y. M., Huat, T. C., Jiram, A. I., Yusri, Y. M., Azahari, A. H., Norparina, I., Noorain, A. and Lokmanhakim, S. (2008) '*Plasmodium knowlesi* in humans, macaques and mosquitoes in peninsular Malaysia', *Parasites & vectors*, 1(1), 26.
- Walker, S. L. Waters, M. F.R. and Lockwood, D.N.J. (2007) 'The role of thalidomide in the management of *erythema nodosum leprosum*', *Leprosy Review*, 78(3), 197-215.
- Walsh, J. J., Coughlan, D., Heneghan, N., Gaynor, C. and Bell, A. (2007) 'A novel artemisinin-quinine hybrid with potent antimalarial activity', *Bioorg Med Chem Lett*, 17(13), 3599-602.
- Wang, J., Huang, L., Li, J., Fan, Q., Long, Y., Li, Y. and Zhou, B. (2010) 'Artemisinin Directly Targets Malarial Mitochondria through Its Specific Mitochondrial Activation', *PLoS ONE*, 5(3), e9582.
- Wein, S., Maynadier, M., Tran Van Ba, C., Cerdan, R., Peyrottes, S., Fraisse, L. and Vial, H. (2010) 'Reliability of antimalarial sensitivity tests depends on drug mechanisms of action', *Journal of clinical microbiology*, 48(5), 1651.

- Weisman, J. L., Liou, A. P., Shelat, A. A., Cohen, F. E., Kiplin Guy, R. and Derisi, J. L. (2006) 'Searching for New Antimalarial Therapeutics amongst Known Drugs', *Chemical Biology & Drug Design*, 67(6), 409-416.
- Wells, T. N. (2011) 'Natural products as starting points for future anti-malarial therapies: going back to our roots?', *Malar J*, 10(Suppl 1), S3.
- Wells, T. N. C. (2010) 'Is the Tide Turning for New Malaria Medicines?', *Science*, 329(5996), 1153-1154.
- Wernsdorfer, W. H. (1980) 'Field evaluation of drug resistance in malaria. *In vitro* micro-test', *Acta Trop*, 37(3), 222-7.
- White, N. J. (2004) 'Antimalarial drug resistance', *The Journal of Clinical Investigation*, 113(8), 1084-1092.
- White, N. J., Pukrittayakamee, S., Phyo, A. P., Rueangweerayut, R., Nosten, F., Jittamala, P., Jeeyapant, A., Jain, J. P., Lefèvre, G., Li, R., Magnusson, B., Diagana, T. T. and Leong, F. J. (2014) 'Spiroindolone KAE609 for *Falciparum* and *Vivax* Malaria', *The New England Journal of Medicine*, 371(5), 403-410.
- WHO (2001) *In vitro micro-test (mark III) for the assessment of the response of Plasmodium falciparum to chloroquine, mefloquine, quinine, amodiaquine, sulfadoxine/pyrimethamine and artemisinin*. Geneva: World Health Organization Press.  
([http://www.who.int/malaria/publications/atoz/ctd\\_mal\\_97\\_20\\_Rev\\_2\\_2001/en/](http://www.who.int/malaria/publications/atoz/ctd_mal_97_20_Rev_2_2001/en/))
- WHO (2010) *Global report on antimalarial drug efficacy and drug resistance: 2000-2010*. Switzerland: World Health Organization Press.  
([http://whqlibdoc.who.int/publications/2010/9789241500470\\_eng.pdf](http://whqlibdoc.who.int/publications/2010/9789241500470_eng.pdf))
- WHO (2013) *World Malaria report: 2013*, France: World Health Organization Press.  
([http://www.who.int/malaria/publications/world\\_malaria\\_report\\_2013/wmr2013\\_no\\_profiles.pdf?ua=1](http://www.who.int/malaria/publications/world_malaria_report_2013/wmr2013_no_profiles.pdf?ua=1))
- Winstanley, P. A. (2000) 'Chemotherapy for *Falciparum* Malaria: The Armoury, the Problems and the Prospects', *Parasitology Today*, 16(4), 146-153.
- Wong, W., Bai, X.-c., Brown, A., Fernandez, I. S., Hanssen, E., Condrón, M., Tan, Y. H., Baum, J., Scheres, S. H. W. and Kühlbrandt, W. (2014) 'Cryo- EM structure of the *Plasmodium falciparum* 80S ribosome bound to the anti- protozoan drug emetine', *eLife*, 3, e03080.
- Wu, T., Nagle, A., Kuhen, K., Gagaring, K., Borboa, R., Francek, C., Chen, Z., Plouffe, D., Goh, A., Lakshminarayana, S. B., Wu, J., Ang, H. Q., Zeng, P., Kang, M. L., Tan, W., Tan, M., Ye, N., Lin, X., Caldwell, C., Ek, J., Skolnik, S., Liu, F., Wang, J., Chang, J., Li, C., Hollenbeck, T., Tuntland, T., Isbell, J., Fischli, C., Brun, R., Rottmann, M., Dartois, V., Keller, T., Diagana, T., Winzeler, E., Glynn, R., Tully, D. C. and Chatterjee, A. K. (2011) 'Imidazolopiperazines: hit to lead

- optimization of new antimalarial agents', *Journal of medicinal chemistry*, 54(14), 5116.
- Wu, T., Nagle, A., Sakata, T., Henson, K., Borboa, R., Chen, Z., Kuhen, K., Plouffe, D., Winzeler, E., Adrian, F., Tuntland, T., Chang, J., Simerson, S., Howard, S., Ek, J., Isbell, J., Deng, X., Gray, N. S., Tully, D. C. and Chatterjee, A. K. (2009) 'Cell-based optimization of novel benzamides as potential antimalarial leads', *Bioorganic & Medicinal Chemistry Letters*, 19(24), 6970-6974.
- Yeh, P. J., Hegreness, M. J., Aiden, A. P. and Kishony, R. (2009) 'Drug interactions and the evolution of antibiotic resistance', *Nature reviews. Microbiology*, 7(6), 460.
- Yeka, A., Banek, K., Bakyaite, N., Staedke, S. G., Kanya, M. R., Talisuna, A., Kironde, F., Nsoya, S. L., Kilian, A., Slater, M., Reingold, A., Rosenthal, P. J., Wabwire-Mangen, F. and Dorsey, G. (2005) 'Artemisinin versus Nonartemisinin Combination Therapy for Uncomplicated Malaria: Randomized Clinical Trials from Four Sites in Uganda', *PLoS Med*, 2(7), e190.
- Yeung, B. K. S., Zou, B., Rottmann, M., Lakshminarayana, S. B., Ang, S. H., Leong, S. Y., Tan, J., Wong, J., Keller-Maerki, S., Fischli, C., Goh, A., Schmitt, E. K., Krastel, P., Francotte, E., Kuhen, K., Plouffe, D., Henson, K., Wagner, T., Winzeler, E. A., Petersen, F., Brun, R., Dartois, V., Diagana, T. T. and Keller, T. H. (2010) 'Spirotetrahydro beta-carbolines (spiroindolones): a new class of potent and orally efficacious compounds for the treatment of malaria', *Journal of medicinal chemistry*, 53(14), 5155.
- Zhanel, G. G., Hoban, D. J. and Harding, G. K. M. (1991) 'The Postantibiotic Effect: A Review of *in Vitro* and *in Vivo* Data', *Annals of Pharmacotherapy*, 25(2), 153-163.
- Zhang, S. and Gerhard, G. S. (2009) 'Heme mediates cytotoxicity from artemisinin and serves as a general anti-proliferation target', *PLoS ONE*, 4(10), e7472.
- Zimmermann, G. R., Lehár, J. and Keith, C. T. (2007) 'Multi- target therapeutics: when the whole is greater than the sum of the parts', *Drug Discovery Today*, 12(1), 34-42.
- Zongo, C., Ouattara, L. P., Savadogo, A., Sanon, S., Barro, N., Koudou, J., Nebie, I. and Traore, A. S. (2011) '*In vitro* Antiplasmodial Activity of Some Medicinal Plants Used in Folk Medicine in Burkina Faso Against Malaria', *Current Research Journal of Biological Sciences*, 3(3), 216.